Regulation of the Ubiquitin RING E3 Ligase Parkin

Viduth Kiran Chaugule

University College London

and

Cancer Research UK London Research Institute

PhD Supervisor: Dr. Helen Walden

A thesis submitted for the degree of

Doctor of Philosophy

University College London

September 2010

Declaration

I Viduth Kiran Chaugule confirm that the work presented in this thesis is my own. Where information has been derived from other sources, I confirm that this has been indicated in the thesis.

Abstract

Regulation of the Ubiquitin RING E3 ligase Parkin

Post-translational modification of proteins by ubiquitin is a central regulatory process in all eukaryotic cells. Substrate selection and type of modification are events catalyzed by the E3 ligase, a component of the ubiquitin pathway. Several ubiquitin E3 ligases are implicated in cancer and other disease states, underlying the need for mechanistic insight of these enzymes.

Parkinson's disease is a neurodegenerative disorder characterised by the loss of dopaminergic neurons from the *substantia nigra*, the presence of Lewy Bodies, and pathogenic aggregates rich in ubiquitin. Autosomal Recessive Juvenile Parkinsonism (AR-JP), which is one of the most common familial forms of the disease, is directly linked to mutations in the *Parkin* gene (*PARK2*). Parkin is a RING E3 and catalyses a range of ubiquitination events (mono, multi mono, K48- and K63- linked poly) in concert with several E2s on a variety of substrates, including itself. Furthermore, Parkin is capable of binding the 26S proteasome and mediates selective degradation of target substrates.

The data presented will demonstrate that the Ubiquitin-like domain (UblD) of Parkin functions to inhibit its auto-ubiquitination via a novel mechanism. Pathogenic Parkin mutations disrupt this inhibition and result in a constitutively active molecule. The inhibition is mediated by an intra-molecular interaction between UblD and the C-terminus of Parkin, and Lysine 48 on UblD participates in this interaction. The study also uncovered unique UblD/Ubiquitin Binding Regions (UBRs) on the C-terminus of Parkin that play a novel role in its RING E3 ligase activity. The observations provide critical mechanistic insights into the myriad functions of Parkin and the underlying basis of Parkinson's disease.

Acknowledgement

I would like to begin by thanking my supervisor Dr. Helen Walden for giving me the unique opportunity to be a part of the first generation of her group, and moreover to work with a challenging project like Parkin. Her constant support, encouragement and enthusiasm were invaluable. I would also like to thank members of the Protein Structure Function Lab in particular, Dr. Ambrose Cole and Laurence Lewis who provided a wonderful environment to work in, forever indulging my questions and accepting me as their 'grumpy' co-worker. I would like to thank Cancer Research UK for supporting my studentship and the numerous facilities, service labs and administrative support at the London Research Institute (LRI).

I would also like to thank Andrea, Dan, Fab, Diego, Dev and others for being great PhD mates and sharing some wonderful experiences over the last four years. Have also had the priceless opportunity to make several friends (Chris, Charlie, Kat, Fred, Martin, Alex and others) as well as share the multi-cultural experience of London (not to mention the weather!). All these experiences have supported me through my PhD and more importantly, the social aspects of my life away from home. Finally, I would like to thank my parents, my brother and his family, and my friends (Amrita, Ogre, Lash, Surabhi, Karan, Shermy, Tan, Ammu) for their continued support, tolerating my long absences and encouraging me throughout of my PhD. My parents in particular I am most thankful, for encouraging me to follow my dreams (even the crazy ones). I hope to have, in a small way, justified their faith in me, and would like to dedicate the thesis to them.

Table of Contents

List of Figures

List of Tables

List of Abbreviations and Symbols

°C	Degrees Celcius
6xHis tag	Hexa-Histidine sequence tag
AIMP2	Aminoacyl tRNA synthase complex-interacting multifunctional protein 2 *(Parkin substrate)*
AMP	Adenosine monophosphate
AR-JP	Autosomal Recessive Juvenile Parkinson's
ATP	Adenosine triphosphate
BAG5	bcl-5-associated anthogene 5
c-Cbl	Casitas B-lineage lymphoma proto-oncogene *(ubiquitin RING E3 ligase)*
C-terminus	carboxy/COOH terminus
CBD	Chitin binding protein
Cdk5	cyclin-dependent kinase 5
CHIP	Carboxyl terminus of the Hsc70-interacting protein *(ubiquitin U-box E3 ligase)*
cIAP2	Inhibitor of Apoptosis protein 2 *(ubiquitin RING E3 ligase)*
CIR	Chain of interacting residues *(within UBC fold of E2)*
CMA	Chaperone mediated autophagy
CRL	Cullin-RING ubiquitin ligases
CTT	C-terminal Thioredoxin tag
cv	column volume
DMSO	Dimethyl sulfoxide
DSS	4,4-dimethyl-4-silapentane-1-sulfonic acid
DTT	Dithiothreitol
DUBs	Deubiquitinating enzymes
E. coli	*Escherichia coli*
ECL	Enhanced chemiluminescence
EDTA	Ethylenediaminetetraacetic acid
EO-PD	Early-Onset Parkinson's Disease
EPL	Expressed protein ligation
EPS15	Epidermal growth factor receptor substrate 15 *(Parkin substrate)*
ER	Endoplasmic reticulum
FancL	Fanconi anemia group protein L *(ubiquitin RING E3 ligase)*
FPLC	Fast protein liquid chromatography
g/mg/μg/ng	Gram/milligram/microgram/nanogram (respectively)
h/min/s	hour/minute/second (respectively)

HECT	Homologous to the E6-AP Carboxyl Terminus *(ubiquitin E3 ligase catalytic domain)*
HOIL-1	Haem-oxidized IRP2 ubiquitin ligase-1 *(ubiquitin RING E3 ligase)*
HOIP	HOIL-1L Interacting Protein *(ubiquitin RING E3 ligase)*
HRP	Horse radish peroxidase
HRS	Hepatocyte growth factor–Regulated tyrosine kinase Substrate
HSP	Heat shock protein
HSQC	Heteronuclear Single Quantum Coherence
HTRA2	High temperature requirement protein A2
IBR	In-Between RING domain
IMPACT	Intein Mediated Purification with an Affinity Chitin-binding Tag
IPTG	Isopropyl β- D-1-thiogalactopyranoside
ISG15	Interferon-stimulated protein 15 *(ubiquitin-like protein)*
kDa	Kilodalton
L/mL/μL	litre/millilitre/microlitre (respectively)
LB	Luria Broth
LC-MS	Liquid chromatography-Mass spectrometry
M/mM/μM/nM	molar/millimolar/micromolar/nanomolar (respectively)
Mb/kb	Megabase/kilobase (respectively)
MBP	Maltose binding protein
MESNA	2-Mercaptoethanesulfonic acid
$MgCl_2$	Magnesium chloride
MPTP	1-methyl-4-phenyl-1,2,3,6-tetrahydropyrindine
N-terminus	amino/NH_2 terminus
NaCl	Sodium chloride
NEDD	Neural precursor cell expressed developmentally down-regulated protein
Ni-NTA	Nickel-nitrilotriacetic acid
NMR	Nuclear Magnetic Resonance
NZF	Npl4 type Zinc Finger *(ubiquitin binding domain)*
OD_{600}	Optical density at 600 nanometer wavelength
PCR	Polymerase chain reaction
PD	Parkinson's disease
PDB	Protein data bank
PDZ	PSD-95/Discs-large/Zona Occludens-1 *(protein-protein interaction domain)*
pH	Potential of hydrogen, $-\log_{10}$ [H+]
pI	Isoelectric point
PICK1	Protein kinase C, alpha *(Parkin substrate)*
PINK1	PTEN Induced putative Kinase-1
ppm	parts per million

PVDF	Polyvinylidene fluoride
RAP80	Receptor associated Protein 80
RCF	Relative centrifugal force
RF	Restriction-free cloning
RING	Really Interesting New Gene *(ubiquitin E3 ligase catalytic domain)*
ROS	Reactive oxygen species
rpm	rotations per minute
RPN	Regulatory particle non-ATPase protein *(proteasomal subunit)*
RT	Room temperature
S	Svedberg sedimentation coefficient
S. cerevisiae	*Saccharomyces cerevisiae*
SCNA	synuclein, alpha (non A4 component of amyloid precursor)
SD	standard deviation
SDS	Sodium dodecyl sulfate
SDS-PAGE	Sodium dodecyl sulfate – polyacrylamide gel electrophoresis
SEC	Size-exclusion chromatography
SUMO	Small Ubiquitin-like Modifier *(ubiquitin-like protein)*
T200 buffer	50 mM Tris pH 8.0, 200 mM NaCl, 250 µM TCEP
T200i	100 mM Tris pH 8.0, 200 mM NaCl, 300 mM imidaizole, 250 µM TCEP
T25	100 mM Tris pH 8.5, 25 mM NaCl, 250 µM TCEP
T500i buffer	75 mM Tris pH 8.0, 500 mM NaCl, 25 mM imidaizole, 250 µM tris TCEP
TAE	Tris Acetate EDTA
TCEP	Tris(2-carboxyethyl)phosphine
TEV	Tobacco etch virus
TRAF6	Tumor Necrosis Factor (TNF) receptor-associated factor 6 *(ubiquitin RING E3 ligase)*
Tris	Tris (hydroxymethyl) aminomethane
Ub	Ubiquitin
UBA	Ubiquitin Activating enzyme
UBA domains	Ubiquitin Associated domains
UBC fold	Ubiquitin conjugating fold *(E2 core fold)*
UBD	Ubiquitin Binding Domain
UBE2Xn	Ubiquitin E2, ‘X’ denotes a letter and ‘n’ a number *(E2 nomenclature)*
UblD	Ubiquitin-like domain *(Parkin specific)*
Ubls	Ubiquitin-like proteins
UBR	UblD/Ub Binding Region *(Parkin specific)*
UFD	Ubiquitin-fold domain
UIM	Ubiquitin Interacting Motif
Ulp1	Ubiquitin-like-specific protease 1

UPR	Unfolded protein response
UV	Ultraviolet
v/v, w/v, w/w	Volume per volume, Weight per volume, Weight per weight (respectively)
WT	Wild type
βME	2-Mercaptoethanol

Single and Three letter codes for Amino Acids

Amino Acid	**One letter code**	**Three letter code**
Alanine	A	Ala
Arginine	R	Arg
Asparagine	N	Asn
Aspartic acid	D	Asp
Cysteine	C	Cys
Glutamic acid	E	Glu
Glutamine	Q	Gln
Glycine	G	Gly
Histidine	H	His
Isoleucine	I	Ile
Leucine	L	Leu
Lysine	K	Lys
Methionine	M	Met
Phenylalanine	F	Phe
Proline	P	Pro
Serine	S	Ser
Threonine	T	Thr
Tryptophan	W	Trp
Tyrosine	Y	Tyr
Valine	V	Val

Chapter 1. Introduction

Ubiquitination is a protein-based post-translation modification (PTM) event that regulates nearly every cellular pathway; cell cycle, DNA repair, transcription, signal transduction, immune response, protein localisation, protein quality control and proteasomal degradation (Pickart, 2001). The modification involves covalent attachment of ubiquitin (Ub) onto a substrate protein. PTMs can also occur through Ubiquitin-like proteins (Ubls) like; Small Ubiquitin-like Modifier (SUMO, called sumoylation), Neural precursor cell expressed, developmentally down-regulated protein 8 (NEDD8, called neddylation) and interferon-stimulated 15kDa protein (ISG15, called ISGylation) among others. Each of the modifiers has their own cohort of proteins to facilitate the PTM event and the following sections introduce those involved in ubiquitination.

1.1 Machinery of Ubiquitination

Ubiquitination occurs through a series of biochemical transactions between three classes of enzymes: E1 or activating enzyme, E2 or the conjugating enzyme and E3 or the ligating enzyme (Pickart, 2001). In humans, the 76-residue ubiquitin (~8.5kDa) is translated either as a polyprotein of tandem ubiquitin repeats (Ubiquitin B (UBB) and Ubiquitin C (UBC)) or a single ubiquitin with an unrelated tail extension (Ubiquitin A-52-residue ribosomal protein (UBA52) and Ribosomal Protein S27A (RPS27A)) (Baker and Board, 1991, Lund et al., 1985, Wiborg et al., 1985). The precursor protein, upon proteolytic processing by a ubiquitin C-terminal hydrolase, yields ubiquitin monomers that enter the ubiquitin pathway (Ozkaynak et al., 1984).

Activation of ubiquitin transpires over two steps; an energy dependent formation of the ubiquitin adenylate intermediate, which is transferred onto E1's catalytic cysteine to form a C-terminal ubiquitin thioester conjugate (Haas et al., 1982). A

loaded E1 thus carries both adenylate and thioester ubiquitin states (Figure 1). Subsequent ubiquitin conjugation of the E2 involves a transthioesterification reaction between the catalytic cysteines of E1 and E2 (E1~ubiquitin → E2~ubiquitin). Nucleophilic attack on the E2~ubiquitin thioester conjugate by the target lysine (ε-amino group) or free amino terminus of the substrate protein results in formation of an isopeptide or peptide bond respectively (*i.e.* ubiquitination).

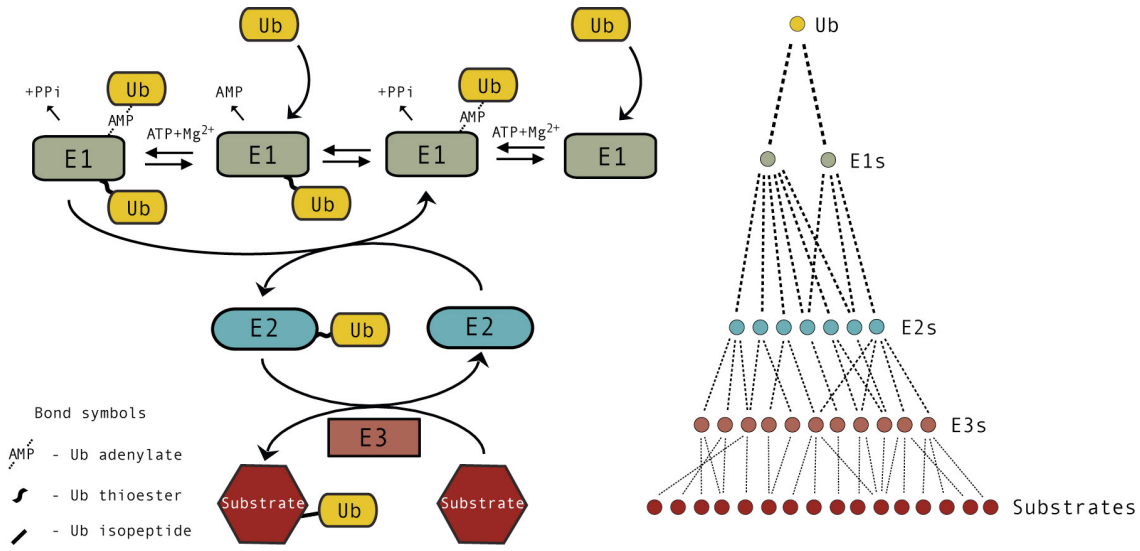

Figure 1: Ubiquitination machinery. A schematic of the ubiquitin (Ub) pathway (left) and the members involved at each step; activation (E1), conjugation (E2) and ligation (E3). Ubiquitin activation is catalyzed by the E1 in an energy intensive process (Adenosine triphosphate (ATP)). A 'loaded' E1 constitutes the ubiquitin adenylate intermediate (E1···AMP···ubiquitin) and the ubiquitin thioester conjugate (E1~ubiquitin) at the active adenylation site and catalytic cysteine site respectively. The ubiquitin thioester conjugate is then passed onto the catalytic cysteine site on the E2 (E1~ubiquitin → E2~ubiquitin) and finally ligated (isopeptide linkage) onto a target lysine of a substrate (substrate-ubiquitin), an event orchestrated by E3 ligases. The flowchart on the right illustrates numerical hierarchy in the ubiquitin pathway with a high degree of orthogonal cross-talk observed towards the functional end of the pathway (E2-E3-

The E3 ligase complex predominantly orchestrates substrate ubiquitination event(s) however the E2 enzymes can catalyse certain events (Nagy and Dikic, 2010, Ciechanover and Ben-Saadon, 2004, Hoeller et al., 2007). E3 ligases are classified based on their catalytic domains; Homologous to the E6-AP Carboxyl Terminus (HECT) domain E3 ligases (Scheffner et al., 1995) or Really Interesting New Gene (RING) domain E3 ligases (reviewed in (Joazeiro and Weissman, 2000)). HECT E3s bear a conserved active site cysteine that accepts ubiquitin from the E2~ubiquitin conjugate before ligating the substrate

with ubiquitin (E2~ubiquitin → E3~ubiquitin → Substrate-ubiquitin). RING E3s bring together substrate and E2~ubiquitin facilitating direct transfer of the ubiquitin moiety (E2~ubiquitin → Substrate-ubiquitin).

A significant number of E2s have been reported, enabling the wide repertoire of ubiquitin based signals. However, the E3s represent an even larger family of enzymes as they and are responsible for the critical facets of ubiquitination; substrate recognition, recruitment of specific E2s and facilitating the ubiquitination event (Deshaies and Joazeiro, 2009, Ye and Rape, 2009). The ubiquitin~E2s conjugation, for all known ubiquitin E2s can established by the E1s, however each E3 recruits one or a few E2s to ligate ubiquitin signals to a set of substrates. Substrates are known to have either a sole E3 or many E3s facilitating ubiquitination. The machinery for ubiquitination thus follows a numerical hierarchy with significant degree of orthogonal crosstalk (Figure 2). Deubiquitinating enzymes (DUBs: enzymes to remove ubiquitin of substrates and disband polyubiquitin structures) and E4s (chain elongating E3 enzymes) are other players that play contrasting roles in the ubiquitin pathway and their cellular functions have been reviewed elsewhere (Hoppe, 2005, Komander et al., 2009a). The following sections set out to introduce E1s, ubiquitin signals and associated receptors, the enzymatic properties of E2s, E3 ligases.

1.2 E1s: activators of ubiquitin signals

Pioneering structure-function studies have revealed the mechanistic details of the Ubiquitin E1 (Lake et al., 2001, Lee and Schindelin, 2008), SUMO E1 (Lois and Lima, 2005, Olsen et al., 2010) and the NEDD8 E1 (Huang et al., 2005, Walden et al., 2003a, Walden et al., 2003b). Briefly, the E1 comprises of three structural elements; the adenylation domain (binds ATP and ubiquitin), catalytic cysteine domain and the ubiquitin-fold domain (UFD, E2 selection). In the E1s for SUMO and NEDD8, the adenylation domains are shared between heterodimers (SUMO Activating Enzyme 1 (SAE1) – Ubiquitin Activating

enzyme 2 (UBA2) for SUMO and NEDD8 Activating Enzyme 1 (NAE1) – UBA3 for NEDD8), while the catalytic cysteine domain and UFD are borne on one protein (UBA2 for SUMO and UBA3 for NEDD8 respectively). In contrast, the E1s for ubiquitin, UBA1 and the recently discovered UBA6 (Jin et al., 2007), are monomeric proteins and bear the three structural elements interspersed on a polypeptide chain (Figure 2) (Schulman and Harper, 2009).

The adenylation domain bears structural homology with the molybdopterin biosynthetic enzyme B (MoeB) and thiamine biosynthesis protein F (ThiF), both bacterial enzymes involved in the biosynthesis of molybdenum cofactor and thiamin respectively. These E1-like enzymes activate the bacterial proteins molybdopterin converting factor subunit 1 (MoaD) and ThiS respectively, both of which bear the Ubl fold, via a mechanism analogous to eukaryotic E1s (Lake et al., 2001, Lehmann et al., 2006, Leimkuhler et al., 2001, Taylor et al., 1998).

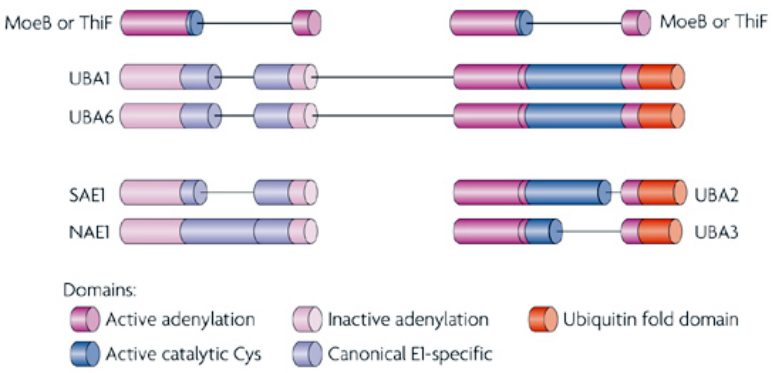

Figure 2: E1 domains. Cartoons depict the structural elements of E1s; adenylation domain (light and dark pink), catalytic cysteine domain (blue) and ubiquitin-fold domain (red), for ubiquitin (UBA1 and UBA6), the Small Ubiquitin-like Modifier (SUMO - SAE1/UBA2) and the Neural precursor cell expressed, developmentally down-regulated protein 8 (NEDD8 - NAE1/UBA3) aligned with the adenylation domains of bacterial E1-like enzymes molybdopterin biosynthetic enzyme B (MoeB)/thiamine biosynthesis protein F (ThiF). UBA is Ubiquitin Activating Enzyme, SAE and NAE is SUMO and NEDD8 Activating Enzyme respectively. Black lines indicate sequence insertions within the conserved domains. Figure adapted from (Schulman and Harper, 2009).

Recognition and activation of ubiquitin, E2 selection and subsequent ubiquitin charging (E2~ubiquitin) can be listed as the fundamental properties for the ubiquitin E1. In the *Saccharomyces cerevisiae* Uba1 structure, a long flexible linker (called ‘crossover loop’) that connects the active adenylation domain with

the catalytic cysteine domain interacts with residue Arg72 on the C-terminal tail of ubiquitin. This residue acts as the crucial determinant of Ubl discrimination by their E1s (Ala and Glu/Gln are present in the corresponding positions of Ubls NEDD8 and the SUMO family respectively) (Lee and Schindelin, 2008, Whitby et al., 1998). In addition, a conserved four-stranded β sheet within the active adenylation domain recognizes the canonical hydrophobic patch of ubiquitin (described in section 1.3). While the UFD confers E2 recognition properties, further structural and biochemical studies are required for deeper understanding of the multiple productive E2 interactions enabled by the ubiquitin E1 (Lee and Schindelin, 2008).

1.3 Ubiquitin: patches and signals

Structurally, ubiquitin (Ub) and ubiquitin-like (Ubl) proteins share the β-grasp ubiquitin superfold (accession number IPR000626) despite low sequence conservation. The 'ubiquitons' share a compact globular structure consisting of a five-stranded β-sheet, a short 3_{10} helix, a 3.5-turn α-helix and a flexible tail on the C-terminus (Figure 3) (Mayer et al., 1998, Vijay-Kumar et al., 1987, Vijay-Kumar et al., 1985).

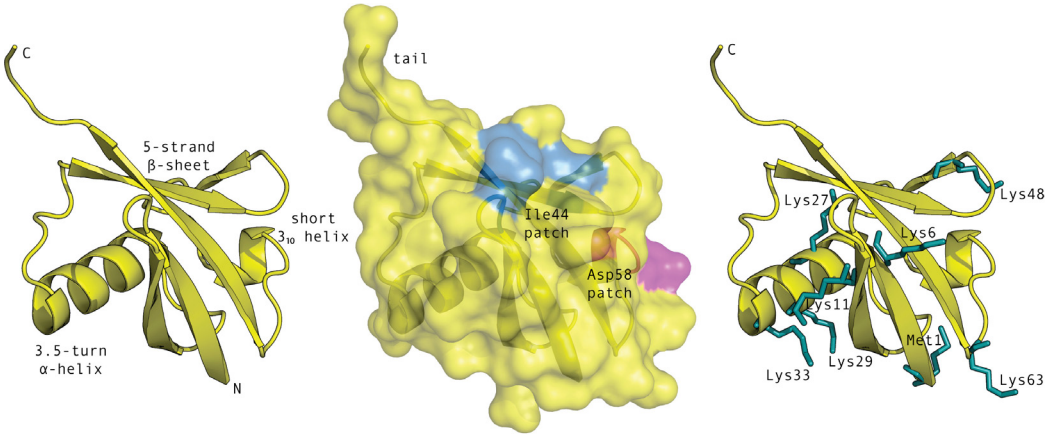

Figure 3: Ubiquitin – Structure, patches and acceptors. Structural features of the β grasp fold in ubiquitin (left) (PDB 1UBQ) alongside a surface representation of the functional patches (hydrophobic (Ile44, blue) patch, acidic (Asp58, pink) patch and the carboxy terminal tail (Arg72-Gly76)) supported by the fold (middle). Ubiquitin ligation occurs through its carboxy terminus, however modification on ubiquitin occurs at any of the seven lysines as well on the amino terminus (right). Structure figures were generated using PyMOL (Schrodinger, 2010).

Functionally important surfaces and regions on the protein include the solvent exposed hydrophobic patch (Leu8, Ile44, Val70 with an extended region surrounding Phe4), an acidic patch (residues surrounding Asp58) and the flexible tail (Leu73, Arg74, Gly75 and Gly76) (Figure 3) (Sloper-Mould et al., 2001, Raiborg et al., 2006).

While ubiquitination entails the ligation of ubiquitin C-terminus onto the target lysine/amino terminus, a chain can be initiated from any of the internal seven lysines within ubiquitin (Lys (x) -linked chains where x can be 6, 11, 27, 29, 33, 48 or 63) or the amino terminus (linear ubiquitin chains). However, non-canonical ubiquitination (on Cys, Ser and Thr acceptors) by viral E3 ligases using cellular E2s have been reported (Cadwell and Coscoy, 2005, Wang et al., 2007, Wang et al., 2009). Consequently, ubiquitin offers a versatile surface for facilitating interactions and in addition is capable of supporting distinct polyubiquitin based signals. Polyubiquitination can be either homotypic (lysine specific and linear linkages) or heterotypic (mixed and branched linkages) and play decisive roles in several cellular pathways (Figure 4A and recently reviewed here (Komander, 2009)).

Monoubiquitination and multi monoubiquitination regulate several cellular pathways including receptor trafficking, DNA repair and transcription regulation (Polo et al., 2003, Ulrich and Walden, 2010). Lys48- linked polyubiquitination is the canonical signal for proteasomal degradation of substrates (Chau et al., 1989), however examples of mono- and Lys11-, Lys63-linked poly-ubiquitinated substrates degraded by the 26S proteasome have also been presented (reviewed in (Finley, 2009)). Cellular functions of Lys63-linked polyubiquitin chain are well established in signalling pathways and DNA damage response pathways, however recent reports have revealed roles for monoubiquitinated and Lys63-linked polyubiquitinated signals in autophagy (reviewed in (Chin et al., 2010, Kirkin et al., 2009)). Structural features of linear (PDB 2W9N) (Komander et al., 2009b), Lys48- (PDB 1AAR) (Cook et al., 1992) and Lys63- (PDB 2ZNV) (Sato et al., 2008) linked diubiquitin chains and more

recently, Lys11- (PDB 2XEW) (Bremm et al., 2010) and Lys6- (PDB 2XK5) linked diubiquitin chains have been characterized.

Structural insights into ubiquitin chain conformations have been vital in understanding the diverse physiological responses they generate. Extended chain conformations are observed in linear and Lys63- linked chains and similar

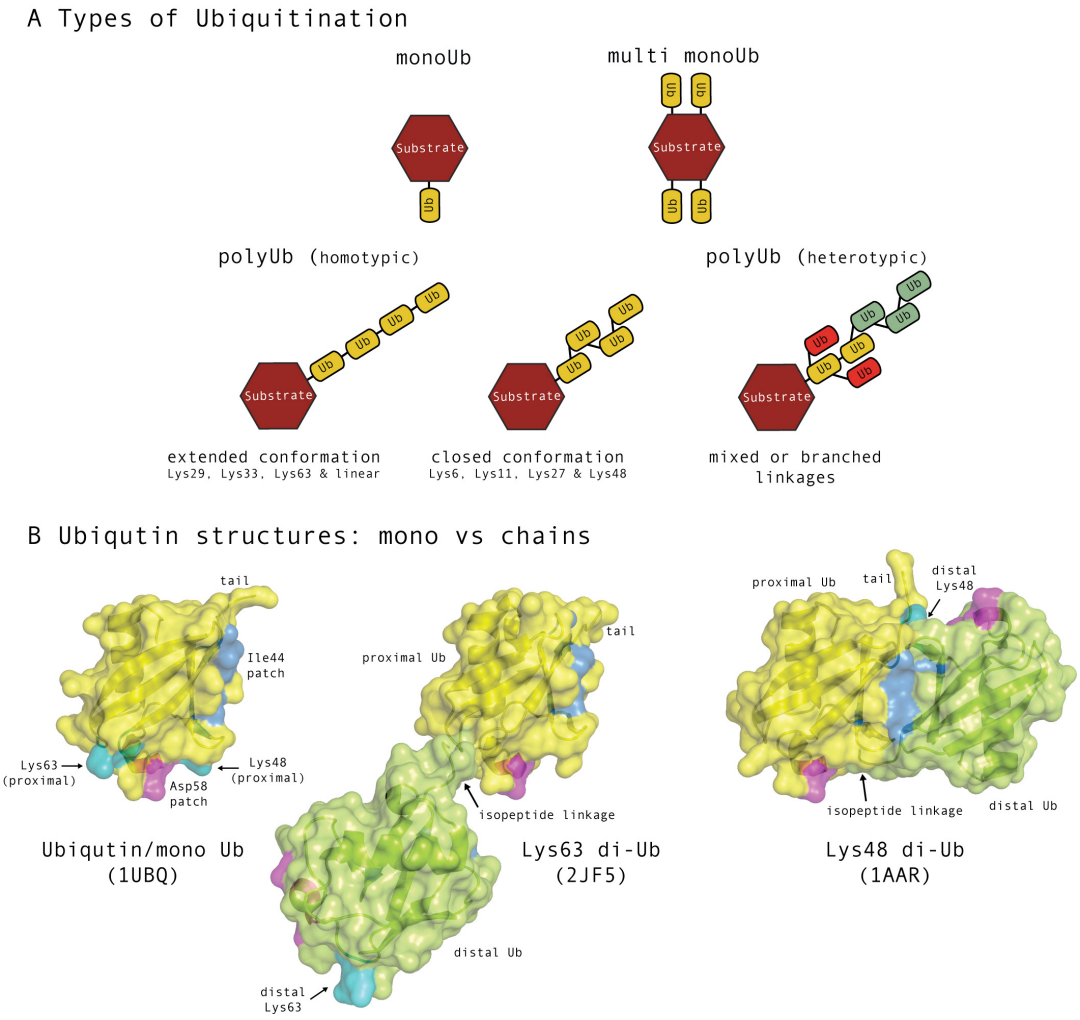

Figure 4: Diversity of Ubiquitin Signals. A. Classification of ubiquitin signals can be based on number (mono/multimono/poly), structure (extended/closed) and composition (homotypic/heterotypic). Ubiquitin chains adopt extended (Lys29/33/63- or linear linkages) or closed conformations (Lys6/11/27/48- linkages) depending on the linkage type. Homotypic ubiquitination refers to polyubiquitination of a single linkage type. In contrast heterotypic refers to either mixed polyubiquitination where two or more linkages occur (yellow and green) or branched polyubiquitination where two or more ubiquitins are linked to different lysines of a single ubiquitin (reds to yellow). **B.** Surface representations of ubiquitin (PDB 1UBQ, left), Lys63 linked di-ubiquitin (PDB 2JF5, middle) and Lys48 linked di-ubiquitin (PDB 1AAR, right) illustrating the functional patches as well as the extended (Lys63 di-Ub) or closed (Lys48 di-Ub) conformations adopted by ubiquitin chains. Proximal and distal ubiquitin moieties in di-ubiquitin structures are coloured yellow and green respectively. Residues Lys48 and Lys63 that support isopeptide linkages with C-terminus of subsequent ubiquitin moieties are coloured cyan ('proximal' Lys48 and Lys63 on the left, distal Lys63 in middle and distal Lys48 on the right). Structure figures were generated using PyMOL (Schrodinger, 2010).

conformations expected in Lys29- and Lys 33- linked structures (Figure 4B) (Fushman and Walker, 2010).

1.4 Ubiquitin: patches and receptors

The hydrophobic patch, regardless of the signal type, is the noncovalent recognition patch for majority of signal receptors or Ubiquitin Binding Domains (UBDs) contained in several proteins (reviewed in (Dikic et al., 2009) and (Hurley et al., 2006)). Thus, substrates bear the ubiquitin signal (mono, multiple mono or polyubiquitination) that is discriminated by various UBD-bearing proteins facilitating downstream transduction of the signals. UBDs themselves are generally small (<100 residues, except the ubiquitin conjugation fold (UBC fold)) and nearly two-dozen have been structurally characterised showing some fold diversity (α-helical, zinc fingers (ZnF), plekstrin homology (PH) domains, UBC and other domains).

In recent years, a surge of structural and biophysical studies has provided the molecular details required to appreciate the multivalent signal-receptor (ubiquitin-UBD) interaction. For example, members of ubiquitin associated (UBA) α-helical UBDs include the UBA2 of human homolog of yeast *Rad23a* (hHR23A) having a selective preference for Lys48 linked polyubiquitin chains, while the UBA of Ubiquilin-1 shows little or no selective criterion in their ubiquitin (mono/chain) binding (Varadan et al., 2005, Zhang et al., 2008). UBDs generally display low binding affinities (100-500 μM) for the monoubiquitin moiety however, affinity can be enhanced through cooperation and avidity mechanisms that have bearing on their downstream events (Sims et al., 2009). Examples of avidity include the double-sided ubiquitin interaction motif (UIM) of Hepatocyte growth factor–Regulated tyrosine kinase Substrate (HRS) (PDB 2D3G) (Hirano et al., 2006, Ren and Hurley, 2010) that play a role in the degradation of internalized receptors in the Endosomal Sorting Complexes Required for Transport (ESCRT) pathway. Tandem UIMs of Receptor

Associated Protein 80 (RAP80) (PDB 3A1Q) (Sato et al., 2009, Sims and Cohen, 2009) binding the extended structure of Lys63-linked ubiquitin chains to initiate DNA repair pathway (Figure 5). UBD cooperation in *trans* is observed between the proteasomal subunits Regulatory Particle Non-ATPase (RPN) 10 (UIM) and 13 (PH domain) (PDB 2KDE and 2KDF) in selecting Lys48-linked chains to initiate substrate degradation (Zhang et al., 2009).

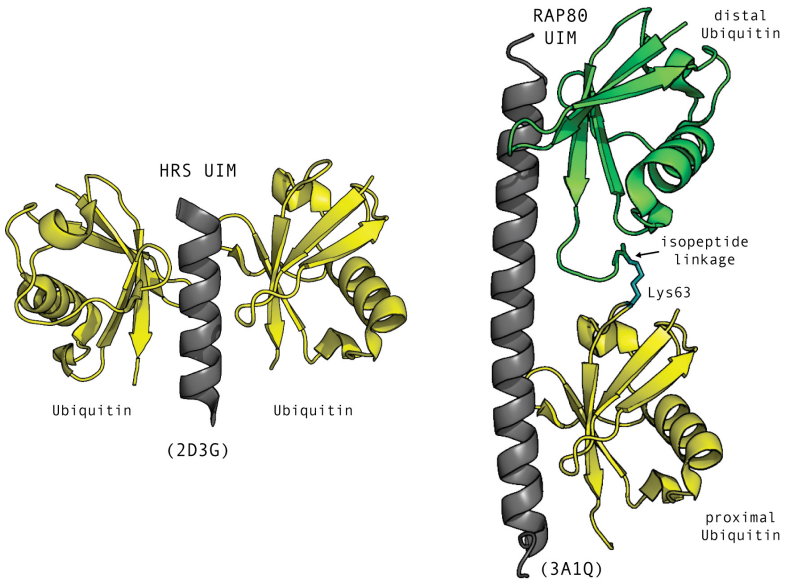

Figure 5: Avidity in Ubiquitin-Ubiquitin Binding Domain (UBD) interactions. Ubiquitin bound structures of double-sided ubiquitin interacting motif (UIM, on left) present in Hepatocyte growth factor–Regulated tyrosine kinase Substrate protein (HRS, PDB 2D3G) and tandem UIM (on right) present in Receptor Associated Protein 80 (RAP80, PDB 3A1Q) illustrate how UBDs enhance binding affinities of non-covalent interactions with ubiquitin. The double-sided HRS UIM presents two interaction surfaces on opposite sides of the helical UBD, each of which binds the hydrophobic patch of ubiquitin. The resulting combined affinity is 2.5-3 fold greater than the individual affinity (Hirano et al., 2006). The extended helical UBD of RAP80 presents two tandem UIMs that exhibit greater affinity and preference for the extended conformation of Lys63-linked ubiquitin chains over monoubiquitin and Lys48-linked (closed conformation) ubiquitin chains (Sato et al., 2009). Structure figures were generated using PyMOL (Schrodinger, 2010).

The Ub/Ubl - UBD interactions have also been observed to influence substrate ubiquitination as described in the case of 'coupled monoubiquitination' (Haglund and Stenmark, 2006). In this event, the interactions between substrate UBD and the E3 ligase (ubiquitinated or Ubl bearing) lead to ubiquitination of the substrate a different site. Subsequently, intramolecular interaction between UBD and ligated ubiquitin could occlude binding of Ub/Ubl bearing E3 or conceal acceptor sites on the ligated Ub, thereby inhibiting successive ubiquitination. The phenomenon has been observed with monoubiquitination of

Epidermal growth factor receptor substrate 15 (EPS15) by E3 ligases, Parkin and Neural precursor cell expressed developmentally down-regulated protein 4 (NEDD4) (Fallon et al., 2006, Woelk et al., 2006). UIMs on EPS15 interact with Parkin's Ubiquitin like Domain (UblD) as well as monoubiquitinated NEDD4 contributing to coupled monoubiquitination (Figure 6).

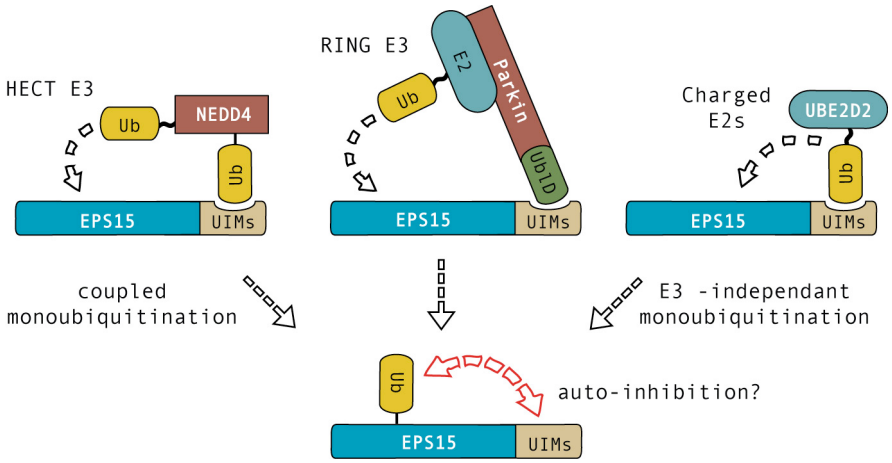

Figure 6: Mechanisms of Ubiquitin Binding Domain (UBD) based ubiquitination. Coupled monoubiquitination is a result of interactions between certain Ubiquitin (Ub)/Ubiquitin-like (Ubl) moieties and UBDs present on the carboxy terminus of Epidermal growth factor receptor substrate 15 (EPS15). Interactions between EPS15 Ubiquitin Interacting Motifs (UIMs, a class of helical UBDs) and ubiquitinated HECT E3 ligase Neural precursor cell expressed developmentally down-regulated protein 4 (NEDD4, top left) or the integral Ubiquitin-like Domain (UblD) of RING E3 ligase Parkin (top centre) leads to coupled monoubiquitination of EPS15. Alternatively, the UIM can interact with the ubiquitin moiety of UBE2D2/UbcH5B~ubiquitin thioester conjugate (top right), resulting in an E3-independant *cis* monoubiquitination event. Subsequently, intramolecular interactions between UBD and ligated ubiquitin (double headed red arrow, bottom) could inhibit repeat events (bottom centre). Figure adapted from (Haglund and Stenmark, 2006). (HECT is Homologous to the E6-AP Carboxyl Terminus and RING is Really Interesting New Gene.)

Interestingly, coupled monoubiquitination can also occur in the absence of an E3, with substrate UBDs binding the ubiquitin charged/loaded E2s and the latter catalysing ubiquitin ligation on the substrate (Hoeller et al., 2006). In addition, UBDs on E2s facilitate polyubiquitin chain building mechanisms, discussed in section 1.5. Taken together, ubiquitin provides a fertile landscape for generating a variety of post-translational modifications and multivalent ubiquitin-UBD interactions enable downstream transmission of these signals.

1.5 E2s: signal-conjugating enzymes

Over three-dozen ubiquitin conjugating enzymes/ubiquitin E2s have been identified in humans all sharing a core ubiquitin conjugation (UBC) fold. The topology of the core domain consists of an N-terminal helix, followed by a four-stranded β-meander (anti-parallel β-sheet), tethered with a 'flap-like' structure comprised of two extended elements in a β-hairpin fold, and finally one to two α-helices at the C-terminus. The catalytic cysteine is located in a shallow groove on the 'flap-like' structure and functionally supported by a conserved 'chain of interacting residues' (CIR - asparagine and histidine and an aromatic residue). Other conserved residues include the hydrophobic pairing of a Pro-Trp/Met that helps tether the 'flap-like' structure to the β-meander (Figure 7) (Burroughs et al., 2008).

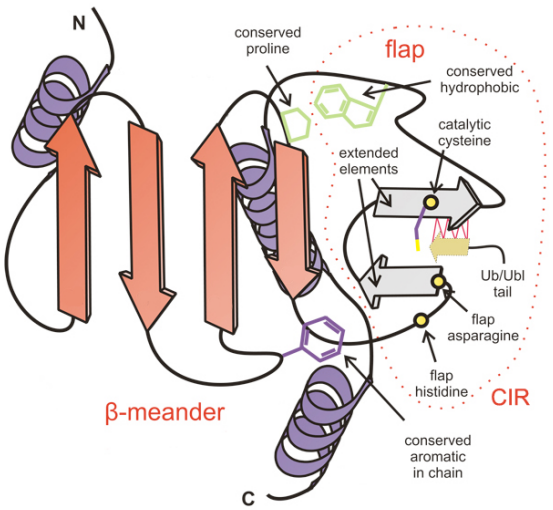

Figure 7: E2 Topology. Conserved structural features of the ubiquitin conjugation (UBC) fold include the β-meander, 'chain of interacting residues' (CIR) and a 'flap-like' element bearing the catalytic cysteine and interactions with ubiquitin tail. Adapted from (Burroughs et al., 2008)

A bioinformatics-driven nomenclature for the various mammalian E2s using the UBE2Xn syntax (X and n denote a letter and number respectively) has been suggested recently (Ye and Rape, 2009). Further structural sub-categorization is based on extensions around the core domain; Class I consists of just the core domain, N and C terminal extensions make up Classes II and III respectively, while Class IV E2s have extensions on both ends (Hofmann and Pickart, 2001, Winn et al., 2004). Proteins that contain the UBC fold but lack the catalytic cysteine are known as E2 variants and have critical roles in chain formations (UBE2V1, 2 and 3 (UEV1, 2 and 3)). A selective list of the mammalian E2s, specialized chain products and other associated features have been compiled in Table 1.

Gene	Other names	Class	Salient roles	Function
UBE2D2	UbcH5B, E2-17K2	I		
UBE2C	UBCX, UbcH10	II	Lys11-linked	Cell cycle regulation
UBE2S	E2-EPF5, E2-24K	III	Lys11-linked	Cell cycle regulation
UBE2R1	Cdc34, Ubc3, E2-32K	III	Lys48-linked	Cell cycle regulation
UBE2K	Ubc1, HIP-2, E2-25K	III	Lys48-linked	Protein quality control
UBE2T	HSPC150	III	Monoubiquitination	DNA repair
UBE2Z	Use1, HOYS7	IV	Functions with Uba6 (E1)	
UBE2G2	Ubc7	I	Lys48-linked, non-lysine sites	Endoplasmic Reticulum (ER) quality control
UBE2J2	NCUBE2, Ubc6	III	Lysine and non-lysine sites, transmembrane domain	
UBE2N	Ubc13, BLU	I	Lys63-linked as heterodimer with UBE2V1/V2	NFκB signaling, DNA repair, Aggresome formation, Macroautophagy
UBE2V1	UEV-1	II	E2 variant, Lys63-linked as heterodimer with UBE2N	
UBE2V2	MMS2, UEV2	I		
UBE2L3	UbcH7, E2-F1	I		Protein quality control
UBE2L6	UbcH8, RIG-B	I	Ubiquitin and ISG15 conjugation	Interferon signaling
UBE2I	Ubc9	I	SUMO conjugation	Cell cycle regulation
UBE2F	NCE2	I	NEDD8 conjugation	Regulation of SCF

Table 1: Diversity of Mammalian E2s. Select list of Mammalian E2s and their associated properties. Adapted from (Ye and Rape, 2009). E2s known to function with Parkin are highlighted (brown).

Principal binding patches on E2s are those establishing E1-E2 and E2-E3 interactions. Restructuring of the ubiquitin E1 during ubiquitin activation reveals the UFD region for E2 interaction via conserved residues in N-terminal helix (Lee and Schindelin, 2008, Huang et al., 2007, Lois and Lima, 2005). The ubiquitin tail packs between the extended elements that bear the catalytic cysteine and asparagine when conjugated to the E2 (Figure 7) (Eddins et al., 2006, Hamilton et al., 2001, Reverter and Lima, 2005, Yunus and Lima, 2006). The CIR (Figure 7) has been suggested to affect deprotonation of the target lysine (or free amino group) as a result facilitating a nucleophilic attack on the thioester (E2~ubiquitin). Concomitantly, CIR's Asn could stabilise the oxyanionic intermediate during isopeptide linkage (Wu et al., 2003, Yunus and

Lima, 2006). Conversely, molecular dynamics simulations propose the trajectory of the attacking amino group, rather than a general base (Asp), helps lower the pK_a, thus favouring its deprotonation and nucleophilic attack on the thioester bond (Hau et al., 2006). The mechanistic details of these events await further biochemical and structural studies.

The N-terminal helix along with two other loops (L1 – loop connecting strands 45 of the β-meander, L2 – the exit loop from the 'flap-like' structure leading to the first of the C-terminal helices) make up the generic E3 interaction surface. A combination of X-ray crystallography, Nuclear Magnetic Resonance (NMR) spectroscopy and interaction mutagenesis experiments have revealed the details and variations of the E2-E3 interface ((Christensen and Klevit, 2009, van Wijk and Timmers, 2010) and reviewed recently in (Ye and Rape, 2009, Deshaies and Joazeiro, 2009)). Despite the distal nature of the E2-E3 interface, E3 binding enhances the rate of ubiquitin offloading/discharge with conserved internal residues are suggested to take part in allosteric transmission mechanics (Figure 8) (Eletr and Kuhlman, 2007, Huang et al., 2009, Ozkan et al., 2005). The E2-RING interface of UBE2L3 (UbcH7) – Casitas B-lineage lymphoma proto-oncogene (c-Cbl) (Zheng et al., 2000), UBE2N (Ubc13) – Tumor Necrosis Factor (TNF) receptor-associated factor 6 (TRAF6) (Yin et al., 2009) and UBE2D2 (UbcH5B) – Inhibitor of Apoptosis protein 2 (cIAP2) (Mace et al., 2008) are depicted in Figure 8.

Examples of sequence elements that co-operate with RING domains in allosteric activation of the E2~ubiquitin thioester have also been presented in context of UBE2G2/Ubc7, an E2 associated with the endoplasmic reticulum (ER). The Ubc7p binding region (U7BR) and G2 Binding Region (G2BR) are *cis* sequence elements to RING domains of ER anchored Conjugation to ER degradation protein-1 (Cue1p) and Autocrine Motility Factor Receptor (AMFR/gp78) E3 ligases respectively. These elements bind UBE2G2 in tandem with the RING domains at a site distinct from the 'canonical' E2-E3 interface and have been observed to enhance UBE2G2 activation as well as E3

mediated substrate ubiquitination (Bazirgan and Hampton, 2008, Biederer et al., 1997, Chen et al., 2006, Das et al., 2009).

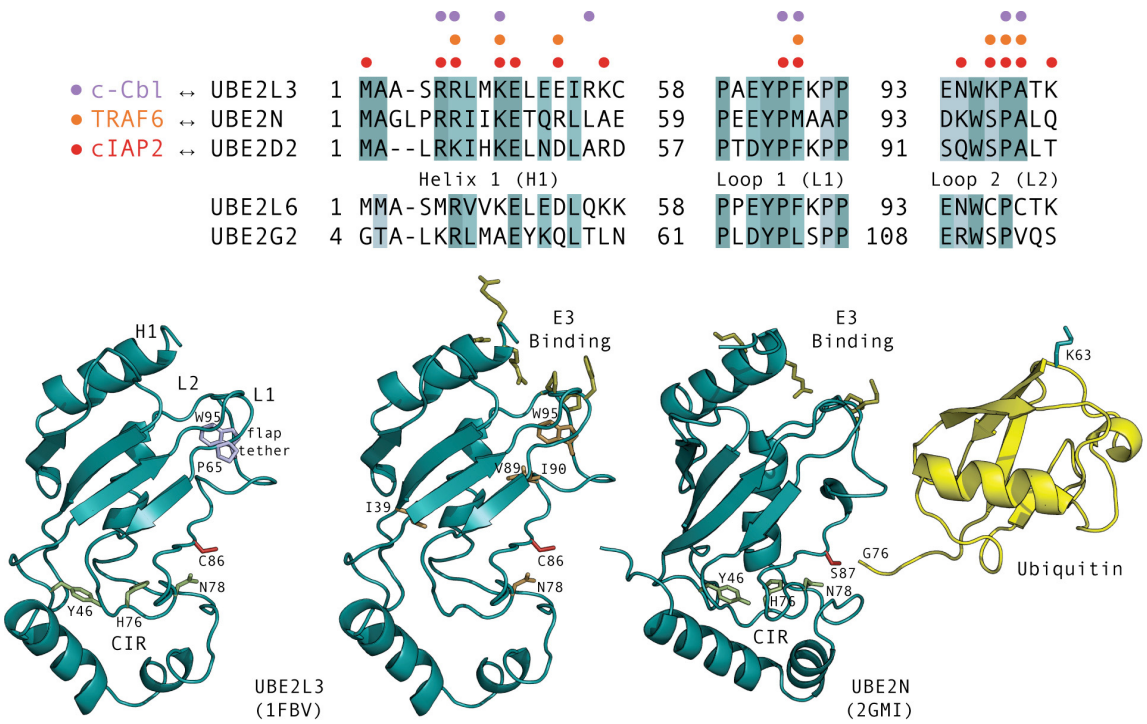

Figure 8: E2 enzyme dynamics. Structural efforts of RING-E2 interactions have revealed three regions on the E2 critical for the interface; helix (H) 1, loops (L) 1 and 2 (loop numbers do not correspond to E2 topology). Multiple sequence alignments (top, generated using ClustalW (Chenna et al., 2003)) depict RING binding regions of select E2s with their interacting residues indicated above with coloured dots; purple, orange and red dots for UBE2L3/UbcH7 - c-Cbl, UBE2N/Ubc13 - TRAF6 and UBE2D2/UbcH5B - cIAP2 interactions respectively. c-Cbl is Casitas B-lineage lymphoma proto-oncogene protein, TRAF6 is Tumor Necrosis Factor (TNF) receptor-associated factor 6, cIAP2 is Inhibitor of Apoptosis protein 2 and RING is Really Interesting New Gene domain. Also aligned are corresponding regions of two other E2s (UBE2L6/UbcH8 and UBE2G2/Ubc7) that function with Parkin. Conserved residues (blue and red sticks) and CIR (green sticks) and the location of RING binding helix 1, loop 1 and 2 are indicated on the UBE2L3/UbcH7 structure (PDB 1FBV, left). Also shown on UBE2L3/UbcH7 structure (PDB 1FBV, middle) are residues that interact with c-Cbl RING and those predicted to be involved in RING mediated allosteric activation of E2 (dark olive and brown sticks respectively) (Ozkan et al., 2005, Zheng et al., 2000). E3 binding residues and the CIR are depicted as sticks (dark olive and green respectively) on UBE2N/Ubc13 (PDB 2GMI), which is covalently linked to ubiquitin via an ester linkage (Ser87 — Gly76, right). Catalytic cysteine (Cys86) of UBE2L3/UbcH7 (left and middle) and the cysteine to serine mutant (Ser87) used to generate the UBE2N/Ubc13 — ubiquitin ester conjugate are shown as red sticks. Structures were generated using PyMOL (Schrodinger, 2010).

As the regions on the UBC fold that support E1 and E3 interactions are partially overlapping (helix1 being the shared interface), E1-E2 and E2-E3 binding events have been observed to be mutually exclusive (Eletr et al., 2005). Furthermore, the transient nature of E2-E3 interactions allow for E2 uncoupling,

ubiquitin recharging of the E2 (via E1) and subsequent E2 reattachment/switching as a strategy to sustain substrate polyubiquitination (Rodrigo-Brenni and Morgan, 2007, Christensen et al., 2007, Windheim et al., 2008, Parker and Ulrich, 2009, Andersen et al., 2005). E2 switching (where an E3 uses two distinct E2s to ubiquitinate a single substrate) enhances the processivity of ubiquitination; defined as the number of ubiquitin moieties ligated on the substrate during a single enzymatic encounter with the E3. In certain scenarios, substrate polyubiquitination can be delineated as a concert with two distinct acts; ubiquitin chain initiation followed by elongation, with different E2s operating in each act.

The pliable UBE2D (UbcH5) family have been reported as the chain initiating partners to the linkage specific E2s. Conversely, numerous E2s have been observed to specialise in linkage specific chain synthesis; UBE2N/UBE2V1/2 (Ubc13/UEV1) for Lys63-linked (Eddins et al., 2006, McKenna et al., 2003, Hau et al., 2006), Lys11-linked by UBE2S (E2-24K) and UBE2C (UbcH10) (Williamson et al., 2009, Jin et al., 2008, Wu et al., 2010), Lys48-linked chains by UBE2K (Ubc1/E2-25K) (Haldeman et al., 1997), UBE2G2 (Ubc7) (Li et al., 2007, Ravid and Hochstrasser, 2007) and UBE2R1 (Cdc34) (Gazdoiu et al., 2007, Petroski and Deshaies, 2005b). Mechanisms of linkage specific chain formation are suggested to involve non-covalent UBC-ubiquitin interactions best demonstrated through structural studies on the heterodimeric UBE2N/UBE2V1/2 (Ubc13/UEV1/2) complexes (Eddins et al., 2006, Hau et al., 2006). Non-covalent ubiquitin interactions and E2 self-association are crucial for chain processivity by UBE2D (UbcH5B), an E2 that lacks intrinsic ability to form linkage specific polyubiquitin chains (Brzovic et al., 2006, Christensen et al., 2007).

An alternative strategy employed to enhance processivity is observed with UBE2G2 (Ubc7), which can preassemble Lys48 linked chains and transfer them *en masse* onto the substrate (Li et al., 2007, Ravid and Hochstrasser, 2007). Interestingly, presence of certain E3s have been observed to enhance the

preassembly of Lys63- and Lys48- linked polyubiquitin chains *in vitro* (Petroski et al., 2007, Li et al., 2007).

Other models for linkage specific ubiquitin chain formation have been described in the context of HECT E3 ligases (refer (Hochstrasser, 2006) for an elegant discussion). An 'indexation model' has been proposed to explain mechanisms involved in tetra-ubiquitin chain synthesis by WW domain-containing protein 1 (WWP1) HECT E3 ligase (Verdecia et al., 2003) and Lys48 linked di-ubiquitin chain synthesis (*in vitro)* by Human papillomavirus E6-associated protein (E6-AP) HECT E3 ligase (Wang and Pickart, 2005). In this model, the catalytic cysteine located on the flexible lobe C-terminal lobe (C-lobe) bears the HECT E3~ubiquitin thioester conjugate. Furthermore, the C-lobe positions the ubiquitin such that Lys48 attacks the E2~ubiquitin thioester (bound to the N-terminal lobe/N-lobe via E2- HECT E3 interactions) resulting in a Lys48 linked di-ubiquitin chain moiety on the HECT active site (HECT E3~ubiquitin + E2~ubiquitin → HECT E3~di-ubiquitin) (Wang and Pickart, 2005). Inherent flexibility of the C-lobe allows the 'unfurling' of the HECT permitting repeat events (chain extension) until a Lys48 linked tetra-ubiquitin chain is formed. Subsequently, a target lysine attacks the HECT E3~tetra-ubiqutin thioester resulting polyubiquitination of the substrate (*en bloc*) (Verdecia et al., 2003).

An alternative 'sequential addition' model has also been proposed with respect to the Reverses SPT-phenotype protein 5 (RSP5) HECT E3 ligase (NEDD4L homolog in *S. cerevisiae*) wherein the ubiquitin is sequentially ligated onto the substrate (repeated cycles of E1~ubiquitin → E2~ubiquitin → E3~ubiquitin → Substrate-ubiquitin) (Kim and Huibregtse, 2009). In this scenario, the catalytic cysteine on the C-lobe positions the HECT E3~ubiquitin thioester to allow nucleophilic attack by Lys63 of the substrate bound ubiquitin or the distal end of the polyubiquitin chain. Taken together, substrate ubiquitination is a multi-faceted process involving ubiquitin, UBDs and various E2s with E3s at the helm.

1.6 RING E3 ligases: conductors of ubiquitin signalling

As indicated earlier, E3 ligases are broadly classified as HECT domain and RING domain E3 ligases. HECT E3s mediate an additional step in the ubiquitin pathway where the ubiquitin moiety is transferred from the E2 onto a conserved cysteine in the HECT domain through a second transthioesterification reaction (Scheffner et al., 1995). The majority of the E3 ligase family contain a RING domain and act as a molecular scaffold enzymes on which the substrate and E2~ubiquitin interact in a catalytically productive manner (Pickart, 2001). Mechanisms of HECT E3 ligases and their role in cellular pathways have been reviewed elsewhere (Bernassola et al., 2008, Scheffner and Staub, 2007). The focus of this section will be on RING E3 ligases primarily as Parkin, the subject of this thesis, is a member of this family. Parkin bears two RING domains flanking an In-Between RING (IBR) domain and is the archetypal member of the RBR/TRIAD; the second largest RING subfamily in humans (Marin et al., 2004). RING motifs, discovered in 1991, were originally considered to be a novel DNA-binding zinc finger motif (Freemont et al., 1991). The association with ubiquitination and inherent E3 ligase activity however, followed nearly a decade later (reviewed in (Joazeiro and Weissman, 2000)). Fortuitously, the discovery of Parkin and association with E3 ligase activity coincided with these reports (Kitada et al., 1998, Shimura et al., 2000).

RING 'finger' domains (Figure 9) are globular domains with a cysteine-rich canonical sequence (InterPro IPR001841) that coordinate two zinc atoms in a unique cross-brace arrangement (Freemont et al., 1991, Barlow et al., 1994, Borden et al., 1995). Numerous variations have been reported including sequence variations (Cys/His swapping or Asp in lieu of Cys) fold variations (Lin11, Isl-1 and Mec-3 (LIM) domains and Plant Homeo Domains (PHDs)) and structural relations (B-box and U-box domains) (reviewed in (Borden and Freemont, 1996), (Aravind and Koonin, 2000, Tao et al., 2008)) (Figure 9). While the majority are associated with ubiquitination, Zn^{2+} coordinating PHDs lack E3 ligase activity (Aravind et al., 2003) and conversely U-box domains do

not coordinate Zn^{2+} however display ubiquitin ligase activity (Aravind and Koonin, 2000).

Furthermore, RING bearing proteins Bard1, Bmi1 and MdmX exhibit ligase activity exclusively through heterodimeric complexes (Brca1/Bard1 (Hashizume et al., 2001), Ring1b/Bmi1 (Wang et al., 2004) and Mdm2/Mdmx (Linares et al., 2003)). An interesting example of heterodimeric RING complex is the 600 kDa linear ubiquitin chain assembly complex (LUBAC) consisting of the haem-oxidized IRP2 ubiquitin ligase-1 (HOIL-1) isoform HOIL-1L and HOIL-1L Interacting Protein (HOIP) (Kirisako et al., 2006). The LUBAC complex has been the only E3 ligase reported to orchestrate the synthesis of linear polyubiquitin chains with a range of E2s, however, the mechanistic details of these events are awaited (refer (Nagy and Dikic, 2010) for proposed theories).

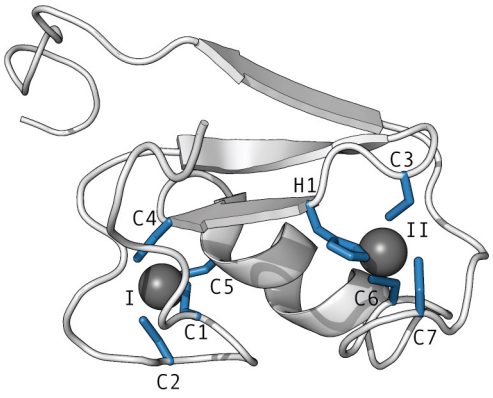

1CHC

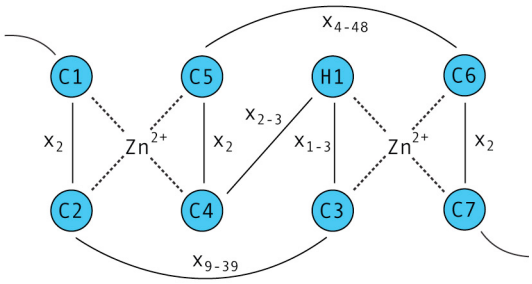

Canonical RING

RING-HC	Cys-x_2-Cys-$x_{(9-39)}$-Cys-$x_{(1-3)}$-His-$x_{(2-3)}$-Cys-x_2-Cys-$x_{(4-48)}$-Cys-x_2-Cys
RING-H2	Cys-x_2-Cys-$x_{(9-39)}$-Cys-$x_{(1-3)}$-His-$x_{(2-3)}$-His-x_2-Cys-$x_{(4-48)}$-Cys-x_2-Cys
$C_2H_2C_4$(Mdm2)	Cys-x_2-Cys-x_{10}-His-x_4-His-x_3-Cys-x_2-Cys-x_{10}-Cys-x_2-Cys
RBQ-1	Cys-x_2-Cys-x_{11}-Cys-x_2-Asn-x_2-Cys-x_2-Cys-x_{12}-Cys-x_2-Cys
RBX1	Cys-x_2-Cys-x_{29}-Cys-x_1-His-x_2-Cys-x_2-Cys-x_{10}-Cys-x_2-Asp
LIM	Cys-x_2-Cys-$x_{(16-23)}$-His-x_2-Cys-x_2-Cys-x_2-Cys-$x_{(16-23)}$-Cys-x_2-Cys
PHD	Cys-x_2-Cys-$x_{(8-21)}$-Cys-$x_{(2-4)}$-Cys-$x_{(4-5)}$-His-x_2-Cys-$x_{(12-46)}$-Cys-x_2-Cys
C_4H_4	Cys-x_2-Cys-x_{13}-Cys-x_1-Cys-x_4-Cys-x_2-Cys-x_{11}-Cys-x_2-Cys
PARKIN → RING1	Cys-x_2-Cys-x_{11}-Cys-x_3-His-x_2-Cys-x_2-Cys-x_{25}-Cys-x_3-Cys
→ RING2	Cys-x_2-Cys-x_9-Cys-x_1-His-x_2-Cys-x_4-Cys-x_4-Cys-x_2-Cys

Figure 9: RING finger domains. Canonical sequences of RING and RING-like variants along with a cartoon representation of the Vmw110 RING domain determined by Nuclear Magnetic Resonance (NMR) spectroscopy (PDB 1CHC) showing cross-brace arrangement. Sequence organisation of the two RING domains of Parkin is also shown. Domain names: RING is Really Interesting New Gene, Mdm2 is Double minute 2 protein, RBQ-1 is Retinoblastoma-Binding Q protein-1, RBX1 is RING-box protein 1, LIM is named after three proteins Lin11, Isl-1 and Mec-3 where it was first found and PHDs is Plant Homeo Domains. 'C' and 'H' are symbols for residues cysteine (Cys) and histidine (His) respectively, while 'x' indicates any residue. Structure figures were generated using PyMOL (Schrodinger, 2010).

Functional homodimerisation is observed in several RING E3 ligases including c-Cbl (Kozlov et al., 2007, Peschard et al., 2007), TRAF6 (Yin et al., 2009), cIAP2 (Mace et al., 2008) as well as the C-terminus of Hsc70-interacting protein (CHIP), a U-box E3 ligase (Zhang et al., 2005). The asymmetric CHIP dimer obstructs a potential E2 binding while the cIAP2 dimer displays twin E2 binding site. Incidentally, the cIAP2 dimer interface requires a conserved aromatic residue located at -3 position from its C-terminus, a residue conserved in Parkin homologs as well (Schlehe et al., 2008). c-Cbl dimerises through a distal UBA domain while the TRAF6 shows an extensive dimer interface through N-terminal zinc fingers and together with the trimeric C-terminal region is suggested to form supramolecular assemblies (Yin et al., 2009).

RINGs can function as monomeric units, with substrate recognition and E2 recruiting elements borne on a single polypeptide chain. For example Fanconi anemia group protein L (FancL), a multi-domain E3 ligase, is responsible for the critical monoubiquitination of FancD2 as part of a DNA damage response pathway which is defective in Fanconi Anemia (FA) patients (Cole et al., 2010). Majority of the RINGs however function as part of multi-subunit complex; cullin-RING ubiquitin ligases (CRLs) (Refer (Deshaies and Joazeiro, 2009) Supplementary Table 1 therein for a comprehensive list of RING E3 ubiquitin ligases). CRLs comprise a modular architecture comprising of rigid central cullin module (CUL 1, 2, 3, 4A, 4B and 5 comprise the cullin family) that docks RING domains (Rbx1 or Rbx2) and associated E2s on a conserved C-terminal region. N-terminus of the cullin modules binds cullin ‘adaptors’ (for example, S-phase kinase-associated protein 1 (SKP1) and the Elongin BC complex) that further associate with numerous ‘substrate receptors’ (members of the F-box family and Suppressor of cytokine signalling (SOCS) box family respectively); the latter conferring substrate specificity to CRLs. (refer (Petroski and Deshaies, 2005a) for an overview of CRL assembly and E3 ligase properties).

Enzymatic properties of RING E3 ligases include substrate recognition, E2 activation and the concomitant ubiquitination of a target lysine on the substrate (Figure 10). Activation of E2s entails the binding RING E3 with E2~ubiquitin and concomitant thioester discharge of E2~ubiquitin. However, not all E2-E3 interactions result in E2 activation, as observed *in vitro* for the c-Cbl-UBE2L3 (UbcH7) (Huang et al., 2009) and Bard1/Brca1-UBE2L3 (UbcH7) (Brzovic et al., 2003) interactions. Detailed mechanisms of this 'activation' are not completely understood however, RING/U-box induced conformation changes within E2~ubiquitin conjugate could play a role in this event. Certain internal residues within the E2 that could play a role in allosteric activation mechanics have also been identified (Ozkan et al., 2005).

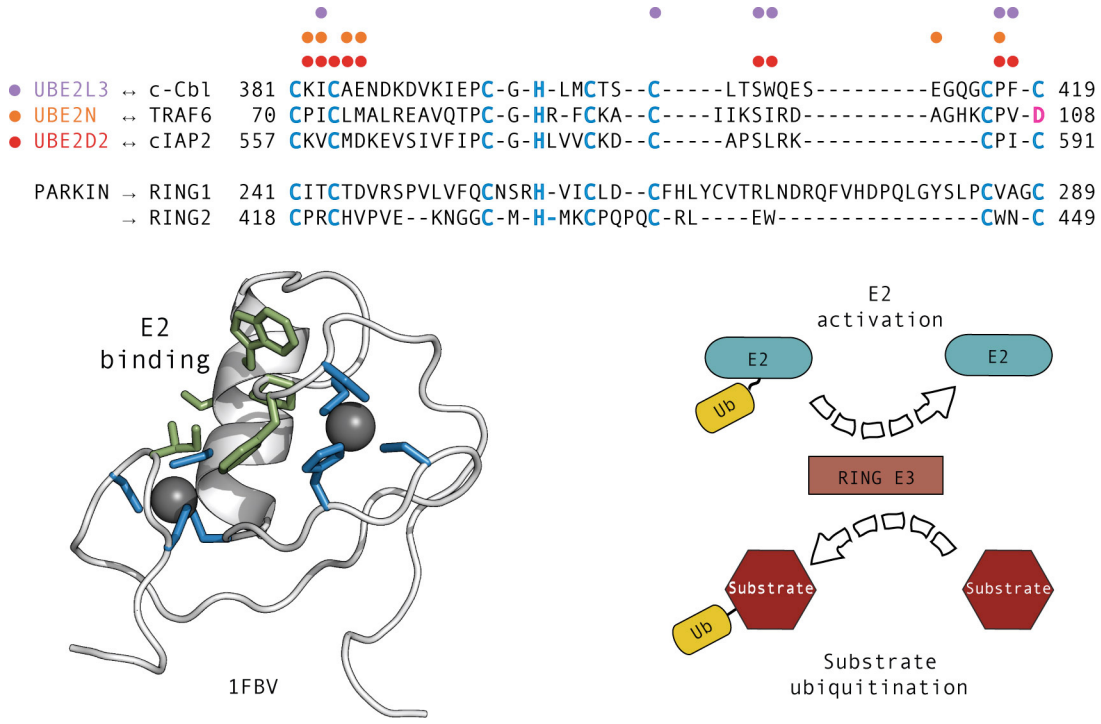

Figure 10: The RING-E2 interface. Multiple sequence alignments (top, generated using ClustalW (Chenna et al., 2003)) depict select RING domains with their E2 interacting residues indicated above with coloured dots; purple, orange and red dots for c-Cbl - UBE2L3/UbcH7, TRAF6 - UBE2N/Ubc13 and cIAP2 - UBE2D2/UbcH5B interactions respectively. c-Cbl is Casitas B-lineage lymphoma proto-oncogene protein, TRAF6 is Tumor Necrosis Factor (TNF) receptor-associated factor 6, cIAP2 is Inhibitor of Apoptosis protein 2 and RING is Really Interesting New Gene domain. Sequence alignments with the two RING domains of Parkin are also shown. Cartoon representation of c-Cbl RING domain (PDB 1FBV) with E2 interaction residues shown as green sticks and zinc co-ordinating residues in blue sticks (bottom left). Structure figures were generated using PyMOL (Schrodinger, 2010). The enzymatic properties of the RING E3 ligases enable E2 activation and concomitant substrate ubiquitination (black dashed arrows, bottom right).

Substrate recognition, the other catalytic property of RING E3 ligases is established through a variety of protein-protein interactions mediated either by internal domains present in monomeric RING E3 ligases (Cole et al., 2010) or through the numerous substrate receptors associated with CRL complexes (Petroski and Deshaies, 2005a). A consensus site for substrate ubiquitination was long considered being absent, however the discovery of a TEK box sequence element neighbouring the target lysine on substrates of the anaphase promoting complex/cyclosome (APC/C) E3 ligase has altered this perspective (Jin et al., 2008). The presence of flanking basic residues could also affect the site of ubiquitination by lowering the pK_a of the target lysine thereby facilitating a nucleophilic attack on the E2~ubiquitin thioester concluding in the ubiquitination of the former (Highbarger et al., 1996). Further mechanistic studies into E2~ubiquitin activation mechanics, target lysine selection and substrate ubiquitination for the numerous E3-substrate complexes identified are awaited.

In summary, substrate ubiquitination is a multifaceted process influenced by several factors including; intrinsic E2 activity (linkage specific E2s or others), E2 switching mechanisms (initiator/elongator), presence of UBDs on E2/E3/substrate (coupled monoubiquitination) and the monomeric/oligomeric state of E3/E2. Parkin, the focus of this study is a RING E3 ligase implicated in Parkinson's disease. The following sections present an overview of the disease state, the molecular players involved as well as the E3 ligase properties of Parkin.

1.7 Introduction to Parkinson's Disease

Parkinson's disease (PD) is a common neurological disorder that is both chronic and progressive and occurs due to loss of dopaminergic neurons in the *substantia nigra pars compacta* (SNc) (reviewed in (Cookson, 2005, Yang et al., 2009)). Loss of dopamine, a catecholamine neurotransmitter, contributes to the movement disorder: bradykinesia (slowness of movement), resting tremor, muscular rigidity and postural instability. Presence of Lewy Bodies (LB, microscopic protein deposits detected accurately only upon autopsy) and eosinophilic cytoplasmic inclusions rich in alpha-synuclein and ubiquitin in surviving neurons, along with loss of dopaminergic neurons, is the pathological definition of idiopathic PD.

Locus	Gene	Inheritance	Function	Reference
PARK1, 4	*SNCA*	AD	Synaptic protein, LB	(Polymeropoulos et al., 1997)
PARK2	*Parkin*	AR	Ubiquitin RING E3 ligase	(Kitada et al., 1998)
PARK3	*Unknown*	AD	Unknown	(Gasser et al., 1998)
PARK5	*UCH-L1**	AD	Ubiquitin C-terminal Hydrolase	(Leroy et al., 1998)
PARK6	*PINK1*	AR	Mitochondrial Kinase	(Valente et al., 2004)
PARK7	*DJ-1*	AR	Oxidative stress response	(Bonifati et al., 2003)
PARK8	*LRRK2*	AD	Kinase and GTPase	(Paisan-Ruiz et al., 2004, Zimprich et al., 2004)
PARK9	*ATP13A2*	AR	Possible ion pump	(Ramirez et al., 2006)
PARK10	*Unknown*	AD	Unknown	(Li et al., 2002)
PARK11	*GIGYF2**	AD	Tyrosine kinase receptor signalling	(Lautier et al., 2008)
PARK12	*Unknown*	X-Linked	Unknown	(Pankratz et al., 2002)
PARK13	*HTRA2*	AD	Mitochondrial Serine protease	(Strauss et al., 2005)
PARK14	*PLA2G6*	AR	Phospholipases A2	(Paisan-Ruiz et al., 2009)
PARK15	*FBXO7*	AR	SCF Ubiquitin E3 ligase complex subunit	(Di Fonzo et al., 2009, Shojaee et al., 2008)
PARK16	*Unknown*	Unknown	Unknown	(Satake et al., 2009)

Table 2: Parkinson's Disease (PD) genes identified in Familial PD. AD and AR stand for autosomal dominant and recessive mode of inheritance respectively. * There are conflicting reports weather UCHL-1 (Healy et al., 2006) and GIGFY2 (Nichols et al., 2009, Vilarino-Guell et al., 2009) are the PD genes corresponding to PARK 5 and PARK11 loci respectively.

The presence of parkinsonian movement disorder symptoms in the absence of LB is termed as 'Parkinsonisms'. PD affects approximately 1% of the population above the age of 50, with around 5% of the cases being rare familial forms with a younger age of onset (<45 years). Linkage and genotypic studies have identified several genes and loci associated with familial PD (Table 2). The following sections will introduce few of the molecular players of PD, describing genetic features, structural and functional features of the associated proteins, contribution to cellular pathway and how they contribute to the pathogenesis of the disease.

1.8 α-synuclein/SNCA: protein crowd dynamics

The first dominant PD gene to be identified was the *SNCA* "synuclein, alpha (non A4 component of amyloid precursor)" (Polymeropoulos et al., 1997). The gene, expressed in several tissues including neurons, is a member of the synuclein family and codes for a 14kDa protein that is functionally undefined. Primary structure analysis reveals a central hydrophobic stretch (~30 residues) sandwiched between hydrophilic regions, on the N-terminus by imperfect KTEGV repeats and a variable C-terminal region rich in glutamic acid and proline (Tobe et al., 1992). The protein adopts no distinct secondary structure in solution however associates, via N-terminal amphiphatic helices, with lipid bilayers especially at pre-synaptic terminals suggestive of a regulatory role in membrane stability (Figure 11A) (Jakes et al., 1994, Davidson et al., 1998).

Self-association is the defining feature of SNCA's role in neurodegenerative diseases. The hydrophobic domain, also called non-amyloid component (NAC), is responsible for SNCA aggregation (Ueda et al., 1993). The C-terminal acidic tail counters the aggregation potential as demonstrated by *in vitro* and *in vivo* experiments (Murray et al., 2003, Tofaris et al., 2006, Periquet et al., 2007). Aggregated SNCA form oligomers, pores and other intermediates that are stabilized upon further aggregation to form heavily insoluble β-pleated fibrils,

which are the major components of Lewy Bodies in PD and related synucleinopathies (Uversky, 2003, Spillantini et al., 1998).

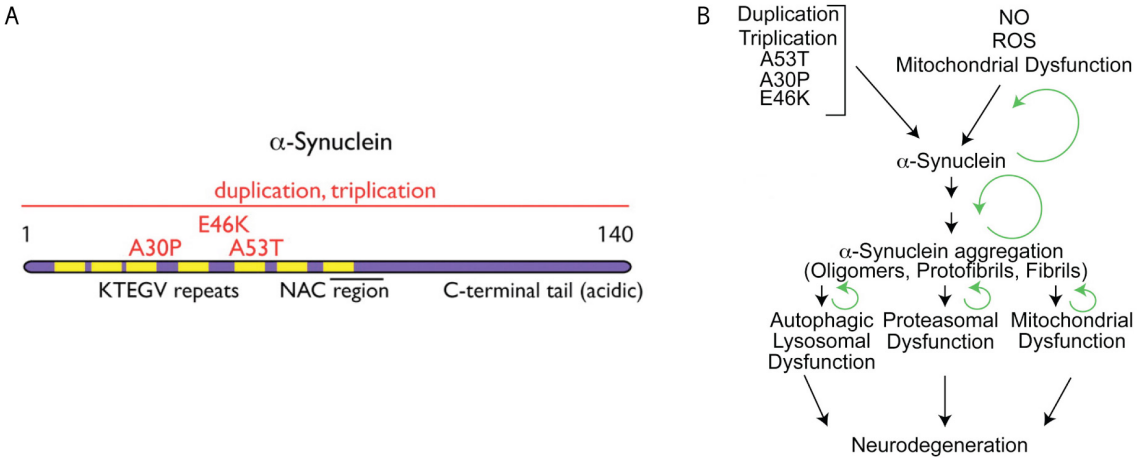

Figure 11: SNCA (α-synuclein) structure and pathways to neurotoxicity. A. Cartoon depicts primary sequence and associated regions of SNCA, with pathogenic mutations indicated above in red. The 14kDa protein bears imperfect KTEGV repeats, a central hydrophobic NAC (non amyloid component) and an acidic carboxy (C) terminal tail (not to scale). Figure adapted from (Cookson and Bandmann, 2010). **B.** Genetic defects (point mutations, duplications and triplications) as well as cellular stresses commonly found in sporadic Parkinson's Disease (PD) (nitric oxide (NO), reactive oxygen species (ROS) and mitochondrial dysfunction) enhance the accumulation and self-aggregation of SNCA thus promoting neurodegeneration. SNCA aggregates inhibit critical cellular pathways (ubiquitin proteasome and autophagic pathways) and are detrimental to the mitochondria thereby further feeding into the cycle (green circular arrows) of SNCA accumulation and self-aggregation. Figure adapted from (Dawson et al., 2010).

The intermediate oligomeric structures, termed protofibrils, are considered to enhance toxicity in dopaminergic neurons. Dopamine-SNCA adducts sustain these intermediates resulting in puncturing of synaptic membranes and vesicles (Lashuel et al., 2002, Xu et al., 2002, Conway et al., 2001). Familial PD mutations (A30P, E46K, A53T, WT duplication and triplication) affect the aggregative property of SNCA. While all mutations promote oligomerisation, the A30P mutation reduces both formation of insoluble fibrils and membrane association (Li et al., 2001, Fredenburg et al., 2007, Chartier-Harlin et al., 2004, Singleton et al., 2003). The viscous cytoplasmic environment (due to macromolecular crowding) along with enhanced SNCA expression observed in neurons renders them susceptible to downstream effects of SNCA mutations (Ueda et al., 1993, Uversky et al., 2002, Shtilerman et al., 2002). Taken together, aggregative toxicity has been attributed to a quantitative phenomenon, as phenotypes of SNCA point mutations are comparable to SNCA duplication

and triplication. Toxic SNCA aggregation, observed in sporadic PD, is enhanced by other factors; environmental agents (reviewed in (Di Monte, 2003), Ser129 phosphorylation (Fujiwara et al., 2002), tyrosine nitration (Giasson et al., 2000) and proteolysis of the C-terminal acidic tail (Kim et al., 2003b).

Pathogenic SNCA aggregates are detrimental to basic cellular pathways further contributing to neuronal toxicity (Figure 11B). The ubiquitin proteasome pathway (UPP) is impaired by direct interaction of A53T SNCA (monomeric and aggregated forms) with subunits of the 26S proteasome and probably contributing to a system overload. This induces endoplasmic reticulum (ER) stress, overloading of the unfolded protein response pathway (UPR), culminating in apoptosis. Cytoplasmic discharge of dopamine vesicles generates reactive oxygen species (ROS) that amplifies oxidative stress leading to mitochondrial dysfunction, release of cytochrome C and culminating in caspase-mediated cell-death (Volles and Lansbury, 2002, Tanaka et al., 2001, Snyder et al., 2003, Smith et al., 2005a). Furthermore, mutant SNCA blocks the chaperone-mediated autophagy (CMA) pathway, via direct binding to lysosomal membrane receptors, thereby antagonizing the protein quality control system that contributes to fatality via macroautophagy (Webb et al., 2003, Stefanis et al., 2001, Cuervo et al., 2004). In summary, SNCA contributes to pathogenesis of familial and sporadic PD primarily due to its aggregative property that disrupts critical physiological processes, many of which involve other PD genes.

1.9 PINK1: Mitochondrial homeostatic kinase

Initially identified in a PTEN (Phosphatase and tensin homologue) activated expression profile screen, PTEN Induced putative Kinase-1 or PINK1 was subsequently associated with the autosomal recessive PARK6 locus (Unoki and Nakamura, 2001, Matsushima-Nishiu et al., 2001, Valente et al., 2004). The translated product is 581residues (~63kDa), migrates at ~66kDa on SDS-PAGE gel, and contains a highly conserved kinase domain (residues 156-509) with a

mitochondrial signal peptide at the very N-terminus (Figure12A). Expectedly, cellular localization is predominantly mitochondrial however a N-terminally processed (~54kDa) fragment is observed at the OMM (outer mitochondrial membrane). The preprotein remains cytoplasmic and is subject to regulation via chaperones (Heat shock protein (HSP) 90/ Cell division cycle 37 homolog (CDC37) complex) and the proteasome. The ratio of isoforms appears related to mitochondrial physiology as well as PD pathogenesis (Gandhi et al., 2006, Lin and Kang, 2008, Muqit et al., 2006, Weihofen et al., 2008).

Ser/Thr kinase activity of PINK1 was initially confirmed through *in vitro* autophosphorylation assays, which proceeded to establish a kinase regulatory role for PINK1 C-terminus (Silvestri et al., 2005). Identification of Tumour necrosis factor receptor-associated protein 1 (TRAP1)/HSP75 as a substrate uncovered a protective role for PINK1 against ROS induced apoptosis, a feature absent in kinase inactive and PD linked PINK1 mutants (Pridgeon et al., 2007). A recent biochemical study by Gandhi *et al.* elegantly established how PINK1 deficiency impaired calcium homeostasis lead to increased ROS, reduced respiration and ATP production, contributing to a fall in $\Delta\Psi m$ (mitochondrial membrane potential) thus triggering cytochrome C mediated apoptosis (Gandhi et al., 2009). Dopaminergic neurons have been shown previously to prefer calcium channels for 'autonomous pacemaking' activities rendering them susceptible to impaired calcium homeostasis (Chan et al., 2007). However, a biochemical link between kinase activity and the mitochondrial Na^+/Ca^{2+} exchanger proved elusive. This study corroborated observations of reduced activity in complexes I and II of the electron transport chain (ETC) in neuronal tissues of PINK1 deficient mouse and fly (Gandhi et al., 2009, Morais et al., 2009, Gautier et al., 2008).

A central role for PINK1 in mitochondrial protein quality control and homeostasis is emerging around the cross talk between PINK1 and other PD genes: DJ-1, High temperature requirement protein A2 (HTRA2) and Parkin. DJ-1, associated with the PARK7 locus and autosomal recessive PD, is a putative

redox-dependent chaperone localised in several cellular compartments including mitochondrial IMS and matrix (Bonifati et al., 2003). It is a structurally dimeric protein with some PD linked mutations (Leu166Pro) located on along the dimer interface (Figure 12B). It has been suggested that acidification of a conserved cysteine (Cys106 in yellow) by ROS initiates migration into the mitochondria as part of the oxidative stress response (Canet-Aviles et al., 2004, Wilson et al., 2003). Indirect evidence of a mitochondrial H_2O_2 scavenging role involving Cys106 has also been presented (Andres-Mateos et al., 2007). Concurrently, neuronal cells from DJ-1 knockout mice showed increased sensitivity to 1-methyl-4-phenyl-1,2,3,6-tetrahydropyrindine (MPTP) induced oxidative stress *in vitro*, while loss of dopaminergic neurons is observed *in vivo*. DJ-1 has been shown to alleviate PINK1 expression in SH-SY5Y cell lines and the two work together in neuronal defence against 1-methyl-4-phenylpyridinium induced cell death (MPP+; the toxic product of MPTP metabolism). (Kim et al., 2005, Tang et al., 2006).

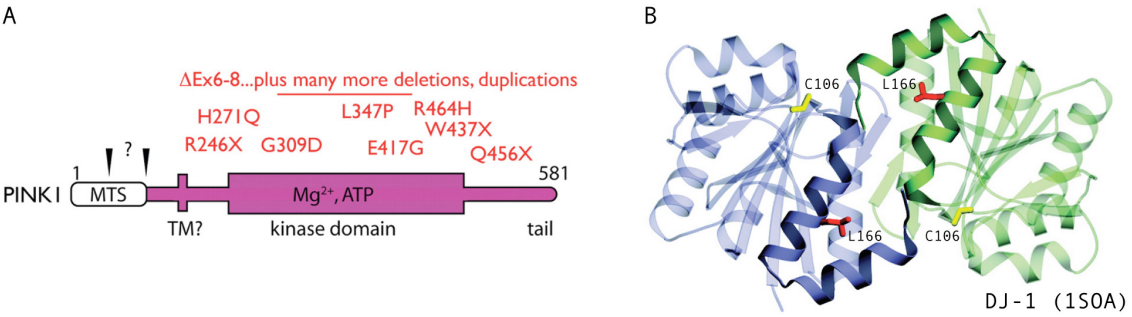

Figure 12: Structure of PINK1 and DJ-1. A. Cartoon depicts the primary sequence profile of PTEN Induced putative Kinase-1 or PINK1. Pathogenic mutations are indicated above in red. The mitochondrial targeting sequence (MTS), predicted cleavage sites (inverted black triangles) and predicted transmembrane (TM) domain lie N-terminal of kinase domain (Figure not to scale, adapted from (Cookson and Bandmann, 2010). **B.** Structure of the Dimeric DJ-1 (PDB 1SOA) highlights the coaxial dimer interface between C-terminal helices of the two monomers, coloured violet and green. Cys-106 (shown in yellow sticks) is a conserved cysteine plays a role in oxidative stress response while Leu-166 (shown in red sticks) is pathogenic mutation site (Leu166Pro) present at the dimer interface. Figure adapted from (Wilson et al., 2003)

HTRA2, associated with the PARK13 locus and autosomal recessive PD, is a serine protease residing in the mitochondrial IMS (inter-membrane space) (Strauss et al., 2005). The translated apoprotein bears a central protease domain flanked by a mitochondrial signal peptide and a putative

transmembrane domain on the N-terminus and a regulatory PSD-95/Discs-large/Zona Occludens-1 (PDZ) domain at the C-terminus. Initially a pro-apoptotic and stress response role for HTRA2 had been suggested (Vaux and Silke, 2003). Under conditions of cellular stress, PINK1 has been reported to bind and induce HTRA2 phosphorylation at a Ser 142 (Ala141 being a PD linked mutation site) thereby activating protease activity, favourable for protein quality control in the mitochondria (Figure 13) (Plun-Favreau et al., 2007). While a mitochondrial protective role for HTRA2 is generally accepted the details of this pathway, especially in PD pathogenesis, are yet to be elucidated. The inception of a metabolic pathway, downstream of PINK1 for HTRA2 has been laid out (Johnson and Kaplitt, 2009, Tain et al., 2009).

A model of mitochondrial quality control pathway via protein ubiquitination and autophagy/lysosomal degradation is emerging around PINK1 and Parkin, a ubiquitin RING E3 ligase associated with the PARK2 locus and autosomal recessive PD (Kitada et al., 1998, Shimura et al., 2000). Genetic linkage between the two genes was first established in *Drosophila*, placing PINK1 upstream in the pathway (Clark et al., 2006, Park et al., 2006, Yang et al., 2006). Oxidative stress induced mitochondrial depolarization initiates PINK1 dependant recruitment of Parkin to the OMM. Parkin catalyzes specific ubiquitination of mitochondrial proteins (Figure 13), like Voltage-dependent anion-selective channel protein 1 (VDAC1), thereby generating a molecular beacon for p62/SQSTM1/ sequestosome-1, the ubiquitin-autophagy adaptor, to induce mitochondrial autophagy/mitophagy (Geisler et al., 2010, Narendra et al., 2009). A parallel model positions PINK1/Parkin as a regulator of mitochondrial morphology (fusion and fission pathways), tweaking the route to mitophagy by enabling mitochondrial recycling (Dagda et al., 2009, Deng et al., 2008, Lutz et al., 2009, Poole et al., 2008, Ziviani et al., 2010). However, certain fundamental questions remain unresolved, in particular the mechanisms by which PINK1 recruits Parkin to damaged mitochondria and directs Parkin's E3 ligase component to generate specific ubiquitin signals on the mitochondria. Clues towards answering the first part of the question come from two recent

reports; PINK1/DJ-1/Parkin complex has been reported to function as a cytoplasmic E3 ligase and cytoplasmic processing of Parkin by HTRA2 abrogates its ligase activity (Park et al., 2009, Xiong et al., 2009). Structure-function aspects of Parkin will be introduced in the following section. This is an exciting period for research in mitochondrial homeostasis, which promises to yield an informative model describing the roles of HTRA2, DJ-1 and PINK1 in autosomal recessive PD.

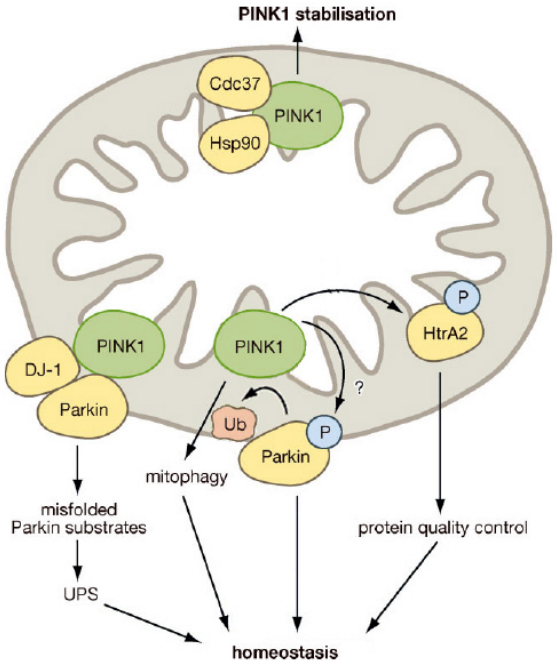

Figure 13: Mitochondrial homeostasis mediated by PINK1. Levels of full-length (and truncated) species of PTEN Induced putative Kinase-1/PINK1 are stabilised by the Heat Shock Protein (HSP) 90 and Cell division cycle 37 homolog (CDC37) chaperone complex. PINK1 has been reported to phosphorylate HTRA2 thereby inducing protease activity that could positively influence mitochondrial protein quality control. Upon oxidative stress, PINK1 recruits Parkin to the outer mitochondrial membrane, possibly through its kinase activity. Parkin generates specific ubiquitin signals on membrane bound mitochondrial proteins that initiate the downstream events leading to mitochondrial autophagy. Furthermore, PINK1/DJ-1/Parkin assemble to form a cytoplasmic E3 ligase complex. Figure adapted from (Deas et al., 2009)

1.10 Parkin: Ubiquitin RING E3 Ligase

1.10.1 Gene structure and pathogenic mutations

Parkin is encoded by one of the largest genes in the human genome; *PARK2*, comprising 12 exons, translating to a 465 amino acid product (52kDa) (Kitada et al., 1998). The gene (1.36 Mbs) makes up for nearly half of FRA6E (3.6Mbs), one of the most regularly observed regions of genomic instability, a common fragile site (CSF) (Denison et al., 2003). The gene is driven by a bi-directional promoter that regulates expression of PACRG (parkin co-regulated gene), a

protein of unknown function regulated by the UPP and associated with *Mycobacterium leprae* infections (Mira et al., 2004, Taylor et al., 2007, West et al., 2003). Up to twelve variable transcript lengths of *PARK2* have been observed in brains of humans and rats. However apart N-terminal truncated species of Parkin (arising due to an alternative translational start site at codon 80) thee is limited evidence of physiological stabilised splice variants (Dagata and Cavallaro, 2004, Henn et al., 2005). The first report of *PARK2* PD linked mutations identified various homozygous deletions of exons and subsequently the CSF core was narrowed to exons 2-8 (Kitada et al., 1998). However, varieties of mutations (multiplications and small deletions/insertions in exons, translated point (missense/nonsense) mutations and splice site mutations) have been identified thereafter spanning the entire gene. Figures 14A,B and Table 3 list the *PARK2* pathogenic exon rearrangements, nonsense-mediated truncations and missense mutations, collated from the PD Mutation Database (PDMD) (http://grenada.lumc.nl/LOVD2/TPI/) and the Human Gene Mutation Database (HGMD) (http://www.hgmd.cf.ac.uk).

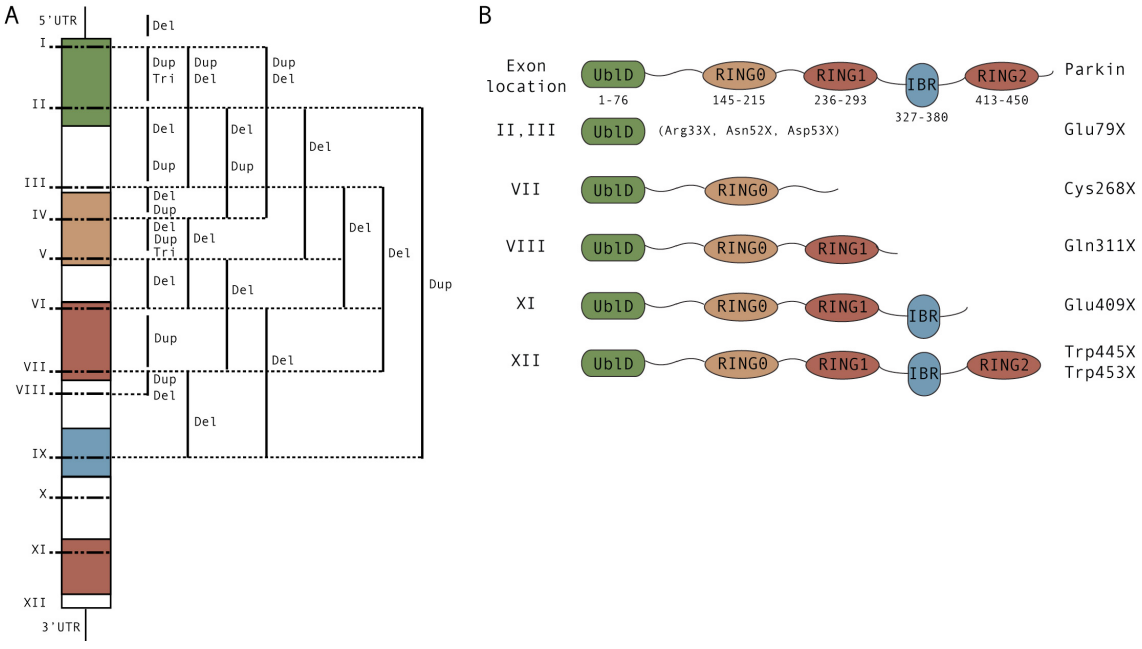

Figure 14: Exon rearrangements and Nonsense mutations. A. An illustration of the Parkin transcript and locations of the observed exon rearrangements; deletions (Del), duplications (Dup) and Triplications (Tri). Figure (not to scale) adapted from (Mata et al., 2004). **B.** Primary structure of full-length Parkin (not to scale) is depicted along with truncations arising from nonsense mutations (right, with exon locations of mutations on the left). Both figures display the following colour scheme for Parkin domains: Ubiquitin-like Domain (UblD, green), Really Interesting New Gene 1 and 2 (RING, dark brown), In-Between Ring (IBR, violet) and RING0 (light brown).

EXON	MUTATION	DOMAIN
I	Met1Leu	Ubiquitin-like Domain (UblD)
II	Gly12Arg Val15Met Asp18Asn Lys32Thr Arg33Gln Pro37Leu Arg42His/Pro/Cys Ala46Pro Thr55Ile Val56Glu	
III	Ala82Glu Asp86Asn Gln100His Arg104Trp	
IV	Tyr143Cys Pro153Arg Lys161Asn Ser167Asn	RING 0
V	Met192Leu/Val Ser193Ile	
VI	Lys211Arg/Asn **Cys212Gly/Tyr** Arg234Gln	
VII	Thr240Arg/Met **Cys253Tyr/Trp** Arg256Cys Val258Met Arg271Ser Asn273Ser Arg275Trp Asp280Asn Gly284Arg **Cys289Gly**	RING 1
VIII	Ile298Ser Gln311His	
IX	Gly328Glu Arg334Cys Ala339Ser Thr351Pro	IBR
X	Arg366Trp Val380Leu	
XI	Asp394Asn Arg396Gly Ala398Thr Arg402Cys/His Thr415Asn **Cys418Arg**	
XII	Gly430Asp **Cys431Phe** Pro437Leu Cys441Arg	RING 2

Table 3: Parkin missense mutations. Pathogenic missense mutations collated from the PD Mutation Database (PDMD) and Human Gene Mutation Database (HGMD) are listed against exon (left) and domain (right) structure. The Ubiquitin-like Domain (UblD, green), Really Interesting New Gene 1 and 2 (RING, dark brown), In-Between Ring (IBR, violet) and RING0 (light brown) constitute the domains of full-length Parkin. Bold letters indicate mutations in zinc-coordinating residues. Mutations Lys27Asn, Lys48Ala in the UblD, IBR zinc-coordinating Cys352Gly and Met434Lys in RING2 have been reported as pathogenic in the literature (Finney et al., 2003, Henn et al., 2005, Matsuda et al., 2006, Safadi and Shaw, 2007, Tomoo et al., 2008). Since they do not appear on the PDMD and HMD lists, they have been excluded from the list.

Mutations described include homozygous, compound heterozygous (different mutation in each allele) and heterozygous mutations. Due to recessive inheritance of the gene, homozygous (loss of function) mutations are the most common cause of Autosomal Recessive Juvenile Parkinson's (AR-JP) as well as Early-Onset Parkinson's Disease (EOPD) (Kitada et al., 1998). Point mutations in the functional domains are linked to an earlier onset and faster disease progression than truncating mutations. The phenotypic correlation of heterozygous and compound heterozygous mutations is yet to be understood completely, however in the absence of AR-JP, these genotypes could increase susceptibility to late-onset PD (Gasser, 2007, Hardy et al., 2009).

1.10.2 Protein structure and localization

Encoded by one of the largest known genes the translated product however, stretches to a mere 465 amino acids with an apparent molecular weight of 52 kDa. Classified as an archetypal RBR (RING-IBR-RING), a recent report of an additional Zn^{2+} binding domain (RING0) makes it a unique multi-domain E3 ligase (Hristova et al., 2009, Marin et al., 2004). Signature sequences of the RING domains in human Parkin (UniProt O60260) are listed in Figure 15.

RING1 and RING2 domains display a single minor linker length variation each from the canonical RING signature (InterPro IPR001841) while the IBR shows two linker length variations from the canonical IBR signature (InterPro IPR002867) (Figure 15, in red). The four domains, RING 1, IBR, RING 2 and RING0, have been shown to bind two zinc ions each, with structural evidence present for the IBR (Beasley et al., 2007, Hristova et al., 2009). Furthermore, RING0 is expected to co-ordinate the zincs in a bipartite manner similar to the IBR (described below). A total of nine missense mutations are observed in five zinc co-ordinating residues (Table 3), all of which would lead to global unfolding of the domain resulting in destabilization of Parkin and is likely to contribute to reduced E3 ligase activity (Gu et al., 2003, Wong et al., 2007).

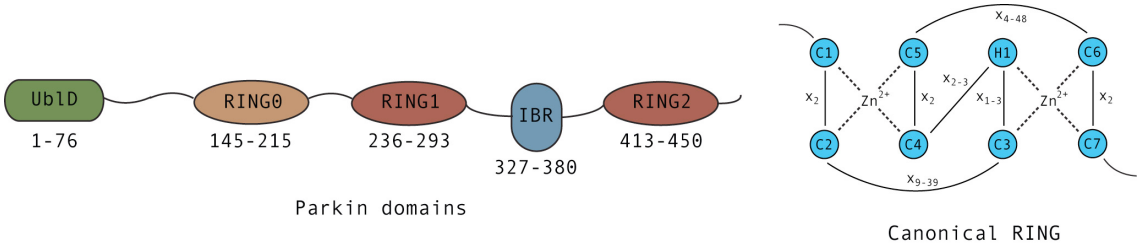

Domain	Primary sequence organisation	Pattern sequence
RING0	Cys-x_3-Cys -x_{11}- Cys -x_2- Cys -|x_{26}|-Cys-x_4-Cys -x_{10}- Cys-x_2-His	C_4|x_{26}|C_3H
RING1	Cys-x_2-Cys -x_{11}- Cys -x_3- His -x_2- Cys-x_2-Cys -x_{25}- Cys-x_3-Cys	C_3HC_4
IBR	Cys-x_4-Cys -x_{14}- Cys -x_7- Cys -x_4- Cys-x_2-Cys -x_4- His-x_3-Cys	C_6HC
RING2	Cys-x_2-Cys -x_9- Cys -x_1- His -x_2- Cys-x_4-Cys -x_4- Cys-x_2-Cys	C_3HC_4
Canonical RING	Cys-x_2-Cys -$x_{(9-39)}$-Cys-$x_{(1-3)}$-His -$x_{(2-3)}$- Cys-x_2-Cys-$x_{(4-48)}$-Cys-x_2-Cys	C_3HC_4
Canonical IBR	Cys-x_4-Cys -$x_{(14-30)}$-Cys-$x_{(1-4)}$-His -x_4- Cys-x_2-Cys -x_4- Cys-x_4-Cys	C_6HC

Figure 15: Parkin domain structure. A cartoon depicting the multi-domain features of full-length Parkin (465 residues) and along with individual domain boundaries (top left). Domain colours: Ubiquitin-like Domain (UblD, green), Really Interesting New Gene 1 and 2 (RING, dark brown), In-Between Ring (IBR, violet) and RING0 (light brown). Topology diagram of the canonical RING domain depicts the distinct RING domain cross-brace. Zinc co-ordinating Cys (C) and His (H) are numbered (blue circles) and Xn represents residue length of the interspaced linker regions (top right). Primary sequence organisation of zinc co-ordinating regions in Parkin compared with canonical RING and IBR sequences (bottom table). RING0 is composed of two zinc fingers, C4 and C3H, separated by a 26-residue linker (Hristova et al., 2009). 'Xn' represents residue length of the interspaced linker regions. Also shown in red are variations of RING 1, 2 and IBR from the canonical sequence.

The IBR structure, solved by nuclear magnetic resonance (NMR) spectroscopy, is unique and is suggestive of enabling E3 function (Beasley et al., 2007). The zinc co-ordinating 'scissor-like' fold contains a modular architecture; a C_4 zinc finger followed by a C_2HC zinc finger in a bilobal arrangement unlike the zinc cross-brace architecture observed in RING domains. While, pathogenic mutant Thr351Pro unfolds the IBR fold, mutations Gly328Glu and Arg334Cys retain wild-type architecture, instead affecting surface properties and perhaps zinc co-ordination respectively. The authors suggest the overall domain architecture could bring together the flanking RING1 and RING2 domains, which in turn could have a bearing on the E3 ligase activity of Parkin. Furthermore, the structure brings residues Val380 (a pathogenic mutation site), Ser378 (phosphorylation site) and Cys323 (potential nitrosylation site) in close proximity of each other. Any mutation/modifications at these residues could affect the IBR structure as well as have a bearing on the RING1 and 2 arrangements and consequently the E3 ligase potential of Parkin (Beasley et al., 2007).

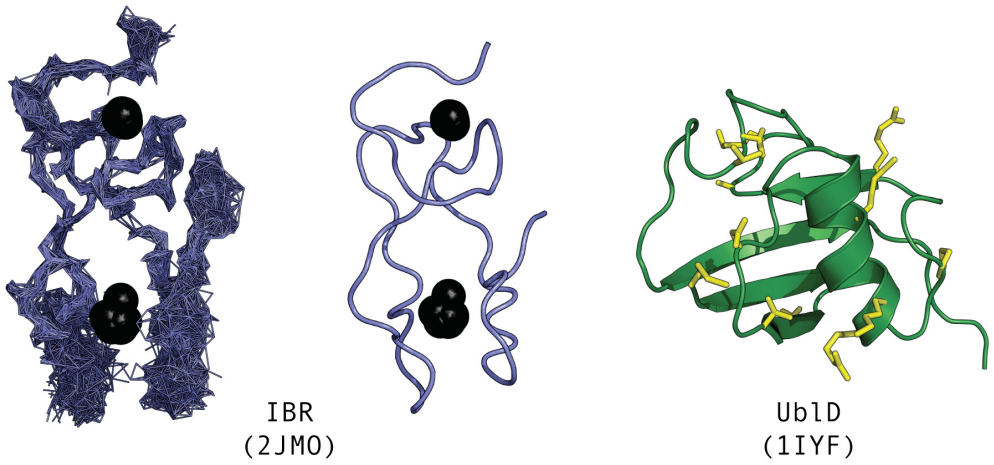

Figure 16: Structures of the In-Between RING (IBR) domain and Ubiquitin-like domain (UblD) of Parkin. Bilobal domain architecture of IBR domain (Ser329 – Cys377) coloured in deep blue (PDB 2JMO). On the left is a backbone overlay of 20 structures deposited and middle is a cartoon representation of the same. Zinc atoms are shown as black spheres. Cartoon representation of the UblD (right, PDB 1IYF) coloured in green and the sites of missense mutations found in this domain shown as yellow sticks. Structure figures were generated using PyMOL (Schrodinger, 2010).

At the N-terminus of the protein lies the Ubiquitin-like Domain (UblD) that shares the β-grasp fold with Ubiquitin along with 32% of sequence identity (Figure 16). Interestingly, over 20% of the total missense mutations observed in Parkin are found spread throughout the UblD, some of which have been reported to cause drastic domain unfolding (Safadi and Shaw, 2007, Tomoo et al., 2008). Interestingly, HOIL-1 is the only other protein that bears a similar domain arrangement to Parkin, however the former bears an additional ubiquitin binding Npl4 type Zinc Finger (NZF) located N-terminal of its RING1 domain (Kirisako et al., 2006). Finally, the last three residues of Parkin (FDV) form a class II PDZ binding motif (ϕXϕ - where ϕ is a hydrophobic residue and X is any residue) (Fallon et al., 2002). Nonsense mediated truncations Trp445X and Trp453X result in loss of this motif with the latter mutation observed to increase aggregation/insolubility of Parkin in cell culture conditions (Henn et al., 2005).

On the tissue level, parkin transcripts were observed in several tissues including the SNc region of the brain (Kitada et al., 1998). Cellular localization of wild-type Parkin is predominantly cytoplasmic (Shimura et al., 2000) with co-localization observed with membranes of the ER (Imai et al., 2001), Golgi apparatus (Huynh et al., 2007), mitochondria (Darios et al., 2003) and synaptic vesicles (Zhang et

al., 2000), as well as neurites (Huynh et al., 2001) and aggresomes (Muqit et al., 2004). Missense mutations have been observed to cause redistribution of Parkin to detergent insoluble inclusion bodies and in some cases aggresomes (Cookson et al., 2003, Sriram et al., 2005, Wang et al., 2005). These studies, conducted in cell lines as over-expression experiments, have lead to the inception of an aggregation theory, which in tandem with mutation-mediated structural destabilization, negatively regulates Parkin's E3 ligase activity and possibly explain its 'loss of function' (Henn et al., 2005, Schlehe et al., 2008, Wang et al., 2005).

1.10.3 E3 properties: E2s, auto-ubiquitination, pathogenic mutations and solubility

Shimura and colleagues ascertained the E3 ligase function of Parkin shortly after association with AR-JP was reported. As described earlier, RING E3 ligases work as scaffold enzymes that select substrates, recruit the charged E2 and facilitate transfer of ubiquitin E2 onto the target lysine of a substrate. UBE2L3/UbcH7 (Imai et al., 2000), UBE2L6/UbcH8 (Zhang et al., 2000), UBE2N/UBE2V1 heterodimer (Ubc13/UEV1) (Doss-Pepe et al., 2005), UBE2G2/Ubc7 and UBE2J2/Ubc6 (Imai et al., 2001) have been reported as cognate E2s for Parkin. Missense mutations, in particular, Thr240Arg proximal to RING1 and Thr415Asn proximal to RING2 have been observed to disrupt UBE2L3 and UBE2L6 binding respectively (Imai et al., 2000, Shimura et al., 2000, Zhang et al., 2000). Furthermore, ubiquitin ligase activity, ascertained via auto-ubiquitination (or self ubiquitination), was abrogated by these mutations. RING2 and RING1 were also proposed to bind the individual components of the UBE2N/UBE2V1 (Ubc13/UEV1) heterodimer (respectively) (Doss-Pepe et al., 2005). Auto-ubiquitination is now the primary assay of choice used to demonstrate the E3 ligase activity of Parkin and several groups have subsequently provided improvements in the experimental design of this assay (Hampe et al., 2006, Matsuda et al., 2006, Hristova et al., 2009).

Described, for the most part, as a single subunit (monomeric) E3 ligase, Parkin has been observed to function as the E3 component of a Skp1, Cullin, F-box (SCF) complex (Staropoli et al., 2003). In addition, Parkin has been shown to cooperate with the chaperone activity of HSP70, as well as, the E4 activity of CHIP (carboxyl terminus of the Hsc70-interacting protein; a U box E3 ligase) thus linking up with the UPR pathway (Imai et al., 2002). These properties not only add to the ligase potency but could also serve as points of regulation. Single subunit Parkin has been shown to synthesise K48-linked and K63-linked ubiquitin chains on substrates (Zhang et al., 2000, Doss-Pepe et al., 2005). Furthermore, Parkin mediated mono- and multi mono- ubiquitination of substrates was observed both *in vitro* and *in vivo* (Fallon et al., 2006, Joch et al., 2007, Moore et al., 2008). This multi-faceted property of ligase function is remarkable for a monomeric RING E3 and invites investigations into how Parkin modulates its ubiquitination potential.

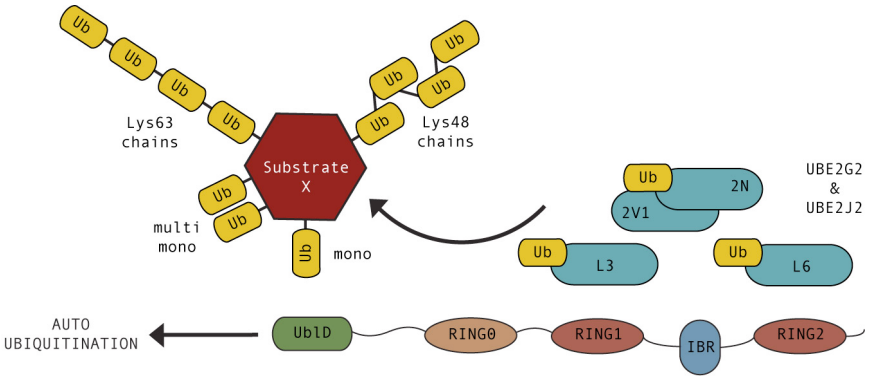

Figure 17: Overview of Parkin's E3 ligase properties. Multi-domain architecture of Parkin depicts the Ubiquitin-like Domain (UblD, green), Really Interesting New Gene 1 and 2 (RING, dark brown), In-Between Ring (IBR, violet) and RING0 (light brown). Parkin also co-operates with several E2s through either the RING1 or RING2 domain; UBE2L3/UbcH7 (RING1) (Imai et al., 2000), UBE2L6/UbcH8 (RING2) (Zhang et al., 2000), UBE2N/UBE2V1 (Ubc13/UEV1) heterodimer (RING1/RING 2 respectively) (Doss-Pepe et al., 2005), UBE2G2 (Ubc7) and UBE2J2 (Ubc6) (Imai et al., 2001). Also summarised are various ubiquitin signals (mono-, multi mono-, Lys48- and Lys63- linked poly- ubiquitination) generated by Parkin on different substrates. Furthermore, Parkin also exhibits auto-ubiquitination, a feature often used to confirm its E3 ligase activity (Hampe et al., 2006, Matsuda et al., 2006, Hristova et al., 2009).

Auto-ubiquitination of Parkin has also been demonstrated as multi monoubiquitination *in vitro* (Matsuda et al., 2006) and *in vivo* (Hampe et al., 2006). Interestingly, the proteasomal degradation of auto-ubiquitinated Parkin has been suggested by multiple reports (Choi et al., 2000, Zhang et al., 2000,

Finney et al., 2003, Ardley et al., 2003, Junn et al., 2002). Taken together, monomeric Parkin co-operates with several E2s to mediate a variety of ubiquitin-based signals (Figure 17) on different substrates (described in section 1.9.4) however mechanisms of these events are yet to be elucidated.

Interestingly, disease mutations studied in the above reports, as well as others (Hampe et al., 2006, Matsuda et al., 2006, Sriram et al., 2005) have either impaired or enhanced ligase activity (measured using auto- and substrate ubiquitination levels) and provide clues towards understanding E3 ligase mechanisms of Parkin. Variations in ligase activity alongside aggregation and destabilization add to the complexity of understanding 'loss of function' in AR-JP. Observed effects of pathogenic mutations on solubility/localization and ligase activity are summarised in Table 4. In majority of the cases, auto-ubiquitination is accompanied with substrate ubiquitination. Non-conforming mutations might impair substrate interaction suggests disassociation of auto- and substrate ubiquitination. Cooperation of the RING domains has been proposed to be crucial for Parkin activity (Rankin et al., 2001). The absence of ligase activity in C-terminal truncations (in particular lacking the RING2 domain) as well as species with RING2 mutations portrays RING2 as the catalytic core (Matsuda et al., 2006, Hampe et al., 2006).

Mutations of interest are the rows shaded in grey (Table 4), some representing exceptions to the above pattern. Mutations Arg42Pro and Arg275Trp are observed to form inclusions, show increased levels of auto-ubiquitination and enhanced non-degradative substrate ubiquitination despite reduced interaction with one of the substrates (Aminoacyl tRNA synthase complex-interacting multifunctional protein 2/AIMP2). Arg256Cys, formed inclusions and enhanced auto-ubiquitination (*in vitro* and *in vivo)* however did not exhibit substrate interaction and ubiquitination. In contrast, the soluble mutants Lys161Asn and Thr240Arg lack any manner of ubiquitination *in vivo* and were termed 'ligase dead' mutants (Sriram et al., 2005).

Parkin Species	Solubility	Inclusion bodies	Ligase activity	
			Auto	Sub.
Wild-type	+	-	✓	✓
Arg33Gln	+	?	?	?
Arg42Pro	-	+	✓	✓
Val56Glu	+	?	?	?
Ala82Glu	+	-	✓	?
Lys161Asn	+	-	✓/ ×	×
Met192Leu	+	-	?	?
Lys211Asn	+	-	✓	?
Lys211X	-	+	?	?
Cys212Tyr	-	+	?	?
Thr240Arg	+	-	✓/ ×	×
Arg256Cys	-	+	✓	×
Cys268X	-	+	?	?
Arg275Trp	-	+	✓	✓
Asp280Asn	+	-	✓	?
Cys289Gly	-	+	✓	?
Gln311X	-	+	×	×
Gly328Glu	+	-	✓	×
Arg334Cys	+	+	✓	?
Glu409X	-	+	×*	×*
Thr415Asn	+	-	×	×
Cys418Arg	-	+	×	×
Gly430Asp	+	-	×/ ✓	×
Cys431Phe	-	+	×/ ✓	×
Pro437Leu	+	-	×	×
Cys441Arg	-	+	×	?
Phe453X	-	+	×/ ✓	×

Table 4: Phenotypic variations of mutant Parkin. Effects of pathogenic mutations (missense and nonsense) on solubility and ligase potential of Parkin are summarised in the table. Experiments were conducted either *in vitro* using 'purified' proteins or *in* vivo as transient over-expression experiments in cell lines. Parkin species are coloured based on domain location of mutation; green - UblD, light brown – RING0, dark brown – RING1 and RING2, violet – IBR. 'Solubility' was assessed by cell extraction using detergents (Triton-X) and comparing Parkin species in supernatant (soluble) versus pellet (insoluble) fractions. Presence of Parkin rich 'Inclusion bodies' was determined via antibody staining/immunofluorescence (IF) experiments. Auto-ubiquitination ('Auto') was tested either *in vitro* using 'purified' proteins or *in vivo* with co-transfections of tagged ubiquitin followed by immunoprecipitation (IP)/western blot (WB) detection techniques. Substrate ubiquitination ('Sub.') assays were conducted *in vivo* by co-transfections of tagged Parkin species, tagged substrates and tagged ubiquitin followed by IP/WB detection techniques.

+/- indicates solubility/insolubility or presences/absence of inclusion bodies. ✓/ × - auto-ubiquitination observed *in vitro* however absent *in vivo*. ×* - Matsuda *et al.* use Lys416X instead of Glu409X. ×/ ✓ - auto-ubiquitination absent *in vitro* but observed *in vivo* suggesting *trans* action by other ubiquitin ligases. ? - not determined.

Wang et al. utilized FLAG-Parkin species in study solubility and inclusion body formation in HEK293 and SH-SY5Y cells. Sriram et al. conducted solubility, inclusion body, auto- and substrate ubiquitination assays with myc-Parkin in SH-SY5Y cells. FLAG-AIMP2 and FLAG-synphillin-1 were substrates tested for ubiquitination. Henn et al. used 3xHA-Parkin species and studied aggregation in N2a and SH-SY5Y cells. Hampe et al. and Matsuda et al. conducted in vitro auto-ubiquitination assays with GST-Parkin (UBE2L3/UbcH7) and MBP-Parkin (UBE2G2/Ubc7) respectively.

References: (Wang et al., 2005, Sriram et al., 2005, Hampe et al., 2006, Matsuda et al., 2006, Henn et al., 2005)

However these mutations show robust auto-ubiquitination *in vitro*, supporting a possible disassociation of ligase properties (auto and substrate ubiquitination) (Hampe et al., 2006, Matsuda et al., 2006). The soluble Thr415Asn, located a few residues N-terminal of the first RING2 cysteine, consistently lacked ligase activity despite the experimental set-up. More recently, Parkin has been observed to mediate K27-linked polyubiquitination on mitochondrial membrane bound substrates (Geisler et al., 2010). The experiments conducted in HeLa and SH-SY5Y cells using FLAG-Parkin species corroborated the above observations for the most part. Notable exceptions were: Arg275Trp was soluble and Lys161Asn showed weak auto-ubiquitination.

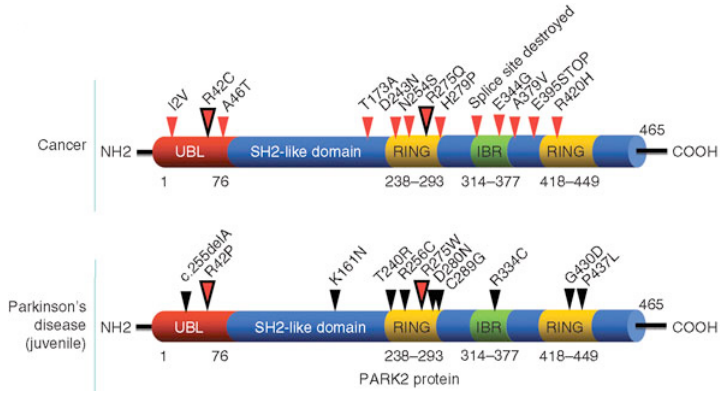

Figure 18: Somatic *PARK2* mutations. *PARK2* mutations found in cancer (top, red arrows) and AR-JP (bottom, black arrows). Larger black-bordered red arrows with indicate sites of mutations shared between the two disease states. Figure adapted from (Veeriah et al., 2010)

A tumour suppressive role for Parkin was uncovered in gliablastoma multiforme (GBM), colon cancer and lung cancer. Somatic mutations in Parkin, similar to those found in AR-JP (Figure 18), impaired auto-ubiquitination, binding and turnover of cyclin E. Parkin, as part of a SCF complex, had been previously shown to regulate cyclin E levels (Staropoli et al., 2003, Veeriah et al., 2010).

1.10.4 E3 properties: substrates, ubiquitin signals and regulators

Substrate recognition and ubiquitination are critical functions of an E3 ligase and Parkin has been reported to ubiquitinate a wide variety of substrates (introduced in the following sections). Each of the domains/motifs within Parkin

has been implicated in substrate recognition however the ubiquitin ligase activity necessitates the RING domains. Ubiquitination signals generated on the substrate include; mono-, multi mono-, K48- and K63- linked poly-ubiquitination, while concomitantly catalysing auto-ubiquitination.

1.10.4.1 Ligase activity: Monoubiquitination potential

The UblD has been shown to direct Parkin's ligase activity, in particular the monoubiquitination potential, to EPS15 and endophilin-A (Figure 19) (Fallon et al., 2006, Trempe et al., 2009). EPS15 is an adaptor molecule for epidermal growth factor receptor (EGFR) and regulates EGF internalization and trafficking. UblD interacted with tandem UIMs located at C-terminus of EPS15 contributing to monoubiquitination of the latter (termed coupled monoubiquitination, described earlier). In contrast, enhanced multiple ubiquitination (auto-ubiquitination) of Parkin was observed, which Fallon *et al.* concluded as EPS15 'activation' of Parkin. UblD interaction with the tandem UIMs of S5a/Rpn10, a subunit of the 26S proteasome, has been biophysically characterized and compared with the EPS15 UIMs interaction. It is noteworthy that Lys48 is the sole residue on the surface of UblD critical for both sets of interactions (Safadi and Shaw, 2010, Sakata et al., 2003). The UIMs of Rpn10 has been shown to assist formation of degradable chains on substrates *in vitro* and RPN10 is functionally regulated by monoubiquitination *in vivo* (Kim et al., 2009, Isasa et al., 2010).

A conserved PaRK extension (Pro-x-Arg-Lys, where x is any amino acid) borne on the C-terminal tail of UblD is responsible for selective recruitment of Parkin to SH3 (SRC Homology-3) domains of endophilin-A and other select BAR (Bin–Amphiphysin–Rvs) domain containing proteins implicated in synaptic vesicle dynamics. Residues Lys48 and Arg42 (a AR-JP mutation site) also play a critical role in this interaction. Upon recruitment, wild-type Parkin proceeds to weakly monoubiquitinate endophilin-A consequently affecting synaptic transmission (Trempe et al., 2009). The UbID is also recognised by Nrdp1/FLRF, a RING E3 ligase that regulates cellular levels of Parkin (Zhong et

al., 2005). Remarkably, Parkin's C-terminal PDZ binding motif is the other region that plays a role in recognition of substrate for monoubiquitination. The PDZ binding motif mediates interactions with Protein interacting with Protein kinase C, alpha (PICK1) and Calcium/calmodulin-dependent serine protein kinase 3 (CASK) however only PICK1 was monoubiquitinated by the E3 thereby regulating synaptic transmission events (Joch et al., 2007, Fallon et al., 2002).

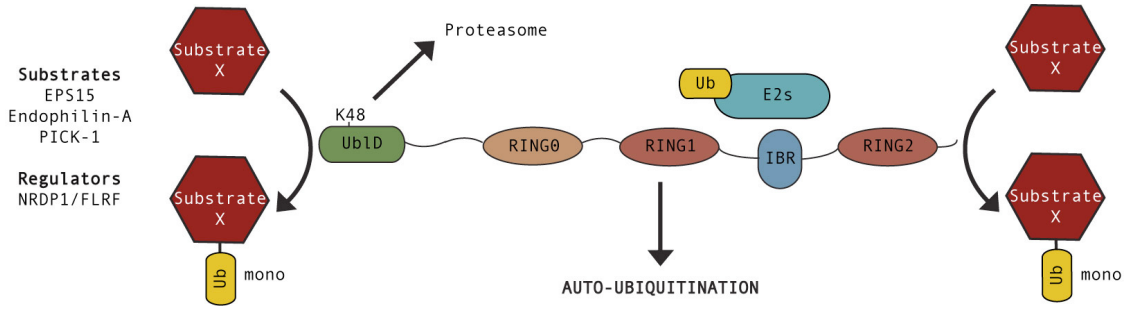

Figure 19: Monoubiquitination potential. Parkin mediates monoubiquitination of substrates Epidermal growth factor receptor substrate 15 (EPS15) (Fallon et al., 2006), endophilin-A (Trempe et al., 2009) and Protein kinase C, alpha (PICK1) (Joch et al., 2007). Concomitant multiple ubiquitination of Parkin (auto-ubiquitination) also observed. Curved arrows indicate regions of substrate recognition; N-terminal Ubiquitin-like Domain (UblD) for EPS15 and endophilin-A while the C-terminal PSD-95/Discs-large/Zona Occludens-1 (PDZ) binding motif for PICK1). In addition, interaction with the Regulatory particle non-ATPase protein (RPN) 10 (subunit of 26S proteasomal) and Nrdp1/FLRF (E3 ligase that regulates cellular levels of Parkin) occurs through the UblD. Tandem ubiquitin interacting motifs (UIM) on EPS15 and RPN10 mediate interaction with UblD, while the binds the UblD of Parkin. Residue Lys48 is crucial for interaction with UIMs of Eps15 and RPN10 and the same residue forms part of the interface with the SH3 domain of endophilin-A.

1.10.4.2 Ligase activity: Non-degradative potential

Indirect association between Parkin's ligase activity and SNCA was established early on. Parkin ubiquitinated the O-glycosylated form of SNCA (αSp22) with UBE2L6/UbcH8 while ubiquitination of synphilin-1, an SNCA interacting protein, was observed with UBE2L3/UbcH7 (Chung et al., 2001, Shimura et al., 2001). Synphilin-1 recognition was mediated primarily by RING2 and the resulting Lys63-linked polyubiquitination enhanced the formation of LB like inclusions rich in synphillin-1, SNCA and Parkin (Lim et al., 2005). Interestingly 14-3-3η, another SNCA interacting protein that functions as a molecular chaperone/adaptor/scaffold, was observed to bind the RING0 domain of Parkin and impair ligase activity (auto- and synphillin-1 ubiquitination). Binding to full-

length Parkin was observed at nanomolar affinities (K_d = 4.2 nM) and pathogenic mutations (Arg42Pro, Lys161Asn and Thr240Arg) appeared to disrupt this interaction (Sato et al., 2006). A similar inhibition of E3 ligase activity was observed upon Cyclin-dependent kinase 5 (Cdk5) mediated phosphorylation of Parkin at Ser131 in the RING0 domain. Furthermore, a phospho-dead mutation (Ser131Ala) displayed increased levels of auto-ubiquitination along with the formation of SNCA/synphillin-1/Parkin rich inclusion bodies in human dopaminergic cells (Avraham et al., 2007).

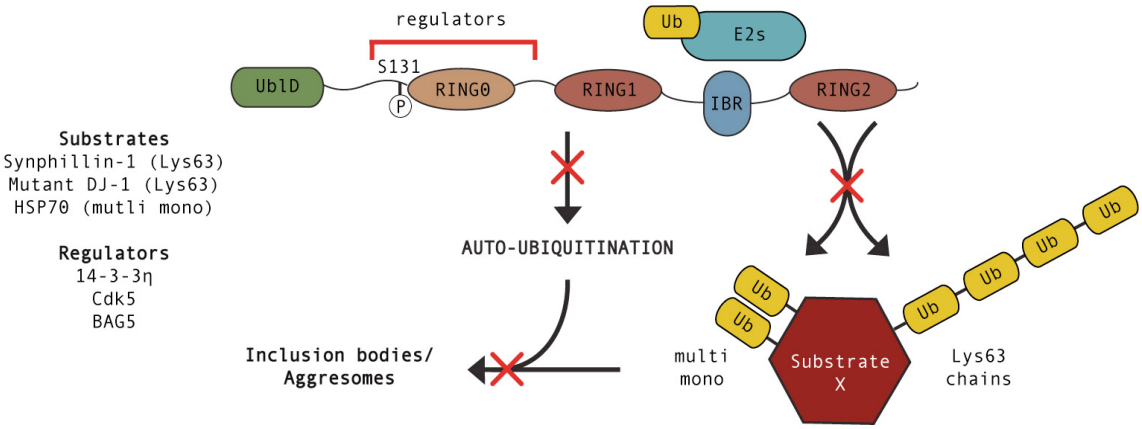

Figure 20: Non-degradative ubiquitination. Parkin catalysed Lys63-linked polyubiquitination of substrates Synphilin-1 (Chung et al., 2001) and mutant, misfolded DJ-1 (Leu166Pro) (Olzmann et al., 2007) resulting in the formation of inclusions bodies/aggresomes. Auto-ubiquitinated Parkin is also sequestered to inclusions/aggresomes. Ligase activity (auto- and synphillin-1 ubiquitination) of Parkin was impaired upon 14-3-3η binding (RING0 domain) and Cdk5 phosphorylation at Ser131 (near RING0) (Sato et al., 2006, Avraham et al., 2007). In addition, Parkin mediated multi monoubiquitination of Heat shock protein (HSP) 70 is negatively regulated by binding of Bcl-2-associated anthogene 5 (BAG5) at the RING0 region (Moore et al., 2008, Kalia et al., 2004).

Parkin mediated K63 linked polyubiquitination of mutant, misfolded DJ-1 (Leu166Pro) with the UBE2N/UBE2V1 (Ubc13/UEV1) heterodimer in SH-SY5Y cells. These signals were recognized by histone deacetylase (HDAC) 6 and sequestered by dynein motors to the aggresome (Olzmann et al., 2007). Parkin was also shown to interact with misfolded DJ-1 through the HSP70/CHIP complex (Moore et al., 2005). Furthermore, non-degradative multi monoubiquitination of HSP70 (via RING2-HSP70 interaction) was also observed in SH-SY5Y cells (Moore et al., 2008). Interestingly, Bcl-2-associated anthogene (BAG) 5, a molecular co-chaperone that bears four BAG repeats,

was observed to negatively regulate the E3 ligase activity and neuroprotective function of Parkin as well as inhibit chaperone HSP70. BAG5 was observed to bind Parkin the RING0 region and impaired auto-ubiquitination (*in vitro*, using E2s UBE2G2/Ubc7 and UBE2J2/Ubc6) as well as the ubiquitination of synphillin-1 in HEK293T cells (Kalia et al., 2004). Non-degradative ubiquitination potential and negative regulation of E3 ligase activity of Parkin are summarised in Figure 20.

1.10.4.3 Ligase activity: Ubiquitin mediated degradation

Parkin catalyses K48 linked poly-ubiquitination on several substrates, a signal that facilitates proteasomal-mediated degradation. Septin5/CDCrel-1, a synaptic vesicle associated GTPase protein, was the first substrate to be identified for Parkin. Substrate selection was through the entire RBR region (although RING2 was sufficient), substrate and auto-ubiquitination was observed with UBE2L6/UbcH8 and a fall in the rate of Septin5 turnover upon proteasomal inhibition and RING2 mutations (Zhang et al., 2000). In addition, Parkin mediated degradative ubiquitination of Sept5_v2/CDCrel-2, a close homologue of Septin5, and levels of both proteins were found to accumulate in AR-JP brains (Choi et al., 2003). Synaptotagmin-XI, another regulator of synaptic transmission, is recognised by RING1 and degraded by Parkin mediated ubiquitination in HEK293 cells (Huynh et al., 2003).

The Parkin/CHIP/Hsp70 complex associates on G protein-coupled receptor 37 (GPR37)/Pael-R as part of the UPR pathway. In cultured neuroblastoma cells (SH-SY5Y), over-expression of Pael-R leads to its unfolding and subsequently ER stress induced cell death. Hsp70 aids in the folding and ER translocation of Pael-R, however upon overloading of the ER translocation machinery, CHIP mediated the dissociation of Hsp70 allowing Parkin to associate with Pael-R via RING2 domain. Parkin mediated degradative ubiquitination of Pael-R occurs in the presence of CHIP that binds the RING0-RING1 domain of Parkin. The ER associated E2s, UBE2G2/Ubc7 and UBE2J2/Ubc6 co-operate with CHIP for its E4 activities on the Parkin substrate Pael-R (Imai et al., 2002, Imai et al., 2001).

Accumulation of substrates in Parkin knockout mice and AR-JP patients has been suggested as criteria for authentic Parkin substrates. AIMP2/p38/JTV1 is one such substrate that follows the criterion. AIMP2 recognition was mediated by RING1 domain however several pathogenic mutations disrupted AIMP2 ubiquitination. Parkin mediated formation of LB like inclusions containing AIMP2 in COS-7 and SH-SY5Y cells as well as in LBs idiopathic PD patients. AIMP2 overexpression induced neuronal toxicity and dopaminergic cell death in cell culture and mice (Corti et al., 2003, Ko et al., 2005). Far upstream element (FUSE) binding protein 1 (FUBP1), a transcriptional activator of c-myc, is another protein whose levels are found elevated in AR-JP, PD and MPTP treated mice brains. AIMP2 was observed to bind FUBP1 and possibly function in the same pathway. Moreover, FUBP1 is subjected to proteasomal degraded by Parkin mediated ubiquitination in SH-SY5Y cells (Kim et al., 2003a, Ko et al., 2006).

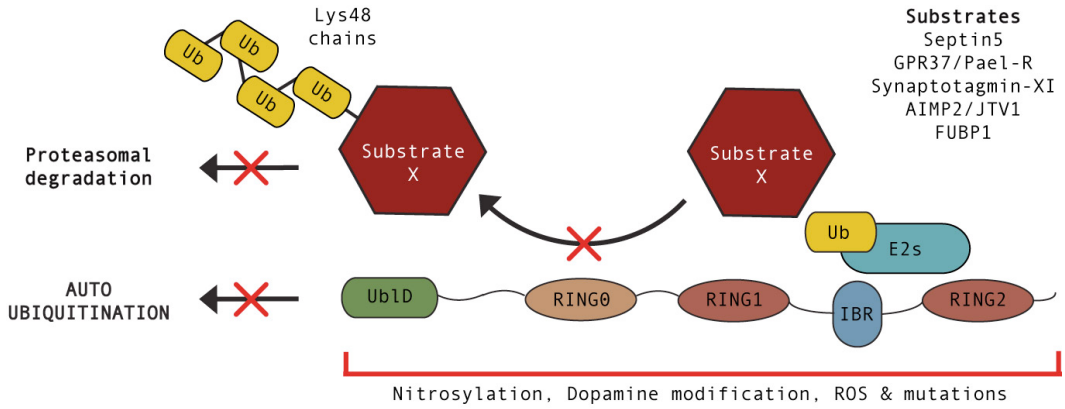

Figure 21: Ubiquitin mediated degradation. Parkin catalyses K48-linked polyubiquitination on various substrates targeting them for proteasomal degradation Substrates include Septin5 (Zhang et al., 2000), G protein-coupled receptor 37 (GPR37)/Pael-R (Imai et al., 2001), Synaptotagmin-XI (Huynh et al., 2003), Aminoacyl tRNA synthase complex-interacting multifunctional protein 2 (AIMP2)/ JTV1 (Corti et al., 2003) and Far upstream element (FUSE) binding protein 1 (FUBP1) (Ko et al., 2006). Ligase activity is impaired by pathogenic mutations, S-nitrosylation of cysteines and covalent modification by dopamine (DA). Reduced Parkin solubility is also observed due to reactive oxygen species (ROS), toxic α-synuclein/SNCA aggregates and DA modification. This 'loss of function' contributes to an accumulation of substrates in Parkin knockout mice and Autosomal Recessive Juvenile Parkinson's patients. However, only AIMP2 and FUBP1 have been observed to accumulate in such conditions (Ko et al., 2005, Ko et al., 2006).

A mutation in Parkin is not the only manner by which ligase activity can be impaired. S-nitrosylation of cysteine residues impair ligase activity in a 'biphasic

manner' (initial increase followed by inactivity) as observed *in vivo* and MPTP induced PD mice. Dopamine (DA) modification of Parkin leads to a similar 'loss of function' phenotype through covalent modification as well as decrease in solubility. Effect of ROS, SNCA aggregation and other cellular stresses contributes to Parkin's insolubility and increases aggresome formation. (Chung et al., 2004, Kawahara et al., 2008, LaVoie et al., 2007, LaVoie et al., 2005, Muqit et al., 2004, Yao et al., 2004). Loss of ligase activity by cellular and environmental factors brings forth a role for Parkin in sporadic PD. The degradative ubiquitination potential of Parkin and affect of cellular factors are summarised in Figure 21.

1.10.5 Neuroprotective functions of Parkin

The neuroprotective role of Parkin is functionally linked with its ubiquitin E3 ligase activity, introduced in the previous sections. However, a global pathway placing the numerous substrates and neuroprotective properties of Parkin in perspective of a physiological pathway, explaining the pathological 'loss of function' in PD, is yet to emerge.

Parkin over-expression has been shown to counter neurotoxicity associated with SNCA in cellular studies and animal model systems (Lo Bianco et al., 2004, Yamada et al., 2005, Yang et al., 2003, Yasuda et al., 2007). Furthermore, Parkin overexpression alleviates the detrimental effects of several cellular and environmental toxins (Jiang et al., 2004, Paterna et al., 2007, Vercammen et al., 2006). The mechanisms of neuroprotection from Parkin over-expression are yet elucidated, hampered by the absence of a direct genetic or biochemical link between SNCA and Parkin (von Coelln et al., 2006, Chung et al., 2001). Furthermore, an equivalent loss of dopaminergic neurons observed in wild type and Parkin null mice treated with environmental toxins (Perez et al., 2005, Thomas et al., 2007) suggested that Parkin over-expression could contribute to non-physiological phenotypes (Dawson and Dawson, 2010).

In recent years, a novel role for Parkin in mitochondrial homeostasis is emerging and involves interaction with other PD genes: PINK1 (Narendra et al., 2009, Geisler et al., 2010, Vives-Bauza et al., 2010), DJ-1 (Irrcher et al., 2010, Hao et al., 2010) and Leucine-Rich Repeat Kinase 2 (LRRK2) (Smith et al., 2005b, Venderova et al., 2009). Animal models (Palacino et al., 2004, Stichel et al., 2007, George et al., 2010) and fly systems (Clark et al., 2006, Park et al., 2006, Yang et al., 2006) support the physiological basis of the Parkin-Mitochondria connection. Studies identifying the ligase role in mitochondrial homeostasis will help assign Parkin's physiological and pathological functions (Figure 22).

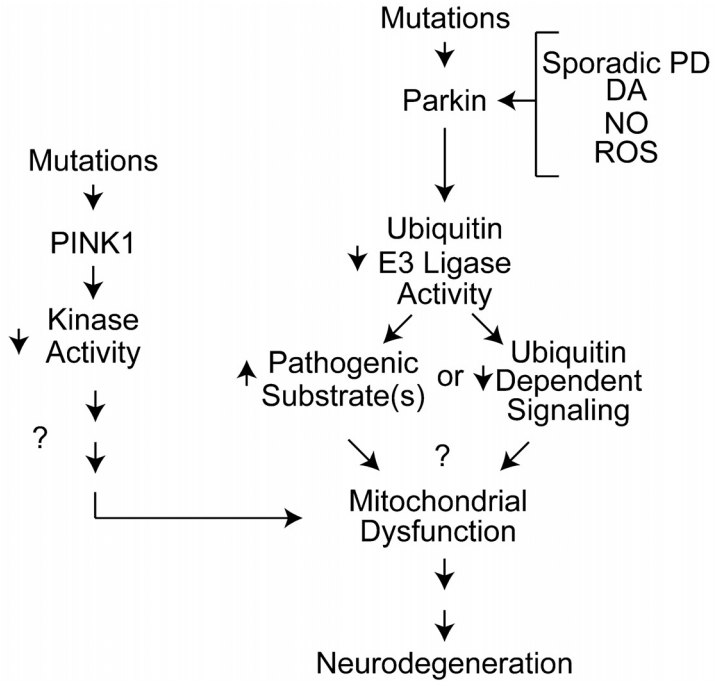

Figure 22: Pathways to Neurodegeneration. E3 ligase properties of Parkin can be impaired by genetic mutations (in Autosomal Recessive Parkinson's Disease (PD)) or by nitric oxide (NO), reactive oxygen species (ROS), dopamine (DA) or in sporadic PD. Consequently, the accumulation/deregulation of substrates (known and as yet unknown) or the loss of Parkin mediated ubiquitin signals could be detrimental to protein quality control pathways and in particular mitochondrial homeostasis. Mutations in PTEN Induced putative Kinase-1/PINK1, a mitochondrial kinase that functions upstream of Parkin, impair its kinase activity. The breakdown of Parkin and PINK1 activities could lead to mitochondrial dysfunction, the mechanistic details of which are still emerging, ultimately leading to neurodegeneration. Figure adapted from (Dawson et al., 2010).

1.11 Aims of this Study

Parkin, a multi-domain ubiquitin RING E3 ligase, has been observed to recruit different E2s (UBE2L3/UbcH7, UBE2L6/UbcH8, UBE2N/UBE2V1 (Ubc13/UEV1) heterodimer, UBE2G2/Ubc7 and UBE2J2/Ubc6) (Imai et al., 2000, Zhang et al., 2000, Doss-Pepe et al., 2005, Imai et al., 2001) to mediate ubiquitination on a variety of substrates, while concomitantly exhibiting auto-ubiquitination (Zhang et al., 2000). Substrate modification events include; monoubiquitination of EPS15, an adaptor molecule for EGFR (Fallon et al., 2006), multi monoubiquitination of HSP70, a molecular chaperone (Moore et al., 2008), Lys63 linked polyubiquitination of synphilin-1, an α-synuclein/SNCA interacting protein (Chung et al., 2001) and Lys48 linked polyubiquitination of AIMP2, subunit of aminoacyl-tRNA synthase complex (Corti et al., 2003) (Refer Figures 19-21 for mores substrates), while multi-monoubiquitination was the favoured auto-ubiquitination signal (Matsuda et al., 2006, Hampe et al., 2006). The multi-faceted properties exhibited by monomeric/single-subunit Parkin make it an attractive model system to examine how RING E3 ligases modulate their ubiquitination potential.

Furthermore, neuroprotective properties and the molecular basis of pathogenesis in AR-JP and idiopathic PD are linked with the ubiquitin E3 ligase activity of Parkin, however the molecular features of the pathway are far from clear. Pathogenic AR-JP mutations have been observed in every domain of Parkin and have variable effects on its E3 ligase activity (reduced solubility, reduced/enhanced auto- and substrate- ubiquitination, summarised in Table 4). Mutations of particular interest are Arg42Pro, Lys161Asn, Thr240Arg and Thr415Asn that lie in the UblD, RING0, RING1 and RING2 domains of Parkin respectively. The Arg42Pro Parkin mutant was observed to form cytoplasmic inclusion bodies/aggresomes (using transient over-expression studies in HEK293 and SH-SY5Y cells) as well as catalyse enhanced ubiquitination of itself and AIMP2 (enhanced auto- and substrate ubiquitination respectively) (Wang et al., 2005, Sriram et al., 2005). Several reports have previously

suggested that auto-ubiquitinated Parkin is subject to proteasomal degradation (Choi et al., 2000, Zhang et al., 2000, Finney et al., 2003, Ardley et al., 2003, Junn et al., 2002). In accordance, Henn *et. al.* noted the proteasomal turnover of Arg42Pro to be three-fold greater than that of wild type Parkin (Henn et al., 2005). In contrast, Parkin mutants Lys161Asn, Thr240Arg and Thr415Asn do not form inclusion bodies or ubiquitinate AIMP2. Nevertheless, robust auto-ubiquitination (*in vitro)* was observed exclusively with the Lys161Asn and Thr240Arg Parkin mutants while the Thr415Asn mutant was termed 'ligase-dead' (Wang et al., 2005, Sriram et al., 2005, Hampe et al., 2006, Matsuda et al., 2006). Investigations into E3 ligase properties of various AR-JP mutations of Parkin could uncover further insights into enzyme regulation and shed some light over pathological 'loss-of-function' mechanisms.

Thus, the broader aims of this study were the structure-function analysis of Parkin, a model RING enzyme, to decipher fundamental mechanisms of RING E3 ligase mediated ubiquitination and examine how these are deregulated in the context of AR-JP. Couple of observations on the E3 ligase properties of Parkin, made prior to commencement of this study, helped direct the objectives of this research. The first came from an article by Matsuda and colleagues who observed the *in vitro* auto-ubiquitination of MBP Parkin (purified recombinant human Parkin with MBP tagged at the N-terminus) with multiple E2s (Matsuda et al., 2006). Further, the report demonstrated that MBP IBR-RING2 (Parkin truncation bearing IBR-RING2 domains) underwent auto-ubiquitination, and the ubiquitin moiety was attached both the MBP tag and the Parkin polypeptide. However, when presented in *trans*, free/unbound MBP was not ubiquitinated by the MBP IBR-RING2 species. The authors proposed that MBP Parkin is 'primed' for ligase activity with the N-terminal tag operating as a pseudo-substrate.

The second observation came from experiments carried out by Simon Leslie and Dr. Helen Walden. Leslie and Walden had previously established the expression and purification protocols of recombinant human Parkin (wild type

and 111C, a truncation that lacked the first 110 residues of Parkin) in *Escherichia coli*. The protein production strategy made use of an N-terminal 6xHis-smt3 (SUMO, *S. cerevisiae*) affinity cum solubility tag for the bacterial expression of human Parkin. Furthermore, production of full-length Parkin using the 6xHis-smt3 tag enabled the cleavage of the fusion protein immediately prior to the N-terminal methionine (by ubiquitin-like-specific protease 1 (Ulp1)), generating wild type Parkin with no overhang or leader sequence. *In vitro* auto-ubiquitination assays undertaken to assess ligase activity of this material (as well as 111C produced using the same strategy) led to some interesting observations. Wild type Parkin (with no overhang or leader sequence) consistently lacked auto-ubiquitination activity while 111C Parkin exhibited robust auto-ubiquitination. Taken together, these observations suggested that modifications to the N-terminus of Parkin (presence of N-terminal MBP tag or deletion of the first 110 residues) influenced Parkin in a way that 'activated' the ubiquitination potential of the E3 ligase. The following chapters will describe the methods (Chapter2) and experiments (Chapters 3-5) carried out during the course of this study, investigating the E3 ligase properties of Parkin, its regulation and effects of AR-JP mutations on this regulation.

Chapter 2. Methods

2.1 Molecular Biology

All experiments carried out in this study made use of recombinant protein expressed and purified from *E. coli*. The following section describes the cloning methods and expression constructs generated. A recombinant vector bearing the *PARK2* (*Parkin*, *Homo sapiens*) open reading frame cloned within the Champion™ pET SUMO (Invitrogen) vector was available in the Walden group at the start of the study. The construct encoded a 6xHis-smt3 (SUMO, *S. cerevisiae*) affinity cum solubility tag that was used for expression and purification of wild type Parkin. Furthermore, this construct served as template for all subsequent genetic manipulations (point mutations, domain deletions/truncation and sequence insertions, Table 5) generated using the Phusion® Mutagenesis kit (Finnzymes) based on manufacturer's protocol.

Point mutations made include Val15Met, Lys27Asn, Lys32Ala, Arg33Gln, Arg42Pro, Ile44Ala, Ala46Pro, Lys48Ala, Arg51Pro, Ser131Glu (and the Ser131Ala + Lys48Ala double mutant), Lys161Glu, Thr240Arg and Thr415Asn. Deletions/truncations made include: UblD (deletion of Gly77 to Val465/C-termius), ΔUblD (deletion of Met1 to Lys76), 95C (deletion of Met1 to Gly94), 321C (deletion of Met1 to Ala320) and ΔRING2 (deletion of Thr414 to Val465/C-terminus) (Table 5). Certain point mutations were also made in a couple of the deletion/truncation constructs: Lys48Ala in the UblD construct, Thr415Asn in ΔUblD construct. Sequence insertions include; incorporation of TEV protease site at several locations between the UblD and RING0 domains of wild type Parkin (Parkin-TEV, experiments described in results section 3.4.2) and insertion of a V5 epitope (GKPIPNPLLGLDST) encoding sequence immediately after the 6xHis-smt3 sequence in UblD construct giving the V5-UblD construct.

Vector	Affinity Tag	Cleavage enzyme	Construct Name	Figure (cartoons represent material used for experiments)	Associated Results section(s)
pET SUMO	6xHis smt3	Ulp1	Wild type/WT Parkin	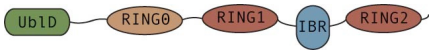	All sections
pET SUMO	6xHis smt3	Ulp1	V15M-, K27N-, K32A-, R33Q-, R42P-, A46P- and R51P- Parkin	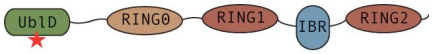	3.3 and 5.5
pET SUMO	6xHis smt3	Ulp1	K48A- and K48R-Parkin		4.2, 4.3 and 5.5
pET SUMO	6xHis smt3	Ulp1	I44A-Parkin		5.2
pET SUMO	6xHis smt3	Ulp1	S131E-Parkin		4.3
			S131E+K48A Parkin		
pET SUMO	6xHis smt3	Ulp1	K161N-Parkin		5.2 and 5.3
			T240R-Parkin		
			T415N-Parkin	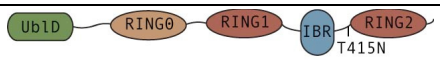	
			ΔUblD + T415N		
pET SUMO	6xHis smt3	Ulp1	ΔUblD		3.2, 4.2, 4.3, and all of 5
pET SUMO	6xHis smt3	Ulp1	321C		5.2 and 5.4
pET SUMO	6xHis smt3	Ulp1	Parkin-Thio		3.2
			ΔRING2	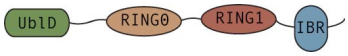	
pET SUMO	6xHis smt3	Ulp1	Parkin TEV	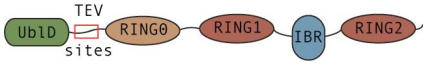	3.4.2
pET SUMO	6xHis smt3	Ulp1	95C		3.4.3
			UblD-Intein-CBD		
pET SUMO	6xHis smt3	Ulp1	UblD		4.2
			UblD K48A		
			V5-UblD	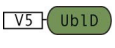	4.4
pRSF-T6	6xHis	-	6xHis-UblD	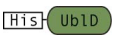 (6xHis tag was retained)	4.2
			6xHis-UblD K48A	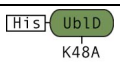 (6xHis tag was retained)	

pRSF-T6	6xHis	TEV protease	14-3-3η	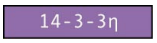	4.3
pRSF-T6	6xHis	-	6xHis-UBE2L3/ UbcH7	 (6xHis tag was retained)	4.3 and 5.3
			6xHis-UBE2L6/ UbcH8	 (6xHis tag was retained)	4.3
pRSF-T6	6xHis	-	6xHis-Ub (Wild type/WT)	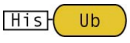 (6xHis tag was retained)	All sections
			F4A, L8A, I44A, V70A and D58A 6xHis-Ub	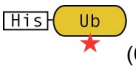 (6xHis tag was retained)	5.2 and 5.3
			K0, K48 and K63 6xHis-Ub	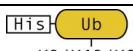 (6xHis tag was retained)	5.5

Table 5: List of expression constructs. Salient features of expression constructs used in this study are listed – parent vector, affinity purification tags, cleavage enzymes used to remove tags, construct name, cartoon representation of purified material (not to scale) and references to Results sections where the material is used are provided. pET SUMO (Invitrogen) and pRSF-T6 (modified pRSF Duet-1, Novogen) were the two parent vectors, both bear a kanamycin resistance gene and bacterial expression driven by a T7*lac* promoter. N-terminal hexa-histidine (6xHis) tag serves as an affinity purification tag in both vectors and in addition, pET SUMO vector features the smt3 (Small Ubiquitin-like Modifier/SUMO, *S. cerevisiae*) solubility tag, cleavable by ubiquitin-like-specific protease 1 (Ulp1). Tobacco etch virus (TEV) protease is used to cleave 6xHis tag from recombinant protein expressed by the pRSF-T6 constructs. Construct names and cartoons (not to scale) refer to purified recombinant material used in the respective experimental sections. 6xHis affinity tags are retained where required. Approximate domain location and nature of point mutations are described or indicated by red stars. Details of TEV sites of the Parkin TEV constructs are presented in section 3.4.2. Parkin domains are: Ubiquitin-like Domain (UblD, green), Really Interesting New Gene 1 and 2 (RING, dark brown), In-Between Ring (IBR, violet) and RING0 (light brown). Ub is ubiquitin, V5 is an epitope tag – GKPIPNPLLGLDST, Thio is Thioredoxin, Intein is the Mxe GyrA Intein (*Mycobacterium xenopi*) protein and CBD is chitin binding protein.

In addition, the pET RSF Duet-1 (Novagen) vector was modified to incorporate the TEV protease site (ENLYFQ|GS, TEV protease cleaves between residues Q and G). The original vector bore two multiple cloning sites (MCS 1 and 2)) each driven by a set of regulatory elements (T7 promoter, *lac* operator, and ribosome binding site (rbs)). A 6xHis coding sequence preceded MCS1 while S tag (KETAAAKFERQHMDS) coding sequence succeeded MCS2. The vector was modified to incorporate a TEV protease site coding sequence upstream of MCS1 and downstream of 6xHis coding sequence between the 6xHis and MCS1, using the Phusion® Mutagenesis kit. The resulting vector, called pET RSF T6, was used as destination vector following the Restriction-free (RF) cloning technique (van den Ent and Lowe, 2006).

Briefly, the RF cloning technique followed a two-step protocol; amplification of target gene by polymerase chain reaction (PCR) followed by a linear amplification reaction. Primers (50bases) were designed such that the 5' half (first 25 bases) and 3'half (last 25 bases) of each primer were complementary to the regions flanking the insertion site (on the destination vector) and fragment of interest (on the template DNA) respectively. The first set of PCR reactions (RF step I) with template DNA (that contained the fragment of interest) and the long primers resulted in a PCR product encoding the region of interest, flanked by 25 base pair sequences complementary to the destination vector. This PCR product functions as the primer pair for the destination vector and extends around the circular plasmid during a linear amplification reaction (RF step II), thus incorporating the PCR fragment into the destination vector (refer (van den Ent and Lowe, 2006) for more details).

In this study, the pET RSF T6 vector served as destination vector for majority for RF cloning reactions, while the MCS1 region (downstream of the 6xHis-TEV protease site encoding sequence) served as the site for insertion. Expression constructs for 6xHis tagged versions of ubiquitin, 14-3-3η, UBE2L3/UbcH7 and UBEL6/UbcH8 were generated using the RF cloning method, each with TEV protease site to enable cleavage of the N-terminal affinity tag. Complementary DNA (cDNA) clones for Ubiquitin C (*H. sapiens,* IMAGE 4076286) and 14-3-3η (*H. sapiens,* IMAGE 3543571) were purchased from the IMAGE consortium, while E2s (*H. sapiens*) were available in the Walden lab. These served as template DNA for the RF step I reaction (Table 5). In addition, Ubiquitin mutants (K0, K48only, K63only, Phe4Ala, Leu8Ala, Ile44Ala, Val70Ala and Asp58Ala) were made using the Phusion® Mutagenesis kit and with assistance from Laurence Lewis (Walden Lab). Expression constructs for 6xHis-UblD and 6xHis-UblD K48A were generated through RF cloning method, using wild-type Parkin and K48A-Parkin constructs as template for the RF step I reaction. pThioHis A (Invitrogen) served as template for Thioredoxin, which was inserted at the C-terminal of Parkin resulting in the Parkin-Thio, construct. pTXB1 (New England Biolabs/NEB) served as template for the *Mycobacterium xenopi gyrA*

Intein gene (Mxe GyrA Intein) + Chitin Binding protein (CBD) + (STOP codon), all of which was inserted downstream of the Gly94 codon in wild type Parkin to give UblD-Intein-CBD construct (Table 5). Furthermore, the RF primers were designed such that upon incorporation of the Intein-CBD coding sequence, the glycine 94 would be mutated to an alanine. The presence of an alanine would improve the autocatalytic cleavage of the C-terminal Intein, as recommended in the IMPACT (Intein Mediated Purification with an Affinity Chitin-binding Tag, New England Biolabs) manual.

Step		**Mutagenesis**		**RF**	
Initial denaturation		98˚C for 30 s		95˚C for 10 s	
Loop	*Denaturing*	25-30x	98˚C for 10 s	35x	95˚C for 10 s
	Annealing		66˚C for 30 s		55˚C for 10 s
	Elongation		72˚C for 30 s per kilobase		68˚C for 120 s per kilobase
Final elongation		72˚C for (*Elongation* time + 30 s)		-	

Table 6: Thermal cycler reaction programs. Reaction programs used for Mutagenesis and Restriction-free (RF) cloning reactions. The same program was used to both steps of the RF method, however elongation times for RF step II were calculated based on total size of the insert and destination vector.

PCRs were carried out in 50 µL reactions comprising of - 0.1 Unit Phusion® High-Fidelity DNA Polymerase (Finnzymes), 1x of associated enzyme buffer, 200 µM deoxynucleotide triphosphates (dNTPs), 0.5 µM of each primer, 3% Dimethyl sulfoxide (DMSO) and 2-10 ng of template DNA. Thermal cycling reactions (Eppendorf) (Table 6) were carried out in either TC-312 (Techne) or GS1 (G-Storm) thermal cyclers, in using thin-walled PCR tubes (Eppendorf). Reaction products were analysed by agarose gel electrophoresis in Tris-Acetate- Ethylenediaminetetraacetic acid (EDTA)/TAE buffer (40 mM Tris Acetate and 1 mM EDTA). Mutagenesis reactions were ligated using Rapid DNA Ligation Kit (Roche) as per manufacturer's protocol. RF step I products were subject to a reaction clean up using QIAquick PCR Purification Kit (Qiagen) prior to RF step II. 'Linear amplification' products of RF step II were

subject to *Dpn1* digestion (to eliminate any unmodified destination vector) for 2 hours at 37˚C before transformation into suitable host cells.

Transformation of mutagenesis/RF products was carried out using chemically competent MAX Efficiency® DH5α™ Competent Cells (Invitrogen) as per manufacturer's protocol and plated on antibiotic selective Luria Broth (LB) agar plates. Colonies were picked, grown overnight in LB (4 mL cultures) for plasmid DNA preparation using QIAprep Spin Miniprep Kit or outsourced to Equipment Park (plasmid DNA prep service, part of the LIF core facility). DNA sequencing using BigDye terminator reactions and capillary sequencing (Applied Biosystems 3730 DNA Analyser) was carried out by Equipment Park. Quality of sequence data was analysed using 4Peaks software while sequence alignments with template (using MegAlign, Lasergene software suite) were carried out to verify results of the intended cloning/mutagenesis experiment. Positive constructs were transformed (40-50 ng of plasmid DNA per transformation) into chemically competent BL21 (DE3) (Stratagene) *E. coli* expression strains (as per manufacturer's protocol), grown overnight (5ml Luria Broth (LB) with 50 μg/mL kanamycin) and an aliquot of the overnight culture was frozen in cryovials (Corning) as 20% v/v glycerol stocks and stored at -80˚C. Plasmid DNA stocks each construct were also maintained at -20˚C.

2.2 Expression and Purification of Proteins

2.2.1 Purification of Parkin (RING domain) constructs

The expression and purification of the wild type/WT Parkin construct was previously established in the Walden Lab by Simon Leslie. The original protocol was successfully adopted, in its entirety, for all pET SUMO based Parkin constructs containing a RING domain. The expression and purification protocols for pET SUMO based UblD constructs (WT, K48A mutant, and V5 tagged species) are described in section 2.2.2.

2.2.1.1 Growth, Expression and Harvest of cells

Expression preps were normally carried out in 6/12 L Luria Broth (LB) culture volumes. A starter culture (50-100 mL LB with 50 μg/mL kanamycin), initiated from fresh transformations of the desired constructs, was grown at 37˚C shaking at 190 rpm. This involved transformation (40-50 ng of the construct plasmid) into chemically competent BL21 (DE3) (Stratagene) *E. coli* expression strains (following manufacturer's protocol) and the entire transformation reaction (transformed cells in super optimal broth (SOC) media) was used to inoculate the starter culture. After overnight growth, 5 mL of this culture was used to inoculate 1 L LB media (with 50 μg/mL kanamycin) held in a 2 L flask. For constructs that comprised of a RING domain, the media was further supplemented with 500 μM zinc chloride.

Cultures were grown at 37°C shaking at 190 rpm until optical density at 600 nm (OD_{600}) reaches 0.4 (roughly 2.5-3 hours). Incubator temperature was lowered to 16˚C and cultures were allowed to grow shaking at 190 rpm until OD_{600} of 0.7-0.8 (roughly 1-1.5 hours after). At this point, protein expression was induced using 25μM Isopropyl β-D-1-thiogalactopyranoside (IPTG). Cultures were grown for another 12-14 hours (overnight) at 16°C shaking at 190 rpm. Cells were harvested by centrifugation at 4000 RCF using Beckmann JS4.2 rotor (J6MC centrifuge) for 15 min at 4˚C. From this stage onwards, samples were maintained at 4˚C or chilled in an ice-bucket (wherever possible).

2.2.1.2 Extraction of soluble material and affinity purification

Harvested cell pellets were re-suspended in cold T500i buffer (75 mM Tris pH 8.0, 500 mM NaCl, 25 mM imidaizole, 250 μM tris (2-carboxyethyl) phosphine (TCEP), 5 mL T500i buffer/1 L cell culture pellet) supplemented with Complete-EDTA free protease inhibitor cocktail tablets (Roche) (1 tablet for every 20ml of T500i buffer used for re-suspension). Re-suspended cells were transferred in pre-chilled 50 mL Falcon tubes (Corning, ≤ 15 mL/falcon) or 100 mL Duran bottles (≤ 40 mL/bottle) depending on the total volume of the re-suspension.

The re-suspended cells (maintained in ice-bucket), were burst open by sonication (Soniprep 150 set at 15 microns amplitude using 19 millimetre probe) - 15-20 s pluses (for Flacon volumes)/ 40-60 s pulses (for bottle volumes), repeated 5-6 times with intermittent pauses (1 min). Subsequently samples were transferred into pre-chilled Oak ridge centrifuge tubes (Nalgene) and clarified by centrifugation at 37000 RCF for 45 min at 4°C using the F0630 fixed angle rotor (Allegra X-24R centrifuge). The supernatants of the high-speed centrifugation step contain soluble fraction of the affinity tagged recombinant protein (6xHis-smt3-(Parkin species).

Supernatants were bound to Nickel-nitrilotriacetic acid (Ni-NTA) beads (Qiagen) pre-equilibrated with T500i buffer, by batch binding method (1 mL of Ni-NTA beads was sufficient for material obtained from a 3 L culture). Binding was carried out in 50 mL Falcon tubes placed on a roller at 4°C. After 30 min of binding, the unbound flow-through was collected, beads were washed with 10 column volumes (cv) of T500i buffer, and flow-through sample was reapplied to beads. The 'bind-wash-bind' step was repeated 3-4 times and enabled enrichment of the affinity tagged material.

2.2.1.3 Affinity tag cleavage and sample concentration

Ni-NTA beads bound with 6xHis-smt3- tagged Parkin species were equilibrated with T200 buffer (50 mM Tris pH 8.0, 200 mM NaCl, 250 µM TCEP) and were subject to on-cleavage with Ulp1. The beads were made up to a 50% v/v suspension (in T200 buffer), the requisite amount of Ulp1 protease was added (1mg of Ulp1 for every mL of Ni-NTA beads) and the cleavage reaction was allowed to proceed overnight at 4°C on a roller. Ulp1 is a cysteine protease that specifically cleaves the smt3/SUMO moiety at its C-terminus, releasing the C-terminally fused protein (in this case, a Parkin species). Furthermore, the 6xHis-smt3 tag remained bound to the Ni-NTA resin while, the cleaved protein is collected in the flow-through.

Following the cleavage reaction, samples were loaded onto a clean glass column and the cleavage flow-through was collected. The beads were further washed with 10 cv of T500i buffer in order to extract any cleaved material bound non-specifically to the beads. Cleavage flow-through and wash fractions, containing the cleaved or 'de-tagged' Parkin species, were pooled and the material was concentrated using appropriate Centriprep concentrators (Millipore) – YM10 (10 kDa molecular weight cut-off (MWCO)) for 321C and YM30 (30 kDa MWCO) for all other Parkin RING domain based constructs

2.2.1.4 Size Exclusion Chromatography (SEC)

Samples containing 'de-tagged' Parkin species were concentrated until the final volume is ≤1.5 mL. Concentrated samples were further purified by SEC runs (Superdex 75 16/60pg or 100/300 GL for 321C species, Superdex 200 26/60pg for all other RING domain based constructs) using the ÄKTApurifier™ fast protein liquid chromatography (FPLC) system (GE Healthcare). Wild type Parkin, various point mutants and domain truncation/deletion species of Parkin (except 321C, discussed in 2.2.1.5), eluted off the SEC as monomers (Figure 23). Sodium dodecyl sulfate – polyacrylamide gel electrophoresis analysis (SDS-PAGE) of SEC elutes confirmed a purity of >95% for all Parkin species.

Protein quantifications were carried out using NanoDrop® ND-1000 UV-Vis Spectrophotometer. Theoretical extinction coefficients (ε) and protein molecular weights, calculated using ProtParam software (http://www.expasy.ch/tools/protparam.html) were used to determine protein concentrations. Pure protein (in T200 buffer containing 10% v/v glycerol) was flash-frozen using liquid nitrogen and stored at -80°C. Protein yields/litre of LB culture; 2-3 mg/L for 321C, 1-1.5 mg/L for wild type, V15M-, K32A-, R33Q-, I44A-, K48A-, R51P, K161N-, S131E-, S131E + K48A Parkin species as well as the ΔUblD, 95C truncations and Parkin-Thio construct. Low yielding constructs (0.5 – 0.8 mg/L) include K27N-, R42P-, A46P-, T240R-, T415N-, ΔUblD + T415N Parkin and the ΔRING2.

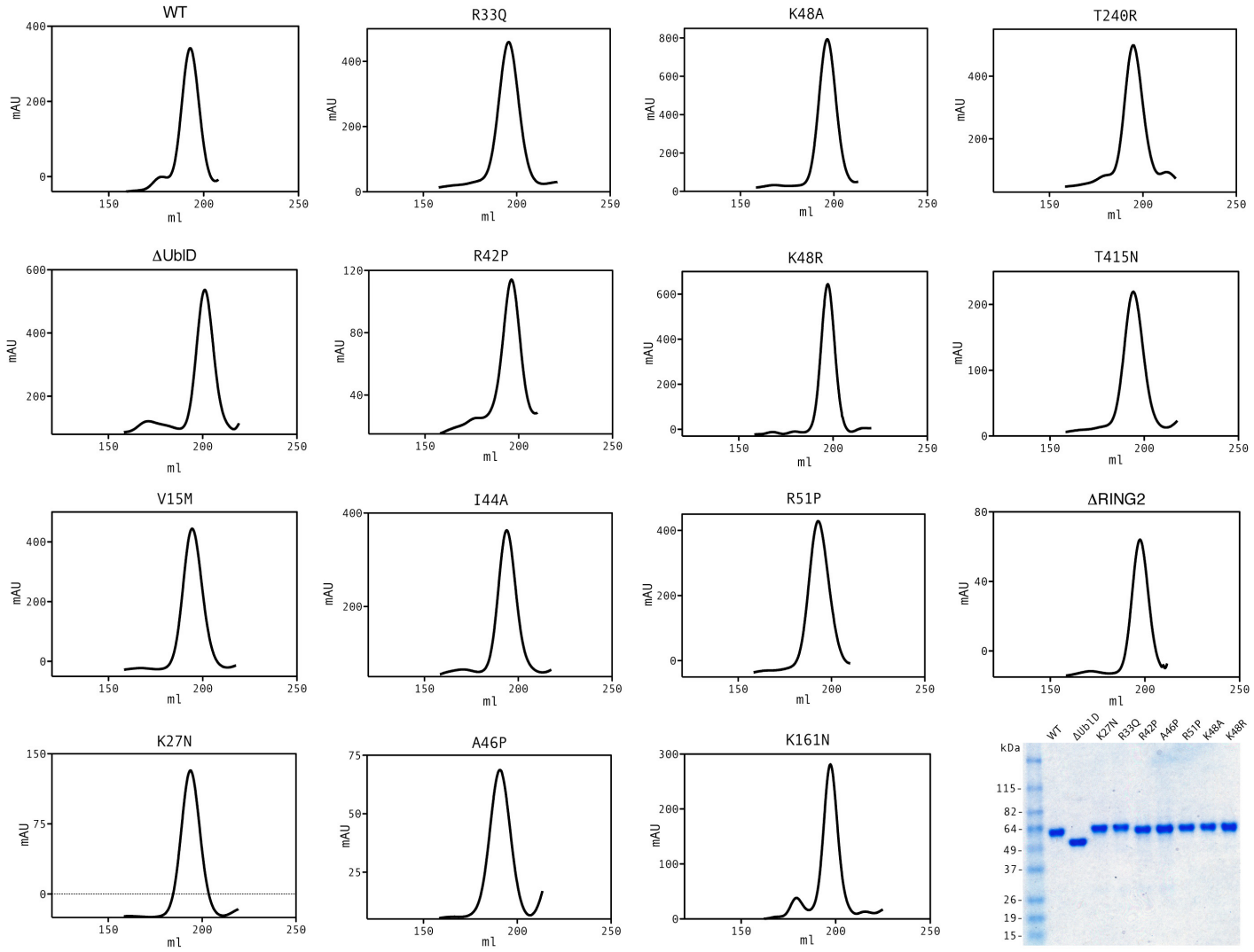

Figure 23: Parkin traces. Results of size exclusion chromatography (SEC) runs for a selection of Parkin species are shown with the species name displayed above each trace. Values on the x-axis indicate elution volumes (in mL) while the y-axis indicate UV absorbance (in milliabsorbance units/mAu). All traces depict quantity of material purified from 6 L LB preps (except T240R and T415N which were 12 L preps each). Parkin species were resolved using the Superdex 200 26/60pg column in 50mM Tris pH 8.0, 200 mM NaCl and 250 μM tris (2-carboxyethyl) phosphine (TCEP) buffer. Coomassie stained gel (bottom right) depicts the input amounts of Parkin species used in auto-ubiquitination assays (1 μg per lane). Traces were generated using GraphPad Prism 5.0c (GraphPad Software, San Diego California).

2.2.1.5 Additional features of the 321C Parkin prep

During SEC purification of the 321C Parkin species (MW ~16 kDa, pI 5.85), majority of the protein appeared to migrate as a monomer however partial oligomerisation was also observed (Figure 47). The nature of 321C oligomeric species was also explored through SEC experiments using the Superdex 75 10/300 GL column. Dilutions of the 'oligomer' (0.5, 1, 2 and 5 mg/mL) and increasing concentrations of the 'monomer' (2, 5, 10 and 15 mg/mL) were separately analysed by SEC to determine if the two species had a concentration dependent dynamic equilibrium. Run were conducted in T200 buffer as was the case during the purification of 321C. However, no changes were observed in SEC profiles and two species eluted at their respective volumes (9.5 – 10.5 mL for oligomer and 11.5 to 12.5 mL for monomer).

The oligomeric species could just be a facet of the over-expression in *E. coli*. Another possibility could be the truncated nature of 321C, thus potentially exposing binding surfaces (normally occupied by the N-terminal regions of Parkin) contributing to soluble aggregation. Further investigations are required to understand the oligomerisation properties of 321C. As monomeric 321C retained its monomer nature even at high concentrations (~1 mM) and was the major species of the SEC purification step, all experiments involving 321C were carried out using the monomer fraction.

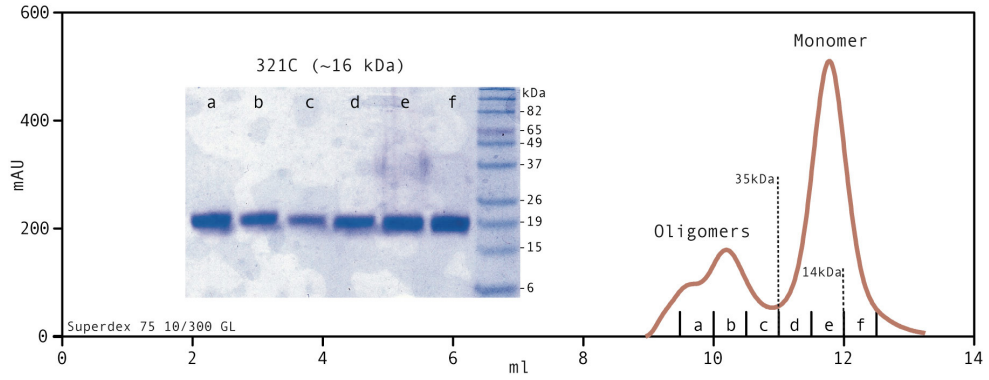

Figure 24: Multiple states of 321C. A chromatogram trace of a Superdex 75 10/300 GL run showing multiple states of 321C (~16 kDa, calibration markers for 14 kDa and 35 kDa are shown for reference) and coomassie blue stained gel (inset) of indicated fractions (9.5 to 12.5 mL – a, b, c, d, e and f) showing purity of protein sample. Protein contained in fractions e and f (11.5 to 12.5 mL) were pooled and used as monomeric Parkin. 321C material was run in 50mM Tris pH 8.0, 200 mM NaCl and 250 μM tris (2-carboxyethyl) phosphine (TCEP) buffer. Traces were generated using GraphPad Prism 5.0c (GraphPad Software, San Diego California).

A small portion of 6xHis-smt3 tag (MW 13.5 kDa, pI 5.87) was also observed to leach off Ni-NTA beads during the Ulp1 mediated on-column cleavage reaction (2.2.1.3) and co-migrated with 321C 'monomer' during SEC as well as on SDS-PAGE analysis. To ensure pure 321C material, the pooled 'monomeric' fractions were subject to an additional affinity purification step using fresh Ni-NTA beads (~1 mL) to separate the 6xHis-smt3 moiety from 321C. Flow-through of this step was further subject to anti-His western blot to confirm the absence of the 6xHis-smt3 moiety.

In addition, remnants of Ulp1 (MW - 25.5 kDa, pI 6.75) were occasionally observed to co-migrate with the monomeric fraction. The monomeric fractions off the SEC step were pooled and buffer exchanged with T25 buffer (100mM Tris pH 8.5, 25 mM NaCl, 250 µM TCEP). Subsequently, an anion exchange chromatography step was carried out to separate the two species. The buffer exchanged protein was loaded on to a MonoQ GL 5/50 (GE Healthcare) column and subject to an elution gradient (25 - 750 mM NaCl) stretching over 20 cv using ÄKTApurifier™ FPLC system. 321C was observed to elute between 120-150 mM salt while the Ulp1 eluted earlier (between 50-70 mM salt) thus resulting in 321C material devoid of Ulp1. In summary, certain additional purifications steps were required to ensure purity of >95% for the 321C material. Protein quantifications were carried out using NanoDrop® ND-1000 UV-Vis Spectrophotometer using values MW - 16 KDa and ε - 30000 (estimated using ProtParam). Pure protein (in T200 buffer containing 10% v/v glycerol) was flash-frozen using liquid nitrogen and stored at -80°C.

2.2.2 Purification of 6xHis tagged constructs

The following protocol applies to all pRSF-T6 based constructs listed in Table5 (6xHis-UblD, 6xHis-UblD K48A, 14-3-3η, 6xHis-UBE2L3/UbcH7, 6xHis-UBE2L6/UbcH8 and 6xHis-Ubiquitin (WT, and mutants) as well as the pET-SUMO based UblD constructs (UblD, UblD K48A, V5-UblD). All constructs (with the exception of 6xHis-UblD K48A) yielded healthy amounts of pure material (2-

5mg/litre of LB culture) thus prep were carried out in culture volumes of 2-4L LB (depending on downstream requirement). Expression and affinity purification of the above constructs followed a similar protocol as described in sections 2.2.1.1 to 2.2.1.2 with few changes at certain steps. Cell cultures were allowed to grow at 37˚C with shaking at 190 rpm until OD_{600} reached 0.6, at which point incubator temperature was reduced to 16˚C and protein expression was induced with 0.5 mM IPTG. Extracts containing soluble over-expressed 6xHis tagged protein were obtained and affinity purification of the tagged species following Ni-NTA batch method was carried out (as in section 2.2.1.2). The following sections describe the subsequent purifications steps for the respective construct.

2.2.2.1 Purification of Ubiquitin and E2s

Ni-NTA beads bound with 6xHis- Ubiquitin species/E2 species were equilibrated in T200 buffer and proteins were batch eluted with imidazole (2x5 cv of T200i buffer). Elutes rich in 6xHis tagged proteins were pooled, and concentrated to final volume of <5 mL. All protein concentration steps for Ubiquitin species were carried out with Amicon Ultra-15 (Millipore) Ultracel-3 (3 kDa MWCO) concentrators while the E2 species were concentrated using the Utracel-10 (10 kDa MWCO). A further SEC step (Superdex 75 16/60pg) was undertaken to polish off the purification. Ubiquitin species were mainly used for *in vitro* ubiquitination reactions thus 6xHis tags were retained as they served as a useful epitope for western blot detection of the ubiquitinated products.

Protein yields of 4-5 mg/litre of LB culture were observed for all the ubiquitin species expressed. 6xHis-E2s species (yields of 2-3 mg/litre of LB culture) were used as baits in pull-down assays (results section 4.3) and in thioester discharge assays (results section 5.2), both of which required the 6xHis tag to be retained. Protein quantifications were carried out using NanoDrop® ND-1000 UV-Vis Spectrophotometer using the given values for MW and ε (estimated using ProtParam); 6xHis-Ubiquitin (WT and mutants): MW - 10.9 KDa and ε -

1500, 6xHis-UBE2L3/UbcH7: MW - 20.9 KDa and ε - 19900, UBE2L6/UbcH8: MW - 19.9 and ε - 18500. Pure protein (in T200 buffer containing 10% v/v glycerol) was flash-frozen using liquid nitrogen and stored at -80°C.

2.2.2.2 Purification of 14-3-3η

The recombinant fusion protein 6xHis-14-3-3η was batch eluted using T200i buffer as described above. Eluted protein was diluted to a final imidazole concentration of <50 mM and concentrated to final volume of <5 mL using Amicon Ultra-15 (Millipore) Ultracel-10 (10 kDa MWCO) concentrators. The 6xHis-14-3-3η fusion protein was subject to TEV protease action (1mg of 6xHis-TEV protease was used to cleave 10mg of the fusion protein) to cleave the N-terminal 6xHis affinity tag. Cleavage reaction was allowed to proceed overnight at 4°C on a roller. The cleavage reaction sample was further purified using SEC (Superdex 200 26/60pg) where the 14-3-3η was observed to run as a dimer. Fractions with pure protein were pooled and subject to an additional affinity purification step using fresh Ni-NTA beads (~1 mL) to eliminate uncleaved fusion protein and 6xHis-TEV protease. Protein quantifications was carried out using NanoDrop® ND-1000 UV-Vis Spectrophotometer using the given values for MW and ε (estimated using ProtParam) using values MW – 28.2 KDa and ε - 28900. Pure protein (in T200 buffer containing 10% v/v glycerol) was flash-frozen using liquid nitrogen and stored at -80°C.

2.2.2.3 Purification of UblD constructs

Affinity purified material from the pRSF-T6 based UblD constructs (6xHis-UblD and 6xHis-UblD K48A) were batch eluted off the Ni-NTA beads using T200i. Subsequent steps in purification were similar to that for ubiquitin (described in section 2.2.2.1). In contrast, affinity purified material from the pET-SUMO based UblD constructs (UblD, UblD K48A, V5-UblD) were not eluted and instead subject to Ulp1 mediated on-column cleavage reactions, as descried in section 2.2.1.3. A further SEC step (Superdex 75 16/60pg) was undertaken to polish off the purification (as described in 2.2.2.1). Amicon Ultra-15 (Millipore) Ultracel-3

(3 kDa MWCO) protein concentrators were successfully used for concentrating all recombinant proteins described in this section. During the purification process, it was observed that UblD (WT or K48A mutant), when in solution, was susceptible to precipitate at protein concentrations approaching 8-10 mg/mL. Attempts to stabilize the protein by the incorporation of glycerol (5% v/v), changing buffers (50 mM (4-(2-hydroxyethyl)-1-piperazineethanesulfonic acid (HEPES) pH 8.0 or phosphate buffered saline (3.2 mM Na_2HPO_4, 0.5 mM KH_2PO_4, 1.3 mM KCl, 135 mM NaCl, pH 7.4)) or changing salt (200-500 mM NaCl or potassium chloride (KCl)) however proved unsuccessful. Thus, during UblD based experiments, care was taken to ensure the protein concentrations of UblD species did not exceed 8 mg/mL.

Protein yields of 1.5-2 mg/litre of LB culture were observed for all UblD based constructs except 6xHisUblD K48A (0.5-1 mg/litre of LB culture). 6xHis-UblD species (WT and K48A) were used as baits in pull down assays while native UblD and UblD K48A were used in K48A-Parkin interaction experiments both of which are described in results section 4.2). V5-UblD was used for peptide array interaction experiments (results section 4.4). Protein quantifications were carried out using NanoDrop® ND-1000 UV-Vis Spectrophotometer using the given values for MW and ε (estimated using ProtParam); 6xHis-UblD (WT and K48A): MW - 11.1 KDa and ε - 12500, UblD (WT and K48A): MW – 8.8 KDa and ε - 11000, V5-UblD: MW – 10.4 and ε - 11000. Pure protein (in T200 buffer containing 10% v/v glycerol) was flash-frozen using liquid nitrogen and stored at -80°C.

2.2.3 Expressed Protein ligation.

The 95C construct of Parkin was expressed and purified as described in section 2.2.1. Expression, affinity purification and Ulp1 mediated on-column cleavage reaction of UblD-Intein-CBD fusion construct was carried out as described in 2.2.1.1 to 2.2.1.3. The flow-through of Ulp1 cleavage (UblD-Intein-CBD, in T200 buffer) was incubated with 10 mM 2-Mercaptoethanesulfonic acid (MESNA,

Sigma) at room temperature for 4-6 hours followed by an overnight incubation at 4˚C. MESNA is a thiol regent that induces autocatalytic cleavage of the Intein-CBD tag located at the C-terminus of the construct (Figure 32A). The protein products of a complete reaction would be 1-94M (UblD with C-terminal thioester derivative) and Intein-CBD tag. A Gly94Ala mutation was also made to improve autocatalytic cleavage of the C-terminal Intein as was suggested in the IMPACT manual (described in 2.1). However, despite the extended MESNA treatment and the Gly94Ala mutation, only about 10-15% of the UblD-Intein-CBD fusion was cleaved to release the 1-94M molecule (yield of 0.8-1 mg from a 4 L prep). Following MESNA treatment, free Intein-CBD tag and unprocessed UblD-Intein-CBD fusion protein was bound to Chitin affinity beads (NEB, binding capacity of 2mg/mL of resin) based on suppliers protocol. An additional SEC step (Superdex 75 10/300 GL) was undertaken in EPL buffer - 100mM Tris pH 8.5, 25 mM NaCl, in order to separate any left over Ulp1, polish up the purification as well as serve as a buffer exchange step

Chemical ligation reactions containing 1-94M with 95C (10:1 molar ratio) and 95C only were carried out overnight at 16˚C in EPL buffer + 10mM MESNA resulting in the formation of Parkin EPL species in the former reaction. The ligation however was not complete and only about 15-20% of the input 95C was observed ligated with 1-94M species resulting in a mixture of 95C and Parkin EPL species. Subsequently, a SEC (SD75 10/300 GL) run separated the unligated 1-94M species, however residual 95C (pI 6.9) species could not be completely separated from Parkin EPL (pI 7.0) despite an anion exchange chromatography step (25-500 mM salt gradient). Samples of freshly prepared 95C and Parkin EPL mixture and the MESNA treated 95C species were used for auto-ubiquitination analysis.

2.3 *In vitro* Ubiquitination assays

2.3.1 Auto-ubiquitination assays

Auto-ubiquitination can be described as an event where an enzyme (usually an ubiquitin E3 ligase or in certain cases ubiquitin conjugating enzyme/E2) catalyses its own ubiquitination. In this study, the auto-ubiquitination properties of Parkin, a RING E3 ligase were explored. The auto-ubiquitination event can be recreated in a test tube reaction wherein purified proteins that make up the basic components of the ubiquitination machinery (ubiquitin, E1, E2 and E3/Parkin, Figure 1), are mixed together in an appropriate buffer (alkaline pH, $MgCl_2$), provided an energy source (ATP) and temperature (37˚C) to facilitate ubiquitination. The reaction protocols used in this study were adapted from (Matsuda et al., 2006). Reaction components were either purchased from Boston Biochem (human recombinant E1/UBA1, ubiquitin E2s: UBE2L3/UbcH7, UBE2L6/UbcH8, UBE2N/UBE2V1 (Ubc13/UEV1) heterodimer, 6xHis-UBE2G2/Ubc7 and UBE2D2/Ubc5B) or purified in-house (6xHis-Ubiquitin (WT and mutants) and Parkin (various species, Table5). Compositions of a typical reaction are described in Table 7.

Component (working stock concentrations)	**Volume / 25 µL reaction**	**Final concentration**
Reaction buffer 10x (500 mM Tris pH 8.0, 20 mM DTT, 50 mM $MgCl_2$)	2.5 µL	1x - 50 mM Tris pH 8.0, 2 mM DTT, 5 mM $MgCl_2$
ATP (25 mM)	4 µL	4 mM
Glycerol (75% v/v)	1.2 µL	~ 5%
E1/UBA1 (110 kDa, 227 nM)	1.6 µL	15 nM
E2 - UBE2L3/UbcH7 (18 kDa, 14 µM)	2 µL	1.1 µM
6xHis-Ubiquitin (10.9 kDa, 184 µM)	0.7 µL	5 µM
E3 - various Parkin species	1-2 µL	0.77 – 1 µM
Water	11-12 µL	-

Table 7: Auto-ubiquitination assay. Setup of a typical auto-ubiquitination assay is described. Components are listed along with their molecular weights (protein) and concentrations of their working stocks. Also shown are volumes of each component used for 25 µL assay reactions and the final concentrations of each component. Final concentration of glycerol takes into account glycerol contributions from E2 and E3 buffer solutions. All other E2s were used at 1.1 µM except for UBE2N/UBE2V1 (Ubc13/UEV1) heterodimer (0.5 µM). Ubiquitin concentrations were constant irrespective of species used. Full-length Parkin (wild type and mutants) and Parkin-Thio species were used at 0.77 µM, while Parkin truncations/deletion (ΔUblD, ΔRING2 and 321C) were at 1 µM. Reactions were carried out at 37˚C for an hour.

Working stocks of reaction components were made for efficient assay setup, and stored at -80˚C. E1 and Ubiquitin (WT and mutants) were stored in 50 mM HEPES pH8.0, E2s in 50 mM HEPES pH 8.0, 50 mM NaCl, 10% (v/v) glycerol, 1mM DTT while E3 (Parkin species) were stored in 50 mM Tris pH 8.0, 200 mM NaCl, 250 µM TCEP, 10% (v/v) glycerol. All reactions were conducted in 25 µL volumes containing 50 mM Tris pH 8.0, 2 mM DTT, 5 mM $MgCl_2$, 4 mM ATP and 5% glycerol at 37˚C for an hour (unless specified otherwise). For assays with wild type Parkin and EPS15 UIMs (WT/ mutant) (section 3.4.1) as well as K48A Parkin and UblD (WT/K48A) (section 4.2), the indicated quantities of EPS15 UIMs species or UblD species were added and final reaction volume was made up to 25 µL with water. Reactions were terminated by boiling samples (100˚C) in 2X SDS loading buffer (150 mM Tris pH 6.8, 4% SDS, 10% glycerol, 200 mM β-mercaptoethanol (βME) and bromophenol blue) for 5 minutes. $1/20^{th}$ and $1/8^{th}$ of the reaction sample was subject to western blot analysis by anti-Parkin (Anti-Human Parkin (1A1) Mouse IgG Monoclonal, IBL) and anti-6xHis (Mouse monoclonal, GE Healthcare) antibodies respectively.

2.3.2 Thioester discharge assay

During ubiquitination, RING E3s catalyse the activation of the E2~ubiquitin thioester conjugate and the concomitant ligation of ubiquitin on the substrate. The rates of ubiquitin discharge from the E2~ubiquitin thioester conjugate can be monitored through a thioester discharge assay. The assay design is analogous to a pulse-chase experiment. The charging of an E2 with ubiquitin forms the pulse chase, followed by an arrest phase where the reaction is depleted of ATP and $MgCl_2$ thereby preventing any further formation of the E2~ubiquitin thioester conjugate (via E1) in the event of a discharge. The reaction is then chased by introduction of a RING E3, which enhances the activation/discharge of the E2~ubiquitin thioester conjugate. The experimental setup for this study (Results section 5.2) was adapted from (Ozkan et al., 2005)

Pulse reactions were setup as 50 µL reactions (300 nM E1, 2 µM 6xHis-E2, 50 µM 6xHis-Ubiquitin and 5 mM ATP in reaction buffer 50 mM HEPES pH 8.0, 2 mM DTT, 5 mM $MgCl_2$ as described in Table 8), and carried out at 37˚C for 10 minutes to facilitate the ubiquitin charging of the E2 (E2~ubiquitin). Subsequently, reactions were arrested by ATPase treatment (10 min at room temperature) and a buffer exchange process to remove $MgCl_2$. Addition of 2.5 units of Ayprase (Sigma, 0.1 units/µL) served as ATPase for this step, in the process taking up the total sample volume to 75 µL. Samples were buffer exchanged into 50 mM Tris pH 8.0, 50 mM NaCl using Zeba™ Spin Desalting Columns (Pierce) according to manufacturer's protocol.

Reaction Component	Volume (50 µL reaction)	Final Concentration
Reaction buffer 10x (500 mM Tris pH 8.0, 20 mM DTT, 50 mM $MgCl_2$)	5 µL	50 mM HEPES pH 8.0, 2 mM DTT, 5 mM $MgCl_2$
ATP (25 mM)	10 µL	5 mM
E1/UBA1 (110 kDa, 4 µM)	3.8 µL	304 nM
E2/6xHis-UBE2L3/UbcH7 (20.2 kDa, 12.4 µM)	8 µL	2 µM
6xHis-Ubiquitin (10.9 kDa, 184 µM)	13.6 µL	50 µM
Water	9.6 µL	-

Table 8: E2 charging reactions. Compositions of 'Pulse' reactions that facilitate charging of E2 (UBE2L3/UbcH7) with ubiquitin are described above. Components are listed along with their molecular weights (protein) and concentrations of their working stocks. Also shown are volumes of each component used for 50 µL assay reactions and the final concentrations of each component. E1/UBA1 is purchased from Boston Biochem, while 6xHis-UBE2L3/UbcH7 and 6xHis-Ubiquitin (various species) are purified in-house. Reaction mixtures were incubated at 37˚C for 10 minutes to facilitate formation of the thioester linked E2~ubiquitin conjugate.

Chase reactions were initiated by addition of 2 µM RING E3 (Parkin species) and total reaction volume was made up to 100 µL with buffer (50 mM Tris pH 8.0, 50 mM NaCl). 10 µL samples were collected at defined intervals and mixed with 10 µL 2xNon-Reducing sample buffer (NR sample buffer - 4 M Urea, 150 mM Tris pH 6.8, 5 mM EDTA, 2% SDS, 10% glycerol and bromophenol blue) to terminate reactions. In addition, a zero time point sample was collected in reducing conditions (2xNR sample buffer + 200 µM βME). $1/10^{th}$ of each time-point sample was subject to western blot analysis using anti-His antibody

(Mouse monoclonal, GE Healthcare) to observe rate of thioester discharge of the E2~ubiquitin (both bearing N-terminal 6xHis tags).

2.3.3 Western blotting/Immunoblotting

Indicated quantities of reaction products (auto-ubiquitination assay and time point samples of thioester discharge assay) were resolved by SDS-PAGE (125 volts for 85 min) using Novex® 8-16% Tris-Glycine Gels (1.5 mm, 10/15wells, Invitrogen) pre-cast gels. Protein transfers onto polyvinylidene fluoride (PVDF) or nitrocellulose membranes were carried out using iBlot® Dry Blotting System (Invitrogen) set at program P2 (23 volts for 7 min and 20 s). Blocking, antibody binding and washing of membranes were carried out using Tris-buffered saline (TBS - 20 mM Tris pH 7.5, 150 mM NaCl, 0.1% (v/v) Polysorbate 20/Tween20 (Sigma) supplemented with either 5% (w/v) milk or 3% (w/v) bovine serum albumin/BSA (Sigma) depending on antibody (refer Table 9).

<table>
<tr><th>Antibody</th><th>Host, Isotype</th><th>Dilution</th><th>Membrane</th><th>Buffer</th><th>Secondary (HRP) Antibody</th></tr>
<tr><td>Anti-Human Parkin (1A1, IBL)</td><td rowspan="2">Mouse IgG monoclonal</td><td>1/5000</td><td>PVDF</td><td rowspan="2">5% (w/v) Milk in TBS</td><td rowspan="2">polyclonal goat anti-mouse HRP - 1/1000 (DAKO)</td></tr>
<tr><td>Anti-His (GE Healthcare)</td><td>1/2000</td><td>PVDF</td></tr>
<tr><td>Anti-Human UblD (In-house/ Pettingill Technology)</td><td rowspan="2">Rabbit polyclonal anti- sera</td><td rowspan="2">1/5000</td><td rowspan="4">Nitrocellulose</td><td rowspan="5">3% (w/v) BSA in TBS</td><td rowspan="2">polyclonal goat anti-rabbit HRP - 1/1000 (DAKO)</td></tr>
<tr><td>Anti-Human IBR-RING2 (In-house/Pettingill Technology)</td></tr>
<tr><td>FK1 (Enzo Lifesciences)</td><td>Mouse IgM monoclonal</td><td rowspan="2">1/1000</td><td>Anti-mouse IgM HRP – 1/5000 (Abcam)</td></tr>
<tr><td>FK2 (Enzo Lifesciences)</td><td>Mouse IgG monoclonal, Biotin conjugate</td><td>Strep-tactin HRP - 1/4000 (IBA)</td></tr>
<tr><td>Anti-V5 HRP (Invitrogen)</td><td>Mouse IgG monoclonal HRP conjugate</td><td>1/5000</td><td>PVDF</td><td>-</td></tr>
</table>

Table 9: Antibody reference list. Features of all antibodies used in this study are listed including: antibody name and supplier, host species used to generate antibody, isotype and secondary modification (if any), working dilution for antibody, membrane preference, binding buffers used and associated secondary antibody. IgG and IgM are immunoglobin G and M respectively, PVDF is polyvinylidene fluoride, HRP is horseradish peroxidase, BSA is bovine serum albumin and TBS is Tris-buffered saline (20 mM Tris pH 7.5, 150 mM NaCl, 0.1% (v/v) Polysorbate 20/Tween20). Pettingill Technology Ltd generated polyclonal rabbit anti-sera against recombinant UblD and 321C.

Membranes were blocked at room temperature for an hour, followed by overnight incubation with primary antibody (at 4˚C). Membranes were washed three times (10 min each) with blocking buffer before binding of secondary antibody (diluted in blocking buffer) for 1-2 hours at room temperature. Membranes were washed as before and then developed using chemiluminescent reagents Amersham™ ECL Western Blotting Detection Reagents (GE Healthcare) and exposed to Amersham Hyperfilm ECL (GE Healthcare).

2.4 Protein interaction assays

2.4.1 Pull-down interaction assays

Pull-down assays involved immobilization of bait proteins, which were subsequently allowed to interact with different prey protein. The bait-prey complex was then subject to salt washes to determine an interaction preference of the bait for the prey. In this study, Ni-NTA beads were used to immobilise 6xHis tagged bait species and any associated prey was detected by SDS-PAGE coomassie staining/immunoblotting techniques. 40-50 μL Ni-NTA beads (maximum binding capacity of 8-10 μg/μL) were saturated with 6xHis-UblD bait species (WT or K48A). The baits were then incubated with 0.5mg of Parkin species (prey); wild type, K48A-Parkin and ΔUblD in 50 mM Tris pH 7.5, 25 mM NaCl, 250 μM TCEP, 5% glycerol, for 2-3 hours at 4˚C.

Beads were subsequently washed with in 10 cv of binding buffer followed by washes with increasing salt concentration. 10 μL beads were boiled with 2x SDS loading buffer after each wash, to be resolved by SDS PAGE and analysed by coomassie staining/western blotting (20x dilutions of each sample) techniques to compare binding preferences of the UblD species for each of the Parkin species (results section 4.2). A similar experiment was carried out using 6xHis-E2s (UBE2L3/UbcH7 or UBE2L6/UbcH8) as baits and Parkin prey

species wild type, ΔUblD, T240R-Parkin (for UBE2L3/UbcH7) or T415N-Parkin (for UBE2L6/UbcH8) (results section 4.3).

2.4.2 Peptide array interactions assays

Peptide arrays (30x20 spot grid) representing the 465 residues of human full-length Parkin as a series of overlapping peptides (21 residues), each individually spotted on cellulose membrane were synthesised by the Peptide Synthesis Laboratory, LRI (described in section 4.4). Arrays were activated for interaction assays by washing with 50% v/v Ethanol, 10% v/v glacial acetic acid solution (15 min) followed by several washes with array interaction buffer/ AI buffer (50mM Tris pH 8.0, 200 mM NaCl, 250 μM TCEP, 0.05% Polysorbate 20/Tween20). Recombinant UblD protein (purification described in section 2.2.2) was labelled at Cys59 using Fluorescein-5-Maleimide (Thermo Scientific) following manufacturer's protocol to generate the fluoro UblD probe while Fluorescein-N-Terminal Ubiquitin was commercially available (Boston Biochem) and was used as the fluoro Ub probe. V5-UblD was expressed and purified as described in section 2.2.2.

Protein probes (0.5mg of V5-UblD, 50 μg of fluoro UblD/Ub), diluted in 25 mL of AI buffer, were incubated with the array for 2-3 hrs at room temperature with continuous rocking. While using fluoro-probes, arrays were protected from prolonged exposure to direct light. Subsequently, 3-5 washes/10 min each) with interaction buffer were carried out to eliminate background and reduce non-specific interactions between the probe and membrane/peptides. Arrays treated with V5-UblD were detected via immunoblotting technique (as described in 2.3.3) using V5 HRP (Invitrogen) antibody. Peptide spots that gave a signal on the anti-V5 HRP blot suggested interactions between V5-UblD and the peptides. Fluoro-probes were detected using fluorescence image scanners (Molecular Dynamics STORM 860) and associated imaging software (ImageQuantTL) available at LIF Equipment Park.

Arrays were stripped of non-covalently bound proteins by incubating with stripping buffer (100 mM Tris pH 6.8, 6 M Guanidine Hydrochloride, 1% SDS, 100 mM βME) at 50˚C for 30 minutes with occasionally shaking. Subsequently, arrays were treated with several washes with water followed by re-activation of the array with 50% v/v Ethanol, 10% v/v glacial acetic acid. Protein stripping efficiency was examined by redetection with anti-V5 HRP. Stripping efficiency of arrays probed with fluoro UblD/Ub was poor thus preventing the re-use of the array. Fresh arrays were made in order to repeat the assays. Interaction assays were conducted at least twice and consistently positive spots were analysed as described in section 4.4.

2.4.3 Nuclear Magnetic Resonance (NMR) spectroscopy experiments

The heteronuclear single quantum coherence (HSQC) presented in this study were conducted with Prof. Gary S. Shaw's group at the University of Western Ontario, Canada. Parkin truncations (321C and ΔUblD) were expressed and purified in the Walden lab and shipped to Canada for these studies. ^{15}N-labelled UblD (Safadi and Shaw, 2007) and ubiquitin (Hamilton et al., 2001) samples were prepared by Dr. Kathryn R Barber based on previously published protocols, HSQC experiments were set up and carried out under the guidance of Prof. Shaw. A Bogue Research Fellowship awarded by University College London (UCL) supported the 7-week research visit.

Briefly, the experiment detects correlations between the ^{1}H atoms and the directly bonded NMR active ^{15}N (or ^{13}C) atoms (Maudsley and Ernst, 1977). The magnetic field experienced by the nucleus (and including those containing isotopically labeled atoms) is affected by the electron distribution around the nucleus (which includes covalently and non-covalently bound atoms). Variations in the local electron density (for example, due to residue-residue interactions during protein binding events) thus affect the local magnetic field, which is reflected in the resonant frequencies (or chemical shifts). These can be measured (in parts per million/ppm) with reference to an internal standard that

is not affected during the course of the experiment (Hammes, 2005). NMR samples prepared for HSQC analysis were ^{15}N -labeled and were hence used to detect any changes in local chemical environment of the amide backbone and side chain amino groups upon protein-protein interactions.

All NMR experiments were collected on a Varian Inova 600 MHz spectrometer equipped with a triple resonance probe using xyz gradients. ^{1}H-^{15}N HSQC spectra were collected using the sensitivity-enhanced method at 25ºC (Kay et al., 1992). Samples (400 µL) were setup in the absence and presence of unlabelled protein. ΔUblD samples: ^{15}N-labelled UblD (125 µM) and ^{15}N-labelled UblD (125 µM) with ΔUblD (125 µM), 321C-UblD samples: ^{15}N-labelled UblD (120 µM) in the absence and presence (3 samples) of 321C (40 µM, 120 µM and 200 µM), ^{15}N-labelled Ub (140 µM) in the presence (3 samples) of 321C (70 µM, 140 µM, 280 µM). All samples were set up in 20mM Tris pH 7.0, 150 mM NaCl, 1 mM DTT, 20 µM 4,4-dimethyl-4-silapentane-1-sulfonic acid (DSS) and 10% D_2O/90% H_2O. Identical spectral parameters were used to collect ^{1}H-^{15}N HSQC spectra of each set of samples (runs lasted about 85 minutes each). ^{1}H chemical shifts were referenced directly using a DSS internal standard. Spectra were processed using a 60º-shifted cosine bell weighting function in both ^{1}H and ^{15}N dimensions and baseline corrected using NMRPipe (Delaglio et al., 1995) and visualised using NMRView (Johnson and Blevins, 1994). Reference peak lists for ^{15}N-UblD and ^{15}N-Ub (from the Shaw lab) were used for automatic peak assignment (with minor manual adjustments) in NMRView, using tolerance levels of 0.2 and 0.02 parts per million (ppm) along nitrogen and proton dimensions respectively. Combined changes in chemical shifts were calculated using the equation $((\Delta\delta H)^2 + (0.2*\Delta\delta N)^2)^{1/2}$ and plotted as histograms using GraphPad Software, San Diego California). $\Delta\delta H$ and $\Delta\delta N$ represent change in proton and nitrogen chemical shifts.

The following chapters (Chapters 3-5) describe experiments carried out in this study and their results.

Chapter 3 Results: Regulation of Parkin's Auto-ubiquitination.

3.1 Background/Preliminary work

The groundwork for the biochemical characterisation of Parkin's E3 ligase had been carried out by Simon Leslie and Dr. Helen Walden before the start of this study. In particular, expression and purification protocols for recombinant human Parkin (wild type and 111C, a truncation that lacked the first 110 residues of Parkin) from *E. coli* were available. The use of a 6xHis-smt3 served the dual role of a solubility tag during expression of in *E. coli* and subsequent affinity (Ni-NTA) purification. More importantly, cleavage of the fusion protein with Ulp1, a cysteine protease that specifically cleaves the smt3/SUMO moiety at its C-terminus, generated Parkin species with no N-terminal sequence overhang. Wild type Parkin (51.7 kDa) purified in this manner migrated at 50-52 kDa when resolved by SDS-PAGE and eluted as a monomer at the corresponding molecular weight during SEC. In addition, 111C Parkin, originally designed based on a breakdown product observed with purified wild type Parkin when left at 4°C for 3-4 days, was expressed and purified using the same strategy.

Subsequently, *in vitro* auto-ubiquitination assays were undertaken to assess ligase activity of the purified material (wild type and 111C). The setup of such an assay included the reconstitution of basic components that make up the ubiquitination pathway (E1, E2, E3, ubiquitin) in a test tube reaction with an appropriate reaction buffer (alkaline condition, $MgCl_2$) and energy source (ATP) to facilitate the ubiquitination event (refer Methods 2.3.1). In contrast to ligase activity established in numerous reports ((Zhang et al., 2000, Corti et al., 2003, Fallon et al., 2006, Matsuda et al., 2006, Hampe et al., 2006, Chung et al., 2001, Olzmann et al., 2007) and others), full-length Parkin consistently lacked

auto-ubiquitination activity with UBE2L3/UbcH7. However, 111C Parkin when tested in a similar assay, was competent for auto-ubiquitination (data not shown). Matsuda and colleagues had earlier established *in vitro* auto-ubiquitination of MBP tagged Parkin with various E2s (Matsuda et al., 2006). Further, the report demonstrated that MBP IBR-RING2 (a Parkin truncation) ubiquitinated both the tag and Parkin polypeptide (presence of a Thrombin protease site between MBP and IBR-RING2 enabled the proteolytic uncoupling of the two proteins upon Thrombin action followed by immunoblotting analysis). However, when presented in *trans*, free/unbound MBP was not ubiquitinated by the MBP IBR-RING2. The authors suggest that MBP Parkin is 'primed' for E3 ligase activity with the N-terminal fusion tag operating as a pseudo-substrate.

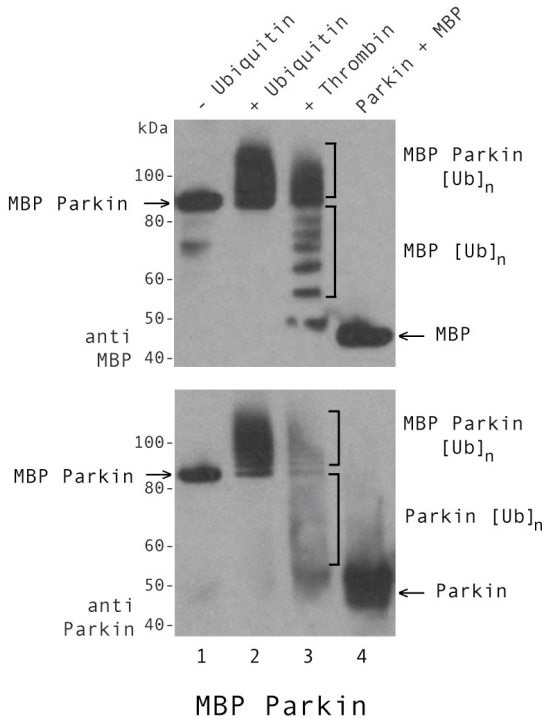

Figure 25: Ubiquitination of fusion tags. Results of auto-ubiquitination reactions with MBP Parkin show robust auto-ubiquitination of the fusion protein (lane 2, lane 1 has no ubiquitin). Reaction products were subject to thrombin to allow proteolytic uncoupling of MBP and Parkin. Immunoblots with Anti-Parkin and Anti-MBP reveal bulk of ubiquitination occurs on the MBP tag (lane 3). Auto-ubiquitination reactions with untagged Parkin in presence free MBP reveals an absence of any modification on either species (lane 4). Brackets indicate ubiquitination. MBP is Maltose binding protein. Reactions (25 µL), were carried out for 2 hours at 4˚C, thrombin cleavage was carried out overnight at 4˚C.

The experimental design was adapted in the Walden lab by Simon Leslie with tagged Parkin species; MBP-Thrombin protease site-Parkin (expression construct gifted by the Tanaka group), Glutathione S-transferase (GST)-TEV protease site-Parkin (purified from insect cell expression systems) and 6xHis-smt3 Parkin (Data not shown). Auto-ubiquitination reactions with MBP Parkin were set up in parallel with reactions containing untagged Parkin and free MBP (Figure 25). While the MBP Parkin fusion protein readily auto-ubiquitinated

(lane 2, Figure 25), with a majority of the ubiquitination occurring on the MBP tag (lane 3, Figure 25), auto-ubiquitination of the untagged Parkin (or ubiquitination of the free MBP tag) was absent. A similar profile was observed with GST-TEV protease site-Parkin and 6xHis-smt3 Parkin fusion proteins (data not shown). In summary, modifications to the N-terminus of Parkin (fusion tags/truncations) appear to positively influence the E3 ligase activity of Parkin. The following sections describe the experiments carried out, as part of this study, investigating how the N-terminal region of Parkin could influence the E3 ligase activity of Parkin.

3.2 Auto-ubiquitination activity

RING E3 ligase activity could be described as a bi-substrate enzymatic reaction, where the RING domain catalyses the activation of E2~ubiquitin thioester conjugate while concomitantly ligating the ubiquitin onto the substrate. In the same way, auto-ubiquitination could be described as an event where the RING E3 recognises itself as a substrate and catalyses self-ubiquitination. In both cases, the transfer of ubiquitin is a *trans* event, *i.e.* from E2 to substrate/E3. Auto-ubiquitination can thus be used to attest E3 ligase activity. The above observations presented an interesting model system where wild type Parkin did not recognize itself as a substrate. While, a truncation of the N-terminus (111C) or the presence of bulky N-terminal tags (MBP-, GST- and smt3-) appeared to facilitate auto-ubiquitination. At the minimum, the loss of the UblD (represented by 111C) appeared to permit the self-recognition and subsequent auto-ubiquitination of Parkin.

To further investigate the above findings, the following expression constructs were cloned through deletion/RF cloning mediated insertions (as described in methods 2.1) of the pET SUMO wild type/WT Parkin expression construct already available: ΔUblD (Gly77 to C-terminus), ΔRING2 (Lys413X, similar to the pathogenic truncation Glu409X) and Parkin-Thio (Parkin with a C-terminal

Thioredoxin tag). The above constructs were expressed and purified based on protocols established in the Walden group, and tested alongside wild type Parkin in auto-ubiquitination assays with UBE2L3/UbcH7 (Figure 26).

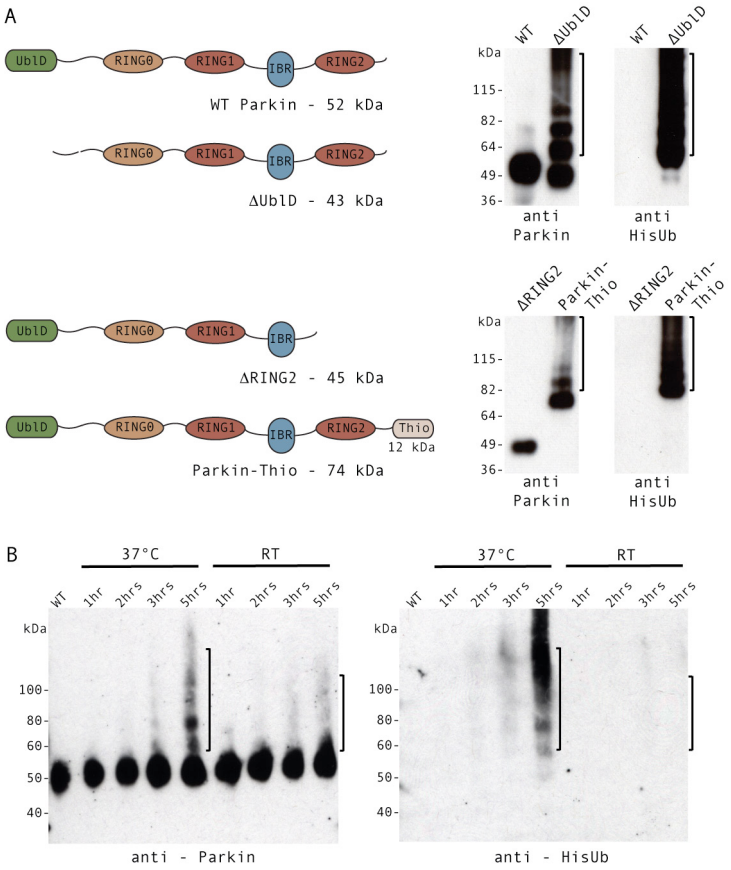

Figure 26: Parkin's auto-ubiquitination profile. A. The presence (wild type/WT Parkin) or absence (ΔUblD) of the Ubiquitin-like Domain (UblD) influences the auto-ubiquitination potential of Parkin (top panel). While wild type Parkin lacks activity, ΔUblD exhibits robust auto-ubiquitination activity. Absence of the carboxy-terminal RING2 domain (ΔRING2) abrogates auto-ubiquitination however attachment of a bulky tag at the carboxy-terminal (Parkin-Thioredoxin/Thio) does not impair catalytic properties of RING2 (bottom panel). Auto-ubiquitination reactions (25 µL) using UBE2L3/UbcH7 as the E2 were carried out at 37˚C for an hour. Cartoons depict domain arrangement of the Parkin species used in the assay. **B.** Latent auto-ubiquitination activity of wild type (WT) Parkin is revealed by the increase in assay reaction time. Reactions (25 µL) were carried out at 37˚C and room temperature (RT) at the indicated time points (hrs – hours) using UBE2L3/UbcH7 as the E2. WT lane contains only wild type Parkin.

Consistent with previous observations, wild type Parkin lacked auto-ubiquitination activity (Figure 26A, top panel). Furthermore, this reflected positively on the reproducibility of protocols established for wild type Parkin (protein production, purification and setup for *in vitro* ubiquitination assays). The cooperation of the RING domains has been proposed to be crucial for Parkin

activity (Rankin et al., 2001) and other studies have shown RING2 to be the catalytic core for Parkin's E3 ligase activity (Hampe et al., 2006, Matsuda et al., 2006). Auto-ubiquitination profile of ΔRING2 and Parkin-Thio together show that Parkin requires RING2 to be present for auto-ubiquitination and the attachment of a bulky tag at its C-terminus did not impair its ligase activity (Figure 26A, bottom panel). Robust auto-ubiquitination of the ΔUblD species confirmed whether the UblD was the minimum domain preventing self-recognition for auto-ubiquitination (Figure 26A, top panel). Interestingly, an increase in assay reaction times resulted in auto-ubiquitination of wild type Parkin, suggesting in part that bacterially produced wild type Parkin was capable of E3 ligase activity (Figure 26B).

Subsequently, auto-ubiquitination of ΔUblD and not wild type Parkin was observed with all E2s known to function with Parkin (Figure 27). Reactions (performed for 90 minutes) show moderately lower levels of activity with UBE2N/UBE2V1 (Ubc13/UEV1) heterodimer and UBE2L6/UbcH8 relative to the other E2s tested. UBE2D2/UbcH5B supported the auto-ubiquitination activity of ΔUblD and has been observed to facilitate monoubiquitination of Parkin substrate PICK1 *in vitro* (Joch et al., 2007) however, an interaction with Parkin could not be detected in co-immunoprecipitation experiments conducted elsewhere (Olzmann et al., 2007, Shimura et al., 2000, Zhang et al., 2000). Lack of auto-ubiquitination with wild type Parkin with any of the associated E2s an unexpected observation. The above observations suggest ubiquitin ligase activity of wild type Parkin is latent and various secondary factors enable E3 activity. The presence of bulky N-terminal (and C-terminal) tags presumably altered the tertiary structure of Parkin thereby 'priming' ligase activity. Correspondingly, increasing the assay reaction time may well have perturbed the protein leading to a gradual improvement in auto-ubiquitination. In addition, N-terminal truncations (ΔUblD and 111C) readily exhibit auto-ubiquitination. Taken together, ubiquitin ligase activity towards Parkin (the substrate, in the case of auto-ubiquitination) appears to be intrinsically suppressed by the UblD.

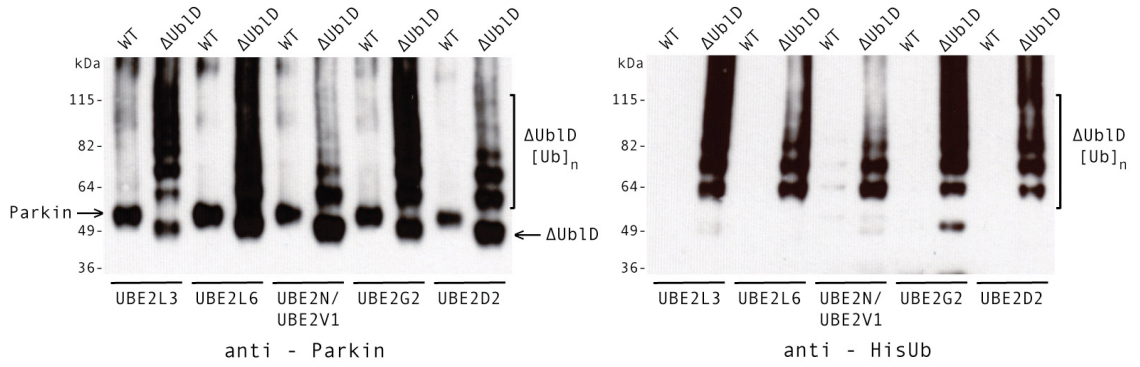

Figure 27: Auto-ubiquitination profile with different E2s. ΔUblD was observed to auto-ubiquitinate with all the E2s tested however similar modification of wild type Parkin was not observed. Auto-ubiquitination reactions (25 µL) of wild type (WT) Parkin (0.77 µM) and ΔUblD (1 µM) were conducted with various E2s (UBE2L3/UbcH7 (1.1 µM), UBE2L6/UbcH8 (1.1 µM), UBE2N/UBE2V1 (Ubc13/UEV1) heterodimer (0.5 µM), UBE2G2/Ubc7 (1.1 µM) and UBE2D2/UbcH5B (1.1 µM). Reactions were conducted at 37˚C for 90 minutes. Brackets indicate ubiquitinated ΔUblD species. UblD is Ubiquitin-like Domain.

3.3 Auto-inhibition of ligase activity: Role for the UblD

The UblD is structurally similar to Ubiquitin, forming a β-grasp globular domain however, shares low (~30%) sequence identity with Ubiquitin (Vijay-Kumar et al., 1987). However, there is a high degree of sequence conservation across species (≥90% identity across higher vertebrates and ≥75% overall similarity) (Figure 25A). Several pathogenic mutations are found within the UblD including 20% of the missense mutations found within the Parkin. Point mutations are spread throughout the UblD (Figure 28A) and some of them have reported to cause domain unfolding (Safadi and Shaw, 2007, Tomoo et al., 2008). The effect of pathogenic mutations Arg33Gln, Arg42Pro and Ala46Pro as well as mutations Lys27Asn and Lys48Ala on the globular structural of the UblD have been analysed by a combination of biophysical techniques and molecular dynamics simulations (Safadi and Shaw, 2007, Tomoo et al., 2008). Lys27Asn, Arg33Gln, Arg42Pro and Ala46Pro caused global unfolding of the while the Lys48Ala mutation had no detrimental affect to UblD's globular structure (Sakata et al., 2003, Safadi and Shaw, 2007, Tomoo et al., 2008). In addition, all the residues show a good degree of conservation across higher vertebrates (Figure 28A). Lys27Asn and Lys48Ala are not listed in the PD and Human

Gene mutation databases (PDMD, HGMD) however have been reported in the literature as pathogenic.

To further investigate the role of UblD in Parkin's E3 ligase activity, the affects of four UblD point mutations (Lys27Asn, Arg33Gln, Arg42Pro and Ala46Pro) on the auto-ubiquitination profile of Parkin were examined (Figure 28C). Tested alongside was a mutation at Arg51 (Arg51Pro), a residue that was weakly conserved between species (Figure 28A and 28C). Auto-ubiquitination of Parkin mutants Lys27Asn, Arg33Gln, Arg42Pro and Ala46Pro (all reported to unfold the UblD) but not wild type confirmed a regulatory role for the domain in Parkin's E3 ligase activity. The Arg51 residue is located within a loop in the UblD structure and displays weak conservation between species. Thus, a severe mutation (Arg51Pro) is expected to have negligible effect to structural integrity of the UblD and the mutant should behave like the wild-type protein in auto-ubiquitination assays. Lack of auto-ubiquitination with Arg51Pro confirmed the rationale behind the mutation.

Residues Val15 and Lys32 were also mutated (Val15Met, Lys32Ala) and tested in similar assay (data not shown). Val15, located on strand β2, contributes to the core hydrophobic network within the UblD structure (helix 1 and strands 1,2 and 5) (Tomoo et al., 2008). Val15Met full-length Parkin did not auto-ubiquitinate in the assay. Given its location and nature, the mutation is not expected to destabilise the global structure. However, the mutation could substantially affect spatial orientation of the central helix against the concave surface presented by the five-stranded sheet. Alternatively, at the genetic level Val15Met could present an alternative start codon for protein translation (analogous to the Met80 that yields an endogenous ΔUblD Parkin (Henn et al., 2005)) yielding a N-terminal UblD truncation that would be unstructured. Residue Lys32 residue located on the surface of the central helix is another pathogenic mutation site (Lys32Thr). The intended Lys32Ala mutation was expected to maintain the hydrogen bond network stabilizing the helix and retain the wild type structure however robust auto-ubiquitination was observed.

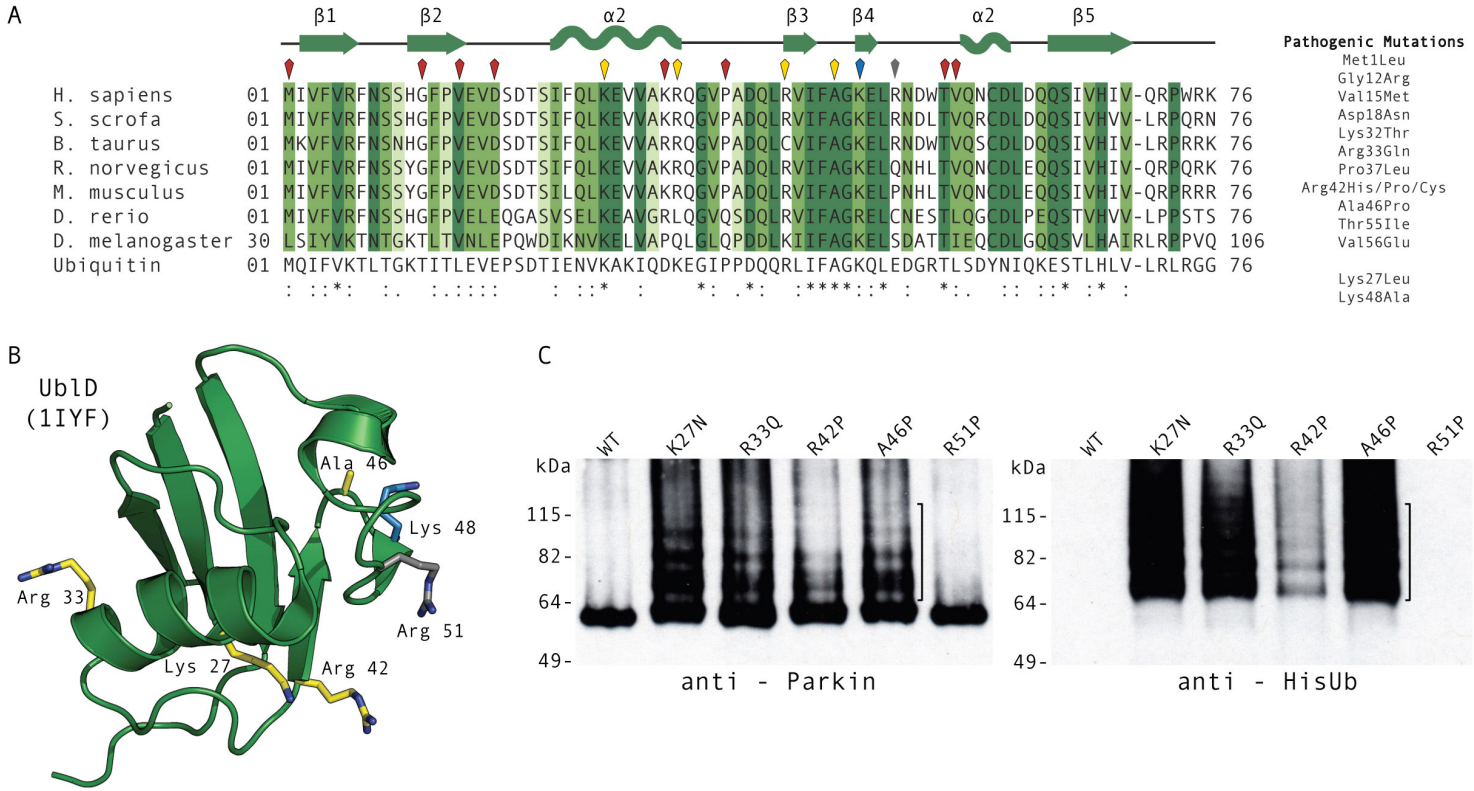

Figure 28: Auto-ubiquitination profile of Parkin Ubiquitin-like Domain (UblD) mutants. A. Multiple sequence alignment (generated using ClustalW (Chenna et al., 2003)) depicts sequence conservation of the Ubiquitin-like Domain (UblD) across Parkin homologues (shades of green) as well as with ubiquitin (bottom row symbols). Secondary structure elements of human UblD are shown above for reference. Sites of pathogenic missense mutations are indicated by maroon and yellow (UblD unfolding mutations (Safadi and Shaw, 2007, Tomoo et al., 2008)) glyphs. Lys 27 and Lys 48 (blue glyph) mutation sites not listed in the databases. Also indicated is the weakly conserved Arg51 (dark grey glyph). Listed alongside are various pathogenic mutations found in the UblD as shown in Table 3 (section 1.10.1). **B.** NMR structure of human UblD (PDB 1IYF) showing residues that were mutated in **C** (same colour scheme as **A**, generated using PyMOL (Schrodinger, 2010)) **C.** Auto-ubiquitination assays with UBE2L3/UbcH7 (1.1 μM) and different full-length species of Parkin (0.77 μM); wild type (WT), UblD mutants Lys27Asn, Arg33Gln, Arg42Pro, Ala46Pro and Arg51Pro. Wild type and Arg51Pro do not auto-ubiquitinate, while mutants that unfold UblD display auto-ubiquitination, demonstrating that loss in structural integrity of UblD activates ligase potential of Parkin. Reactions (25 μL) were conducted at 37˚C for an hour. Brackets indicate ubiquitinated species.

These observations suggest secondary roles for the numerous UblD pathogenic mutations that require further investigations. Nevertheless, point mutations that have been shown to unfold the UblD structure appear to augment auto-ubiquitination of Parkin. Along the same lines, bulky N-terminal tags could displace UblD in the context of the full-length protein and perturb the tertiary structure of Parkin. Given that the UblD was the minimum domain preventing self-recognition and subsequent auto-ubiquitination, the above experiment confirms a role UblD as an auto-inhibition module. More importantly, the series of observations are indicative of a dynamic tertiary conformation for Parkin and UblD possibly will participate in an intra-molecular interaction with the rest of the molecule.

3.4 Validation of UblD as Auto-inhibitory module

3.4.1 Substrate UIM strategy:

Inhibition of auto-ubiquitination was offset by the presence of bulky N-terminal tags, domain truncation (ΔUblD) and by certain UblD pathogenic mutations. The UblD has been shown to recognize the UIMs of EPS15 resulting in Parkin mediated monoubiquitination of EPS15 as well as multi monoubiquitination of Parkin (Fallon et al., 2006). Custom peptides representing the EPS15 UIMs and mutant peptides were synthesised by the Peptide Synthesis Laboratory (PSL), a Core Technology facility at the London Research Institute. EPS15 bear two C-terminal tandem UIMs with UIM II is predicted to be double-sided UIM based on sequence comparison with Hrs UIM ((Hirano et al., 2006) and (Figure 29A)). UIMs interact with the hydrophobic patch on Ubiquitin (Ile44 and surrounding residues), a surface that is conserved on the UblD (Figure 29A). Point mutations, similar to those disrupting the Hrs UIM - Ubiquitin interaction, were designed for the Eps15 UIMs and synthesised as peptides (Figure 29A). EPS 15 UIMs incubated with wild type Parkin are likely to interact with the UblD, consequently disrupting the auto-inhibitory state while mutant UIMs should have little or no effect on wild type Parkin. To test this hypothesis, the peptides were used in auto-ubiquitination assays with wild type Parkin (Figure 29B).

Weak auto-ubiquitination of full length Parkin (0.77 μM) was observed at high concentrations (50x molar excess) of EPS15 UIMs (EPS15 WT UIMs) in the presence of UBE2L3 however, mutant UIMs (EPS15 m UIMs) had no effect Parkin. As the *in vitro* ubiquitination reaction mixture contained ubiquitin (~5x molar excess), UIM-ubiquitin interactions could also occur. Furthermore, weak affinities observed between UBDs and ubiquitin could partially explain low auto-ubiquitination activity observed *in vitro*. The interaction had an affinity of 318 ± 21 μM by surface plasmon resonance (SPR) (Hirano et al., 2006), while the affinity of Parkin's UblD to both the UIMs was 139 ± 19 μM by NMR and 193 ± 30 μM by isothermal calorimetry (ITC) (Safadi and Shaw, 2010).

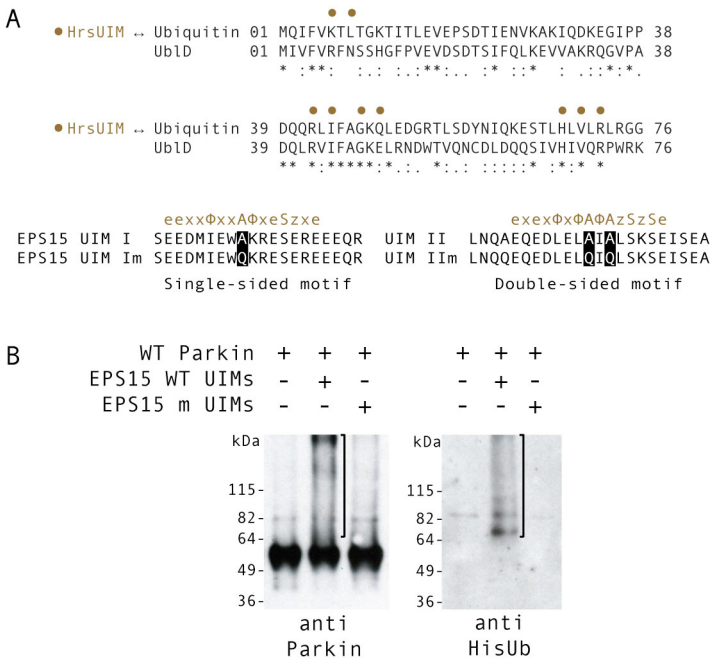

Figure 29: Parkin - EPS15 Ubiquitin Interaction Motifs (UIMs) assay. A. Alignment of ubiquitin and UblD sequences (top, generated using ClustalW (Chenna et al., 2003)) show conservation of residues that participate in the ubiquitin – HRS UIM interaction (gold circles). Also shown are sequences of wild type and mutant (m) EPS15 UIM peptides (I, II and Im and IIm respectively, Ala to Gln mutations are highlighted) used in this assay, aligned with UIM consensus signature for single-sided and double-sided ubiquitin interactions (x is any residue, z is bulky hydrophobic/polar, e is negatively charge, Φ is hydrophobic). HRS is Hepatocyte growth factor–Regulated tyrosine kinase Substrate, EPS15 is Epidermal growth factor receptor substrate 15 **B.** Auto-ubiquitination reactions (25 μL) with wild type (WT) Parkin (0.77 μM) in the presence of 50x molar excess of EPS15 wild type (WT) or mutant (m) UIMs shows activation of ligase potential with the former. Reactions were conducted at 37˚C for an hour. Brackets indicate ubiquitinated species.

While the above experiment contained the UIMs as two peptides, a better strategy might have been to synthesise them as a single polypeptide chain. Due to the residue content of the UIMs, difficulties were observed during the purification of the synthesised peptides and a longer peptide (UIMs I and II) would have compounded the issue. Experiments with EPS15 UIMs purified as recombinant protein from *E. coli* were planned. However, due to technical difficulties faced during cloning of the expression construct, the material could not be purified nor were assays conducted. Nevertheless, the experiment proved to be a partially successful as is showed UblD mediated auto-inhibition of E3 ligase activity in wild type Parkin could be suppressed by UblD interactions with substrate domains.

3.4.2 TEV protease induced Parkin auto-ubiquitination:

Another strategy used for validating the role of the UblD as an auto-inhibitory module was the TEV protease induced activation assay. As stated earlier, purified Parkin stored at 4°C for 3-4 days was susceptible to breakdown leading to the 111C truncation. In addition, a limited proteolysis assay using subtilisin A (serine endopeptidase with broad specificity) on wild type Parkin revealed additional proteolytic susceptible sites in the neighbourhood of residue 110 - Gly84, His124, Gly135 and Ser141 (data not shown, Figure 30 black arrows). Taken together, the region between the UblD and RING0 (Gly77 to Asn144) appeared unstructured and surface exposed, consequently amenable to incorporate a modification such as a TEV protease site. It was speculated that a stably integrated TEV site within this region should have little effect on auto-ubiquitination profile of wild type Parkin. Proteolytic cleavage would then disengage the UblD from the rest of the protein thus permitting auto-ubiquitination. A Parkin-TEV variant, inducible for auto-ubiquitination upon TEV protease action would be a useful tool to study mechanisms of E3 ligase activity.

To put the theory to test, a number of mutations were designed to incorporate a TEV protease within this region and were tested in auto-ubiquitination assays (Figure 30). Unfortunately, several of these mutations rendered Parkin capable of auto-ubiquitination prior to TEV protease activity (red squares and blue circle Figure 30). Surprisingly, the two species that were stable (yellow triangle and green star, Figure 30) either did not cleave or did not auto-ubiquitinate. These sites overlapped the Cdk5 phosphorylation site (Ser131, indicated in the figure), a region that has been shown to regulate Parkin's ligase activity (Avraham et al., 2007). There appeared to be a secondary role of this region that required further investigations. The Parkin-TEV variant, while an attractive concept, proved to intractable in the absence of structural information to guide the assay design.

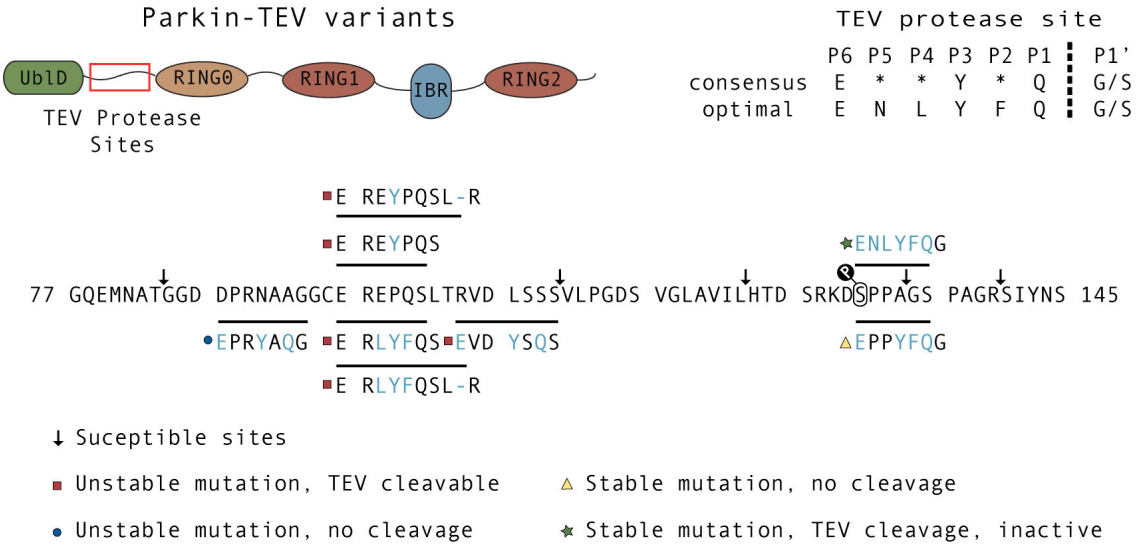

Figure 30: Protease induced Parkin auto-ubiquitination. Strategy and summary of for the Tobacco etch virus (TEV) protease induced auto-ubiquitination of Parkin-TEV experiments. Cartoon indicates linker region of Parkin (red box) that was targeted for incorporation of TEV protease sites (top left). Shown along side are consensus and optimal sequences of a TEV protease site (top right, '*' indicates any residue, dashed line indicates peptide bond hydrolysed by TEV protease). Sequence of the Gly77 to Ser145 (UblD to RING0) linker region (middle), with subtilisin A susceptible sites indicated with black arrows. Residues marked by thin black lines served as sites for the insertion of sequences encoding the TEV protease site (in black are Parkin residues retained, in blue are residues mutated/inserted). Parkin-TEV variants were either unstable (exhibited auto-ubiquitination, TEV protease cleavage was either observed (red box) or absent (blue circle)) or stable but were not cleaved by TEV protease action (auto-ubiquitination absent, yellow triangle). Another Parkin-TEV variant (green star) was stable, cleaved by the protease, however was inactive. This site overlapped serine 131 (encircled), the location of cyclin-dependent kinase 5 (Cdk5) mediated phosphorylation of Parkin.

3.4.3 Expressed Protein Ligation of Parkin

A strategy involving protein-protein ligation was designed to validate the auto-inhibitory role for UblD. As the ΔUblD was constitutively active towards auto-ubiquitination, reattaching the UblD, a folded globular protein should in theory, revert the species to an auto-inhibited state as observed with wild type Parkin. Thus, the structural reconstitution of an auto-inhibited Parkin state is made possible through this strategy. Given that inhibition of auto-ubiquitination is a novel observation, one that contradicts several critical aspects of Parkin biology, it was felt necessary present multiple lines of evidence to shore up this observation. The experiment involved the use of Expressed Protein Ligation (EPL) a technique successfully used incorporate amino acids analogs, synthetic labels and probes and post-translational modifications exclusively at specific locations on a desired protein (reviewed in (Schwarzer and Cole, 2005) and (Muralidharan and Muir, 2006)). EPL involves an autocatalytic chemical ligation reaction between protein fragments and is analogous to intein/extein splicing process observed during protein translation (Figure 31 and (Muir, 2003).

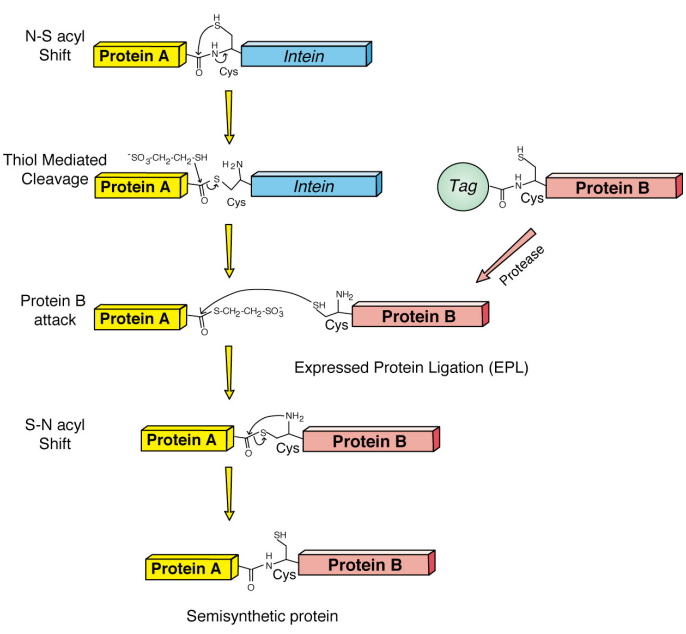

Figure 31: Expressed Protein Ligation (EPL). EPL involves autocatalytic chemical ligation of two protein fragments (A to B). Protein A is expressed with a carboxy (C-) terminal Intein fusion that can be cleaved by a thiol reagent (2-Mercaptoethanesulfonic acid (MESNA) is depicted) resulting in a reactive thioester derivative at the C-terminus. Protein B bears an amino (N-) terminal cysteine expressed using a fusion tag. Proteolytic cleavage of the protein B reveals the N-terminal cysteine, which attacks the C-terminal thioester derivative leading to the autocatalytic ligation (EPL) of the two proteins. Figure adapted from Intein Mediated Purification with an Affinity Chitin-binding Tag (IMPACT) manual (New England Biolabs).

Briefly, the process of chemically ligating protein A to protein B requires the former to bear an N-terminal cysteine residue, while the latter requires a

thioester linked leaving group moiety at the C-terminus. Recombinant expression of protein A fused with a C-terminal Intein tag, followed by an intein-mediated, thiol induced cleavage that facilitates formation of a C-terminal thioester derivative. The two proteins can then be ligated by autocatalytic chemical ligation reaction in the presence of thiol reagents (Figure 31).

The strategy for the Parkin EPL experiment involved production of the UblD with a C-terminal Intein tag and the ΔUblD truncation with a N-terminal cysteine (Figure 32A). Ligation of these fragments would yield full length Parkin EPL species, predicted to resemble the tertiary structure of wild type Parkin as well as its auto-ubiquitination profile. Two cysteines are present in the proximity of the UblD; Cys59 - present within the UblD and Cys95 present in the UblD-RING0 linker region. Due to its location, Cys95 was selected as the preferred site for the ΔUblD truncation (95C) and was cloned, expressed and purified. The *Mycobacterium xenopi gyrA* Intein gene (Mxe GyrA Intein) and Chitin Binding Domain (CBD) (from the pTXB1 vector, New England Biolabs) was cloned as a fusion construct C-terminal to residue 94 of Parkin (see 2.1 and 2.2.3 for details).

The UblD-Intein-CBD fusion protein was cleaved using 2-mercaptoethanesulfonic acid (MESNA) as the thiol reagent, further purified to remove free Intein-CBD tag and residual uncleaved fusion protein (see Methods for details). UblD with C-terminal thioester derivative (1-95M) was used for chemical ligation with 95C. The ligation reaction was incomplete despite an overnight incubation, however Parkin EPL was successfully synthesised (Figure 32B) Size-exclusion chromatography eliminated residual the 1-95M species, however the residual 95C could not separated completely despite a subsequent anion exchange chromatography (monoQ) step. Nevertheless, unligated 95C and the mixture of Parkin EPL and 95C were assayed for auto-ubiquitination (Figure 32C). To differentiate between Parkin EPL and 95C, differential antibodies; anti IBR-RING2 and anti UblD, were used (Figure 32C).

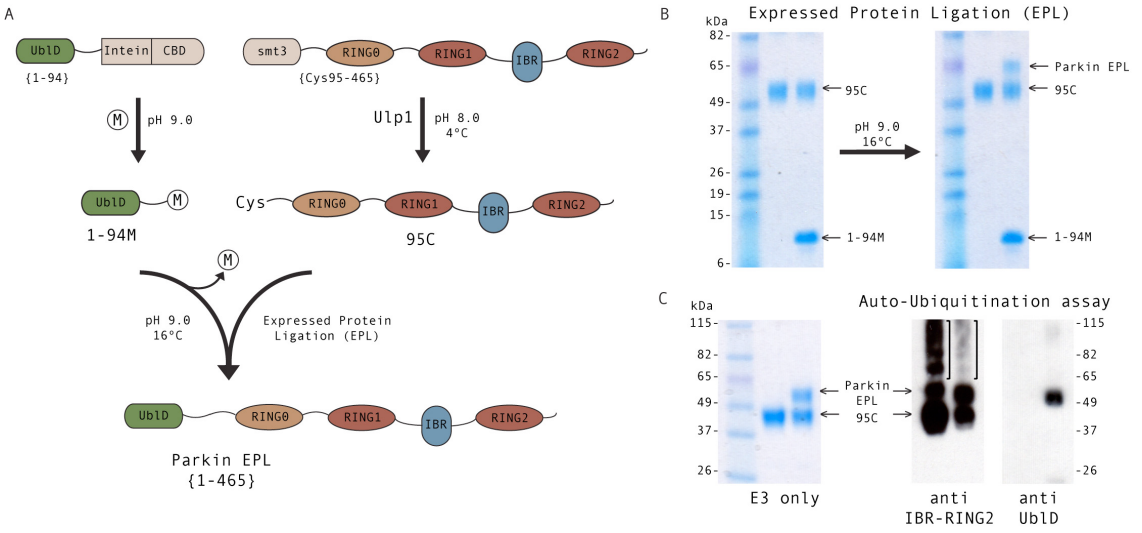

Figure 32: Parkin Expressed Protein Ligation (EPL) assay. A. Strategy for Parkin EPL assay. The UblD-Intein-Chitin Binding protein (UBD) fusion was cleaved and activated for EPL through thiol action (M - 2-mercaptoethanesulfonic acid or MESNA) generating the 1-94M (residues 1-94 with C-terminal thioester derivative) species. 95C Parkin was expressed and purified as a smt3/SUMO (Small Ubiquitin-like Modifier) fusion and cleaved by Ubiquitin-like protease 1 to reveal the amino terminal cysteine. Ligation of the two species resulted in Parkin EPL. **B.** Coomassie stained gels of reactions set up for expressed protein ligation step. 95C alone and 95C with 10X excess 1-94M (on left) were treated with 10 mM MESNA overnight at 16˚C. Reaction products (on right) revealed partial ligation of 1-94M to 95C. **C.** Auto-ubiquitination reactions (25 µL) with 95C (1 µM) and mixture of 95C/Parkin EPL (1 µg of mix) revealed the latter species did not auto-ubiquitinate (detected by anti-UblD immunoblot) while 95C readily auto-ubiquitinated (anti-IBR-RING2 immunoblot). On left is a coomassie stained gel of the E3 species used in the assay.

As expected, 95C readily auto-ubiquitinated, represented by the slow migrating bands in both the lanes in the anti-IBR-RING2 western blot. The weaker profile observed in the second lane corresponds to the lower amount of 95C present in the reaction. The anti-UblD blot does not pick up the 95C species in either lane, however readily recognizes the Parkin EPL species. Moreover, absence of any higher molecular weight bands suggests that auto-ubiquitination does not occur with Parkin EPL. Thus, Parkin EPL resembles wild type in its auto-ubiquitination profile, possibly its auto-inhibited tertiary structure, and validating the role for the UblD as the auto-inhibitory module.

To conclude this section of results, the above experiments demonstrate that full-length Parkin does not auto-ubiquitinate with any of its cognate E2s. The N-terminal UblD appears function as an auto-inhibitory module for Parkin's auto-ubiquitination. Bulky N-terminal tags, truncations lacking the UblD,

destabilizing/pathogenic mutations within the UblD, and UblD directed substrate interactions disrupt this inhibition resulting in a constitutively active molecule. Re-ligating the UblD onto ΔUblD Parkin truncation restores its auto-inhibitory function. Furthermore, the above observations suggest auto-inhibition could be mediated by an intra-molecular interaction between the UblD and Parkin's C-terminus. Intra-molecular interaction as a possible mechanism for auto-inhibition will be explored in the following chapter.

Chapter 4. Results: Intra-molecular interaction of Parkin

4.1 Background

Auto-ubiquitination, like substrate ubiquitination by RING E3 ligases, involves E2 activation and substrate recognition. Absence of auto-ubiquitination of full-length Parkin implies either one of both those events are disrupted. Thus, auto-inhibition mediated by the UblD involves disruption of self-recognition or the masking of target lysines on the Parkin surface, both of which require an intra-molecular interaction between the UblD and the catalytic C-terminus of Parkin (Figure 30). Several other questions arise from this hypothesis; could substrate interactions (as is the case with UblD - EPS15 and endophilin-A) disrupt this interface or alternatively can ubiquitination of substrates occur independent of this interface? Could substrate and auto-ubiquitination occur as mutually exclusive events?

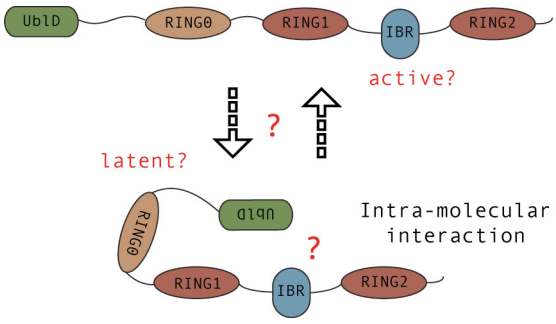

Figure 33: Model for auto-inhibition of Parkin's ligase activity. Cartoon describing two possible states of Parkin (active and latent) with UblD mediated intra-molecular interaction rendering the ligase inactive/latent. Mechanisms of activation and inhibition are yet to be described in detail.

To investigate substrate ubiquitination, the bacterial expression and purification of recombinant AIMP2 ('authentic' Parkin substrate, see 1.10.4.3 and (Corti et al., 2003, Ko et al., 2005)) was attempted using MBP, GST and 6xHis-smt3 tags, with little or no success. While a small percentage soluble MBP-AIMP2 could be affinity purified, soluble material was not observed with the other two

fusion proteins. Moreover, removal of the MBP tag using thrombin protease resulted in precipitation of recombinant AIMP2 (data not shown). The expression and purification of AIMP2 required further optimisation however could not be addressed within the time frame of this study. The following sections describe experiments investigating the intra-molecular interaction within Parkin, the nature of the interface and the mechanism of auto-inhibition.

4.2 Lysine 48 mediated intra-molecular interaction of Parkin

Lysine 48, located in the β3-β4 loop, is conserved across Parkin species and with Ubiquitin (Figure 28 A and B). Ubiquitin mediated proteasomal degradation of substrates is signalled by Lys48-linked polyubiquitin chains, underlying its importance in the ubiquitin (Chau et al., 1989). Lys48Ala UblD mutation has been reported as an AR-JP mutation in numerous studies (Finney et al., 2003, Henn et al., 2005, Safadi and Shaw, 2007, Tomoo et al., 2008) however, is not listed in the mutation databases (PDMD and HGMD). The Lys48 side chain appears to have no conformational constrains within the UblD structure and the Lys to Ala mutation does not lead to domain unfolding (Safadi and Shaw, 2007, Tomoo et al., 2008). The residues in strands β3 and β4 of UblD form the interaction interface with Rpn10 with Lys48 playing a significant role in this interface (Sakata et al., 2003). Recently, the residue has also been shown to participate in interactions with EPS15 UIM and the SH3 domain of endophilin-1 (Safadi and Shaw, 2010, Trempe et al., 2009). As the residue participates in a contrasting set of interactions (proteasome and substrates), Lys48 is an ideal candidate to be engaged in the proposed intra-molecular inhibitory interaction.

Mutations Lys48Ala and Lys48Arg (a conserved substitution observed in zebra fish Parkin, Figure 28A) were tested for auto-ubiquitination. Lys48Ala Parkin (K48A-Parkin) was capable of auto-ubiquitination while Lys48Arg lacked this profile (Figure 34A). In addition, full-length Parkin species (WT and K48A) when subjected to proteolytic digest with a broad-spectrum endopeptidase (subtilisin

A), showed divergent digestion profiles (Figure 34B). 100 μg of respective Parkin species in 100 μL of buffer containing 50 mM Tris pH 8.0, 200 mM NaCl, 250 μM TCEP and 5% (v/v) glycerol were digested overnight at 4°C with indicated quantities of protease (% w/w). K48A-Parkin was susceptible to digestion even at low protease concentrations, while wild type Parkin was more resistant indicative of a shielded tertiary structure. In the context of Parkin's intra-molecular interaction, the above results revealed a potential interaction surface on the UblD that can be modified (K48A) to 'open-up' the molecule. More importantly, a correlation between intra-molecular interaction and auto-inhibition could now be examined within an enzymatic assay.

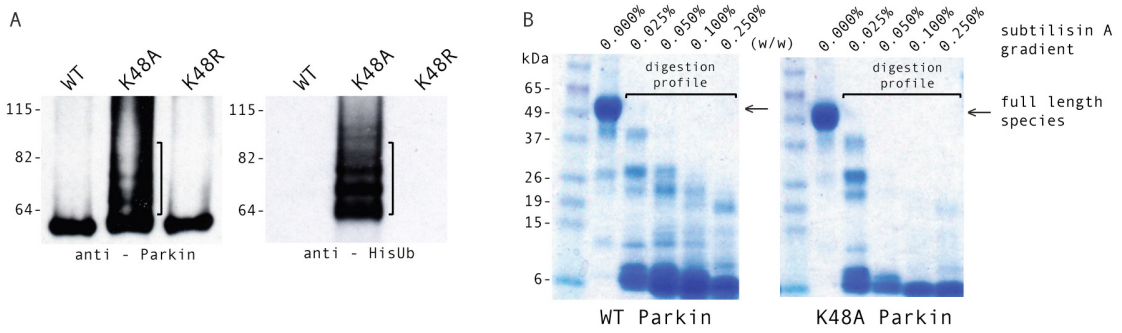

Figure 34: Role for Lysine 48 in Parkin auto-inhibition. A. Auto-ubiquitination reactions with wild type (WT), K48A- and K48R- Parkin show activity only in lanes with K48A-Parkin (indicated by brackets) suggesting a role for the charged nature of the residue in auto-inhibition of Parkin ligase activity. Reactions (25 μL) were conducted with 0.77 μM of each of the Parkin species and UBE2L3/UbcH7 (1.1 μM) at 37°C for an hour. **B.** Divergent digestion profiles observed for WT and K48A- Parkin species reveal the latter (on right) to be prone to subtilisin A proteolysis even at low protease concentrations (indicated above in weight per weight percentage) suggesting an exposed conformation for the mutant. In contrast, WT Parkin is observed to be more resistant to proteolysis indicative of a closed tertiary structure. Proteolytic digests were carried out overnight at 4°C in 100 μL reactions containing 100 μg of respective Parkin species.

Accordingly, pull-down experiments were carried out using, 6xHis-UblD (wild-type and K48A) as bait and different Parkin species (wild-type, K48A-Parkin and ΔUblD) as the prey, in order to establish an interaction preference (Figure 35). K48A-Parkin was also subject to auto-ubiquitination in the presence of increasing concentrations of free UblD and UblD K48A, to examine the effect of *trans* interactions (with the C-terminus of K48A-Parkin) on the auto-ubiquitination profile of K48A-Parkin (Figure 36). Pull-down experiments (section 2.4.1 for methods) using 6xHis-UblD as the bait protein showed a

stronger binding of the bait to K48A-Parkin and the ΔUblD species when compared wild type (Figure 35, left panel). In contrast, the 6xHis-UblD K48A bait protein lacked a preference for the prey or exhibit any stable interactions (Figure 35, right panel) suggesting the mutation alters the UblD surface responsible for the interaction with C-terminus of Parkin.

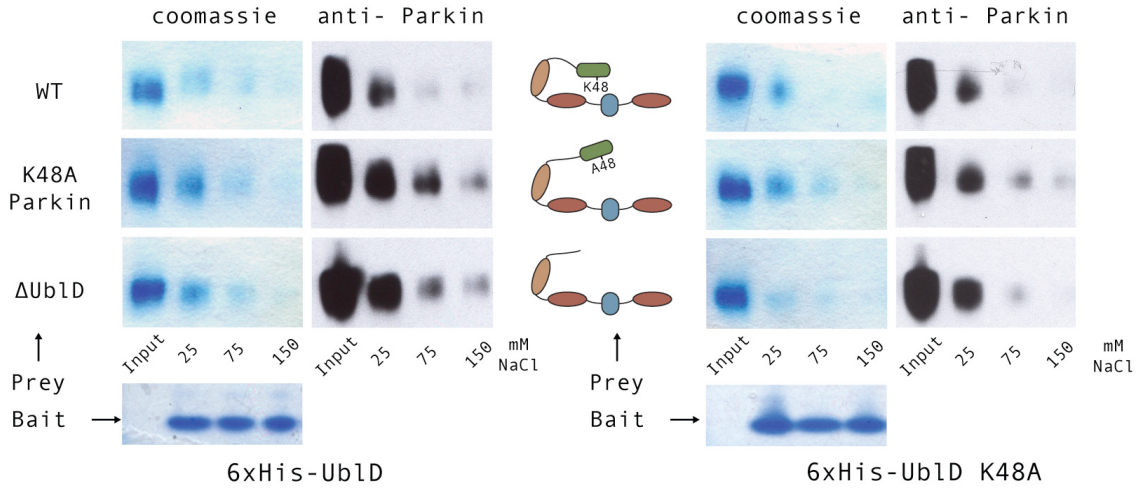

Figure 35: Intra-molecular interaction - role for Lysine 48. Results of pull-down assays with 6xHis-Ubiqutin-like Domain (UblD, left panel) or 6xHis-UblD K48A (right panel) as bait proteins with wild type (WT) Parkin, K48A-Parkin and ΔUblD (first, second and third row respectively, also shown as cartoons in centre) as the prey species. 6xHis-UblD displays an interaction preference for K48A-Parkin and ΔUblD species over WT Parkin suggesting the carboxy-terminal UblD binding surface mutant Parkin species is available for interaction (in *trans*) with the bait UblD species. The same surface, in WT Parkin would be occupied by the amino-terminal UblD domain hence occluded from interaction. 6xHis-UblD K48A shows weak interactions with the prey species suggesting the Lys48Ala mutation perturbs UblD surface responsible for interaction with carboxy terminus of Parkin. Baits were bound to nickel-nitrilotriacetic acid (Ni-NTA) beads (40 μL) were incubated with 0.5 mg of each of the prey species in 50 mM Tris pH 7.5, 25 mM NaCl, 250 μM TCEP, 5% glycerol, for 2-3 hours at 4˚C. Beads were washed (10 column volumes) with binding buffer and subsequent washes of increasing salt concentration (indicated below third row), with samples (10 μL) taken at every step for sodium dodecyl sulfate – polyacrylamide gel electrophoresis (SDS-PAGE) and coomassie/immunoblot (anti-Parkin) detection. Input lanes represent 5% of prey species used in the pull downs. Samples are diluted 20 fold for immunoblots and probed with anti-Parkin antibody that recognises a carboxy terminal epitope on Parkin.

Concomitantly, increasing concentrations of free UblD (8-32 fold molar excess with increments of 8) in a K48A-Parkin auto-ubiquitination assay (0.77 μM in 25 μL reactions) gradually reduced levels of auto-ubiquitination (Figure 36, on left). At least a 16 fold molar excess of UblD was required to observe significant reduction in activity and complete inactivation could not be observed. On the other hand, a similar excess of UblD K48A in a similar assay did not

significantly impede auto-ubiquitination. (Figure 36, on right) Overall, the interaction of UblD appears weak, however sufficient to regulate auto-ubiquitination in the K48A Parkin species, confirming the presence of an intra-molecular inhibitory interaction within Parkin, mediated by the UblD.

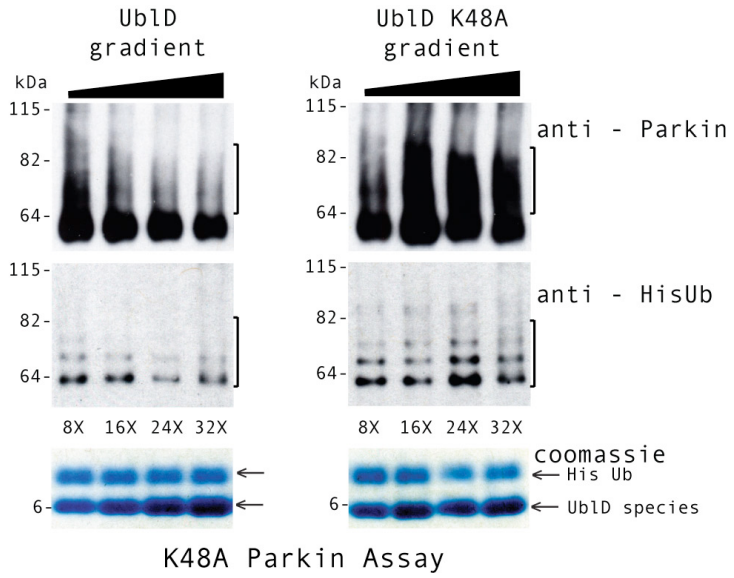

Figure 36: Inhibition of ligase activity - role for Lysine 48. Auto-ubiquitination assays with K48A-Parkin conducted in the presence of increasing quantities of UblD species (wild type, left and Lys48Ala, right). Reduction in levels of auto-ubiquitination is observed with increasing quantities of UblD (at least a 16 fold excess), however a similar inhibition was not observable upon titration with UblD K48A. Reactions (25 μL) containing 0.77 μM of K48A-Parkin and UBE2L3/UbcH7 (1.1 μM) were mixed with indicated (8, 16, 24 and 32 fold molar excess) quantities of UblD/UblD K48A and incubated at 37˚C for an hour.

Attempts to further quantify UblD interaction with K48A-Parkin through isothermal calorimetry (ITC) based experiments were met with a few technical challenges. Briefly, ITC measures the heat change (indirectly, using a reference cell) arising from a sample cell (containing protein ‘a’ of the two-protein complex, a - b) upon interactions with a ligand (protein b), injected at high concentrations through a syringe until the complex is saturated. The raw data generated from the experiment is computed to give values for binding affinity (K_a), enthalpy changes (ΔH), and binding stoichiometry (n) for the interaction (refer (Freyer and Lewis, 2008) for practical aspects of ITC). The ITC experiment for this study was designed such that K48A-Parkin was held in the

sample cell and the UblD (ligand) injected at high concentrations. As described earlier (see 2.2.2.3), UblD was unstable at concentrations exceeding 8 mg/mL and proved tricky to accommodate within the experimental setup. Sequential ITC runs, with UblD at a stable concentration (6 mg/ml), were planned in order to achieve complex saturation however the K48A-Parkin was observed to be precipitate after extended incubations in the sample cell (held at 25˚C, with each run lasting for 80-90 minutes). Finally, the protein locations were swapped, placing UblD in the sample cell and K48A-Parkin in the syringe. The latter species (~52 kDa) could be concentrated up to 0.45 mM, however when injected at concentrations of 0.20 to 0.25 mM, protein precipitation was observed in the sample cell which was analysed to be K48A-Parkin. Further optimisation of protein material was required to generate quantitative data for the interaction however, could not be addressed within the course of this study.

Interestingly, 6xHis-Ubiquitin baits exhibited faint binding with the K48A Parkin and ΔUblD species, with prey being washed away at physiological salt levels (150 mM). However, increasing concentration of inactive ubiquitin (Arg74X) did not impair auto-ubiquitination of K48A-Parkin (data not shown), as was observed with UblD. The relevance of a Parkin-ubiquitin interaction will be discussed at a later stage. In context of wild type Parkin, cross talk between UblD and the RING domains would be expected for the former to influence the 'business-end' of the E3 ligase (Figure 30). Thus, spatial orientation of the UblD could be influenced by the 'linker-region' (Gly77 to Asn235 including the RING0 domain), as well as secondary interactions along the molecule. The 'linker-region' is subject to several levels of regulation (phosphorylation, binding of adaptors 14-3-3η and BAG5) as well as involved in substrate recognition (Pael-R) (Sato et al., 2006, Imai et al., 2001, Avraham et al., 2007, Kalia et al., 2004). However, the interplay between intra-molecular inhibitory interaction within Parkin established here and the above events requires further investigations.

The above observations introduce the molecular basis of UblD mediated inhibition of Parkin's auto-ubiquitination. A direct correlation of UblD's

interaction with Parkin's C-terminus and regulation of auto-ubiquitination was established. Furthermore, Lysine 48 (and neighbouring residues), previously shown to direct Parkin interactions with substrates and the proteasome, is critical for the intra-molecular auto-inhibitory interaction. These data represent first experimental investigations into the inherent regulation of Parkin's ligase activity and could hold a greater significance in the disease perspective as well as for understanding mechanisms of RING E3 regulation.

4.3 UblD interaction: Effect on Parkin E2s and Adaptors

UblD mediated intra-molecular interaction could possibly occlude the E2-RING interaction thereby inhibiting auto-ubiquitination. The effect of UblD mediated intra-molecular interaction on Parkin-E2 binding was tested in pull-down assays using 6xHis-UBE2L3/UbcH7 and 6xHis-UBE2L6/UbcH8 as baits and wild type Parkin and ΔUblD as prey proteins (Figure 37A). In addition, auto-ubiquitination assays with wild-type Parkin were carried out in the presence of increasing quantities of UBE2L3/UbcH7 and UBE2L6/UbcH8 (Figure 37B) to examine possible competition of binding regions.

A small degree of Parkin-E2 binding was observed however, the bound Parkin species washed away at salt levels greater than 50mM NaCl, in contrast to the binding observed in UblD based pull-downs. The levels of wild-type Parkin pulled-down were comparable to ΔUblD for both the E2s (Figure 37A) suggesting the UblD interaction surface on the C-terminus of Parkin is distinct from the Parkin-E2 interaction surface. The use of E2~ubiquitin thioester conjugates as baits may well have improved the observed levels of E2-E3 interactions thereby revealing subtle differences between the binding events (ΔUblD with E2~ubiqutin versus WT with E2~ubiqutin) however, this was not planned as part of the original experiment and requires further investigation. Nevertheless, an increase in E2 concentration in auto-ubiquitination assays (and consequently an increased E2~ubiquitin concentration in the reaction)

showed no induction of Parkin's auto-ubiquitination (Figure 37B) collectively suggesting that, E2 interaction events and intra-molecular inhibition occur independently.

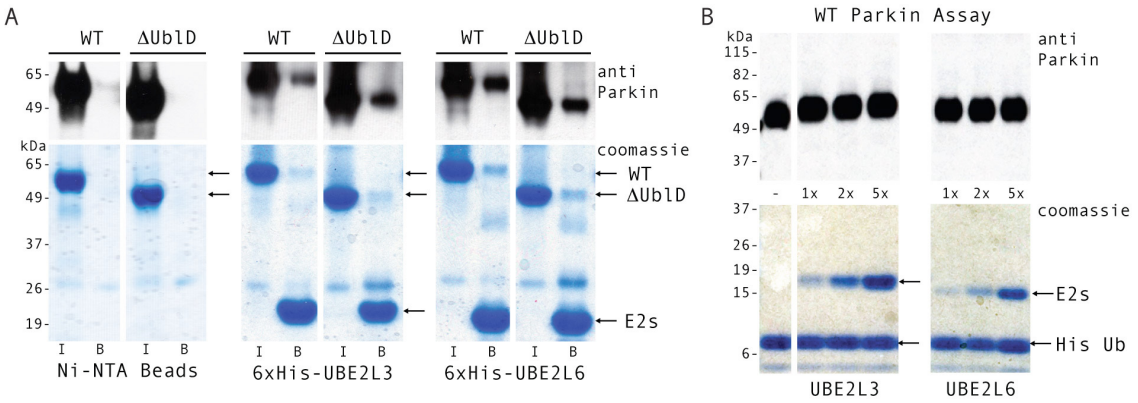

Figure 37: E2 binding assays. A. Pull-down assays using 6xHis tagged UBE2L3/UbcH7 or UBE2L6/UbcH8 show similar levels of interaction with both the prey proteins: wild type (WT) Parkin and ΔUblD, while the beads only control (left panel) shows no interaction. 50 μL nickel-nitrilotriacetic acid (Ni-NTA) beads were saturated with 6xHis tagged E2s and acted as baits for 0.5 mg of prey proteins (indicated above) in 50 mM Tris pH 7.5, 25 mM NaCl, 250 μM Tris (2-carboxyethyl) phosphine (TCEP) buffer, 5% (v/v) glycerol). Binding was carried out for 2-3 hours at 4˚C. Input lanes (I) represent 5% of prey proteins. Bead lanes (B) indicate prey pulled down after 10 column volume (cv) low salt wash (50 mM). Samples were diluted 20 fold for immunoblots. **B.** Auto-ubiquitination assays with wild-type Parkin (0.77 μM) with increasing quantities of E2 (1x, 2x and 5x indicate 1.1, 2.2 and 5.5 μM respectively) to ascertain if excess E2 could relieve UblD mediated auto-inhibition. Lack of auto-ubiquitination suggests E2 interaction events and intra-molecular inhibition occur independently. Reactions (25 μL) were conducted at 37˚C for an hour. v/v is volume per volume.

As introduced earlier, the Gly77 to Asn235 linker-region is subject to regulation by Cdk5 phosphorylation (at Ser131) and the binding of adaptors 14-3-3η and BAG5 (Sato et al., 2006, Avraham et al., 2007, Kalia et al., 2004). In addition, each of the events resulted in either abrogation of auto-ubiquitination (all three) or Parkin mediated substrate ubiquitination (binding of BAG5 and Cdk5 phosphorylation inhibited synphillin-1 ubiquitination). Binding of the 14-3-3η protein with Parkin was observed to nanomolar affinities (K_d = 4.2 nM) by SPR technique (Sato et al., 2006), and provides an attractive target to study how an intra-molecular interaction within Parkin would influence adaptor interaction. In addition, binding of 14-3-3η was observed independent of the phosphorylation status of Parkin, although the authors do not rule out a phospho event enhancing binding (Sato et al., 2006).

The following experiments were designed to examine the relationship between Parkin-adaptor regulatory mechanisms and the UblD mediated intra-molecular inhibitory interactions. A phosphomimetic mutation of Parkin was designed (Ser131Glu) alongside a double mutant (Lys48Ala + Ser131Glu) to examine (indirectly) if phosphorylation on the linker-region could regulate the 'open' state of Parkin (Figure 38). Furthermore, the mutant (Ser131Glu) was also used in binding assays with 14-3-3η alongside WT Parkin (Figure 39) to study if the adaptor could alter the 'open' state of Parkin. The S131E-Parkin retained wild type characteristics in an auto-ubiquitination assay, however the double mutant was observed to auto-ubiquitinate, suggesting the two events might not co-operate as was predicted (Figure 38).

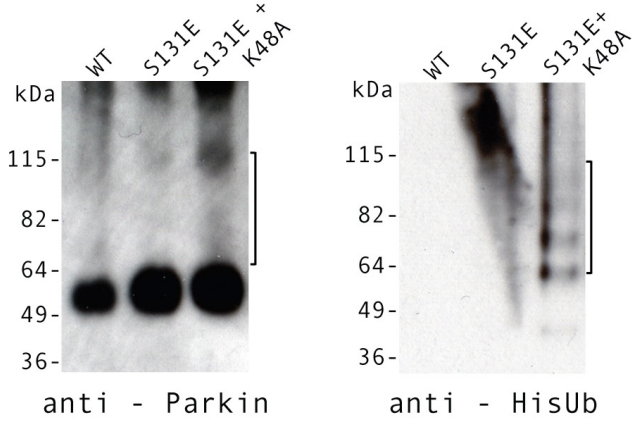

Figure 38: Phosphomimetic Parkin mutant assay. Auto-ubiquitination assays with wild type (WT), Ser131Glu (phosphomimetic mutant) and Ser131Glu + Lys48Ala (double mutant) species of Parkin (0.77 μM each) show ligase activity with the double mutant species, while the phosphomimetic mutant resembles WT-Parkin in its auto-ubiquitination profile. Reactions (25 μL) were conducted with UBE2L3/UbcH7 (1.1 μM) at 37°C for an hour.

A phosphomimetic mutation (Ser to Glu) may not adequately represent the physiological phosphorylation state however, comparing rates of auto-ubiquitination (K48A-Parkin versus S131E+K48A Parkin) could reveal the finer aspects of Parkin phosphorylation and requires further work. Additional phosphorylation sites (Ser101, Ser131 ('linker' sites), Ser296 (RING1-IBR linker) and Ser378 (IBR)) have also been observed to regulate Parkin's response to the UPR pathway (Yamamoto et al., 2005). More recently, the 'activation' of Parkin's E3 ligase activity mediated by PINK1 phosphorylation was observed (Kim et al., 2008, Sha et al., 2010) as well as contested

(Narendra et al., 2010). Auto-inhibition, presented here for the first time, represents a fundamental regulation of Parkin's activity. However, modifications such as phosphorylation, could tweak other functional facets of Parkin's activity (substrate interaction, binding of adaptors) thereby regulating the E3 ligase potential of Parkin.

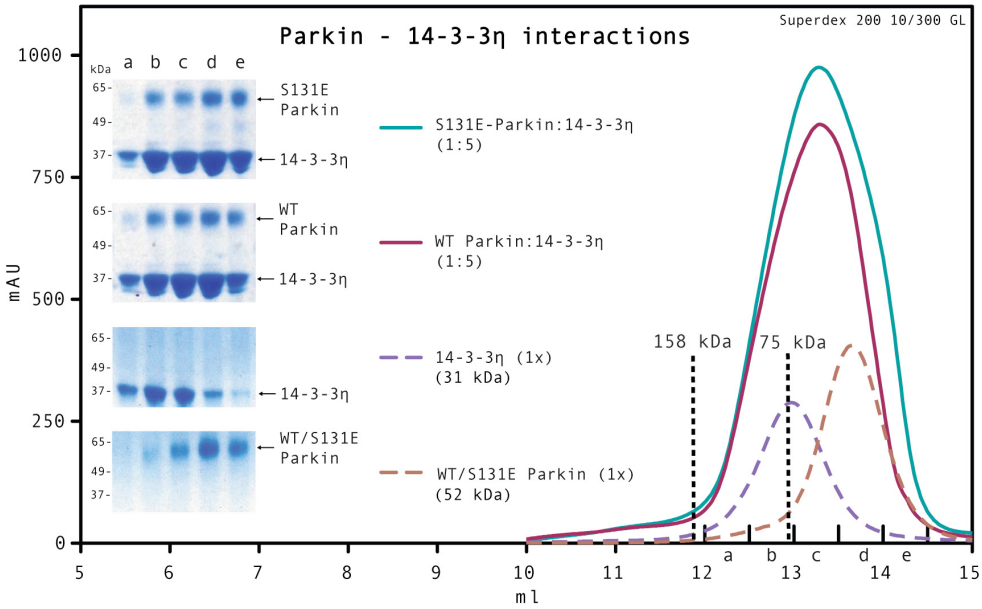

Figure 39: Interactions with 14-3-3η. Results of size exclusion chromatography (SEC) based analysis of 14-3-3η interactions with Parkin. The elution profiles overlaid are; monomeric wild type (WT) or Ser131Glu (phosphomimetic mutant) Parkin (brown dashes, 1x - 0.5 mg), dimeric 14-3-3**η** (violet, 1x - 0.3 mg), WT Parkin with 14-3-3**η** in 1:5 molar ratio of monomers (maroon) and Ser131Glu with 14-3-3**η** in 1:5 molar ratio of monomers (teal). Absence of a shifted elution profile representing a trimeric protein complex (Parkin (WT/S131E) with dimeric 14-3-3**η**) indicates a lack of protein complex formation during SEC analysis. Values along x-axis indicate elution volumes in (mL). Indicated fractions a to e (12 mL to 14.5 mL) for each run were analysed by sodium dodecyl sulfate – polyacrylamide gel electrophoresis (SDS-PAGE) and stained with coomassie brilliant blue. Monomeric molecular weights of individual proteins are indicated in brackets. SEC runs (250 μL samples) were conducted using Superdex 200 10/300 GL in 50 mM Tris pH 8.0, 50 mM NaCl and 250 μM Tris (2-carboxyethyl) phosphine (TCEP) buffer. Calibration markers for 75 kDa and 158 kDa are shown for reference. Traces were generated using GraphPad Prism 5.0c (GraphPad, San Diego, CA).

Parkin-14-3-3η interactions, analysed using size exclusion chromatography (SEC), were largely absent regardless of the Parkin species used as a binding partner. The 31kDa protein migrates as a dimer on a size exclusion column (purple dashed trace (Figure 39)) while all the Parkin species (~52kDa) traced identical profiles, represented by the brown dashed trace of WT Parkin. Low salt levels (50mM) were maintained in the interaction buffer to promote binding, and

increasing levels of 14-3-3η (1x, 2x and 5x) were also tested however, the expected offset representing a trimeric complex (Parkin and dimeric 14-3-3η - 114kDa) or a tetrameric (166 kDa) complex was not observed. S131E-Parkin (Figure 39, teal coloured trace), K48A-Parkin and K48A+S131 Parkin species (data not shown) were also tested for 14-3-3η interactions however, protein complex formation was once again not observed. In addition, 14-3-3η showed no effect on *in vitro* auto-ubiquitination profile of K48A Parkin as well as of the double mutant (K48A+S131E) (data not shown). Sato and colleagues had demonstrated 14-3-3η interactions with Parkin purified from insect cell expression systems, hence post-translation modifications can be expected to assist the interaction. Material used in the above assays was purified from a bacterial expression system and similar modifications are not expected.

Further investigations into 14-3-3η - Parkin interactions (optimization of an ITC based binding assay, effect of pathogenic mutations on binding (mutants Ala82Glu, Lys161Asn and Lys211Asn were cloned, expressed and purified), use of multi phosphomimetic mutants/phospho peptides for interaction analysis) were required to understand the molecular basis of how the E3 ligase is regulated by 14-3-3η. However, certain developments in other aspects of this study, in particular the details of C-terminal regions on Parkin that were expected to be involved in the intra-molecular inhibitory interactions presented themselves (discussed below). Subsequently, experiments relating to the description of the novel intramolecular inhibitory interaction were taken up, leaving insufficient time to appropriately address the questions arising from this section.

4.4 UblD interaction mapping

The above results (section 4.2) demonstrate intra-molecular interaction mediated by the UblD regulates auto-ubiquitination of Parkin. The molecular detail of this interaction would help understand how the regulation occurs and

whether the mechanism influences substrate ubiquitination. While the above experiments benefited from the UblD structure, apart from the IBR structure, no other information was available to direct experiments. Consequently, peptide-array interaction experiments were designed to identify possible candidate regions to guide subsequent biochemical and biophysical experiments. A target protein can be split into an array of overlapping peptide fragments followed by 'SPOT synthesis' of each peptide on a cellulose membrane (technique and applications reviewed in (Hilper et al., 2007)). The membrane is incubated with the probe protein to allow peptide interactions, washed stringently, and analysed to determine the peptide spots retaining interaction with the probe protein (analogous to epitope mapping).

Peptides arrays of Parkin were synthesised by the Peptide Synthesis Laboratory, LRI. The peptides stretched over 21 residues with a +1 residue shift for each subsequent peptide in the array until the whole Parkin sequence is mapped (spot n = residues n to n+20, where n lies between 1 and 445). UblD tagged with the V5 epitope tag (GKPIPNPLLGLDST) and labelled with a fluorophore (thioether linkage between UblD Cys59 and Fluorescein-5-Maleimide) was used as probes (V5-UblD and Fluoro UblD, respectively, Figure 40A and B). In addition, based on the weak binding observed in the pull-down assays, fluorescein-N-terminal Ubiquitin was also used as a probe (Fluoro Ub, Figure 40C). Concomitantly, probes were made to interact with a +3 shift sparse array, *i.e.* a +3 residue shift along the Parkin sequence in each subsequent peptide spot, and was used to confirm hits obtained from the fine (+1 shift) interaction assay (data not shown). The arrays that were generated represented the entire Parkin sequence however, for the purpose of this study, interacting peptides observed in the UblD were not pursued further and excluded from the figures. Positive interactions were those that were represented in both the array types, fine (+1 shift) and sparse (+3 shift). Positive interactions observed were classified as major hits when they covered at least five consecutive peptide spots (Figure 40D), while interactions observed in 3-5 consecutive peptide spots were listed as minor hits (Figure 40E).

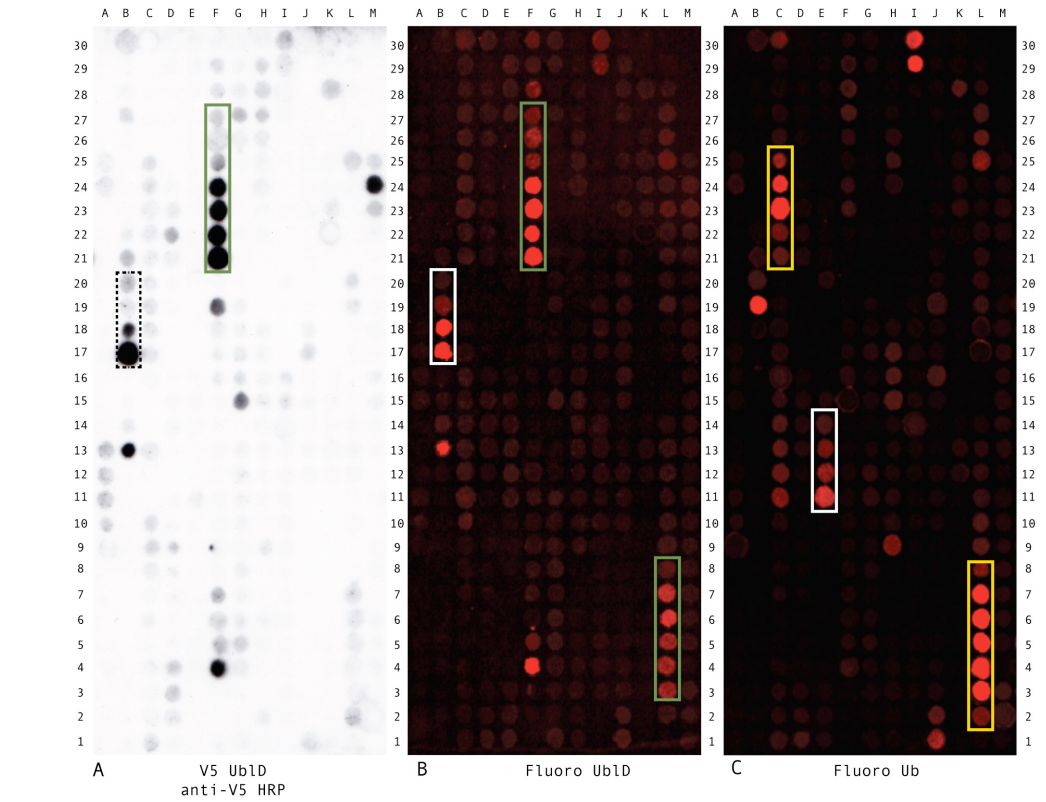

D Major Hits

Grid	UblD	Ub	Sequence	PD Mutations	Other features*
C 21-25	✗	✓	141 SIYNSFYVY**C**KGP**C**QRVQPGKLRVQ 165	Y143C, P153R, K161N	14-3-3η, BAG5 binding
F 21-27	✓	✗	231 TNSRN**I**T**C**I**C**TDVRSPVLVF**Q**C**N**SRH 257	R234Q, T240R/M, **C253Y/W**, R256C	UBE2L3 binding
L 2-8	✓	✓	392 RVDERAAEQARWEAASKETIK**K**TTKP**C** 418	D394N, R396G, A398T, R402H/C, E409X, T415N, **C418R**	UBE2L6 binding

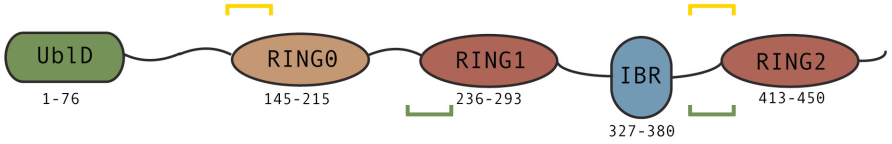

E Minor Hits

Grid	UblD	Ub	Sequence	PD Mutations	Other features*
B 17-20	✓	?	107 LSSSVLPGDSVGLAVILHTDSRKD 130	none	none
E 11-14	✗	✓	191 RMSGE**C**QSPH**C**PGTSAEFFFK**C**GA 214	M192L/V, S193I, K211R/N, **C212G/Y**	14-3-3η, BAG5 binding

Figure 40: Peptide array interactions. Parkin peptide array showing peptide spots interacting with probes **A.** V5-UblD, **B.** Fluoro UblD and **C.** Fluoro Ub. Positive interaction spots are classified as **D.** major and **E.** minor. Rectangles in **A**, **B** & **C** represent major and minor hits - green for UblD, yellow for Ub and black dashed/white for minor hits. Interaction with V5-UblD was detected by anti-V5 horseradish peroxidase antibody. Image Storm scanner (λ595nm) was used to detect interactions of the fluorophore labelled probes. Grid reference in **D** and **E** represents positive interaction spots and stated alongside is the nature of probe, associated sequence, PD mutations and other features. Zinc co-ordinating residues are in bold. * Indicates the features listed do not include substrate interactions. Cartoons representing domain arrangement of Parkin are not to scale and the locations of the observed interactions, indicated by brackets (green for UblD, yellow for Ub and black dashed for minor hits) are approximate. UblD is Ubiquitin-like domain, Ub is ubiquitin, RING is Really Interesting New Gene and IBR is In-between RING. E2s – UBE2L3/UbcH7, UBE2L6/UbcH8.

Distinct interaction regions were observed for UblD and ubiquitin apart from spots L 2-8 representing the sole overlapping region. The two major hits observed with the UblD (F 21-27 and L 2-8) appear to with have common characteristics with the reported Parkin-E2 binding patches (Shimura et al., 2000, Zhang et al., 2000, Ardley et al., 2001). A major ubiquitin interacting region (C 21-27) was situated in the RING0 domain leading into the C_4 zinc finger, N-terminal half of the predicted bipartite zinc co-ordinating region. In addition, the C-terminal of the second zinc co-ordinating region predicted in RING0 was a minor site (E 11-14) of ubiquitin binding. Interestingly, the N-terminal zinc-finger is observed analogous to the ubiquitin interacting NZF-like zinc finger present in HOIL-1 (Figure 41A) (Hristova et al., 2009, Kirisako et al., 2006), however a possible ubiquitin-RING0 interaction has not yet been examined.

Over 20 PD mutations were collectively represented within the major and minor hits of the array interactions. More importantly, several missense mutations of interest (grey shaded rows in table 4) appear in major interaction hits (red glyphs (Figure 40)); destabilizing Arg256Cys (F 21-27) formed aggresomes, exhibited enhanced auto-ubiquitination (*in vitro* and *in vivo*) however lacked substrate ubiquitination, soluble mutations Lys161Asn (C 21-27) and Thr240Arg (F 21-27) that lack substrate ubiquitination *in vivo* however show robust auto-ubiquitination *in vitro*, and finally the soluble Thr415Asn (L 2-8) 'ligase-dead' mutation.

The major hits C 21-27, F 21-27 and L 2-8 are, from this point forwards, generically referred to as UblD/Ub Binding Regions (UBRs) I, II and III respectively. A high degree of sequence conservation across species was observed in all regions. While this was expected of UBRs I and II as they coincide with genuine domains of Parkin (RING0 and RINGI respectively). However UBR III, incidentally displays a superior sequence identity (92% to 55%) across species between the three UBRs, does not overlap with any known Parkin domains/motifs (Figure 40D and 41).

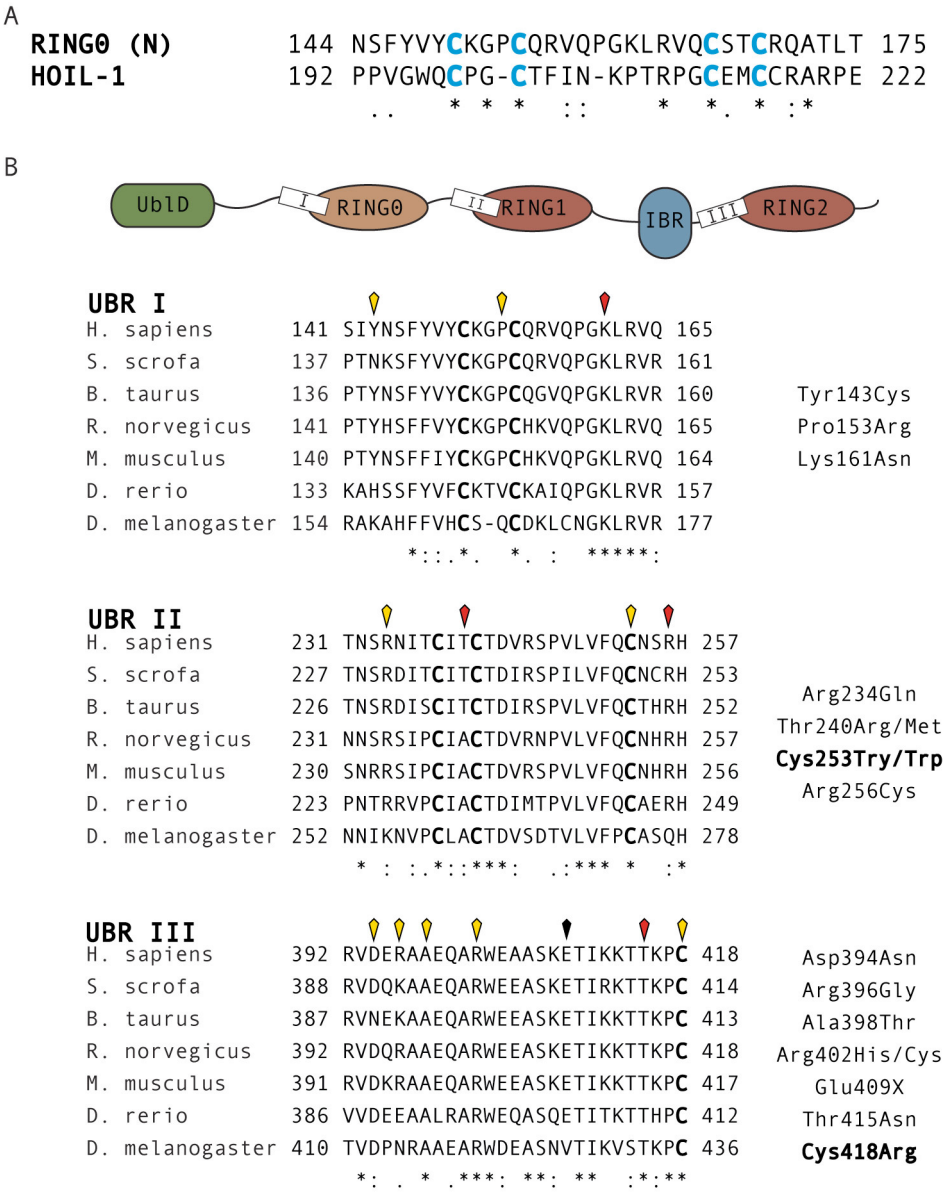

Figure 41: Parkin UblD/Ub Binding Regions (UBRs). A. Sequence alignments (of amino-terminal zinc finger motif of Parkin's RING0 domain with Npl4 type Zinc Finger (NZF)-like zinc finger present in Haem-oxidized IRP2 ubiquitin ligase-1 (HOIL-1). Predicted zinc co-ordinating cysteines are in bold blue letters. UBR I overlaps the RING0 domain (see cartoon and top panel in **B**). **B.** Cartoon representation of Parkin with approximate locations of UBR I, II and III (not to scale). Multiple sequence alignment depicts sequence conservation of the UBRs I, II and III (top, middle and bottom respectively) across Parkin homologues. Also indicated are sites of pathogenic mutations found in each UBR (yellow and red glyphs for missense mutations and black for nonsense mutations, nature of mutations are listed alongside). Zinc-coordinating cysteines are in bold letters. All sequence alignments were generated using ClustalW (Chenna et al., 2003). UblD is Ubiquitin-like domain, RING is Really Interesting New Gene and IBR is In-between RING.

UBR III also bears four lysine residues or potential targets for ubiquitination, which could be masked by the UblD interaction as a regulatory mechanism against auto-ubiquitination. Furthermore, several PD mutations appeared to

punctuate the UBR III that is a shared UblD and Ub interaction patch, all of which would suggest a decisive role for this region.

In summary, pull-down experiments demonstrate an interaction between the UblD and C-terminus of Parkin (ΔUblD). Lys48 in the UblD is crucial residue for this interface and increasing concentrations of free UblD but not Lys48Ala UblD are capable of reducing auto-ubiquitination of full-length K48A Parkin. Full-length Parkin and ΔUblD appeared to bind E2s (UBE2L3/UbcH7 and UBE2L6/UbcH8) equally well, demonstrating that an E2 was not competing with UblD for Parkin interaction. In addition, several factors (kinase action, binding of adaptors) have been reported to regulate Parkin's E3 ligase activity. The intra-molecular interaction of Parkin, mediated by the Lys48 surface of UblD is an inherent feature of molecule, one that principally establishes inhibition of auto-ubiquitination. Finally, peptide based interaction mapping proposes an unexpected Parkin-ubiquitin interaction as well three UBRs to investigate mechanisms of UblD mediated auto-inhibition. The concluding chapter will describe experiments designed to validate the UBRs and propose a model for Parkin ligase activity.

Chapter 5. Results: Novel Interactions of Parkin

5.1 Background

The enzymatic activity of RING E3 ligases involves substrate recognition, activation of E2s and facilitating substrate ubiquitination (*trans* event: E2~ubiquitin → Substrate). The significance of a potential RING E3-ubiquitin interaction within this pathway is not immediately clear. Alternatively, inhibition of Parkin auto-ubiquitination/self-recognition may involve UblD mediated masking of target lysines. In theory, the UBR III containing four lysines could be concealed from ubiquitin (on a charged E2) by the UblD thereby inhibiting auto-ubiquitination of Parkin. Could an intra-molecular inhibition involve co-operation between the three UBRs? UBRs III and I suggest ubiquitin binding while UBRs II and III display UblD interaction. Functional co-operation could be mediated by an enclosed structure of Parkin, further supporting the importance of an intra-molecular interaction (Figure 42). A trade-off between UblD and ubiquitin interactions could also play a crucial role in the synthesis of ubiquitin chains by Parkin.

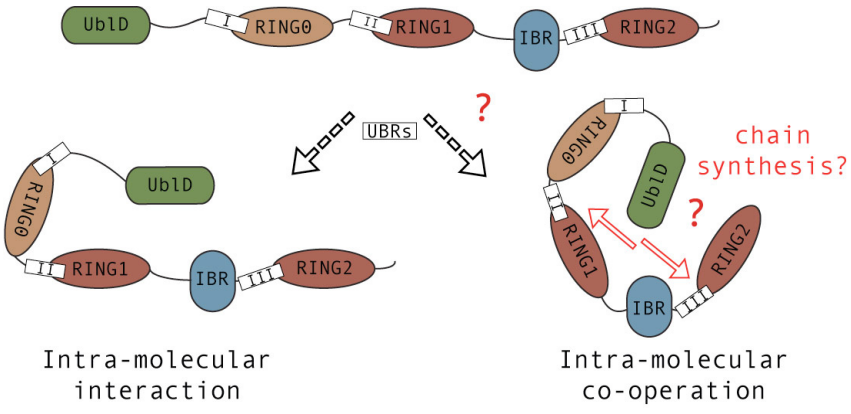

Figure 42: Molecular dynamics of Parkin. Cartoons (not to scale) representing location of Parkin UblD/Ub Binding Regions (UBRs) I, II and III (top, UblD is Ubiquitin-like Domain, Ub is ubiquitin, RING is Really Interesting New Gene, IBR is In-between RING). UblD mediated intra-molecular interaction in Parkin that inhibits auto-ubiquitination (bottom left) and proposed trade-off between UblD/Ub and UBRs interactions that could regulate ubiquitination events (bottom right).

The following sections describe experiments exploring the dynamics of an intra-molecular UblD based interaction, a probable Parkin-ubiquitin interaction and how these events could influence the RING E3 ligase properties.

5.2 Validation of Peptide Interaction Array

The UBR III presented an attractive region to focus validation experiments, primarily due to its ability to potentially interact with both UblD and ubiquitin. Auto-ubiquitination assays with ubiquitin mutants were designed to identify a functional relevance of the ubiquitin interaction. Point mutations in the hydrophobic (Phe4Ala, Leu8Ala, Ile44Ala and Val70Ala) and acidic (Asp58Ala) patches were introduced and used as source ubiquitin in ΔUblD auto-ubiquitination assays (Figure 43A). Assays were also conducted in the absence of the E3 to observe if the mutants impaired charging of the E2 (UBE3L3/UbcH7) (Figure 43C). Concomitantly, select PD missense mutations represented in the UBRs (UBR I - Lys161Asn, UBR II - Thr240Arg and UBR III - Thr415Asn, Figure 41) were also purified and tested in auto-ubiquitination assays (K161N-, T240R- and T415N-Parkin) (Figure 43D).

Unexpectedly, auto-ubiquitination of the ΔUblD species was completely abrogated by the Ile44Ala mutation and marginal activity was observed with the Lue8Ala and Val70Ala mutations (Figure 43A). Together these residues form the core hydrophobic patch on ubiquitin. Similar loss of activity was observed when the Ile44Ala ubiquitin mutant was used with K48A-Parkin, pathogenic UblD mutations (Lys27Asn, Arg33Gln, Arg42Pro and Ala46Pro) as well the 321C truncation (Glu321 to C-terminus, contains IBR-RING2) (Figure 43B). The levels of ΔUblD auto-ubiquitination with wild type ubiquitin, and ubiquitin mutants Phe4Ala and Asp58Ala were comparable (Figure 43C) moreover, the formation of E2~ubiquitin thioester conjugate (UBE2L3/UbcH7) was not significantly effected by any of the mutations (Figure 43C).

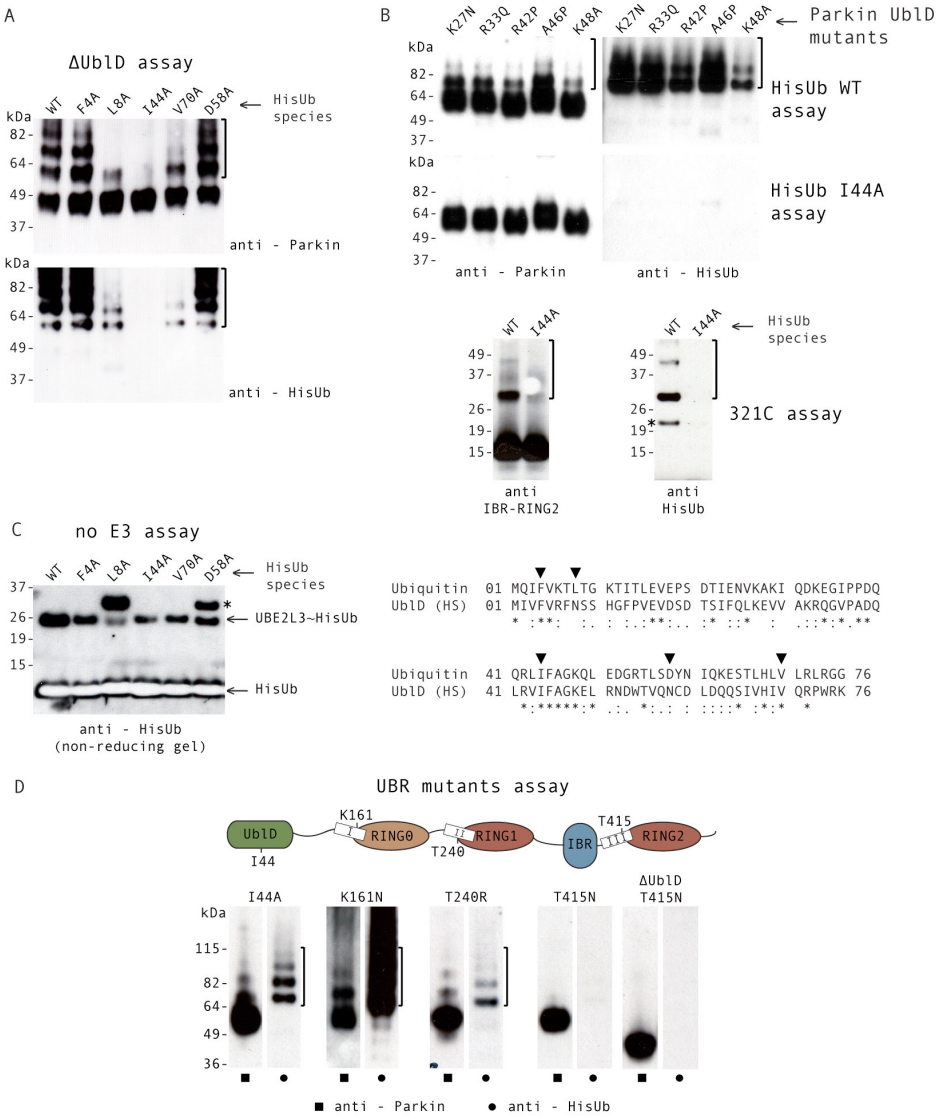

Figure 43: Auto-ubiquitination assays with Ubiquitin and Parkin mutants. A. Reduced auto-ubiquitination observed with hydrophobic patch mutants of ubiquitin (Leu8Ala, Ile44Ala and Val70Ala) while the acidic patch mutant (Asp58Ala) shows no effect on ΔUblD auto-ubiquitination profile. **B.** Auto-ubiquitination of Parkin mutants (Lys27Asn, Arg33Gln, Arg42Pro, Ala46Pro, Lys48Ala and 321C (deletion of Met1 to Ala320 in Parkin) was impaired due to Ile44Ala mutation on the hydrophobic patch of ubiquitin. **C.** None of the ubiquitin mutants however, significantly effect formation of the E2~ubiquitin thioester as the charged E2 species (UBE2L3/UbcH7~ubiquitin) was observed in non-reducing conditions and in the absence of an E3 (no E3 assay). ClustalW generated sequence alignment of ubiquitin and UblD (human) indicating conservation of residues (bottom). Inverted black triangles indicate location of residues mutated in ubiquitin for the ΔUblD assay. **D.** Auto-ubiquitination assays with Parkin mutants (residue location depicted on cartoon of Parkin structure); Ile44Ala (UblD hydrophobic mutant), Lys161Asn (UBR I mutant), Thr240Arg (UBR II mutant), Thr415Asn (UBR III mutant) and ΔUblD+T415N (ΔUblD containing Thr415Asn mutation). Auto-ubiquitination was observed with all mutants, except the 'ligase-dead' T415N-Parkin as well as ΔUblD+T415N Parkin. All ubiquitination assays were conducted as 25 µL reactions containing 0.77 µM of full-length Parkin species or 1 µM 321C and ΔUblD+T415N species or no E3, in the presence of 1.1 µM UBE2L3/UbcH7 at 37˚C for an hour. Brackets indicate ubiquitinated species. In 'no E3 assay', reaction samples were treated with 2xbuffer containing 4 M Urea, 150 mM Tris pH 6.8, 5 mM ethylenediaminetetraacetic acid (EDTA), 2% SDS, 10% glycerol and bromophenol blue for analysis in non-reducing conditions. UblD is Ubiquitin-like domain, Ub is ubiquitin, UBR is UblD/Ub Binding Regions.'*' indicates non-specific band.

The hydrophobic patch (Phe4, Ile44 and Val70) on UblD could represent an extended surface supporting intra-molecular interaction in Parkin and accordingly the Ile44Ala full-length Parkin mutant (I44A-Parkin) was active for auto-ubiquitination (Figure 43D). Furthermore, auto-ubiquitination was successfully observed in PD-linked K161N- and T240R-Parkin (UBR I and UBR III respectively) (Figure 37B) although T240R-Parkin activity was weaker of the two. Lys161Asn and Thr240Arg are drastic charge switching mutations and could possibly disrupt intra-molecular inhibition in a mechanism similar to the Lys48Ala mutation. True to its label, the 'ligase-dead' T415N mutation as well as the ΔUblD+T415N Parkin tested alongside lacked auto-ubiquitination activity. At this stage, a correlation of the observed loss of activity observed with T415N-Parkin and hydrophobic mutants of ubiquitin is tempting as the Thr415 lies in the UBR III on Parkin (Figure 40, a region that interacts with both UblD and ubiquitin.

5.3 Novel requisite for ubiquitin ligase activity of Parkin

The catalytic properties of RING E3s include activation of E2s and concomitant substrate ubiquitination (or auto-ubiquitination) (described earlier, Section 3.2). The auto-ubiquitination potential of Parkin was inhibited by a novel intra-molecular interaction mediated by the UblD present on the N-terminus of Parkin. The above experiments reveal two contrasting mutations that inhibit Parkin's auto-ubiquitination as well; the Ile44Ala on the hydrophobic patch of ubiquitin and Thr415Asn located on UBR III near the C-terminus of Parkin. Furthermore, both these mutations negatively regulate the E3 ligase activity of Parkin in a ΔUblD background (Figure 43A and 43D) implying a distinct inhibitory mechanism.

Subsequently, E2~ubiquitin thioester discharge assays that characterize E2 activation properties of Parkin were carried out to examine the inhibitory mechanisms of the above mutations. These assays allow a comparison of E2

activation rates or rates at which ubiquitin is discharged from the E2~ubiquitin thioester conjugate and their setup is analogous to a pulse-chase experiment (Figure 44A). Conjugation of ubiquitin and E2 (by E1 and ATP/$MgCl_2$) forms the pulse phase of the reaction. The reaction is then arrested by depletion of ATP/$MgCl_2$ (Apyrase/ATPase action followed by buffer exchange) thereby preventing recharging of the E2 (via E1) in an event of a thioester discharge. The reaction is then chased by the RING E3, which enhances E2 activation or the discharge of ubiquitin from the thioester E2~ubiquitin conjugate (Petroski and Deshaies, 2005b). In case of UBE2L3/UbcH7, which lacks intrinsic capability of ubiquitin chain synthesis, the RING mediated E2 activation event results in either the discharge of ubiquitin or discharge of ubiquitin followed by ligation onto a primary amine (lysine or N-terminus via isopeptide or peptide linkage).

Thioester discharge assays were carried out using a combination of WT/mutant species of Parkin and ubiquitin to examine whether UBE2L3/UbcH7 charged with Ile44Ala mutant ubiquitin could be activated by constitutively active species of Parkin (ΔUblD) (Figure 44C) and whether UBE2L3/UbcH7~ubiquitin could be activated by the ΔUblD+T415N Parkin species (Figure 44E). In the absence of a RING E3, activation of UBE2L3 (illustrated by ratio of charged (E2~ubiquitin) versus uncharged/discharged E2) was muted (Figure 44B) however addition of ΔUblD contributed to ubiquitin discharge (Figure 44C) rapidly accompanied by ubiquitination of the E2 and ΔUblD auto-ubiquitination (confirmed by subjecting samples to reducing conditions, data not shown). E2 ubiquitination, could arise due to robust ligase activity of the ΔUblD species contributing to reaction by-products of *in vitro* assays or alternatively, E2s could act as pseudo-substrates for Parkin.

A similar set-up with ΔUblD and I44A-Ubiquitin led to rapid discharge of the ubiquitin conjugated UBE2L3, however no E2 ubiquitination was observed (Figure 44D). A double mutant (ΔUblD+T415N) appeared to catalyse ubiquitin discharge quicker than the ‘no E3’ reaction however was comparatively slower

than other Parkin species tested alongside. The T415N mutation has been suggested to inactivate RING2 (Hampe et al., 2006, Matsuda et al., 2006), thus activation of the E2~ubiquitin thioester by the RING1 domain of Parkin cannot be excluded. Further analysis, using RING truncations or combinations of RING-E2 interaction abrogating mutants is required to understand 'ligase-dead' mechanisms of T415N-Parkin.

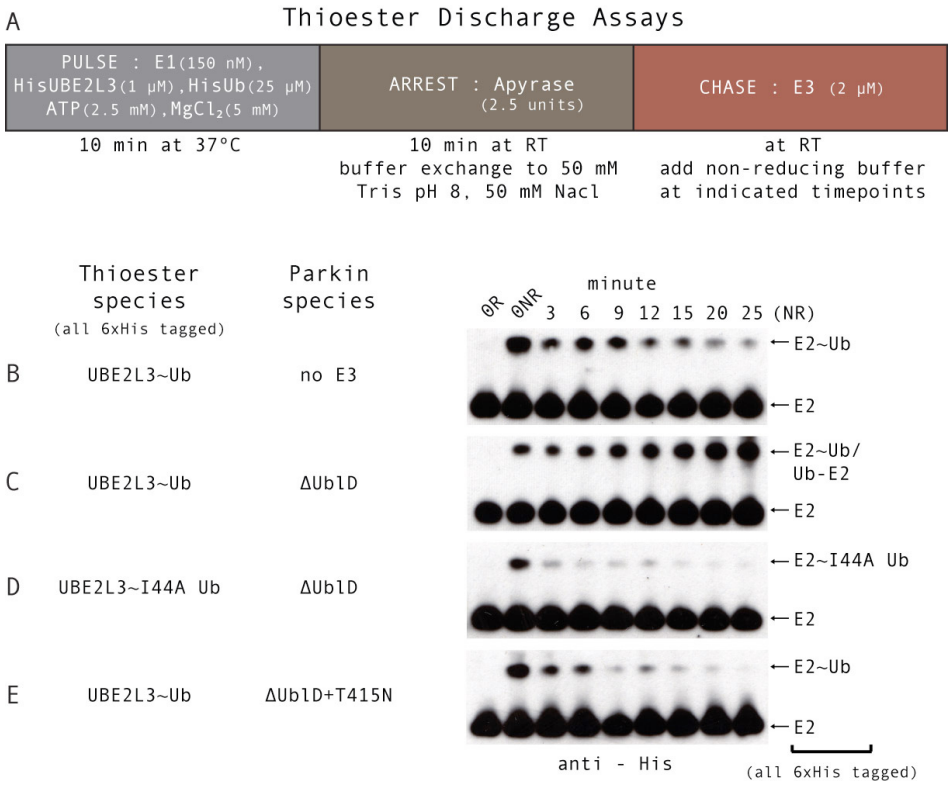

Figure 44: E2~ubiquitin thioester discharge assays. A. Schematic describing the pulse-chase format of the E2~Ub thioester discharge assay with reaction times and temperatures for each stage indicated. All E2 and ubiquitin species are 6xHis- tagged to enabled detection by anti-His immunoblot. E2~ubiquitin/E3 species present in each chase reaction are listed alongside the corresponding immunoblots of chase samples. Chase reactions are; UBE2L3/UbcH7~ubiquitin only (in **B**), UBE2L3/UbcH7~ubiquitin with ΔUblD (in **C**), UBE2L3/UbcH7~Ile44Ala ubiquitin with ΔUblD (in **D**) and UBE2L3/UbcH7~ubiquitin with ΔUblD+Thr415Asn Parkin (in **E**). Thioester discharge (hydrolysis of E2~ubiquitin conjugate) is muted in absence of E3 (**B**). However, rapid thioester discharge (**D**) and rapid thioester discharge followed by E2 ubiquitination (Ub-E2) (**C**) are observed in chase reactions containing UBE2L3/UbcH7~Ile44Ala ubiquitin with ΔUblD and UBE2L3/UbcH7~ubiquitin with ΔUblD, respectively. Discharge of UBE2L3/UbcH7~ubiquitin by ΔUblD+Thr415Asn Parkin is quicker than no E3 reaction (**E**). Lanes in each immunoblot comprise of reaction samples collected at chase time points indicated. Chase reactions were conducted as single reaction mixtures (100 μl) and chase samples (10 μl) were collected at the indicate time points in 2x Non-Reducing (NR) sample buffer containing 4 M Urea, 150 mM Tris pH 6.8, 5 mM ethylenediaminetetraacetic acid (EDTA), 2% SDS, 10% glycerol and bromophenol blue. In addition, a zero time point reduced (0R) sample was collected with 2xNR buffer containing 200 μM β-mercaptoethanol. ATP is adenosine triphosphate, min is minutes and RT is room temperature.

Nevertheless, the concomitant absence of auto-ubiquitination when Ile44Ala Ubiquitin is used despite observed activation of the UBE2L3~I44AUb (Figure 43D and 44E) provides experimental evidence of a novel requisite for Parkin's ubiquitin ligase potential *i.e.* interaction with the hydrophobic patch of ubiquitin.

5.4 Interactions between UblD/Ubiquitin and Parkin

The above results propose cross-talk between the hydrophobic patch of ubiquitin and UBR III could perform crucial roles in events surrounding ligase activity of Parkin (auto- or substrate ubiquitination). While peptide array interaction assays revealed multiple UblD interactions along Parkin's C-terminus, interactions at protein/domain levels need to be examined to understand the cross-talk mechanisms and how they affect ligase activity.

The molecular details of these interactions were addressed using NMR spectroscopy conducted in collaboration with Prof. Gary S. Shaw's group at the University of Western Ontario, Canada. A N-terminal truncation of Parkin, 321C, containing IBR and RING2 domains as well as the UBR III was expressed and purified in the Walden lab and shipped to Canada for these studies. Interestingly, partial oligomerisation of this species is observed (see Methods 2.2.1.5) however, the monomer fraction could be sufficiently isolated and was utilised for subsequent experiments. ^{15}N-labelled UblD samples were prepared with Parkin truncations (ΔUblD and 321C) at different ratios as part of standard [1H, 15N]-heteronuclear single quantum coherence (HSQC) experiments. In addition, ^{15}N-labelled ubiquitin were prepared with 321C to compare the interaction surface of IBR-RING2. Dr. Kathryn R Barber prepared all 15N-labelled reagents and spectroscopy experiments were carried out under the guidance of Prof. Shaw. A Bogue Research Fellowship awarded by University College London (UCL) supported the 7-week research visit. The results

discussed below are part of an on-going collaboration between the Walden and Shaw labs and should be considered as work-in-progress/preliminary data.

Based on all preceding results that suggest an intra-molecular interaction within Parkin, a dramatic effect of ^{15}N-UblD spectra was expected upon addition of unlabelled ΔUblD, as observed in (Figure 45). The disappearance of the majority of the peaks in a ^{15}N-UblD spectra is indicative of global changes in the chemical environment of UblD residues. A similar experiment with ^{15}N-K48A UblD as the labelled species showed a less dramatic effect (data not shown). Multiple interactions between UblD and ΔUblD (Parkin C-terminus), as suggested by peptide array experiments, and different titrants (ΔUblD with pathogenic missense mutations and other Parkin truncations) could be used in tandem to enhance the output.

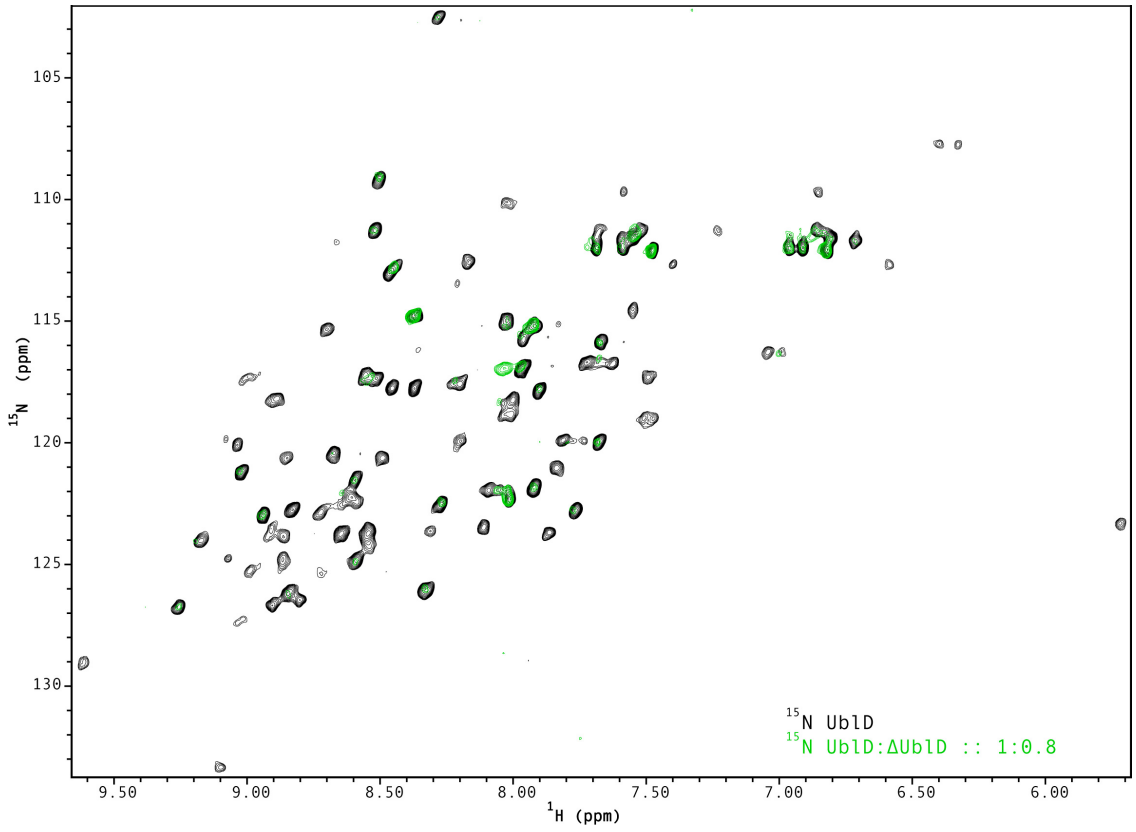

Figure 45: Ubiquitin-like Domain (UblD) interactions with ΔUblD. Overlay of ^{1}H-^{15}N HSQC spectra showing interactions of ΔUblD with ^{15}N labelled UblD. Spectra were collected using 150 μM UblD in 20 mM Tris pH 7.0, 150 mM NaCl, 1 mM Dithiothreitol (DTT) at 25˚C. Black contours indicate basal UblD spectra and green contours show effect of ΔUblD (120 μM) addition. ppm - parts per million.

321C interaction experiments with ^{15}N-UblD and ^{15}N-Ub were more informative for identifying interacting residues and contrasting the binding regions. Reference peak lists for ^{15}N-UblD and ^{15}N-Ub (from the Shaw lab) were used for automatic peak assignment (with minor manual adjustments) in NMRView (Johnson and Blevins, 1994), with tolerance levels of 0.2 and 0.02 parts per million (ppm) along nitrogen and proton dimensions respectively. HSQC spectra were recorded and peak assignment carried out for each addition of the 321C. Slow and intermediate exchange rates of UblD peaks were predominantly observed upon 321C titration (Figure 46A), in contrast to the fast exchange rates of ubiquitin peak (linear peak movement) (Figure 47A). Saturation of ubiquitin - 321C interaction was not observed despite addition of 2x excess 321C, however the UblD - 321C complex appeared closer to saturation as sample approached a ratio of 1:2. Combined changes in chemical shifts were calculated using the equation $((\Delta\delta H)^2 + (0.2*\Delta\delta N)^2)^{1/2}$ and plotted as histograms. $\Delta\delta$H and $\Delta\delta$N represent change in proton and nitrogen chemical shifts (in ppm) for labelled UblD (0x versus 1.6x excess 321C) and labelled Ub (0.5x versus 2x excess 321C) (Figure 46B and 47B). Residues that were perturbed greater than set thresholds (Mean + 1 Standard Deviation (SD), 0.024 ppm for UblD and 0.033 ppm for Ub) are indicated in the respective histograms.

Chemical shifts greater than the threshold of 0.033 ppm (equivalent to the calculated Mean + 1 SD for Ub) were mapped on the respective structures (Figure 48 A and B) (PDB 1IYF and 1UBQ) (Vijay-Kumar et al., 1987, Sakata et al., 2003). Unexpectedly, analogous surfaces on the UblD and ubiquitin were significantly perturbed upon interaction with 321C. Residues Val5, His11, Phe13, Ile44, His68 and Ile69 along the β-sheet of UblD show the largest changes while peaks corresponding to Gly12, Val67 and Val70 (indicated by asterisks in (Figure 46B) disappeared altogether or could not be assigned despite increasing the tolerance levels (0.5 and 0.05 ppm for ^{15}N and ^{1}H dimensions respectively). In addition, chemical shifts in Phe4, Asn8 and Ala46 were greater than the internal threshold for UblD (Mean + 1 SD, (Figure 46B).

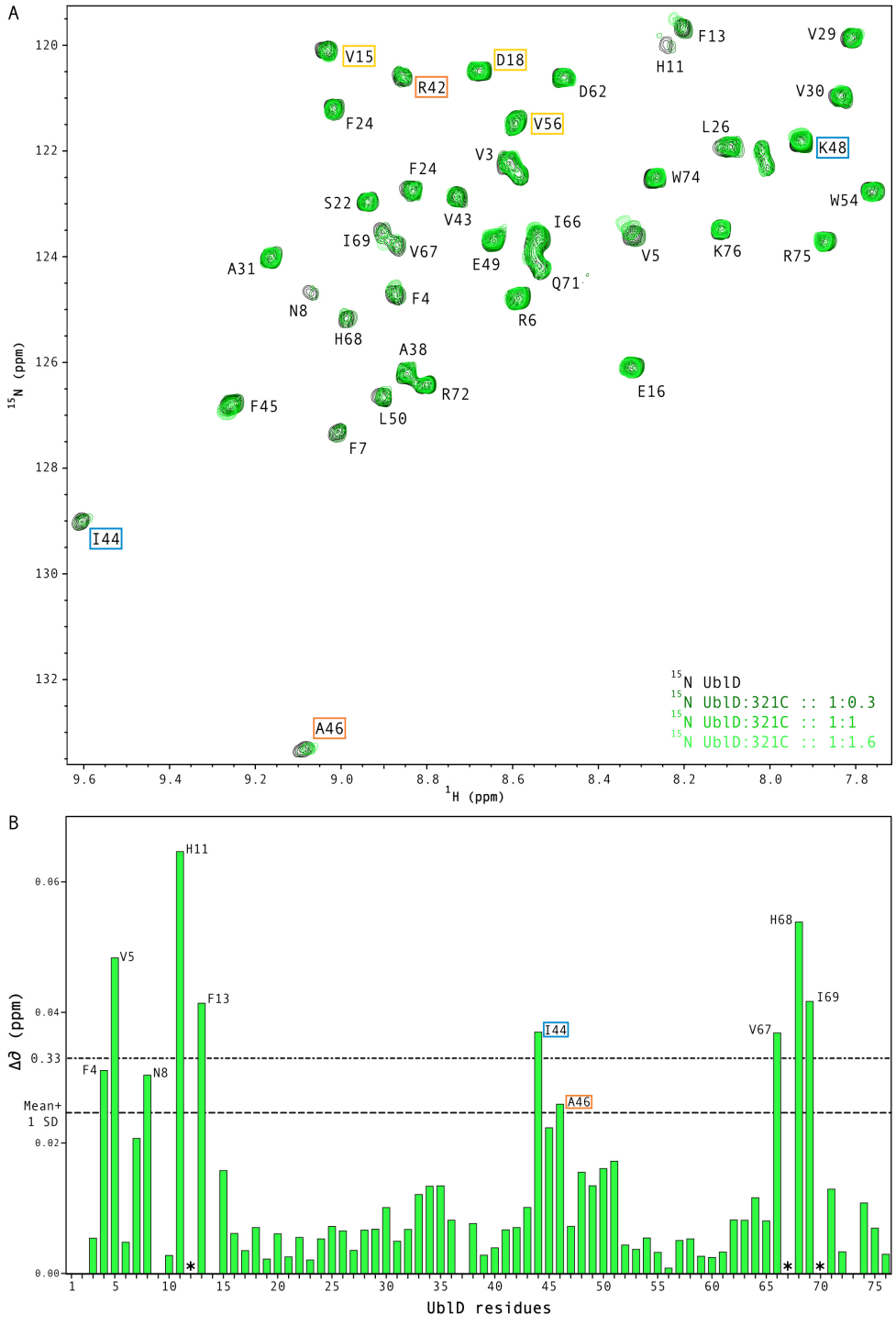

Figure 46: ^{15}N-UblD interactions with 321C. A. ^{1}H-^{15}N HSQC spectra of ^{15}N labelled Ubiquitin-like domain/UblD (select region) overlaid with spectra of 321C interaction experiments (basal state in black contours and gradient of green coloured contours corresponding to increasing 321C concentrations (bottom right)). Assigned peaks are labelled and select residues are boxed (yellow/orange for sites of Parkinson Disease missense mutations, blue for residues mutated in Sections 4.2 and 5.2 of this study). Spectra were collected using 120 μM UblD in 20 mM Tris pH 8.0, 150 mM NaCl, 1 mM Dithiothreitol (DTT) at 25˚C. **B.** Histograms show combined changes in chemical shifts $[((\Delta\delta H)^2 + (0.2*\Delta\delta N)^2)^{1/2}]$ for the residues assigned (x axis). * indicate residues that disappear or could not be automatically assigned. Residues perturbed more than Mean + Standard Deviation (SD = 0.024 parts per million (ppm); dashed line) are labelled. Threshold for comparison with shifts in Ub spectra (0.33 ppm) is also shown (dashed and dotted line).

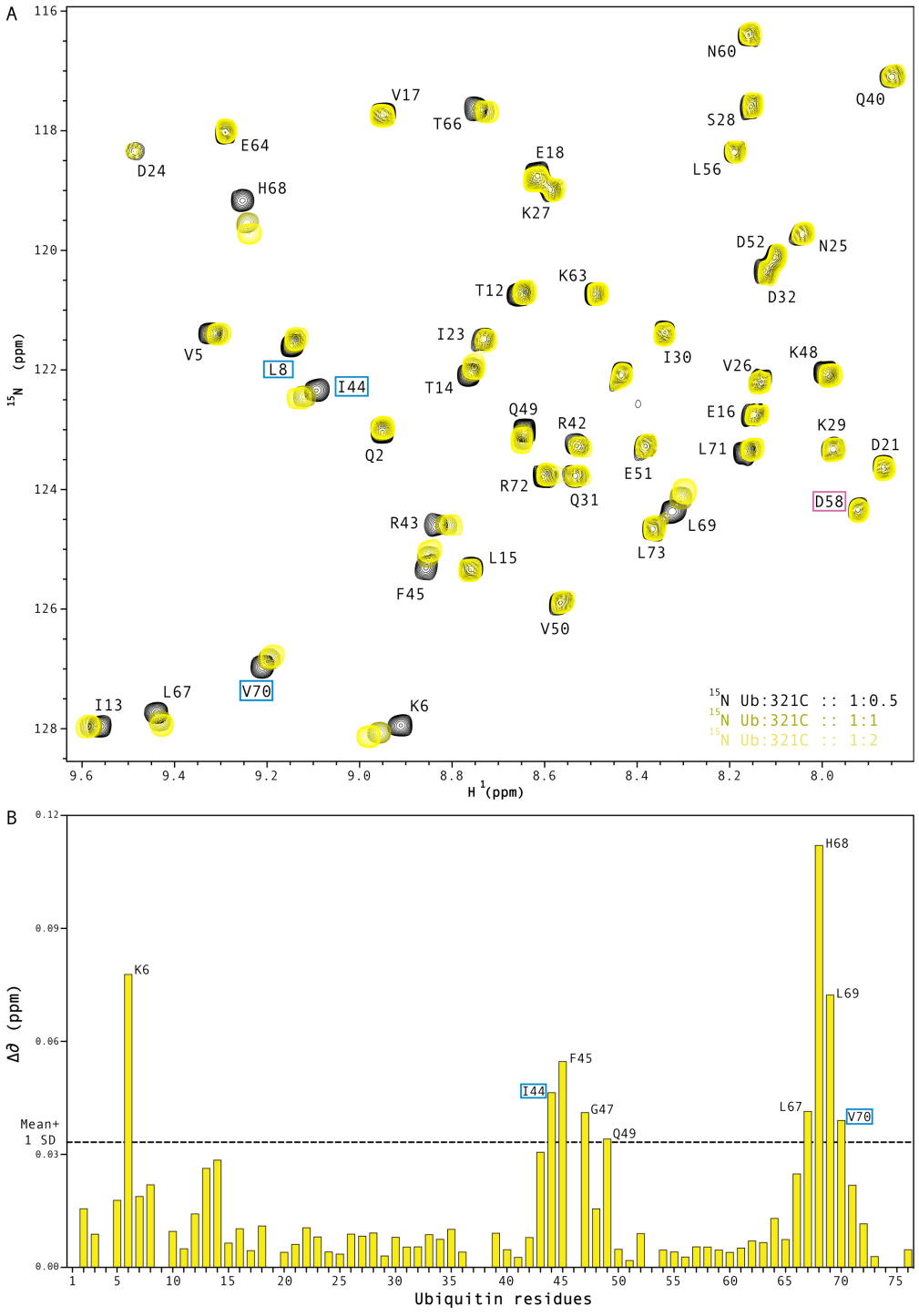

Figure 47: ^{15}N-Ub interactions with 321C. A. ^{1}H-^{15}N HSQC spectra of ^{15}N labelled ubiquitin/Ub (select region) overlaid with spectra of 321C interaction experiments (basal state in black contours and gradient of yellow coloured contours corresponding to increasing 321C concentrations (bottom right)). Assigned peaks are labelled and select residues are boxed (blue/pink for residues mutated in Section 5.2 of this study). Spectra were collected using 140 μM UblD in 20 mM Tris pH 7.0, 150 mM NaCl, 1 mM Dithiothreitol (DTT) at 25˚C. **B.** Histograms show combined changes in chemical shifts $[((\Delta\delta H)^2 + (0.2*\Delta\delta N)^2)^{1/2}]$ for the residues assigned (x axis). Residues perturbed more than Mean + Standard Deviation (SD = 0.033 parts per million (ppm); dashed line) are labelled.

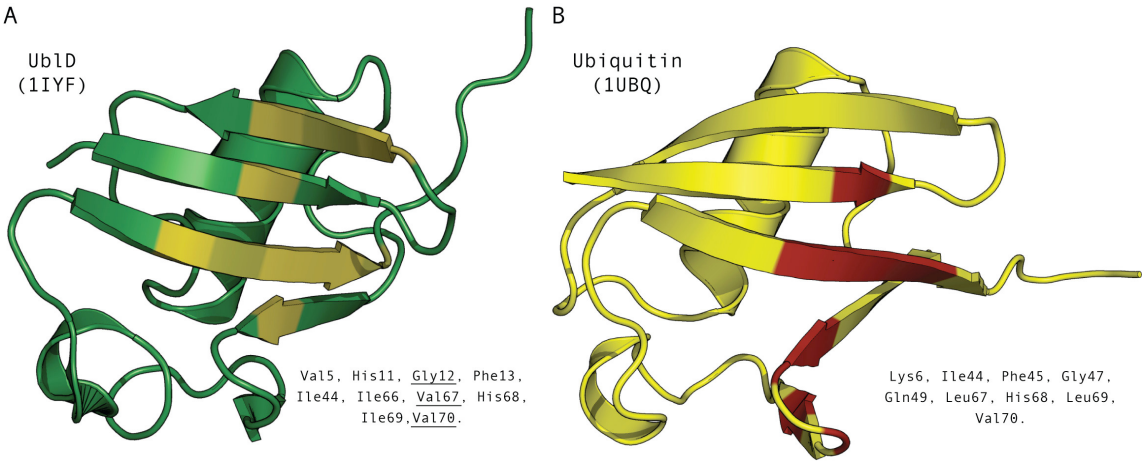

Figure 48: 321C interaction surface on Ubiquitin-like Domain (UblD) and Ubiquitin. A. UblD and **B.** Ubiquitin Nuclear magnetic resonance (NMR) chemical shift perturbations upon 321C titrations were mapped on their respective structures (PDB 1IYF and 1UBQ). Residues that perturbed greater than the set threshold (0.033 ppm) were coloured olive on UblD, red on Ubiquitin and listed alongside. UblD residues that disappeared/could not be picked are coloured dark olive and underlined.

Residues Lys6, Ile44, Phe45, Gly47, Gln49, Leu67, His68, Leu69 and Val70 on ubiquitin correspond to a similar surface for 321C interaction (Figure 48B). In the context of the ligase activity of Parkin, residues Gly12, Ile44 and Ala46 on the UblD, Ile44 and Val70 on ubiquitin are noteworthy. Gly12 and Ala46 are sites of PD missense mutations (Gly12Arg and Ala46Pro). The latter along with the Ile44Ala mutation relieve UblD mediated auto-inhibition of Parkin. Conversely, auto-ubiquitination of ΔUblD is abrogated by the Ile44Ala ubiquitin mutant and reduced in case of Val70Ala mutation (Figure 43A)

The above experiments were initially executed as titration based experiments where 321C (at high concentrations) was added to the same NMR sample tube after every data collection. However, its was observed that 321C in the sample tube gradually began to precipitate over 2-3 rounds of data collection (verified by subjecting precipitant to SDS-PAGE analysis) where each run lasted for around 85 minutes at 25°C. Subsequently, multiple samples were prepared, each with increasing proportions of 321C with the labelled material kept as constant. This approach proved successful however, rapidly used up the

purified 321C samples that were shipped to the Shaw lab prior to the visit. After the initial data collections confirmed 321C interactions with both ^{15}N-UblD and ^{15}N-Ub, a final set of experiments were planned to collect data at a range of 321C concentrations (0 to 2.5 fold excess) with the labelled reagents. These experiments would also provide for a broader set of peak shifts required to determine values of binding affinities. Unexpectedly however, these experiments did not reproduce the chemical shifts observed during the initial runs and a complete data set could not achieved within the fellowship period. Nevertheless, the visit was partially successful in confirming UblD and ubiquitin interactions with C-terminus of Parkin.

Given the UBR III is represented within 321C truncation of Parkin, a majority of the perturbations on both the spectra could be associated to interactions with this region. Interaction with the hydrophobic patch on ubiquitin was earlier shown to be a prerequisite for ubiquitin ligase activity of Parkin. Consequently, an intra-molecular interaction with the UblD could shield UBR III from ubiquitin thereby preventing auto-ubiquitination. Pathogenic mutations along the UblD - UBR III interface could disrupt this interaction resulting in constitutively active Parkin. Alternatively, as might be the case with T415N-Parkin, mutations that disrupt the Ub-UBR III interface result in 'ligase-dead' Parkin. Further analysis towards establishing binding affinities of the bivalent interactions observed with 321C and characterising effects of pathogenic mutations are required to validate this hypothesis.

5.5 'Mixed signals' from Parkin

Auto-ubiquitination of pure but tagged Parkin has been demonstrated as multi monoubiquitination *in vitro* (Matsuda et al., 2006, Hampe et al., 2006) and *in vivo* (Hampe et al., 2006). Both the reports conclude Parkin is an E3 ligase with monoubiquitination capacity and secondary factor like E4s (CHIP (Imai et al., 2002, Imai et al., 2001)) or chain-specific E2s (UBE2N/UBE2V1 (Ubc13/UEV1)

heterodimer (Doss-Pepe et al., 2005, Olzmann et al., 2007)) are required to mediate substrate polyubiquitination. Furthermore, UblD directed substrate interaction of Parkin activated its monoubiquitination potential towards EPS15 and endophilin-A (Fallon et al., 2006, Trempe et al., 2009). In both cases, Parkin auto-ubiquitination was observed, with multi-monoubiquitination confirmed in the former. Conversely, as introduced earlier, Parkin has been reported to catalyse K48-linked (Zhang et al., 2000, Corti et al., 2003) and K63-linked (Chung et al., 2001, Olzmann et al., 2007) polyubiquitin chains on different substrates.

The data presented here demonstrates inhibition of Parkin auto-ubiquitination by UblD domain. Thus, ubiquitin chain building capability of Parkin was investigated using full-length Parkin UblD mutations (pathogenic A42P-Parkin and directed by rationale; K48A-Parkin, I44A-Parkin) as well as the ΔUblD truncation. Furthermore UBE2L3/UbcH7 was used the E2 of choice as it lacks intrinsic capability of ubiquitin chain synthesis. Auto-ubiquitination assays were conducted using wild-type ubiquitin and mutants bearing no lysines (K0Ub) and single lysine mutants K48Ub and K63Ub (Figure 49A). In addition, auto-ubiquitination reactions with wild-type ubiquitin were subject to western blot analysis using antibodies that recognize mono and polyubiquitin (FK2) alongside those that exclusively recognise polyubiquitin species (FK1) (Figure 49B).

Auto-ubiquitination reactions with wild type and lysine mutants of ubiquitin show activity with all the Parkin species tested. Moderately lower levels of activity were observed with 6xHis-tagged K0Ub in all Parkin species (reactions 2 in (Figure 49A). As the mutant is incapable of chain formation, multi-monoubiquitination was observed (at least three ubiquitins ligated) confirming the previous observations. A gradual trend of decreasing auto-ubiquitination, in the order of wild-type ubiquitin, K48Ub and K63Ub (reactions 1, 3 & 4 respectively in (Figure 49A)), was observed in Parkin UblD mutants. The observations suggest multi-monoubiquitination is the underlying modification

with possibility of K48- and K63-linked polyubiquitin chains. This was confirmed by detection with FK2 antibodies however, signal levels were not comparable to detection by the anti-His antibody except in the case of ΔUblD (Figure 49B). Unexpectedly, none of the UblD mutant species of Parkin showed polyubiquitination as observed with lack of high molecular weight species when probed with the polyubiquitin specific FK1 antibody. Absence of signal could be due technical factors and the possibility polyubiquitin chain synthesis by UblD mutants cannot be ruled out completely. Nevertheless, polyubiquitination of ΔUblD was readily detected demonstrating, for the first time, that synthesis of polyubiquitin chains is an intrinsic property of Parkin.

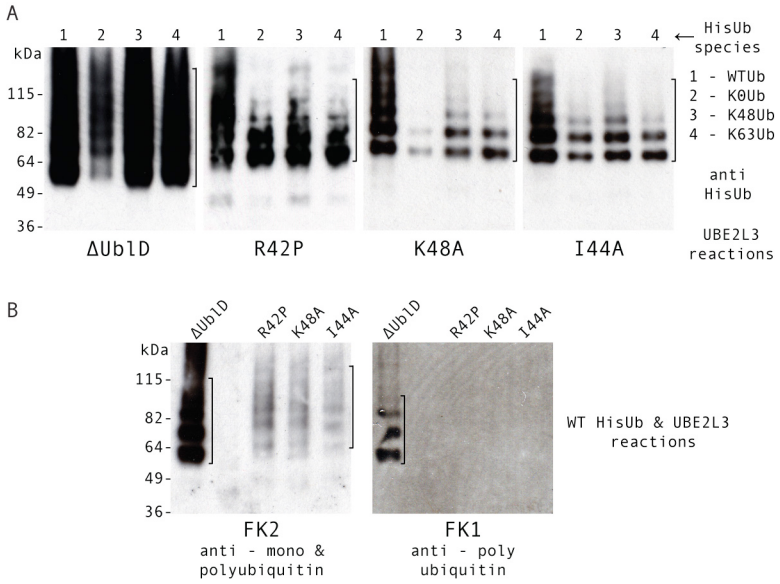

Figure 49: Analysis of ubiquitin chain synthesis. A. Auto-ubiquitination reactions with ΔUblD (1 μM) and Parkin UblD mutants; Arg42Pro, Lys48Ala and Ile44Ala (0.77 μM each). UBE2L3/UbcH7 (1.1 μM) was the E2 used for all reactions, while 6xHis tagged Ubiquitin wild type K0, K48 and K63 were used in reactions 1, 2, 3 and 4 respectively. **B.** Reaction products of auto-ubiquitination with wild type ubiquitin (reactions 1 in **A.**) were analysed by antibodies that recognise mono and polyubiquitin species (FK2) and those exclusive for polyubiquitin chains (FK1). Immunoblots revealed polyubiquitination potential of ΔUblD, while Parkin mutants were pre-dominantly mono-ubiquitinated.

Unconfirmed observations suggest a similar pattern with the UBR I mutant K161N-Parkin and UBR II mutant T240R-Parkin, however polyubiquitination could not be confirmed with the latter (data not shown). Further experiments are required to establish the ubiquitination profile of various pathogenic mutations and more importantly, their effect on auto-inhibition. Mixed ubiquitin signals

generated by artificially activated Parkin species reveals another level in the ubiquitin ligase potential of Parkin with the UblD as the primary regulatory module of all the levels. UBRs III and I show ubiquitin interaction and the hydrophobic patch on ubiquitin was observed to be necessary for Parkin's ubiquitin ligase. Thus, a trade-off between UblD/ubiquitin interactions and intra-molecular co-operation between UBRs could play a crucial role in ubiquitin chain synthesis and specificity.

In summary, the hydrophobic patch on ubiquitin was earlier shown as a novel requisite for enabling the ubiquitin ligase potential of Parkin. Mechanisms of intra-molecular inhibition by the UblD are likely to involve the regulation of Parkin-Ubiquitin interaction, indirectly suggested by analogous surfaces on ubiquitin and UblD for interaction with 321C. UBR III, represented in 321C and earlier shown (section 4.5) to exhibit bivalent (UblD/Ub) interaction properties, is a probable candidate for such a surface. Finally, intrinsic polyubiquitination capacity of Parkin was demonstrated for the first time by the ΔUblD species.

Chapter 6. Discussion

6.1 Synopsis

Parkin is a multifaceted RBR E3 ligase, observed to co-operate with several E2s, recognise a diverse group of substrates and catalyse distinct ubiquitination events including auto-ubiquitination. In addition, several mutations in the *Parkin* gene are causative of AR-JP and affect the E3 ligase properties of Parkin in different ways. Thus, the examination of Parkin's E3 ligase properties will offer deeper insight into fundamental mechanisms of ubiquitin E3 ligases (substrate recognition and ubiquitin chain synthesis) and how they are regulated/deregulated.

The work presented here introduces the regulation of the E3 ligase activity of Parkin as an inherent property, mediated by the UblD. Contrary to numerous reports over the last decade, wild type Parkin does not exhibit auto-ubiquitination with any of its cognate E2s. The N-terminal UblD domain was demonstrated as an auto-inhibitory module that is disrupted by the presence of bulky N-terminal tags and UblD directed substrate interactions. Pathogenic mutations within the UblD that unfold the globular domain and domain deletion (ΔUblD) disrupt the inhibition resulting in a constitutively active molecule. Accordingly, auto-inhibition can be restored in the ΔUblD truncation upon N-terminal re-ligation of the UblD.

Auto-inhibition of Parkin or the intrinsic inhibition of ligase activity was observed to arise due to an intra-molecular interaction between the UblD and Parkin's C-terminus. A conserved residue (Lys48) in the UblD is crucial for the intra-molecular interaction and essential RING-E2 interactions were not hindered by the 'closed' tertiary structure of Parkin. Interaction mapping experiments reveal at least two surfaces on the C-terminus of Parkin (UBRs II and III) that could

support the intra-molecular interface with the UblD. Furthermore, novel Parkin-ubiquitin interaction surfaces were also revealed (UBRs I and III).

Consequently, the hydrophobic patch on ubiquitin was demonstrated as a novel requisite enabling the ubiquitin ligase potential of Parkin. The C-terminal region of Parkin (321C which includes the IBR-RING2 domains) was shown to interact with analogous surfaces on ubiquitin and UblD. Auto-inhibition of Parkin is expected to involve UblD mediated preclusion of a Parkin-Ubiquitin interaction. Finally, the capacity to synthesise polyubiquitin chains was demonstrated as an intrinsic feature of Parkin and is likely to involve dynamic cross talk between UblD, the UBRs and ubiquitin.

6.2 Structure-function characterisation of Parkin UBR III.

The above studies introduce unique interaction surfaces that could prove critical in understanding the mechanisms of E3 ligase activity in Parkin and dysfunction in the disease context. A prerequisite for ubiquitin interaction in RING E3 ligase activity is a novel property described for Parkin and furthermore inherent regulation of this interaction, mediated by the UblD is proposed from the above observations. To understand the nature of the unique bivalent interactions observed with 321C, structural features of the UBR III were re-examined. PSIPRED, a secondary structure prediction software (http://bioinf.cs.ucl.ac.uk/psipred/) predicted residues Asp394 to Thr414 of the UBRIII to form a helical structure with high degree of confidence (Figure 50A). Unexpectedly, primary sequence analysis of the UBR III revealed an uncanny resemblance to UIM motifs. The eexxϕxxAϕe/zSzxe signature represents the canonical sequence for a UIM motif, where 'e' represents negatively charged, ϕ for hydrophobic, z for bulky hydrophobic/polar and x represents any residue (Hirano et al., 2006, Hofmann and Falquet, 2001). These α-helical UBDs pack against the hydrophobic patch of ubiquitin with the conserved Ala and Ser residues (underlined) making extensive contacts with the core hydrophobic residues

Ile44, Val70 and Leu8 ((Swanson et al., 2003) and reviewed in (Dikic et al., 2009, Hurley et al., 2006). Multiple sequence alignments between UBR III and single-sided UIMs (1:1::UBD:ubiquitin interactions) revealed two stretches, Asp392 to Lys406 (UBR IIIa) and Glu399 to Lys413 (UBR IIIb), staggered by five residues, that resemble a UIM each (Figure 50B). However, neither of them follows the UIM canonical sequence, absence of the conserved Ser being the most notable exception (Ala403 and Thr410 in the respective stretches).

Helical wheel projections (α-helix) of the predicted UBR III helix shows polarized surfaces for the two putative UIMs (Figure 43C). However, alignments with double-sided UIMs (1:2::UBD:ubiquitin interactions), represented by the canonical sequence exexϕxϕAϕAzSzS/Ae (repeating UIMs with a +2 offset, refer (Hirano et al., 2006) for more details) showed even less agreement (data not shown). Pathogenic missense mutations punctuate more of UBR IIIa (Figure 50C) in particular mutations Asp394Asn and Ala398Thr would disrupt supporting interactions in a 'UIM' - UblD/Ub complex. The Glu409X mutation would result in truncation of the predicted helix, more importantly in loss of RING2. However, Thr415, the site of the 'ligase-dead' Parkin mutation T415N, lies at the foot of UBRIIIb and two residues N-terminal of the first zinc coordinating cysteine in RING2. Given the analogous nature of the UblD/Ub - 321C interaction surface, it is likely either UBRIIIa or UBRIIIb would behave as the sole UIM-like motif in UBR III.

Interestingly, UblD residues shown to interact with EPS15 UIMs (Parkin substrate) are comparable to those perturbed in the presence of 321C ((Safadi and Shaw, 2010) and Figure 46 of this study, compiled in Figure 50D). Both RPN10 (Parkin interactor) and EPS15 have tandem UIMs with UIM II of EPS15 is predicted to be a double-sided UIM (Hirano et al., 2006). UblD was observed to prefer UIM I for the S5A interaction while both the UIMs of EPS15 participate in the UblD interaction (Safadi and Shaw, 2010). Authentication of UBR III as a UIM-like motif and correlation with observed UblD interactions would be an attractive prospect for future work.

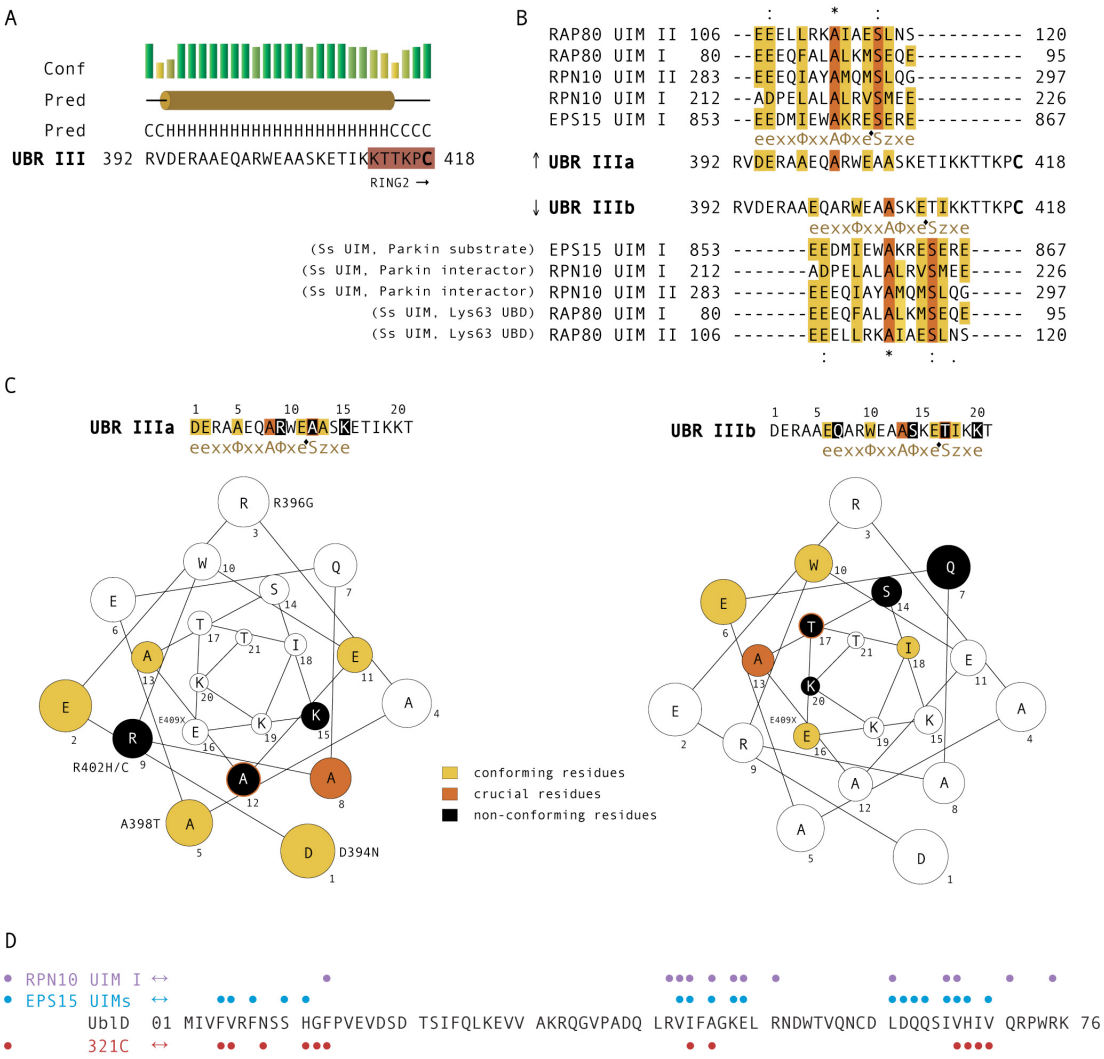

Figure 50: Structure-function analysis of UblD/Ub Binding Region (UBR) III. A. Secondary structure prediction of the UBR III by PSIPRED showing high probability of helical structure between Asp394 and Thr414. Overlap with RING2 domain highlighted in brown and in bold is the zinc co-ordinating cysteine. **B.** Sequence alignments (ClustalW {Chenna, 2003 #430} generated and manually adjusted) of putative Ubiquitin Interacting Motifs (UIM)-like motifs UBR IIIa and IIIb with UIM consensus sequence and known single-sided (Ss) UIM motifs. (x is any residue, z is bulky hydrophobic/polar, e is negatively charge, Φ is hydrophobic and e• indicates position can be occupied by e/z). Residues conforming to consensus signature are coloured yellow and orange the latter specifies crucial residues. In bold is zinc co-ordinating cysteine of RING2. **C.** α-Helical wheel projections of predicted UBR III helix (Asp394 to Thr414, renumbered 1-21 for clarity) showing polarised orientation of the putative UIMs, UBR IIIa (left) and UBR IIIb (right). Conforming and crucial residues are coloured yellow and orange respectively. Black and black with orange border indicate non-conforming resides, the latter denotes absence of crucial UIM residue. Location and nature of PD mutations within UBR IIIa and IIIb are indicated in the respective wheels. **D.** UblD residues that participate in interaction with RPN10 UIM I (purple dots) (Safadi and Shaw, 2010), EPS15 UIMs (blue dots) (Safadi and Shaw, 2010), and 321C (maroon dots; from Figure 48 in this study). UblD is ubiquitin like Domain, Ub is ubiquitin, RPN is Regulatory particle non-ATPase protein, RAP80 is Receptor associated Protein 80, and EPS 15 is Epidermal growth factor receptor substrate 15.

6.3 Implications for Parkinson's disease

In the context of the disease state, the data presented here demonstrates that ligase activity profile of Parkin most certainly is an indicator of function/dysfunction. At the basal level, the UblD inhibits auto-ubiquitination through an intra-molecular interaction where ligase activity is rendered latent. Substrate interactions mediated by the UblD activate the monoubiquitination potential of Parkin and its concomitant auto-ubiquitination. Auto-ubiquitination can also result from Parkin UblD mutants in particular those that unfold the N-terminal domain. Substrate recognition by C-terminal domains of Parkin could result in a rearrangement of the intra-molecular inhibited state thereby releasing the polyubiquitination potential of Parkin. Preliminary observations with pathogenic mutations in the UBRs that exhibit auto-ubiquitination (Lys161Asn, data not shown) as well as ΔUblD polyubiquitination support this theory.

It has been previously suggested that Parkin may be physiologically processesed to release the UblD (Schlossmacher et al., 2002) and caspase cleavage upon induction of apoptosis (Kahns et al., 2003, Kahns et al., 2002). The translation of N-terminally truncated Parkin resulting in loss of the UblD was attributed to an alternative start site (codon 80) (Henn et al., 2005). The effect of ligase activity, however, was not addressed in the above reports. Given the data presented here, the above events are likely to activate auto-ubiquitination of Parkin.

Conventionally, auto-ubiquitination has been used as a marker for ligase activity of Parkin. In addition, relative solubility levels of wild type and mutant Parkin reflect folded state and stability of the enzyme. Finally, comparative analyses of substrate ubiquitination levels determine function/dysfunction of the Parkin species. Deletion of the UblD had no effect on solubility and cellular localization of Parkin (Henn et al., 2005, Kyratzi et al., 2007). Other reports have

demonstrated that deletion of UblD resulted in the loss of substrate ubiquitination but not substrate binding/colocalization; AIMP2 (Corti et al., 2003) and Synaptotagmin-XI (Huynh et al., 2003) however the same deletion did not affect auto-ubiquitination (Finney et al., 2003). Conversely UblD mutants, in particular Arg42Pro, resulted in drastic destabilisation of Parkin and the formation of inclusion bodies (Henn et al., 2005, Kyratzi et al., 2007, Wang et al., 2005, Hampe et al., 2006) while auto-ubiquitination was observed *in vitro* (Matsuda et al., 2006) with 'increased' levels *in vivo* (Sriram et al., 2005). Furthermore, the same report observed enhanced non-degradative ubiquitination of Parkin substrates AIMP2 (despite reduced binding) and Synphilin-1 (increased binding), with accumulation of the former in inclusion bodies. On the contrary, a higher rate of proteasomal turnover for Arg42Pro and other UblD mutants was observed elsewhere (Henn et al., 2005).

Data presented here shows auto-ubiquitination of wild-type Parkin is inhibited thus changing the baseline for comparison of ligase activity and, more importantly shifting the focus toward substrate ubiquitination. In theory, 'activated' Parkin (tagged/mutant/N-terminal truncated) could result in incessant auto-ubiquitination and indiscriminate substrate ubiquitination leading to redistribution to inclusion bodies/aggresomes (Cookson et al., 2003, Muqit et al., 2004). Alternatively, proteasomal turnover of auto-ubiquitinated Parkin could also occur (Choi et al., 2000, Zhang et al., 2000, Ardley et al., 2003, Junn et al., 2002) contributing to loss of the required ubiquitin signal on Parkin substrates. Auto-ubiquitination of 'activated' Parkin could be also enhanced by E3 independent monoubiquitination, a *cis* event arising from interaction between UBD element (Parkin UBRs) and ubiquitin moiety conjugated to an E2. Interestingly, auto-ubiquitination was observed in species with mutations in zinc co-ordinating residues Cys289Gly (RING1, *in vitro* (Matsuda et al., 2006)), Cys431Phe (RING2, *in vivo* (Sriram et al., 2005)). As these mutations are likely to unfold the catalytic RING domains rendering the ligase inactive, a UBD mediated ubiquitination could explain the 'auto-ubiquitination' events. Compounding these issues however, is the use of over-expressed tagged

Parkin to establish the mechanism of dysfunction. Loss-of-function is considered the pathogenic mechanism in AR-JP and majority of the mutations in the *Parkin* gene are heterozygous recessive. On the contrary, the above referenced reports portray a toxic gain of function for several of these mutations and furthermore over expression of Parkin, a common method used in the above studies could lead to non-physiological phenotypes (Kyratzi et al., 2007, Dawson and Dawson, 2010).

The present study establishes the hydrophobic patch on Ubiquitin as a novel requisite of the ligase activity. UblD mediated auto-inhibition is likely to involve regulation of the Parkin-Ubiquitin cross-talk providing novel insights into regulation of Parkin ligase activity. Accordingly, some of the pathogenic missense mutations in the proposed ubiquitin interaction surfaces (14 mutations in UBRs I, II and minor hit E11-14) could disrupt the ubiquitin interaction resulting in ligase inactivation. Conversely, mixed ubiquitin signals generated by the ΔUblD (and possibly other mutations) could also be interpreted as loss-of-function. Deregulation of Parkin could render the ligase incapable of catalysing precise ubiquitin signals on substrates, thus contributing to loss of downstream functions. Further analysis into mechanisms of Parkin inactivation is required to understand true function of the E3 ligase and loss-of-function mechanism in AR-JP pathogenesis.

6.4 Implications for the Ubiquitin pathway

There are several proteins in the human proteome with integral ubiquitin like domains, primarily involved in various protein quality control systems as well as other cellular processes (reviewed in (Grabbe and Dikic, 2009, Welchman et al., 2005)}. Intra-molecular inhibitory interactions were first reported within the UV excision repair protein RAD23 homolog B (hHR23B) (Ryu et al., 2003). The multi-domain protein includes an N-terminal Ubl domain (binds RPN10 subunit of 26S proteasome) and a xeroderma pigmentosum complementation group C

(XPC)-binding domain flanked by two UBA domains (UBA domains 1 and 2, the latter preferentially binds Lys48-linked polyubiquitin chains (Varadan et al., 2005)). The protein has crucial functions in the nucleotide excision repair (NER) pathway in response to DNA damage as well as a 'proteasomal shuttle' (Schauber et al., 1998, Sugasawa et al., 1998). The latter function involves interactions between UBA domain 2 with Lys48-linked polyubiquitinated substrates and subsequent transfer to the 26S proteasome mediated by Ubl interactions with proteasomal subunits thereby regulating the turnover of polyubiquitinated substrates. Regulation of this function involves intramolecular interaction between Ubl and UBA domains thereby maintaining the protein in a 'closed' or inactive conformation (Ryu et al., 2003).

A similar closed/inactive state was revealed in this study for wild type Parkin, probably mediated by the UblD – UBR interactions. In addition, Parkin (UblD) interactions with RPN10 (UIM 1), proteasomal regulatory subunit have been observed (Sakata et al., 2003), and biophysically characterized (Safadi and Shaw, 2010). The UblD surface that supports interactions with RPN10 UIM I and the intra-molecular inhibitory interaction of Parkin are similar (Figure 50D), thus regulating Parkin-proteasome cross talk. However, a functional relevance of this binding is unclear and is likely to involve proteasomal degradation of auto-ubiquitinated/deregulated Parkin and/or its associated substrates (Upadhya and Hegde, 2003). A recent bioinformatics driven study in to multiple members of IAP family of RING E3 ligase uncovered a conserved UBA domain found to preferentially bind Lys63-linked polyubiquitin chains of potential significance in NF-kappaB signalling (Gyrd-Hansen et al., 2008). The presence of cryptic UblD/Ub binding regions in Parkin (UBR III and RING0) could help direct experiments that establish 'novel ubiquitin receptor' functions for the E3 ligase. Alternatively, the presence of Parkin UBDs could be decisive in mechanisms of ubiquitin chain synthesis, a role previously proposed while describing acceptor lysine selection for ubiquitin chain type specificity by HECT E3 ligases (Wang and Pickart, 2005, Kim and Huibregtse, 2009) as well as for

promoting the formation of degradable ubiquitin chains by RING/U-box E3 ligases under the influence of RPN10 UIMs (in *trans*) (Kim et al., 2009).

This study proposes regulation of the E3 ligase activity as a novel role for Ubl domains. The mechanism of intra-molecular inhibition and/or a regulatory role for Ubls could be could be extended to other members of the E3 ligase family. Auto-inhibition of Smurf ligase activity has been observed and mediated by intra-molecular interaction through the C2 domain (Wiesner et al., 2007). Elongin-B, a subunit of the von-Hippel-Landu (VHL) E3 ubiquitin ligase complex also contains the Ubl domain, however has not been functional characterised. Interactions between the Ubl domains of Ubiquitin Specific Protease (USP) 7 and the viral ring finger protein Herpes simplex virus type 1 immediate-early regulatory protein (ICP0) represses the auto-ubiquitination mediated destruction of the viral protein (Zhu et al., 2007, Canning et al., 2004).

Regulation of ligase activity is critical to ensure ubiquitin signals are generated at the right place and right time. The heterodimeric LUBAC complex, consisting of HOIL-1L and HOIP is an interesting case of a RING E3 ligase complex capable of synthesising linear ubiquitin chains with a range of E2 enzymes (Kirisako et al., 2006) however, the mechanistic details of these events are awaited. Parkin shares the UbID/RING-IBR-RING domain arrangement with that of HOIL-1L however, the former bears two potential UBDs/UBRs located in RING0 (UBR I and minor hit E11-14) and UBRIII while the latter bears a ubiquitin binding Npl4 type Zinc Finger (NZF) domain for at a similar location as the first zinc finger of RING0. A recent report exploring the physiological state of Parkin in mouse brain, heart and skeletal muscle tissues observed the E3 ligase to be part of a non-covalent ~110kDa heterogeneous complex (Van Humbeeck et al., 2008). Another report observed Parkin/DJ1/PINK1 operate as a complex when over-expressed in SH-SY5Y neuroblastoma cells, are predominantly localised in the cytoplasm and had E3 ligase properties (auto- and substrate ubiquitination (synphillin-1)) (Xiong et al., 2009). Furthermore, Parkin has been observed to function as the RING component of an SCF

complex in the degradation of cyclinE (Staropoli et al., 2003). Wild type Parkin, as observed in this study, needs to be activated (or relieved of the UblD mediated intramolecular inhibitory interaction) for the molecule to exhibit its E3 ligase properties. Taken together, it is plausible that Parkin operates in different semi-CRL like complexes; each with a Parkin 'effecter' molecule that bears a UBD (or at least a Parkin UblD binding domain) thus, selectively activates the ligase when required.

Activation of the dormant ligase allows additional control of E3 ligase enzymatic activity. Mechanisms of enhanced SCF ligase activity upon conjugation of the ubiquitin-like protein Nedd8 have been demonstrated (Duda et al., 2008, Saha and Deshaies, 2008, Yamoah et al., 2008). Differential regulation of the E2 enzymatic properties upon sumoylation has also been observed; UBE2K/Ubc1 (Pichler et al., 2005) and UBE2I/Ubc9 (Knipscheer et al., 2008). Degradative auto-ubiquitination of the RING E3 ligase cIAP1 induced by small-molecules presents a case for therapeutic strategies directed towards an E3 ligase (Sekine et al., 2008). Perhaps the strongest argument for activation of Parkin's E3 ligase potential comes from PINK1-Parkin interaction for mitochondria homeostasis. Recent reports have demonstrated that PINK1 selectively recruits Parkin to damaged mitochondria (Narendra et al., 2008) and activates its E3 ligase potential (Matsuda et al., 2010, Narendra et al., 2010) while pathogenic mutations in Parkin disrupts clearance of damaged mitochondria (Geisler et al., 2010, Lee et al., 2010). However, the mechanism of Parkin recruitment and activation is unclear and is likely to involve disruption of the UblD mediated auto-inhibition of Parkin.

6.5 Future perspectives

The data presented here establishes a novel E3 ligase inhibitory mechanism for Parkin's UblD, likely to be its fundamental role. However, other functions of UblD have previously been demonstrated; substrate recognition (Fallon et al.,

2006, Trempe et al., 2009) and interaction with proteasome (Sakata et al., 2003). Given the prerequisite of ubiquitin's hydrophobic patch for Parkin's E3 ligase activity, the presence of multiple UBRs and possible competition between UblD and ubiquitin for UBR interaction together predict a dynamic role for the UblD in ubiquitin chain synthesis. Recently, a similar requirement of ubiquitin interaction was reported for polyubiquitin chain synthesis by HECT E3 ligases Rsp5 (French et al., 2009) and Smurf (Ogunjimi et al., 2010).

Authentication of UBR III as UIM(s) would be the first port of call and mutations predicted to disrupt UIM-ubiquitin interactions followed by auto-ubiquitination assays would present some clues. An interesting outcome would be if both IIIa and IIIb prove to be functional UIMs. In theory, UBR III could provide a molecular groove over which UblD could swivel, exposing/concealing adjacent UBRs and ubiquitin interactions thus regulating ubiquitin chain formation. Structural characterisation would also reveal deeper mechanistic insights of the interface. Validation of the RING0 region (contains UBR I and minor hit E11-14) as a possible zinc-finger based UBD needs to be addressed. Presence of two (or three) 'UBDs' on a single subunit RING E3 ligase could help direct specificity of the growing chain and possibly enhance processivity.

In summary, this study shows the tertiary arrangement of Parkin domains influences its activity. A mechanistic insight into UblD mediated intra-molecular regulation of RING E3 ligase activity was presented along with the effect of certain pathogenic mutations to this regulation. Novel requirements for ligase activity were uncovered along with predictions of Parkin UBDs and ubiquitin interactions that could play a crucial role in diverse E3 ligase activities exhibited by Parkin.

Chapter 7. References

ANDERSEN, P. L., ZHOU, H., PASTUSHOK, L., MORAES, T., MCKENNA, S., ZIOLA, B., ELLISON, M. J., DIXIT, V. M. & XIAO, W. (2005) Distinct regulation of Ubc13 functions by the two ubiquitin-conjugating enzyme variants Mms2 and Uev1A. *J Cell Biol,* 170**,** 745-55.

ANDRES-MATEOS, E., PERIER, C., ZHANG, L., BLANCHARD-FILLION, B., GRECO, T. M., THOMAS, B., KO, H. S., SASAKI, M., ISCHIROPOULOS, H., PRZEDBORSKI, S., DAWSON, T. M. & DAWSON, V. L. (2007) DJ-1 gene deletion reveals that DJ-1 is an atypical peroxiredoxin-like peroxidase. *Proc Natl Acad Sci U S A,* 104**,** 14807-12.

ARAVIND, L., IYER, L. M. & KOONIN, E. V. (2003) Scores of RINGS but no PHDs in ubiquitin signaling. *Cell Cycle,* 2**,** 123-6.

ARAVIND, L. & KOONIN, E. V. (2000) The U box is a modified RING finger - a common domain in ubiquitination. *Curr Biol,* 10**,** R132-4.

ARDLEY, H. C., SCOTT, G. B., ROSE, S. A., TAN, N. G., MARKHAM, A. F. & ROBINSON, P. A. (2003) Inhibition of proteasomal activity causes inclusion formation in neuronal and non-neuronal cells overexpressing Parkin. *Mol Biol Cell,* 14**,** 4541-56.

ARDLEY, H. C., TAN, N. G., ROSE, S. A., MARKHAM, A. F. & ROBINSON, P. A. (2001) Features of the parkin/ariadne-like ubiquitin ligase, HHARI, that regulate its interaction with the ubiquitin-conjugating enzyme, Ubch7. *J Biol Chem,* 276**,** 19640-7.

AVRAHAM, E., ROTT, R., LIANI, E., SZARGEL, R. & ENGELENDER, S. (2007) Phosphorylation of Parkin by the cyclin-dependent kinase 5 at the linker region modulates its ubiquitin-ligase activity and aggregation. *J Biol Chem,* 282**,** 12842-50.

BAKER, R. T. & BOARD, P. G. (1991) The human ubiquitin-52 amino acid fusion protein gene shares several structural features with mammalian ribosomal protein genes. *Nucleic Acids Res,* 19**,** 1035-40.

BARLOW, P. N., LUISI, B., MILNER, A., ELLIOTT, M. & EVERETT, R. (1994) Structure of the C3HC4 domain by 1H-nuclear magnetic resonance spectroscopy. A new structural class of zinc-finger. *J Mol Biol,* 237**,** 201-11.

BAZIRGAN, O. A. & HAMPTON, R. Y. (2008) Cue1p is an activator of Ubc7p E2 activity in vitro and in vivo. *J Biol Chem,* 283**,** 12797-810.

BEASLEY, S. A., HRISTOVA, V. A. & SHAW, G. S. (2007) Structure of the Parkin in-between-ring domain provides insights for E3-ligase dysfunction in autosomal recessive Parkinson's disease. *Proc Natl Acad Sci U S A,* 104**,** 3095-100.

BERNASSOLA, F., KARIN, M., CIECHANOVER, A. & MELINO, G. (2008) The HECT family of E3 ubiquitin ligases: multiple players in cancer development. *Cancer Cell,* 14**,** 10-21.

BIEDERER, T., VOLKWEIN, C. & SOMMER, T. (1997) Role of Cue1p in ubiquitination and degradation at the ER surface. *Science,* 278**,** 1806-9.

BONIFATI, V., RIZZU, P., VAN BAREN, M. J., SCHAAP, O., BREEDVELD, G. J., KRIEGER, E., DEKKER, M. C., SQUITIERI, F., IBANEZ, P., JOOSSE, M., VAN DONGEN, J. W., VANACORE, N., VAN SWIETEN, J. C., BRICE, A., MECO, G., VAN DUIJN, C. M.,

OOSTRA, B. A. & HEUTINK, P. (2003) Mutations in the DJ-1 gene associated with autosomal recessive early-onset parkinsonism. *Science,* 299**,** 256-9.

BORDEN, K. L., BODDY, M. N., LALLY, J., O'REILLY, N. J., MARTIN, S., HOWE, K., SOLOMON, E. & FREEMONT, P. S. (1995) The solution structure of the RING finger domain from the acute promyelocytic leukaemia proto-oncoprotein PML. *EMBO J,* 14**,** 1532-41.

BORDEN, K. L. & FREEMONT, P. S. (1996) The RING finger domain: a recent example of a sequence-structure family. *Curr Opin Struct Biol,* 6**,** 395-401.

BREMM, A., FREUND, S. M. & KOMANDER, D. (2010) Lys11-linked ubiquitin chains adopt compact conformations and are preferentially hydrolyzed by the deubiquitinase Cezanne. *Nat Struct Mol Biol,* 17**,** 939-47.

BRZOVIC, P. S., KEEFFE, J. R., NISHIKAWA, H., MIYAMOTO, K., FOX, D., 3RD, FUKUDA, M., OHTA, T. & KLEVIT, R. (2003) Binding and recognition in the assembly of an active BRCA1/BARD1 ubiquitin-ligase complex. *Proc Natl Acad Sci U S A,* 100**,** 5646-51.

BRZOVIC, P. S., LISSOUNOV, A., CHRISTENSEN, D. E., HOYT, D. W. & KLEVIT, R. E. (2006) A UbcH5/ubiquitin noncovalent complex is required for processive BRCA1-directed ubiquitination. *Mol Cell,* 21**,** 873-80.

BURROUGHS, A. M., JAFFEE, M., IYER, L. M. & ARAVIND, L. (2008) Anatomy of the E2 ligase fold: implications for enzymology and evolution of ubiquitin/Ub-like protein conjugation. *J Struct Biol,* 162**,** 205-18.

CADWELL, K. & COSCOY, L. (2005) Ubiquitination on nonlysine residues by a viral E3 ubiquitin ligase. *Science,* 309**,** 127-30.

CANET-AVILES, R. M., WILSON, M. A., MILLER, D. W., AHMAD, R., MCLENDON, C., BANDYOPADHYAY, S., BAPTISTA, M. J., RINGE, D., PETSKO, G. A. & COOKSON, M. R. (2004) The Parkinson's disease protein DJ-1 is neuroprotective due to cysteine-sulfinic acid-driven mitochondrial localization. *Proc Natl Acad Sci U S A,* 101**,** 9103-8.

CANNING, M., BOUTELL, C., PARKINSON, J. & EVERETT, R. D. (2004) A RING finger ubiquitin ligase is protected from autocatalyzed ubiquitination and degradation by binding to ubiquitin-specific protease USP7. *J Biol Chem,* 279**,** 38160-8.

CHAN, C. S., GUZMAN, J. N., ILIJIC, E., MERCER, J. N., RICK, C., TKATCH, T., MEREDITH, G. E. & SURMEIER, D. J. (2007) 'Rejuvenation' protects neurons in mouse models of Parkinson's disease. *Nature,* 447**,** 1081-6.

CHARTIER-HARLIN, M. C., KACHERGUS, J., ROUMIER, C., MOUROUX, V., DOUAY, X., LINCOLN, S., LEVECQUE, C., LARVOR, L., ANDRIEUX, J., HULIHAN, M., WAUCQUIER, N., DEFEBVRE, L., AMOUYEL, P., FARRER, M. & DESTEE, A. (2004) Alpha-synuclein locus duplication as a cause of familial Parkinson's disease. *Lancet,* 364**,** 1167-9.

CHAU, V., TOBIAS, J. W., BACHMAIR, A., MARRIOTT, D., ECKER, D. J., GONDA, D. K. & VARSHAVSKY, A. (1989) A multiubiquitin chain is confined to specific lysine in a targeted short-lived protein. *Science,* 243**,** 1576-83.

CHEN, B., MARIANO, J., TSAI, Y. C., CHAN, A. H., COHEN, M. & WEISSMAN, A. M. (2006) The activity of a human endoplasmic reticulum-associated degradation E3, gp78, requires its Cue domain, RING finger, and an E2-binding site. *Proc Natl Acad Sci U S A,* 103**,** 341-6.

CHENNA, R., SUGAWARA, H., KOIKE, T., LOPEZ, R., GIBSON, T. J., HIGGINS, D. G. & THOMPSON, J. D. (2003) Multiple sequence alignment with the Clustal series of programs. *Nucleic Acids Res,* 31**,** 3497-500.

CHIN, L. S., OLZMANN, J. A. & LI, L. (2010) Parkin-mediated ubiquitin signalling in aggresome formation and autophagy. *Biochem Soc Trans,* 38**,** 144-9.

CHOI, P., OSTREROVA-GOLTS, N., SPARKMAN, D., COCHRAN, E., LEE, J. M. & WOLOZIN, B. (2000) Parkin is metabolized by the ubiquitin/proteosome system. *Neuroreport,* 11**,** 2635-8.

CHOI, P., SNYDER, H., PETRUCELLI, L., THEISLER, C., CHONG, M., ZHANG, Y., LIM, K., CHUNG, K. K., KEHOE, K., D'ADAMIO, L., LEE, J. M., COCHRAN, E., BOWSER, R., DAWSON, T. M. & WOLOZIN, B. (2003) SEPT5_v2 is a parkin-binding protein. *Brain Res Mol Brain Res,* 117**,** 179-89.

CHRISTENSEN, D. E., BRZOVIC, P. S. & KLEVIT, R. E. (2007) E2-BRCA1 RING interactions dictate synthesis of mono- or specific polyubiquitin chain linkages. *Nat Struct Mol Biol,* 14**,** 941-8.

CHRISTENSEN, D. E. & KLEVIT, R. E. (2009) Dynamic interactions of proteins in complex networks: identifying the complete set of interacting E2s for functional investigation of E3-dependent protein ubiquitination. *FEBS J,* 276**,** 5381-9.

CHUNG, K. K., THOMAS, B., LI, X., PLETNIKOVA, O., TRONCOSO, J. C., MARSH, L., DAWSON, V. L. & DAWSON, T. M. (2004) S-nitrosylation of parkin regulates ubiquitination and compromises parkin's protective function. *Science,* 304**,** 1328-31.

CHUNG, K. K., ZHANG, Y., LIM, K. L., TANAKA, Y., HUANG, H., GAO, J., ROSS, C. A., DAWSON, V. L. & DAWSON, T. M. (2001) Parkin ubiquitinates the alpha-synuclein-interacting protein, synphilin-1: implications for Lewy-body formation in Parkinson disease. *Nat Med,* 7**,** 1144-50.

CIECHANOVER, A. & BEN-SAADON, R. (2004) N-terminal ubiquitination: more protein substrates join in. *Trends Cell Biol,* 14**,** 103-6.

CLARK, I. E., DODSON, M. W., JIANG, C., CAO, J. H., HUH, J. R., SEOL, J. H., YOO, S. J., HAY, B. A. & GUO, M. (2006) Drosophila pink1 is required for mitochondrial function and interacts genetically with parkin. *Nature,* 441**,** 1162-6.

COLE, A. R., LEWIS, L. P. & WALDEN, H. (2010) The structure of the catalytic subunit FANCL of the Fanconi anemia core complex. *Nat Struct Mol Biol,* 17**,** 294-8.

CONWAY, K. A., ROCHET, J. C., BIEGANSKI, R. M. & LANSBURY, P. T., JR. (2001) Kinetic stabilization of the alpha-synuclein protofibril by a dopamine-alpha-synuclein adduct. *Science,* 294**,** 1346-9.

COOK, W. J., JEFFREY, L. C., CARSON, M., CHEN, Z. & PICKART, C. M. (1992) Structure of a diubiquitin conjugate and a model for interaction with ubiquitin conjugating enzyme (E2). *J Biol Chem,* 267**,** 16467-71.

COOKSON, M. R. (2005) The biochemistry of Parkinson's disease. *Annu Rev Biochem,* 74**,** 29-52.

COOKSON, M. R. & BANDMANN, O. (2010) Parkinson's disease: insights from pathways. *Hum Mol Genet,* 19**,** R21-7.

COOKSON, M. R., LOCKHART, P. J., MCLENDON, C., O'FARRELL, C., SCHLOSSMACHER, M. & FARRER, M. J. (2003) RING finger 1 mutations in Parkin produce altered localization of the protein. *Hum Mol Genet,* 12**,** 2957-65.

CORTI, O., HAMPE, C., KOUTNIKOVA, H., DARIOS, F., JACQUIER, S., PRIGENT, A., ROBINSON, J. C., PRADIER, L., RUBERG, M., MIRANDE, M., HIRSCH, E., ROONEY, T., FOURNIER, A. & BRICE, A. (2003) The p38 subunit of the aminoacyl-tRNA synthetase complex is a Parkin substrate: linking protein biosynthesis and neurodegeneration. *Hum Mol Genet,* 12**,** 1427-37.

CUERVO, A. M., STEFANIS, L., FREDENBURG, R., LANSBURY, P. T. & SULZER, D. (2004) Impaired degradation of mutant alpha-synuclein by chaperone-mediated autophagy. *Science,* 305**,** 1292-5.

DAGATA, V. & CAVALLARO, S. (2004) Parkin transcript variants in rat and human brain. *Neurochem Res,* 29**,** 1715-24.

DAGDA, R. K., CHERRA, S. J., 3RD, KULICH, S. M., TANDON, A., PARK, D. & CHU, C. T. (2009) Loss of PINK1 function promotes mitophagy through effects on oxidative stress and mitochondrial fission. *J Biol Chem,* 284**,** 13843-55.

DARIOS, F., CORTI, O., LUCKING, C. B., HAMPE, C., MURIEL, M. P., ABBAS, N., GU, W. J., HIRSCH, E. C., ROONEY, T., RUBERG, M. & BRICE, A. (2003) Parkin prevents mitochondrial swelling and cytochrome c release in mitochondria-dependent cell death. *Hum Mol Genet,* 12**,** 517-26.

DAS, R., MARIANO, J., TSAI, Y. C., KALATHUR, R. C., KOSTOVA, Z., LI, J., TARASOV, S. G., MCFEETERS, R. L., ALTIERI, A. S., JI, X., BYRD, R. A. & WEISSMAN, A. M. (2009) Allosteric activation of E2-RING finger-mediated ubiquitylation by a structurally defined specific E2-binding region of gp78. *Mol Cell,* 34**,** 674-85.

DAVIDSON, W. S., JONAS, A., CLAYTON, D. F. & GEORGE, J. M. (1998) Stabilization of alpha-synuclein secondary structure upon binding to synthetic membranes. *J Biol Chem,* 273**,** 9443-9.

DAWSON, T. M. & DAWSON, V. L. (2010) The role of parkin in familial and sporadic Parkinson's disease. *Mov Disord,* 25 Suppl 1**,** S32-9.

DAWSON, T. M., KO, H. S. & DAWSON, V. L. (2010) Genetic animal models of Parkinson's disease. *Neuron,* 66**,** 646-61.

DEAS, E., PLUN-FAVREAU, H. & WOOD, N. W. (2009) PINK1 function in health and disease. *EMBO Mol Med,* 1**,** 152-65.

DELAGLIO, F., GRZESIEK, S., VUISTER, G. W., ZHU, G., PFEIFER, J. & BAX, A. (1995) NMRPipe: a multidimensional spectral processing system based on UNIX pipes. *J Biomol NMR,* 6**,** 277-93.

DENG, H., DODSON, M. W., HUANG, H. & GUO, M. (2008) The Parkinson's disease genes pink1 and parkin promote mitochondrial fission and/or inhibit fusion in Drosophila. *Proc Natl Acad Sci U S A,* 105**,** 14503-8.

DENISON, S. R., CALLAHAN, G., BECKER, N. A., PHILLIPS, L. A. & SMITH, D. I. (2003) Characterization of FRA6E and its potential role in autosomal recessive juvenile parkinsonism and ovarian cancer. *Genes Chromosomes Cancer,* 38**,** 40-52.

DESHAIES, R. J. & JOAZEIRO, C. A. (2009) RING domain E3 ubiquitin ligases. *Annu Rev Biochem,* 78**,** 399-434.

DI FONZO, A., DEKKER, M. C., MONTAGNA, P., BARUZZI, A., YONOVA, E. H., CORREIA GUEDES, L., SZCZERBINSKA, A., ZHAO, T., DUBBEL-HULSMAN, L. O., WOUTERS, C. H., DE GRAAFF, E., OYEN, W. J., SIMONS, E. J., BREEDVELD, G. J., OOSTRA, B. A., HORSTINK, M. W. & BONIFATI, V. (2009) FBXO7 mutations cause autosomal recessive, early-onset parkinsonian-pyramidal syndrome. *Neurology,* 72**,** 240-5.

DI MONTE, D. A. (2003) The environment and Parkinson's disease: is the nigrostriatal system preferentially targeted by neurotoxins? *Lancet Neurol,* 2**,** 531-8.

DIKIC, I., WAKATSUKI, S. & WALTERS, K. J. (2009) Ubiquitin-binding domains - from structures to functions. *Nat Rev Mol Cell Biol,* 10**,** 659-71.

DOSS-PEPE, E. W., CHEN, L. & MADURA, K. (2005) Alpha-synuclein and parkin contribute to the assembly of ubiquitin lysine 63-linked multiubiquitin chains. *J Biol Chem,* 280**,** 16619-24.

DUDA, D. M., BORG, L. A., SCOTT, D. C., HUNT, H. W., HAMMEL, M. & SCHULMAN, B. A. (2008) Structural insights into NEDD8 activation of cullin-RING ligases: conformational control of conjugation. *Cell,* 134**,** 995-1006.

EDDINS, M. J., CARLILE, C. M., GOMEZ, K. M., PICKART, C. M. & WOLBERGER, C. (2006) Mms2-Ubc13 covalently bound to ubiquitin reveals the structural basis of linkage-specific polyubiquitin chain formation. *Nat Struct Mol Biol,* 13**,** 915-20.

ELETR, Z. M., HUANG, D. T., DUDA, D. M., SCHULMAN, B. A. & KUHLMAN, B. (2005) E2 conjugating enzymes must disengage from their E1 enzymes before E3-dependent ubiquitin and ubiquitin-like transfer. *Nat Struct Mol Biol,* 12**,** 933-4.

ELETR, Z. M. & KUHLMAN, B. (2007) Sequence determinants of E2-E6AP binding affinity and specificity. *J Mol Biol,* 369**,** 419-28.

FALLON, L., BELANGER, C. M., CORERA, A. T., KONTOGIANNEA, M., REGAN-KLAPISZ, E., MOREAU, F., VOORTMAN, J., HABER, M., ROULEAU, G., THORARINSDOTTIR, T., BRICE, A., VAN BERGEN EN HENEGOUWEN, P. M. & FON, E. A. (2006) A regulated interaction with the UIM protein Eps15 implicates parkin in EGF receptor trafficking and PI(3)K-Akt signalling. *Nat Cell Biol,* 8**,** 834-42.

FALLON, L., MOREAU, F., CROFT, B. G., LABIB, N., GU, W. J. & FON, E. A. (2002) Parkin and CASK/LIN-2 associate via a PDZ-mediated interaction and are co-localized in lipid rafts and postsynaptic densities in brain. *J Biol Chem,* 277**,** 486-91.

FINLEY, D. (2009) Recognition and processing of ubiquitin-protein conjugates by the proteasome. *Annu Rev Biochem,* 78**,** 477-513.

FINNEY, N., WALTHER, F., MANTEL, P. Y., STAUFFER, D., ROVELLI, G. & DEV, K. K. (2003) The cellular protein level of parkin is regulated by its ubiquitin-like domain. *J Biol Chem,* 278**,** 16054-8.

FREDENBURG, R. A., ROSPIGLIOSI, C., MERAY, R. K., KESSLER, J. C., LASHUEL, H. A., ELIEZER, D. & LANSBURY, P. T., JR. (2007) The impact of the E46K mutation on the properties of alpha-synuclein in its monomeric and oligomeric states. *Biochemistry,* 46**,** 7107-18.

FREEMONT, P. S., HANSON, I. M. & TROWSDALE, J. (1991) A novel cysteine-rich sequence motif. *Cell,* 64**,** 483-4.

FRENCH, M. E., KRETZMANN, B. R. & HICKE, L. (2009) Regulation of the RSP5 ubiquitin ligase by an intrinsic ubiquitin-binding site. *J Biol Chem,* 284**,** 12071-9.

FREYER, M. W. & LEWIS, E. A. (2008) Isothermal titration calorimetry: experimental design, data analysis, and probing macromolecule/ligand binding and kinetic interactions. *Methods Cell Biol,* 84**,** 79-113.

FUJIWARA, H., HASEGAWA, M., DOHMAE, N., KAWASHIMA, A., MASLIAH, E., GOLDBERG, M. S., SHEN, J., TAKIO, K. & IWATSUBO, T. (2002) alpha-Synuclein is phosphorylated in synucleinopathy lesions. *Nat Cell Biol,* 4**,** 160-4.

FUSHMAN, D. & WALKER, O. (2010) Exploring the linkage dependence of polyubiquitin conformations using molecular modeling. *J Mol Biol,* 395**,** 803-14.

GANDHI, S., MUQIT, M. M., STANYER, L., HEALY, D. G., ABOU-SLEIMAN, P. M., HARGREAVES, I., HEALES, S., GANGULY, M., PARSONS, L., LEES, A. J., LATCHMAN, D. S., HOLTON, J. L., WOOD, N. W. & REVESZ, T. (2006) PINK1 protein in normal human brain and Parkinson's disease. *Brain,* 129**,** 1720-31.

GANDHI, S., WOOD-KACZMAR, A., YAO, Z., PLUN-FAVREAU, H., DEAS, E., KLUPSCH, K., DOWNWARD, J., LATCHMAN, D. S., TABRIZI, S. J., WOOD, N. W., DUCHEN, M. R. & ABRAMOV, A. Y. (2009) PINK1-associated Parkinson's disease is caused by neuronal vulnerability to calcium-induced cell death. *Mol Cell,* 33**,** 627-38.

GASSER, T. (2007) Update on the genetics of Parkinson's disease. *Mov Disord,* 22 Suppl 17**,** S343-50.

GASSER, T., MULLER-MYHSOK, B., WSZOLEK, Z. K., OEHLMANN, R., CALNE, D. B., BONIFATI, V., BEREZNAI, B., FABRIZIO, E., VIEREGGE, P. & HORSTMANN, R. D. (1998) A susceptibility locus for Parkinson's disease maps to chromosome 2p13. *Nat Genet,* 18**,** 262-5.

GAUTIER, C. A., KITADA, T. & SHEN, J. (2008) Loss of PINK1 causes mitochondrial functional defects and increased sensitivity to oxidative stress. *Proc Natl Acad Sci U S A,* 105**,** 11364-9.

GAZDOIU, S., YAMOAH, K., WU, K. & PAN, Z. Q. (2007) Human Cdc34 employs distinct sites to coordinate attachment of ubiquitin to a substrate and assembly of polyubiquitin chains. *Mol Cell Biol,* 27**,** 7041-52.

GEISLER, S., HOLMSTROM, K. M., SKUJAT, D., FIESEL, F. C., ROTHFUSS, O. C., KAHLE, P. J. & SPRINGER, W. (2010) PINK1/Parkin-mediated mitophagy is dependent on VDAC1 and p62/SQSTM1. *Nat Cell Biol,* 12**,** 119-31.

GEORGE, S., MOK, S. S., NURJONO, M., AYTON, S., FINKELSTEIN, D. I., MASTERS, C. L., LI, Q. X. & CULVENOR, J. G. (2010) alpha-synuclein transgenic mice reveal compensatory increases in Parkinson's disease-associated proteins DJ-1 and Parkin and have enhanced alpha-synuclein and PINK1 levels after rotenone treatment. *J Mol Neurosci,* 42**,** 243-54.

GIASSON, B. I., DUDA, J. E., MURRAY, I. V., CHEN, Q., SOUZA, J. M., HURTIG, H. I., ISCHIROPOULOS, H., TROJANOWSKI, J. Q. & LEE, V. M. (2000) Oxidative damage linked to neurodegeneration by selective alpha-synuclein nitration in synucleinopathy lesions. *Science,* 290**,** 985-9.

GRABBE, C. & DIKIC, I. (2009) Functional roles of ubiquitin-like domain (ULD) and ubiquitin-binding domain (UBD) containing proteins. *Chem Rev,* 109**,** 1481-94.

GU, W. J., CORTI, O., ARAUJO, F., HAMPE, C., JACQUIER, S., LUCKING, C. B., ABBAS, N., DUYCKAERTS, C., ROONEY, T., PRADIER, L., RUBERG, M. & BRICE, A. (2003) The C289G and C418R missense mutations cause rapid sequestration of human Parkin into insoluble aggregates. *Neurobiol Dis,* 14**,** 357-64.

GYRD-HANSEN, M., DARDING, M., MIASARI, M., SANTORO, M. M., ZENDER, L., XUE, W., TENEV, T., DA FONSECA, P. C., ZVELEBIL, M., BUJNICKI, J. M., LOWE, S., SILKE, J. & MEIER, P. (2008) IAPs contain an evolutionarily conserved ubiquitin-binding domain that regulates NF-kappaB as well as cell survival and oncogenesis. *Nat Cell Biol,* 10**,** 1309-17.

HAAS, A. L., WARMS, J. V., HERSHKO, A. & ROSE, I. A. (1982) Ubiquitin-activating enzyme. Mechanism and role in protein-ubiquitin conjugation. *J Biol Chem,* 257**,** 2543-8.

HAGLUND, K. & STENMARK, H. (2006) Working out coupled monoubiquitination. *Nat Cell Biol,* 8**,** 1218-9.

HALDEMAN, M. T., XIA, G., KASPEREK, E. M. & PICKART, C. M. (1997) Structure and function of ubiquitin conjugating enzyme E2-25K: the tail is a core-dependent activity element. *Biochemistry,* 36**,** 10526-37.

HAMILTON, K. S., ELLISON, M. J., BARBER, K. R., WILLIAMS, R. S., HUZIL, J. T., MCKENNA, S., PTAK, C., GLOVER, M. & SHAW, G. S. (2001) Structure of a conjugating enzyme-ubiquitin thiolester intermediate reveals a novel role for the ubiquitin tail. *Structure,* 9**,** 897-904.

HAMMES, G. G. (2005). Spectroscopy for the biological sciences. Wiley-InterScience, New York.

HAMPE, C., ARDILA-OSORIO, H., FOURNIER, M., BRICE, A. & CORTI, O. (2006) Biochemical analysis of Parkinson's disease-causing variants of Parkin, an E3 ubiquitin-protein ligase with monoubiquitylation capacity. *Hum Mol Genet,* 15**,** 2059-75.

HAO, L. Y., GIASSON, B. I. & BONINI, N. M. (2010) DJ-1 is critical for mitochondrial function and rescues PINK1 loss of function. *Proc Natl Acad Sci U S A,* 107**,** 9747-52.

HARDY, J., LEWIS, P., REVESZ, T., LEES, A. & PAISAN-RUIZ, C. (2009) The genetics of Parkinson's syndromes: a critical review. *Curr Opin Genet Dev,* 19**,** 254-65.

HASHIZUME, R., FUKUDA, M., MAEDA, I., NISHIKAWA, H., OYAKE, D., YABUKI, Y., OGATA, H. & OHTA, T. (2001) The RING heterodimer BRCA1-BARD1 is a ubiquitin ligase inactivated by a breast cancer-derived mutation. *J Biol Chem,* 276**,** 14537-40.

HAU, D. D., LEWIS, M. J., SALTIBUS, L. F., PASTUSHOK, L., XIAO, W. & SPYRACOPOULOS, L. (2006) Structure and interactions of the ubiquitin-conjugating enzyme variant human Uev1a: implications for enzymatic synthesis of polyubiquitin chains. *Biochemistry,* 45**,** 9866-77.

HEALY, D. G., ABOU-SLEIMAN, P. M., CASAS, J. P., AHMADI, K. R., LYNCH, T., GANDHI, S., MUQIT, M. M., FOLTYNIE, T., BARKER, R., BHATIA, K. P., QUINN, N. P., LEES, A. J., GIBSON, J. M., HOLTON, J. L., REVESZ, T., GOLDSTEIN, D. B. & WOOD, N. W. (2006) UCHL-1 is not a Parkinson's disease susceptibility gene. *Ann Neurol,* 59**,** 627-33.

HENN, I. H., GOSTNER, J. M., LACKNER, P., TATZELT, J. & WINKLHOFER, K. F. (2005) Pathogenic mutations inactivate parkin by distinct mechanisms. *J Neurochem,* 92**,** 114-22.

HIGHBARGER, L. A., GERLT, J. A. & KENYON, G. L. (1996) Mechanism of the reaction catalyzed by acetoacetate decarboxylase. Importance of lysine 116 in determining the pKa of active-site lysine 115. *Biochemistry,* 35**,** 41-6.

HILPER, K., WINKLER, D. F. & HANCOCK, R. E. (2007) Cellulose-bound peptide arrays: preparation and applications. *Biotechnol Genet Eng Rev,* 24**,** 31-106.

HIRANO, S., KAWASAKI, M., URA, H., KATO, R., RAIBORG, C., STENMARK, H. & WAKATSUKI, S. (2006) Double-sided ubiquitin binding of Hrs-UIM in endosomal protein sorting. *Nat Struct Mol Biol,* 13**,** 272-7.

HOCHSTRASSER, M. (2006) Lingering mysteries of ubiquitin-chain assembly. *Cell,* 124**,** 27-34.

HOELLER, D., CROSETTO, N., BLAGOEV, B., RAIBORG, C., TIKKANEN, R., WAGNER, S., KOWANETZ, K., BREITLING, R., MANN, M., STENMARK, H. & DIKIC, I. (2006) Regulation of ubiquitin-binding proteins by monoubiquitination. *Nat Cell Biol,* 8**,** 163-9.

HOELLER, D., HECKER, C. M., WAGNER, S., ROGOV, V., DOTSCH, V. & DIKIC, I. (2007) E3-independent monoubiquitination of ubiquitin-binding proteins. *Mol Cell,* 26**,** 891-8.

HOFMANN, K. & FALQUET, L. (2001) A ubiquitin-interacting motif conserved in components of the proteasomal and lysosomal protein degradation systems. *Trends Biochem Sci,* 26**,** 347-50.

HOFMANN, R. M. & PICKART, C. M. (2001) In vitro assembly and recognition of Lys-63 polyubiquitin chains. *J Biol Chem,* 276**,** 27936-43.

HOPPE, T. (2005) Multiubiquitylation by E4 enzymes: 'one size' doesn't fit all. *Trends Biochem Sci,* 30**,** 183-7.

HRISTOVA, V. A., BEASLEY, S. A., RYLETT, R. J. & SHAW, G. S. (2009) Identification of a novel Zn2+-binding domain in the autosomal recessive juvenile Parkinson-related E3 ligase parkin. *J Biol Chem,* 284**,** 14978-86.

HUANG, A., DE JONG, R. N., WIENK, H., WINKLER, G. S., TIMMERS, H. T. & BOELENS, R. (2009) E2-c-Cbl recognition is necessary but not sufficient for ubiquitination activity. *J Mol Biol,* 385**,** 507-19.

HUANG, D. T., HUNT, H. W., ZHUANG, M., OHI, M. D., HOLTON, J. M. & SCHULMAN, B. A. (2007) Basis for a ubiquitin-like protein thioester switch toggling E1-E2 affinity. *Nature,* 445**,** 394-8.

HUANG, D. T., PAYDAR, A., ZHUANG, M., WADDELL, M. B., HOLTON, J. M. & SCHULMAN, B. A. (2005) Structural basis for recruitment of Ubc12 by an E2 binding domain in NEDD8's E1. *Mol Cell,* 17**,** 341-50.

HURLEY, J. H., LEE, S. & PRAG, G. (2006) Ubiquitin-binding domains. *Biochem J,* 399**,** 361-72.

HUYNH, D. P., DY, M., NGUYEN, D., KIEHL, T. R. & PULST, S. M. (2001) Differential expression and tissue distribution of parkin isoforms during mouse development. *Brain Res Dev Brain Res,* 130**,** 173-81.

HUYNH, D. P., NGUYEN, D. T., PULST-KORENBERG, J. B., BRICE, A. & PULST, S. M. (2007) Parkin is an E3 ubiquitin-ligase for normal and mutant ataxin-2 and prevents ataxin-2-induced cell death. *Exp Neurol,* 203**,** 531-41.

HUYNH, D. P., SCOLES, D. R., NGUYEN, D. & PULST, S. M. (2003) The autosomal recessive juvenile Parkinson disease gene product, parkin, interacts with and ubiquitinates synaptotagmin XI. *Hum Mol Genet,* 12**,** 2587-97.

IMAI, Y., SODA, M., HATAKEYAMA, S., AKAGI, T., HASHIKAWA, T., NAKAYAMA, K. I. & TAKAHASHI, R. (2002) CHIP is associated with Parkin, a gene responsible for familial Parkinson's disease, and enhances its ubiquitin ligase activity. *Mol Cell,* 10**,** 55-67.

IMAI, Y., SODA, M., INOUE, H., HATTORI, N., MIZUNO, Y. & TAKAHASHI, R. (2001) An unfolded putative transmembrane polypeptide, which can lead to endoplasmic reticulum stress, is a substrate of Parkin. *Cell,* 105**,** 891-902.

IMAI, Y., SODA, M. & TAKAHASHI, R. (2000) Parkin suppresses unfolded protein stress-induced cell death through its E3 ubiquitin-protein ligase activity. *J Biol Chem,* 275**,** 35661-4.

IRRCHER, I., ALEYASIN, H., SEIFERT, E. L., HEWITT, S. J., CHHABRA, S., PHILLIPS, M., LUTZ, A. K., ROUSSEAUX, M. W., BEVILACQUA, L., JAHANI-ASL, A., CALLAGHAN, S., MACLAURIN, J. G., WINKLHOFER, K. F., RIZZU, P., RIPPSTEIN, P., KIM, R. H., CHEN, C. X., FON, E. A., SLACK, R. S., HARPER, M. E., MCBRIDE, H. M., MAK, T. W. & PARK, D. S. (2010) Loss of the Parkinson's disease-linked gene DJ-1 perturbs mitochondrial dynamics. *Hum Mol Genet*.

ISASA, M., KATZ, E. J., KIM, W., YUGO, V., GONZALEZ, S., KIRKPATRICK, D. S., THOMSON, T. M., FINLEY, D., GYGI, S. P. & CROSAS, B. (2010) Monoubiquitination of RPN10 regulates substrate recruitment to the proteasome. *Mol Cell,* 38**,** 733-45.

JAKES, R., SPILLANTINI, M. G. & GOEDERT, M. (1994) Identification of two distinct synucleins from human brain. *FEBS Lett,* 345**,** 27-32.

JIANG, H., REN, Y., ZHAO, J. & FENG, J. (2004) Parkin protects human dopaminergic neuroblastoma cells against dopamine-induced apoptosis. *Hum Mol Genet,* 13**,** 1745-54.

JIN, J., LI, X., GYGI, S. P. & HARPER, J. W. (2007) Dual E1 activation systems for ubiquitin differentially regulate E2 enzyme charging. *Nature,* 447**,** 1135-8.

JIN, L., WILLIAMSON, A., BANERJEE, S., PHILIPP, I. & RAPE, M. (2008) Mechanism of ubiquitin-chain formation by the human anaphase-promoting complex. *Cell,* 133**,** 653-65.

JOAZEIRO, C. A. & WEISSMAN, A. M. (2000) RING finger proteins: mediators of ubiquitin ligase activity. *Cell,* 102**,** 549-52.

JOCH, M., ASE, A. R., CHEN, C. X., MACDONALD, P. A., KONTOGIANNEA, M., CORERA, A. T., BRICE, A., SEGUELA, P. & FON, E. A. (2007) Parkin-mediated monoubiquitination of the PDZ protein PICK1 regulates the activity of acid-sensing ion channels. *Mol Biol Cell,* 18**,** 3105-18.

JOHNSON, B. A. & BLEVINS, R. A. (1994) NMR View: A computer program for the visualization and analysis of NMR data. *Journal of Biomolecular NMR,* 4**,** 603-614.

JOHNSON, F. & KAPLITT, M. G. (2009) Novel mitochondrial substrates of omi indicate a new regulatory role in neurodegenerative disorders. *PLoS One,* 4**,** e7100.

JUNN, E., LEE, S. S., SUHR, U. T. & MOURADIAN, M. M. (2002) Parkin accumulation in aggresomes due to proteasome impairment. *J Biol Chem,* 277**,** 47870-7.

KAHNS, S., KALAI, M., JAKOBSEN, L. D., CLARK, B. F., VANDENABEELE, P. & JENSEN, P. H. (2003) Caspase-1 and caspase-8 cleave and inactivate cellular parkin. *J Biol Chem,* 278**,** 23376-80.

KAHNS, S., LYKKEBO, S., JAKOBSEN, L. D., NIELSEN, M. S. & JENSEN, P. H. (2002) Caspase-mediated parkin cleavage in apoptotic cell death. *J Biol Chem,* 277**,** 15303-8.

KALIA, S. K., LEE, S., SMITH, P. D., LIU, L., CROCKER, S. J., THORARINSDOTTIR, T. E., GLOVER, J. R., FON, E. A., PARK, D. S. & LOZANO, A. M. (2004) BAG5 inhibits parkin and enhances dopaminergic neuron degeneration. *Neuron,* 44**,** 931-45.

KAWAHARA, K., HASHIMOTO, M., BAR-ON, P., HO, G. J., CREWS, L., MIZUNO, H., ROCKENSTEIN, E., IMAM, S. Z. & MASLIAH, E. (2008) alpha-Synuclein aggregates interfere with Parkin solubility and distribution: role in the pathogenesis of Parkinson disease. *J Biol Chem,* 283**,** 6979-87.

KAY, L., KEIFER, P. & SAARINEN, T. (1992) Pure absorption gradient enhanced heteronuclear single quantum correlation spectroscopy with improved sensitivity. *Journal of the American Chemical Society,* 114**,** 10663-10665.

KIM, H. C. & HUIBREGTSE, J. M. (2009) Polyubiquitination by HECT E3s and the determinants of chain type specificity. *Mol Cell Biol,* 29**,** 3307-18.

KIM, H. T., KIM, K. P., UCHIKI, T., GYGI, S. P. & GOLDBERG, A. L. (2009) S5a promotes protein degradation by blocking synthesis of nondegradable forked ubiquitin chains. *EMBO J,* 28**,** 1867-77.

KIM, M. J., PARK, B. J., KANG, Y. S., KIM, H. J., PARK, J. H., KANG, J. W., LEE, S. W., HAN, J. M., LEE, H. W. & KIM, S. (2003a) Downregulation of FUSE-binding protein and c-myc by tRNA synthetase cofactor p38 is required for lung cell differentiation. *Nat Genet,* 34**,** 330-6.

KIM, R. H., SMITH, P. D., ALEYASIN, H., HAYLEY, S., MOUNT, M. P., POWNALL, S., WAKEHAM, A., YOU-TEN, A. J., KALIA, S. K., HORNE, P., WESTAWAY, D., LOZANO, A. M., ANISMAN, H., PARK, D. S. & MAK, T. W. (2005) Hypersensitivity of DJ-1-deficient mice to 1-methyl-4-phenyl-1,2,3,6-tetrahydropyrindine (MPTP) and oxidative stress. *Proc Natl Acad Sci U S A,* 102**,** 5215-20.

KIM, S. J., SUNG, J. Y., UM, J. W., HATTORI, N., MIZUNO, Y., TANAKA, K., PAIK, S. R., KIM, J. & CHUNG, K. C. (2003b) Parkin cleaves intracellular alpha-synuclein inclusions via the activation of calpain. *J Biol Chem,* 278**,** 41890-9.

KIM, Y., PARK, J., KIM, S., SONG, S., KWON, S. K., LEE, S. H., KITADA, T., KIM, J. M. & CHUNG, J. (2008) PINK1 controls mitochondrial localization of Parkin through direct phosphorylation. *Biochem Biophys Res Commun,* 377**,** 975-80.

KIRISAKO, T., KAMEI, K., MURATA, S., KATO, M., FUKUMOTO, H., KANIE, M., SANO, S., TOKUNAGA, F., TANAKA, K. & IWAI, K. (2006) A ubiquitin ligase complex assembles linear polyubiquitin chains. *EMBO J,* 25**,** 4877-87.

KIRKIN, V., MCEWAN, D. G., NOVAK, I. & DIKIC, I. (2009) A role for ubiquitin in selective autophagy. *Mol Cell,* 34**,** 259-69.

KITADA, T., ASAKAWA, S., HATTORI, N., MATSUMINE, H., YAMAMURA, Y., MINOSHIMA, S., YOKOCHI, M., MIZUNO, Y. & SHIMIZU, N. (1998) Mutations in the parkin gene cause autosomal recessive juvenile parkinsonism. *Nature,* 392**,** 605-8.

KNIPSCHEER, P., FLOTHO, A., KLUG, H., OLSEN, J. V., VAN DIJK, W. J., FISH, A., JOHNSON, E. S., MANN, M., SIXMA, T. K. & PICHLER, A. (2008) Ubc9 sumoylation regulates SUMO target discrimination. *Mol Cell,* 31**,** 371-82.

KO, H. S., KIM, S. W., SRIRAM, S. R., DAWSON, V. L. & DAWSON, T. M. (2006) Identification of far upstream element-binding protein-1 as an authentic Parkin substrate. *J Biol Chem,* 281**,** 16193-6.

KO, H. S., VON COELLN, R., SRIRAM, S. R., KIM, S. W., CHUNG, K. K., PLETNIKOVA, O., TRONCOSO, J., JOHNSON, B., SAFFARY, R., GOH, E. L., SONG, H., PARK, B. J., KIM, M. J., KIM, S., DAWSON, V. L. & DAWSON, T. M. (2005) Accumulation of the authentic parkin substrate aminoacyl-tRNA synthetase cofactor, p38/JTV-1, leads to catecholaminergic cell death. *J Neurosci,* 25**,** 7968-78.

KOMANDER, D. (2009) The emerging complexity of protein ubiquitination. *Biochem Soc Trans,* 37**,** 937-53.

KOMANDER, D., CLAGUE, M. J. & URBE, S. (2009a) Breaking the chains: structure and function of the deubiquitinases. *Nat Rev Mol Cell Biol,* 10**,** 550-63.

KOMANDER, D., REYES-TURCU, F., LICCHESI, J. D., ODENWAELDER, P., WILKINSON, K. D. & BARFORD, D. (2009b) Molecular discrimination of structurally equivalent Lys 63-linked and linear polyubiquitin chains. *EMBO Rep,* 10**,** 466-73.

KOZLOV, G., PESCHARD, P., ZIMMERMAN, B., LIN, T., MOLDOVEANU, T., MANSUR-AZZAM, N., GEHRING, K. & PARK, M. (2007) Structural basis for UBA-mediated dimerization of c-Cbl ubiquitin ligase. *J Biol Chem,* 282**,** 27547-55.

KYRATZI, E., PAVLAKI, M., KONTOSTAVLAKI, D., RIDEOUT, H. J. & STEFANIS, L. (2007) Differential effects of Parkin and its mutants on protein aggregation, the ubiquitin-proteasome system, and neuronal cell death in human neuroblastoma cells. *J Neurochem,* 102**,** 1292-303.

LAKE, M. W., WUEBBENS, M. M., RAJAGOPALAN, K. V. & SCHINDELIN, H. (2001) Mechanism of ubiquitin activation revealed by the structure of a bacterial MoeB-MoaD complex. *Nature,* 414**,** 325-9.

LASHUEL, H. A., PETRE, B. M., WALL, J., SIMON, M., NOWAK, R. J., WALZ, T. & LANSBURY, P. T., JR. (2002) Alpha-synuclein, especially the Parkinson's disease-associated mutants, forms pore-like annular and tubular protofibrils. *J Mol Biol,* 322**,** 1089-102.

LAUTIER, C., GOLDWURM, S., DURR, A., GIOVANNONE, B., TSIARAS, W. G., PEZZOLI, G., BRICE, A. & SMITH, R. J. (2008) Mutations in the GIGYF2 (TNRC15) gene at the PARK11 locus in familial Parkinson disease. *Am J Hum Genet,* 82**,** 822-33.

LAVOIE, M. J., CORTESE, G. P., OSTASZEWSKI, B. L. & SCHLOSSMACHER, M. G. (2007) The effects of oxidative stress on parkin and other E3 ligases. *J Neurochem,* 103**,** 2354-68.

LAVOIE, M. J., OSTASZEWSKI, B. L., WEIHOFEN, A., SCHLOSSMACHER, M. G. & SELKOE, D. J. (2005) Dopamine covalently modifies and functionally inactivates parkin. *Nat Med,* 11**,** 1214-21.

LEE, I. & SCHINDELIN, H. (2008) Structural insights into E1-catalyzed ubiquitin activation and transfer to conjugating enzymes. *Cell,* 134**,** 268-78.

LEE, J. Y., NAGANO, Y., TAYLOR, J. P., LIM, K. L. & YAO, T. P. (2010) Disease-causing mutations in parkin impair mitochondrial ubiquitination, aggregation, and HDAC6-dependent mitophagy. *J Cell Biol,* 189**,** 671-9.

LEHMANN, C., BEGLEY, T. P. & EALICK, S. E. (2006) Structure of the Escherichia coli ThiS-ThiF complex, a key component of the sulfur transfer system in thiamin biosynthesis. *Biochemistry,* 45**,** 11-9.

LEIMKUHLER, S., WUEBBENS, M. M. & RAJAGOPALAN, K. V. (2001) Characterization of Escherichia coli MoeB and its involvement in the activation of molybdopterin synthase for the biosynthesis of the molybdenum cofactor. *J Biol Chem,* 276**,** 34695-701.

LEROY, E., BOYER, R., AUBURGER, G., LEUBE, B., ULM, G., MEZEY, E., HARTA, G., BROWNSTEIN, M. J., JONNALAGADA, S., CHERNOVA, T., DEHEJIA, A., LAVEDAN, C., GASSER, T., STEINBACH, P. J., WILKINSON, K. D. & POLYMEROPOULOS, M. H. (1998) The ubiquitin pathway in Parkinson's disease. *Nature,* 395**,** 451-2.

LI, J., UVERSKY, V. N. & FINK, A. L. (2001) Effect of familial Parkinson's disease point mutations A30P and A53T on the structural properties, aggregation, and fibrillation of human alpha-synuclein. *Biochemistry,* 40**,** 11604-13.

LI, W., TU, D., BRUNGER, A. T. & YE, Y. (2007) A ubiquitin ligase transfers preformed polyubiquitin chains from a conjugating enzyme to a substrate. *Nature,* 446**,** 333-7.

LI, Y. J., SCOTT, W. K., HEDGES, D. J., ZHANG, F., GASKELL, P. C., NANCE, M. A., WATTS, R. L., HUBBLE, J. P., KOLLER, W. C., PAHWA, R., STERN, M. B., HINER, B. C., JANKOVIC, J., ALLEN, F. A., JR., GOETZ, C. G., MASTAGLIA, F., STAJICH, J. M., GIBSON, R. A., MIDDLETON, L. T., SAUNDERS, A. M., SCOTT, B. L., SMALL, G. W., NICODEMUS, K. K., REED, A. D., SCHMECHEL, D. E., WELSH-BOHMER, K. A., CONNEALLY, P. M., ROSES, A. D., GILBERT, J. R., VANCE, J. M., HAINES, J. L. & PERICAK-VANCE, M. A. (2002) Age at onset in two common neurodegenerative diseases is genetically controlled. *Am J Hum Genet,* 70**,** 985-93.

LIM, K. L., CHEW, K. C., TAN, J. M., WANG, C., CHUNG, K. K., ZHANG, Y., TANAKA, Y., SMITH, W., ENGELENDER, S., ROSS, C. A., DAWSON, V. L. & DAWSON, T. M. (2005) Parkin mediates nonclassical, proteasomal-independent ubiquitination of synphilin-1: implications for Lewy body formation. *J Neurosci,* 25**,** 2002-9.

LIN, W. & KANG, U. J. (2008) Characterization of PINK1 processing, stability, and subcellular localization. *J Neurochem,* 106**,** 464-74.

LINARES, L. K., HENGSTERMANN, A., CIECHANOVER, A., MULLER, S. & SCHEFFNER, M. (2003) HdmX stimulates Hdm2-mediated ubiquitination and degradation of p53. *Proc Natl Acad Sci U S A,* 100**,** 12009-14.

LO BIANCO, C., SCHNEIDER, B. L., BAUER, M., SAJADI, A., BRICE, A., IWATSUBO, T. & AEBISCHER, P. (2004) Lentiviral vector delivery of parkin prevents dopaminergic degeneration in an alpha-synuclein rat model of Parkinson's disease. *Proc Natl Acad Sci U S A,* 101**,** 17510-5.

LOIS, L. M. & LIMA, C. D. (2005) Structures of the SUMO E1 provide mechanistic insights into SUMO activation and E2 recruitment to E1. *EMBO J,* 24**,** 439-51.

LUND, P. K., MOATS-STAATS, B. M., SIMMONS, J. G., HOYT, E., D'ERCOLE, A. J., MARTIN, F. & VAN WYK, J. J. (1985) Nucleotide sequence analysis of a cDNA encoding human ubiquitin reveals that ubiquitin is synthesized as a precursor. *J Biol Chem,* 260**,** 7609-13.

LUTZ, A. K., EXNER, N., FETT, M. E., SCHLEHE, J. S., KLOOS, K., LAMMERMANN, K., BRUNNER, B., KURZ-DREXLER, A., VOGEL, F., REICHERT, A. S., BOUMAN, L., VOGT-WEISENHORN, D., WURST, W., TATZELT, J., HAASS, C. & WINKLHOFER, K. F. (2009) Loss of parkin or PINK1 function increases Drp1-dependent mitochondrial fragmentation. *J Biol Chem,* 284**,** 22938-51.

MACE, P. D., LINKE, K., FELTHAM, R., SCHUMACHER, F. R., SMITH, C. A., VAUX, D. L., SILKE, J. & DAY, C. L. (2008) Structures of the cIAP2 RING domain reveal conformational changes associated with ubiquitin-conjugating enzyme (E2) recruitment. *J Biol Chem,* 283**,** 31633-40.

MARIN, I., LUCAS, J. I., GRADILLA, A. C. & FERRUS, A. (2004) Parkin and relatives: the RBR family of ubiquitin ligases. *Physiol Genomics,* 17**,** 253-63.

MATA, I. F., LOCKHART, P. J. & FARRER, M. J. (2004) Parkin genetics: one model for Parkinson's disease. *Hum Mol Genet,* 13 Spec No 1**,** R127-33.

MATSUDA, N., KITAMI, T., SUZUKI, T., MIZUNO, Y., HATTORI, N. & TANAKA, K. (2006) Diverse effects of pathogenic mutations of Parkin that catalyze multiple monoubiquitylation in vitro. *J Biol Chem,* 281**,** 3204-9.

MATSUDA, N., SATO, S., SHIBA, K., OKATSU, K., SAISHO, K., GAUTIER, C. A., SOU, Y. S., SAIKI, S., KAWAJIRI, S., SATO, F., KIMURA, M., KOMATSU, M., HATTORI, N. & TANAKA, K. (2010) PINK1 stabilized by mitochondrial depolarization recruits Parkin to damaged mitochondria and activates latent Parkin for mitophagy. *J Cell Biol,* 189**,** 211-21.

MATSUSHIMA-NISHIU, M., UNOKI, M., ONO, K., TSUNODA, T., MINAGUCHI, T., KURAMOTO, H., NISHIDA, M., SATOH, T., TANAKA, T. & NAKAMURA, Y. (2001) Growth and gene expression profile analyses of endometrial cancer cells expressing exogenous PTEN. *Cancer Res,* 61**,** 3741-9.

MAUDSLEY, A. A. AND ERNST, R. R. (1977). Indirect detection of magnetic resonance by heteronuclear two dimensional spectroscopy. Chem. Phys. Leff., 50 (3), 368-372.

MAYER, R. J., LANDON, M. & LAYFIELD, R. (1998) Ubiquitin superfolds: intrinsic and attachable regulators of cellular activities? *Fold Des,* 3**,** R97-9.

MCKENNA, S., MORAES, T., PASTUSHOK, L., PTAK, C., XIAO, W., SPYRACOPOULOS, L. & ELLISON, M. J. (2003) An NMR-based model of the ubiquitin-bound human ubiquitin conjugation complex Mms2.Ubc13. The structural basis for lysine 63 chain catalysis. *J Biol Chem,* 278**,** 13151-8.

MIRA, M. T., ALCAIS, A., NGUYEN, V. T., MORAES, M. O., DI FLUMERI, C., VU, H. T., MAI, C. P., NGUYEN, T. H., NGUYEN, N. B., PHAM, X. K., SARNO, E. N., ALTER, A., MONTPETIT, A., MORAES, M. E., MORAES, J. R., DORE, C., GALLANT, C. J., LEPAGE, P., VERNER, A., VAN DE VOSSE, E., HUDSON, T. J., ABEL, L. & SCHURR, E. (2004) Susceptibility to leprosy is associated with PARK2 and PACRG. *Nature,* 427**,** 636-40.

MOORE, D. J., WEST, A. B., DIKEMAN, D. A., DAWSON, V. L. & DAWSON, T. M. (2008) Parkin mediates the degradation-independent ubiquitination of Hsp70. *J Neurochem,* 105**,** 1806-19.

MOORE, D. J., ZHANG, L., TRONCOSO, J., LEE, M. K., HATTORI, N., MIZUNO, Y., DAWSON, T. M. & DAWSON, V. L. (2005) Association of DJ-1 and parkin mediated by pathogenic DJ-1 mutations and oxidative stress. *Hum Mol Genet,* 14**,** 71-84.

MORAIS, V. A., VERSTREKEN, P., ROETHIG, A., SMET, J., SNELLINX, A., VANBRABANT, M., HADDAD, D., FREZZA, C., MANDEMAKERS, W., VOGT-WEISENHORN, D., VAN COSTER, R., WURST, W., SCORRANO, L. & DE STROOPER, B. (2009) Parkinson's disease mutations in PINK1 result in decreased Complex I activity and deficient synaptic function. *EMBO Mol Med,* 1**,** 99-111.

MUIR, T. W. (2003) Semisynthesis of proteins by expressed protein ligation. *Annu Rev Biochem,* 72**,** 249-89.

MUQIT, M. M., ABOU-SLEIMAN, P. M., SAURIN, A. T., HARVEY, K., GANDHI, S., DEAS, E., EATON, S., PAYNE SMITH, M. D., VENNER, K., MATILLA, A., HEALY, D. G., GILKS, W. P., LEES, A. J., HOLTON, J., REVESZ, T., PARKER, P. J., HARVEY, R. J., WOOD, N. W. & LATCHMAN, D. S. (2006) Altered cleavage and localization of PINK1 to aggresomes in the presence of proteasomal stress. *J Neurochem,* 98**,** 156-69.

MUQIT, M. M., DAVIDSON, S. M., PAYNE SMITH, M. D., MACCORMAC, L. P., KAHNS, S., JENSEN, P. H., WOOD, N. W. & LATCHMAN, D. S. (2004) Parkin is recruited into aggresomes in a stress-specific manner: over-expression of parkin reduces aggresome formation but can be dissociated from parkin's effect on neuronal survival. *Hum Mol Genet,* 13**,** 117-35.

MURALIDHARAN, V. & MUIR, T. W. (2006) Protein ligation: an enabling technology for the biophysical analysis of proteins. *Nat Methods,* 3**,** 429-38.

MURRAY, I. V., GIASSON, B. I., QUINN, S. M., KOPPAKA, V., AXELSEN, P. H., ISCHIROPOULOS, H., TROJANOWSKI, J. Q. & LEE, V. M. (2003) Role of alpha-synuclein carboxy-terminus on fibril formation in vitro. *Biochemistry,* 42**,** 8530-40.

NAGY, V. & DIKIC, I. (2010) Ubiquitin ligase complexes: from substrate selectivity to conjugational specificity. *Biol Chem,* 391**,** 163-9.

NARENDRA, D., TANAKA, A., SUEN, D. F. & YOULE, R. J. (2008) Parkin is recruited selectively to impaired mitochondria and promotes their autophagy. *J Cell Biol,* 183**,** 795-803.

NARENDRA, D., TANAKA, A., SUEN, D. F. & YOULE, R. J. (2009) Parkin-induced mitophagy in the pathogenesis of Parkinson disease. *Autophagy,* 5**,** 706-8.

NARENDRA, D. P., JIN, S. M., TANAKA, A., SUEN, D. F., GAUTIER, C. A., SHEN, J., COOKSON, M. R. & YOULE, R. J. (2010) PINK1 is selectively stabilized on impaired mitochondria to activate Parkin. *PLoS Biol,* 8**,** e1000298.

NICHOLS, W. C., KISSELL, D. K., PANKRATZ, N., PAUCIULO, M. W., ELSAESSER, V. E., CLARK, K. A., HALTER, C. A., RUDOLPH, A., WOJCIESZEK, J., PFEIFFER, R. F. & FOROUD, T. (2009) Variation in GIGYF2 is not associated with Parkinson disease. *Neurology,* 72**,** 1886-92.

OGUNJIMI, A. A., WIESNER, S., BRIANT, D. J., VARELAS, X., SICHERI, F., FORMAN-KAY, J. & WRANA, J. L. (2010) The ubiquitin binding region of the Smurf HECT domain

facilitates polyubiquitylation and binding of ubiquitylated substrates. *J Biol Chem,* 285**,** 6308-15.

OLSEN, S. K., CAPILI, A. D., LU, X., TAN, D. S. & LIMA, C. D. (2010) Active site remodelling accompanies thioester bond formation in the SUMO E1. *Nature,* 463**,** 906-12.

OLZMANN, J. A., LI, L., CHUDAEV, M. V., CHEN, J., PEREZ, F. A., PALMITER, R. D. & CHIN, L. S. (2007) Parkin-mediated K63-linked polyubiquitination targets misfolded DJ-1 to aggresomes via binding to HDAC6. *J Cell Biol,* 178**,** 1025-38.

OZKAN, E., YU, H. & DEISENHOFER, J. (2005) Mechanistic insight into the allosteric activation of a ubiquitin-conjugating enzyme by RING-type ubiquitin ligases. *Proc Natl Acad Sci U S A,* 102**,** 18890-5.

OZKAYNAK, E., FINLEY, D. & VARSHAVSKY, A. (1984) The yeast ubiquitin gene: head-to-tail repeats encoding a polyubiquitin precursor protein. *Nature,* 312**,** 663-6.

PAISAN-RUIZ, C., BHATIA, K. P., LI, A., HERNANDEZ, D., DAVIS, M., WOOD, N. W., HARDY, J., HOULDEN, H., SINGLETON, A. & SCHNEIDER, S. A. (2009) Characterization of PLA2G6 as a locus for dystonia-parkinsonism. *Ann Neurol,* 65**,** 19-23.

PAISAN-RUIZ, C., JAIN, S., EVANS, E. W., GILKS, W. P., SIMON, J., VAN DER BRUG, M., LOPEZ DE MUNAIN, A., APARICIO, S., GIL, A. M., KHAN, N., JOHNSON, J., MARTINEZ, J. R., NICHOLL, D., CARRERA, I. M., PENA, A. S., DE SILVA, R., LEES, A., MARTI-MASSO, J. F., PEREZ-TUR, J., WOOD, N. W. & SINGLETON, A. B. (2004) Cloning of the gene containing mutations that cause PARK8-linked Parkinson's disease. *Neuron,* 44**,** 595-600.

PALACINO, J. J., SAGI, D., GOLDBERG, M. S., KRAUSS, S., MOTZ, C., WACKER, M., KLOSE, J. & SHEN, J. (2004) Mitochondrial dysfunction and oxidative damage in parkin-deficient mice. *J Biol Chem,* 279**,** 18614-22.

PANKRATZ, N., NICHOLS, W. C., UNIACKE, S. K., HALTER, C., RUDOLPH, A., SHULTS, C., CONNEALLY, P. M. & FOROUD, T. (2002) Genome screen to identify susceptibility genes for Parkinson disease in a sample without parkin mutations. *Am J Hum Genet,* 71**,** 124-35.

PARK, H. M., KIM, G. Y., NAM, M. K., SEONG, G. H., HAN, C., CHUNG, K. C., KANG, S. & RHIM, H. (2009) The serine protease HtrA2/Omi cleaves Parkin and irreversibly inactivates its E3 ubiquitin ligase activity. *Biochem Biophys Res Commun,* 387**,** 537-42.

PARK, J., LEE, S. B., LEE, S., KIM, Y., SONG, S., KIM, S., BAE, E., KIM, J., SHONG, M., KIM, J. M. & CHUNG, J. (2006) Mitochondrial dysfunction in Drosophila PINK1 mutants is complemented by parkin. *Nature,* 441**,** 1157-61.

PARKER, J. L. & ULRICH, H. D. (2009) Mechanistic analysis of PCNA poly-ubiquitylation by the ubiquitin protein ligases Rad18 and Rad5. *EMBO J,* 28**,** 3657-66.

PATERNA, J. C., LENG, A., WEBER, E., FELDON, J. & BUELER, H. (2007) DJ-1 and Parkin modulate dopamine-dependent behavior and inhibit MPTP-induced nigral dopamine neuron loss in mice. *Mol Ther,* 15**,** 698-704.

PEREZ, F. A., CURTIS, W. R. & PALMITER, R. D. (2005) Parkin-deficient mice are not more sensitive to 6-hydroxydopamine or methamphetamine neurotoxicity. *BMC Neurosci,* 6**,** 71.

PERIQUET, M., FULGA, T., MYLLYKANGAS, L., SCHLOSSMACHER, M. G. & FEANY, M. B. (2007) Aggregated alpha-synuclein mediates dopaminergic neurotoxicity in vivo. *J Neurosci,* 27**,** 3338-46.

PESCHARD, P., KOZLOV, G., LIN, T., MIRZA, I. A., BERGHUIS, A. M., LIPKOWITZ, S., PARK, M. & GEHRING, K. (2007) Structural basis for ubiquitin-mediated dimerization and activation of the ubiquitin protein ligase Cbl-b. *Mol Cell,* 27**,** 474-85.

PETROSKI, M. D. & DESHAIES, R. J. (2005a) Function and regulation of cullin-RING ubiquitin ligases. *Nat Rev Mol Cell Biol,* 6**,** 9-20.

PETROSKI, M. D. & DESHAIES, R. J. (2005b) Mechanism of lysine 48-linked ubiquitin-chain synthesis by the cullin-RING ubiquitin-ligase complex SCF-Cdc34. *Cell,* 123**,** 1107-20.

PETROSKI, M. D., ZHOU, X., DONG, G., DANIEL-ISSAKANI, S., PAYAN, D. G. & HUANG, J. (2007) Substrate modification with lysine 63-linked ubiquitin chains through the UBC13-UEV1A ubiquitin-conjugating enzyme. *J Biol Chem,* 282**,** 29936-45.

PICHLER, A., KNIPSCHEER, P., OBERHOFER, E., VAN DIJK, W. J., KORNER, R., OLSEN, J. V., JENTSCH, S., MELCHIOR, F. & SIXMA, T. K. (2005) SUMO modification of the ubiquitin-conjugating enzyme E2-25K. *Nat Struct Mol Biol,* 12**,** 264-9.

PICKART, C. M. (2001) Mechanisms underlying ubiquitination. *Annu Rev Biochem,* 70**,** 503-33.

PLUN-FAVREAU, H., KLUPSCH, K., MOISOI, N., GANDHI, S., KJAER, S., FRITH, D., HARVEY, K., DEAS, E., HARVEY, R. J., MCDONALD, N., WOOD, N. W., MARTINS, L. M. & DOWNWARD, J. (2007) The mitochondrial protease HtrA2 is regulated by Parkinson's disease-associated kinase PINK1. *Nat Cell Biol,* 9**,** 1243-52.

POLO, S., CONFALONIERI, S., SALCINI, A. E. & DI FIORE, P. P. (2003) EH and UIM: endocytosis and more. *Sci STKE,* 2003**,** re17.

POLYMEROPOULOS, M. H., LAVEDAN, C., LEROY, E., IDE, S. E., DEHEJIA, A., DUTRA, A., PIKE, B., ROOT, H., RUBENSTEIN, J., BOYER, R., STENROOS, E. S., CHANDRASEKHARAPPA, S., ATHANASSIADOU, A., PAPAPETROPOULOS, T., JOHNSON, W. G., LAZZARINI, A. M., DUVOISIN, R. C., DI IORIO, G., GOLBE, L. I. & NUSSBAUM, R. L. (1997) Mutation in the alpha-synuclein gene identified in families with Parkinson's disease. *Science,* 276**,** 2045-7.

POOLE, A. C., THOMAS, R. E., ANDREWS, L. A., MCBRIDE, H. M., WHITWORTH, A. J. & PALLANCK, L. J. (2008) The PINK1/Parkin pathway regulates mitochondrial morphology. *Proc Natl Acad Sci U S A,* 105**,** 1638-43.

PRIDGEON, J. W., OLZMANN, J. A., CHIN, L. S. & LI, L. (2007) PINK1 protects against oxidative stress by phosphorylating mitochondrial chaperone TRAP1. *PLoS Biol,* 5**,** e172.

RAIBORG, C., SLAGSVOLD, T. & STENMARK, H. (2006) A new side to ubiquitin. *Trends Biochem Sci,* 31**,** 541-4.

RAMIREZ, A., HEIMBACH, A., GRUNDEMANN, J., STILLER, B., HAMPSHIRE, D., CID, L. P., GOEBEL, I., MUBAIDIN, A. F., WRIEKAT, A. L., ROEPER, J., AL-DIN, A., HILLMER, A. M., KARSAK, M., LISS, B., WOODS, C. G., BEHRENS, M. I. & KUBISCH, C. (2006) Hereditary parkinsonism with dementia is caused by mutations in ATP13A2, encoding a lysosomal type 5 P-type ATPase. *Nat Genet,* 38**,** 1184-91.

RANKIN, C. A., JOAZEIRO, C. A., FLOOR, E. & HUNTER, T. (2001) E3 ubiquitin-protein ligase activity of Parkin is dependent on cooperative interaction of RING finger (TRIAD) elements. *J Biomed Sci,* 8**,** 421-9.

RAVID, T. & HOCHSTRASSER, M. (2007) Autoregulation of an E2 enzyme by ubiquitin-chain assembly on its catalytic residue. *Nat Cell Biol,* 9**,** 422-7.

REN, X. & HURLEY, J. H. (2010) VHS domains of ESCRT-0 cooperate in high-avidity binding to polyubiquitinated cargo. *EMBO J,* 29**,** 1045-54.

REVERTER, D. & LIMA, C. D. (2005) Insights into E3 ligase activity revealed by a SUMO-RanGAP1-Ubc9-Nup358 complex. *Nature,* 435**,** 687-92.

RODRIGO-BRENNI, M. C. & MORGAN, D. O. (2007) Sequential E2s drive polyubiquitin chain assembly on APC targets. *Cell,* 130**,** 127-39.

RYU, K. S., LEE, K. J., BAE, S. H., KIM, B. K., KIM, K. A. & CHOI, B. S. (2003) Binding surface mapping of intra- and interdomain interactions among hHR23B, ubiquitin, and polyubiquitin binding site 2 of S5a. *J Biol Chem,* 278**,** 36621-7.

SAFADI, S. S. & SHAW, G. S. (2007) A disease state mutation unfolds the parkin ubiquitin-like domain. *Biochemistry,* 46**,** 14162-9.

SAFADI, S. S. & SHAW, G. S. (2010) Differential interaction of the E3 ligase parkin with the proteasomal subunit S5a and the endocytic protein Eps15. *J Biol Chem,* 285**,** 1424-34.

SAHA, A. & DESHAIES, R. J. (2008) Multimodal activation of the ubiquitin ligase SCF by Nedd8 conjugation. *Mol Cell,* 32**,** 21-31.

SAKATA, E., YAMAGUCHI, Y., KURIMOTO, E., KIKUCHI, J., YOKOYAMA, S., YAMADA, S., KAWAHARA, H., YOKOSAWA, H., HATTORI, N., MIZUNO, Y., TANAKA, K. & KATO, K. (2003) Parkin binds the Rpn10 subunit of 26S proteasomes through its ubiquitin-like domain. *EMBO Rep,* 4**,** 301-6.

SATAKE, W., NAKABAYASHI, Y., MIZUTA, I., HIROTA, Y., ITO, C., KUBO, M., KAWAGUCHI, T., TSUNODA, T., WATANABE, M., TAKEDA, A., TOMIYAMA, H., NAKASHIMA, K., HASEGAWA, K., OBATA, F., YOSHIKAWA, T., KAWAKAMI, H., SAKODA, S., YAMAMOTO, M., HATTORI, N., MURATA, M., NAKAMURA, Y. & TODA, T. (2009) Genome-wide association study identifies common variants at four loci as genetic risk factors for Parkinson's disease. *Nat Genet,* 41**,** 1303-7.

SATO, S., CHIBA, T., SAKATA, E., KATO, K., MIZUNO, Y., HATTORI, N. & TANAKA, K. (2006) 14-3-3eta is a novel regulator of parkin ubiquitin ligase. *EMBO J,* 25**,** 211-21.

SATO, Y., YOSHIKAWA, A., MIMURA, H., YAMASHITA, M., YAMAGATA, A. & FUKAI, S. (2009) Structural basis for specific recognition of Lys 63-linked polyubiquitin chains by tandem UIMs of RAP80. *EMBO J,* 28**,** 2461-8.

SATO, Y., YOSHIKAWA, A., YAMAGATA, A., MIMURA, H., YAMASHITA, M., OOKATA, K., NUREKI, O., IWAI, K., KOMADA, M. & FUKAI, S. (2008) Structural basis for specific cleavage of Lys 63-linked polyubiquitin chains. *Nature,* 455**,** 358-62.

SCHAUBER, C., CHEN, L., TONGAONKAR, P., VEGA, I., LAMBERTSON, D., POTTS, W. & MADURA, K. (1998) Rad23 links DNA repair to the ubiquitin/proteasome pathway. *Nature,* 391**,** 715-8.

SCHEFFNER, M., NUBER, U. & HUIBREGTSE, J. M. (1995) Protein ubiquitination involving an E1-E2-E3 enzyme ubiquitin thioester cascade. *Nature,* 373**,** 81-3.

SCHEFFNER, M. & STAUB, O. (2007) HECT E3s and human disease. *BMC Biochem,* 8 Suppl 1**,** S6.

SCHLEHE, J. S., LUTZ, A. K., PILSL, A., LAMMERMANN, K., GRGUR, K., HENN, I. H., TATZELT, J. & WINKLHOFER, K. F. (2008) Aberrant folding of pathogenic Parkin mutants: aggregation versus degradation. *J Biol Chem,* 283**,** 13771-9.

SCHLOSSMACHER, M. G., FROSCH, M. P., GAI, W. P., MEDINA, M., SHARMA, N., FORNO, L., OCHIISHI, T., SHIMURA, H., SHARON, R., HATTORI, N., LANGSTON, J. W., MIZUNO, Y., HYMAN, B. T., SELKOE, D. J. & KOSIK, K. S. (2002) Parkin localizes to the Lewy bodies of Parkinson disease and dementia with Lewy bodies. *Am J Pathol,* 160**,** 1655-67.

SCHRODINGER, LLC (2010) The PyMOL Molecular Graphics System, Version 1.3r1.

SCHULMAN, B. A. & HARPER, J. W. (2009) Ubiquitin-like protein activation by E1 enzymes: the apex for downstream signalling pathways. *Nat Rev Mol Cell Biol,* 10**,** 319-31.

SCHWARZER, D. & COLE, P. A. (2005) Protein semisynthesis and expressed protein ligation: chasing a protein's tail. *Curr Opin Chem Biol,* 9**,** 561-9.

SEKINE, K., TAKUBO, K., KIKUCHI, R., NISHIMOTO, M., KITAGAWA, M., ABE, F., NISHIKAWA, K., TSURUO, T. & NAITO, M. (2008) Small molecules destabilize cIAP1 by activating auto-ubiquitylation. *J Biol Chem,* 283**,** 8961-8.

SHA, D., CHIN, L. S. & LI, L. (2010) Phosphorylation of parkin by Parkinson disease-linked kinase PINK1 activates parkin E3 ligase function and NF-kappaB signaling. *Hum Mol Genet,* 19**,** 352-63.

SHIMURA, H., HATTORI, N., KUBO, S., MIZUNO, Y., ASAKAWA, S., MINOSHIMA, S., SHIMIZU, N., IWAI, K., CHIBA, T., TANAKA, K. & SUZUKI, T. (2000) Familial Parkinson disease gene product, parkin, is a ubiquitin-protein ligase. *Nat Genet,* 25**,** 302-5.

SHIMURA, H., SCHLOSSMACHER, M. G., HATTORI, N., FROSCH, M. P., TROCKENBACHER, A., SCHNEIDER, R., MIZUNO, Y., KOSIK, K. S. & SELKOE, D. J. (2001) Ubiquitination of a new form of alpha-synuclein by parkin from human brain: implications for Parkinson's disease. *Science,* 293**,** 263-9.

SHOJAEE, S., SINA, F., BANIHOSSEINI, S. S., KAZEMI, M. H., KALHOR, R., SHAHIDI, G. A., FAKHRAI-RAD, H., RONAGHI, M. & ELAHI, E. (2008) Genome-wide linkage analysis of a Parkinsonian-pyramidal syndrome pedigree by 500 K SNP arrays. *Am J Hum Genet,* 82**,** 1375-84.

SHTILERMAN, M. D., DING, T. T. & LANSBURY, P. T., JR. (2002) Molecular crowding accelerates fibrillization of alpha-synuclein: could an increase in the cytoplasmic protein concentration induce Parkinson's disease? *Biochemistry,* 41**,** 3855-60.

SILVESTRI, L., CAPUTO, V., BELLACCHIO, E., ATORINO, L., DALLAPICCOLA, B., VALENTE, E. M. & CASARI, G. (2005) Mitochondrial import and enzymatic activity of PINK1 mutants associated to recessive parkinsonism. *Hum Mol Genet,* 14**,** 3477-92.

SIMS, J. J. & COHEN, R. E. (2009) Linkage-specific avidity defines the lysine 63-linked polyubiquitin-binding preference of rap80. *Mol Cell,* 33**,** 775-83.

SIMS, J. J., HARIRINIA, A., DICKINSON, B. C., FUSHMAN, D. & COHEN, R. E. (2009) Avid interactions underlie the Lys63-linked polyubiquitin binding specificities observed for UBA domains. *Nat Struct Mol Biol,* 16**,** 883-9.

SINGLETON, A. B., FARRER, M., JOHNSON, J., SINGLETON, A., HAGUE, S., KACHERGUS, J., HULIHAN, M., PEURALINNA, T., DUTRA, A., NUSSBAUM, R., LINCOLN, S., CRAWLEY, A., HANSON, M., MARAGANORE, D., ADLER, C., COOKSON, M. R., MUENTER, M., BAPTISTA, M., MILLER, D., BLANCATO, J., HARDY, J. & GWINN-HARDY, K. (2003) alpha-Synuclein locus triplication causes Parkinson's disease. *Science,* 302**,** 841.

SLOPER-MOULD, K. E., JEMC, J. C., PICKART, C. M. & HICKE, L. (2001) Distinct functional surface regions on ubiquitin. *J Biol Chem,* 276**,** 30483-9.

SMITH, W. W., JIANG, H., PEI, Z., TANAKA, Y., MORITA, H., SAWA, A., DAWSON, V. L., DAWSON, T. M. & ROSS, C. A. (2005a) Endoplasmic reticulum stress and mitochondrial cell death pathways mediate A53T mutant alpha-synuclein-induced toxicity. *Hum Mol Genet,* 14**,** 3801-11.

SMITH, W. W., PEI, Z., JIANG, H., MOORE, D. J., LIANG, Y., WEST, A. B., DAWSON, V. L., DAWSON, T. M. & ROSS, C. A. (2005b) Leucine-rich repeat kinase 2 (LRRK2) interacts with parkin, and mutant LRRK2 induces neuronal degeneration. *Proc Natl Acad Sci U S A,* 102**,** 18676-81.

SNYDER, H., MENSAH, K., THEISLER, C., LEE, J., MATOUSCHEK, A. & WOLOZIN, B. (2003) Aggregated and monomeric alpha-synuclein bind to the S6' proteasomal protein and inhibit proteasomal function. *J Biol Chem,* 278**,** 11753-9.

SPILLANTINI, M. G., CROWTHER, R. A., JAKES, R., HASEGAWA, M. & GOEDERT, M. (1998) alpha-Synuclein in filamentous inclusions of Lewy bodies from Parkinson's disease and dementia with lewy bodies. *Proc Natl Acad Sci U S A,* 95**,** 6469-73.

SRIRAM, S. R., LI, X., KO, H. S., CHUNG, K. K., WONG, E., LIM, K. L., DAWSON, V. L. & DAWSON, T. M. (2005) Familial-associated mutations differentially disrupt the solubility, localization, binding and ubiquitination properties of parkin. *Hum Mol Genet,* 14**,** 2571-86.

STAROPOLI, J. F., MCDERMOTT, C., MARTINAT, C., SCHULMAN, B., DEMIREVA, E. & ABELIOVICH, A. (2003) Parkin is a component of an SCF-like ubiquitin ligase complex and protects postmitotic neurons from kainate excitotoxicity. *Neuron,* 37**,** 735-49.

STEFANIS, L., LARSEN, K. E., RIDEOUT, H. J., SULZER, D. & GREENE, L. A. (2001) Expression of A53T mutant but not wild-type alpha-synuclein in PC12 cells induces alterations of the ubiquitin-dependent degradation system, loss of dopamine release, and autophagic cell death. *J Neurosci,* 21**,** 9549-60.

STICHEL, C. C., ZHU, X. R., BADER, V., LINNARTZ, B., SCHMIDT, S. & LUBBERT, H. (2007) Mono- and double-mutant mouse models of Parkinson's disease display severe mitochondrial damage. *Hum Mol Genet,* 16**,** 2377-93.

STRAUSS, K. M., MARTINS, L. M., PLUN-FAVREAU, H., MARX, F. P., KAUTZMANN, S., BERG, D., GASSER, T., WSZOLEK, Z., MULLER, T., BORNEMANN, A., WOLBURG, H., DOWNWARD, J., RIESS, O., SCHULZ, J. B. & KRUGER, R. (2005) Loss of function mutations in the gene encoding Omi/HtrA2 in Parkinson's disease. *Hum Mol Genet,* 14**,** 2099-111.

SUGASAWA, K., NG, J. M., MASUTANI, C., IWAI, S., VAN DER SPEK, P. J., EKER, A. P., HANAOKA, F., BOOTSMA, D. & HOEIJMAKERS, J. H. (1998) Xeroderma pigmentosum group C protein complex is the initiator of global genome nucleotide excision repair. *Mol Cell,* 2**,** 223-32.

SWANSON, K. A., KANG, R. S., STAMENOVA, S. D., HICKE, L. & RADHAKRISHNAN, I. (2003) Solution structure of Vps27 UIM-ubiquitin complex important for endosomal sorting and receptor downregulation. *EMBO J,* 22**,** 4597-606.

TAIN, L. S., CHOWDHURY, R. B., TAO, R. N., PLUN-FAVREAU, H., MOISOI, N., MARTINS, L. M., DOWNWARD, J., WHITWORTH, A. J. & TAPON, N. (2009) Drosophila HtrA2 is dispensable for apoptosis but acts downstream of PINK1 independently from Parkin. *Cell Death Differ,* 16**,** 1118-25.

TANAKA, Y., ENGELENDER, S., IGARASHI, S., RAO, R. K., WANNER, T., TANZI, R. E., SAWA, A., V, L. D., DAWSON, T. M. & ROSS, C. A. (2001) Inducible expression of mutant alpha-synuclein decreases proteasome activity and increases sensitivity to mitochondria-dependent apoptosis. *Hum Mol Genet,* 10**,** 919-26.

TANG, B., XIONG, H., SUN, P., ZHANG, Y., WANG, D., HU, Z., ZHU, Z., MA, H., PAN, Q., XIA, J. H., XIA, K. & ZHANG, Z. (2006) Association of PINK1 and DJ-1 confers digenic inheritance of early-onset Parkinson's disease. *Hum Mol Genet,* 15**,** 1816-25.

TAO, H., SIMMONS, B. N., SINGIREDDY, S., JAKKIDI, M., SHORT, K. M., COX, T. C. & MASSIAH, M. A. (2008) Structure of the MID1 tandem B-boxes reveals an interaction reminiscent of intermolecular ring heterodimers. *Biochemistry,* 47**,** 2450-7.

TAYLOR, J. M., SONG, Y. J., HUANG, Y., FARRER, M. J., DELATYCKI, M. B., HALLIDAY, G. M. & LOCKHART, P. J. (2007) Parkin Co-Regulated Gene (PACRG) is regulated by the ubiquitin-proteasomal system and is present in the pathological features of Parkinsonian diseases. *Neurobiol Dis,* 27**,** 238-47.

TAYLOR, S. V., KELLEHER, N. L., KINSLAND, C., CHIU, H. J., COSTELLO, C. A., BACKSTROM, A. D., MCLAFFERTY, F. W. & BEGLEY, T. P. (1998) Thiamin biosynthesis in Escherichia coli. Identification of ThiS thiocarboxylate as the immediate sulfur donor in the thiazole formation. *J Biol Chem,* 273**,** 16555-60.

THOMAS, B., VON COELLN, R., MANDIR, A. S., TRINKAUS, D. B., FARAH, M. H., LEONG LIM, K., CALINGASAN, N. Y., FLINT BEAL, M., DAWSON, V. L. & DAWSON, T. M. (2007) MPTP and DSP-4 susceptibility of substantia nigra and locus coeruleus catecholaminergic neurons in mice is independent of parkin activity. *Neurobiol Dis,* 26**,** 312-22.

TOBE, T., NAKAJO, S., TANAKA, A., MITOYA, A., OMATA, K., NAKAYA, K., TOMITA, M. & NAKAMURA, Y. (1992) Cloning and characterization of the cDNA encoding a novel brain-specific 14-kDa protein. *J Neurochem,* 59**,** 1624-9.

TOFARIS, G. K., GARCIA REITBOCK, P., HUMBY, T., LAMBOURNE, S. L., O'CONNELL, M., GHETTI, B., GOSSAGE, H., EMSON, P. C., WILKINSON, L. S., GOEDERT, M. & SPILLANTINI, M. G. (2006) Pathological changes in dopaminergic nerve cells of the substantia nigra and olfactory bulb in mice transgenic for truncated human alpha-synuclein(1-120): implications for Lewy body disorders. *J Neurosci,* 26**,** 3942-50.

TOMOO, K., MUKAI, Y., IN, Y., MIYAGAWA, H., KITAMURA, K., YAMANO, A., SHINDO, H. & ISHIDA, T. (2008) Crystal structure and molecular dynamics simulation of ubiquitin-like domain of murine parkin. *Biochim Biophys Acta,* 1784**,** 1059-67.

TREMPE, J. F., CHEN, C. X., GRENIER, K., CAMACHO, E. M., KOZLOV, G., MCPHERSON, P. S., GEHRING, K. & FON, E. A. (2009) SH3 domains from a subset of BAR proteins define a Ubl-binding domain and implicate parkin in synaptic ubiquitination. *Mol Cell,* 36**,** 1034-47.

UEDA, K., FUKUSHIMA, H., MASLIAH, E., XIA, Y., IWAI, A., YOSHIMOTO, M., OTERO, D. A., KONDO, J., IHARA, Y. & SAITOH, T. (1993) Molecular cloning of cDNA encoding an unrecognized component of amyloid in Alzheimer disease. *Proc Natl Acad Sci U S A,* 90**,** 11282-6.

ULRICH, H. D. & WALDEN, H. (2010) Ubiquitin signalling in DNA replication and repair. *Nat Rev Mol Cell Biol,* 11**,** 479-89.

UNOKI, M. & NAKAMURA, Y. (2001) Growth-suppressive effects of BPOZ and EGR2, two genes involved in the PTEN signaling pathway. *Oncogene,* 20**,** 4457-65.

UPADHYA, S. C. & HEGDE, A. N. (2003) A potential proteasome-interacting motif within the ubiquitin-like domain of parkin and other proteins. *Trends Biochem Sci,* 28**,** 280-3.

UVERSKY, V. N. (2003) A protein-chameleon: conformational plasticity of alpha-synuclein, a disordered protein involved in neurodegenerative disorders. *J Biomol Struct Dyn,* 21**,** 211-34.

UVERSKY, V. N., E, M. C., BOWER, K. S., LI, J. & FINK, A. L. (2002) Accelerated alpha-synuclein fibrillation in crowded milieu. *FEBS Lett,* 515**,** 99-103.

VALENTE, E. M., ABOU-SLEIMAN, P. M., CAPUTO, V., MUQIT, M. M., HARVEY, K., GISPERT, S., ALI, Z., DEL TURCO, D., BENTIVOGLIO, A. R., HEALY, D. G., ALBANESE, A., NUSSBAUM, R., GONZALEZ-MALDONADO, R., DELLER, T., SALVI, S., CORTELLI, P., GILKS, W. P., LATCHMAN, D. S., HARVEY, R. J., DALLAPICCOLA, B., AUBURGER, G. & WOOD, N. W. (2004) Hereditary early-onset Parkinson's disease caused by mutations in PINK1. *Science,* 304**,** 1158-60.

VAN DEN ENT, F. & LOWE, J. (2006) RF cloning: a restriction-free method for inserting target genes into plasmids. *J Biochem Biophys Methods,* 67**,** 67-74.

VAN HUMBEECK, C., WAELKENS, E., CORTI, O., BRICE, A. & VANDENBERGHE, W. (2008) Parkin occurs in a stable, non-covalent, approximately 110-kDa complex in brain. *Eur J Neurosci,* 27**,** 284-93.

VAN WIJK, S. J. & TIMMERS, H. T. (2010) The family of ubiquitin-conjugating enzymes (E2s): deciding between life and death of proteins. *FASEB J,* 24**,** 981-93.

VARADAN, R., ASSFALG, M., RAASI, S., PICKART, C. & FUSHMAN, D. (2005) Structural determinants for selective recognition of a Lys48-linked polyubiquitin chain by a UBA domain. *Mol Cell,* 18**,** 687-98.

VAUX, D. L. & SILKE, J. (2003) HtrA2/Omi, a sheep in wolf's clothing. *Cell,* 115**,** 251-3.

VEERIAH, S., TAYLOR, B. S., MENG, S., FANG, F., YILMAZ, E., VIVANCO, I., JANAKIRAMAN, M., SCHULTZ, N., HANRAHAN, A. J., PAO, W., LADANYI, M., SANDER, C., HEGUY, A., HOLLAND, E. C., PATY, P. B., MISCHEL, P. S., LIAU, L., CLOUGHESY, T. F., MELLINGHOFF, I. K., SOLIT, D. B. & CHAN, T. A. (2010) Somatic mutations of the Parkinson's disease-associated gene PARK2 in glioblastoma and other human malignancies. *Nat Genet,* 42**,** 77-82.

VENDEROVA, K., KABBACH, G., ABDEL-MESSIH, E., ZHANG, Y., PARKS, R. J., IMAI, Y., GEHRKE, S., NGSEE, J., LAVOIE, M. J., SLACK, R. S., RAO, Y., ZHANG, Z., LU, B., HAQUE, M. E. & PARK, D. S. (2009) Leucine-Rich Repeat Kinase 2 interacts with Parkin, DJ-1 and PINK-1 in a Drosophila melanogaster model of Parkinson's disease. *Hum Mol Genet,* 18**,** 4390-404.

VERCAMMEN, L., VAN DER PERREN, A., VAUDANO, E., GIJSBERS, R., DEBYSER, Z., VAN DEN HAUTE, C. & BAEKELANDT, V. (2006) Parkin protects against neurotoxicity in the 6-hydroxydopamine rat model for Parkinson's disease. *Mol Ther,* 14**,** 716-23.

VERDECIA, M. A., JOAZEIRO, C. A., WELLS, N. J., FERRER, J. L., BOWMAN, M. E., HUNTER, T. & NOEL, J. P. (2003) Conformational flexibility underlies ubiquitin ligation mediated by the WWP1 HECT domain E3 ligase. *Mol Cell,* 11**,** 249-59.

VIJAY-KUMAR, S., BUGG, C. E. & COOK, W. J. (1987) Structure of ubiquitin refined at 1.8 A resolution. *J Mol Biol,* 194**,** 531-44.

VIJAY-KUMAR, S., BUGG, C. E., WILKINSON, K. D. & COOK, W. J. (1985) Three-dimensional structure of ubiquitin at 2.8 A resolution. *Proc Natl Acad Sci U S A,* 82**,** 3582-5.

VILARINO-GUELL, C., ROSS, O. A., SOTO, A. I., FARRER, M. J., HAUGARVOLL, K., AASLY, J. O., UITTI, R. J. & WSZOLEK, Z. K. (2009) Reported mutations in GIGYF2 are not a common cause of Parkinson's disease. *Mov Disord,* 24**,** 619-20.

VIVES-BAUZA, C., ZHOU, C., HUANG, Y., CUI, M., DE VRIES, R. L., KIM, J., MAY, J., TOCILESCU, M. A., LIU, W., KO, H. S., MAGRANE, J., MOORE, D. J., DAWSON, V. L., GRAILHE, R., DAWSON, T. M., LI, C., TIEU, K. & PRZEDBORSKI, S. (2010) PINK1-dependent recruitment of Parkin to mitochondria in mitophagy. *Proc Natl Acad Sci U S A,* 107**,** 378-83.

VOLLES, M. J. & LANSBURY, P. T., JR. (2002) Vesicle permeabilization by protofibrillar alpha-synuclein is sensitive to Parkinson's disease-linked mutations and occurs by a pore-like mechanism. *Biochemistry,* 41**,** 4595-602.

VON COELLN, R., THOMAS, B., ANDRABI, S. A., LIM, K. L., SAVITT, J. M., SAFFARY, R., STIRLING, W., BRUNO, K., HESS, E. J., LEE, M. K., DAWSON, V. L. & DAWSON, T. M. (2006) Inclusion body formation and neurodegeneration are parkin independent in a mouse model of alpha-synucleinopathy. *J Neurosci,* 26**,** 3685-96.

WALDEN, H., PODGORSKI, M. S., HUANG, D. T., MILLER, D. W., HOWARD, R. J., MINOR, D. L., JR., HOLTON, J. M. & SCHULMAN, B. A. (2003a) The structure of the APPBP1-UBA3-NEDD8-ATP complex reveals the basis for selective ubiquitin-like protein activation by an E1. *Mol Cell,* 12**,** 1427-37.

WALDEN, H., PODGORSKI, M. S. & SCHULMAN, B. A. (2003b) Insights into the ubiquitin transfer cascade from the structure of the activating enzyme for NEDD8. *Nature,* 422**,** 330-4.

WANG, C., TAN, J. M., HO, M. W., ZAIDEN, N., WONG, S. H., CHEW, C. L., ENG, P. W., LIM, T. M., DAWSON, T. M. & LIM, K. L. (2005) Alterations in the solubility and intracellular localization of parkin by several familial Parkinson's disease-linked point mutations. *J Neurochem,* 93**,** 422-31.

WANG, H., WANG, L., ERDJUMENT-BROMAGE, H., VIDAL, M., TEMPST, P., JONES, R. S. & ZHANG, Y. (2004) Role of histone H2A ubiquitination in Polycomb silencing. *Nature,* 431**,** 873-8.

WANG, M. & PICKART, C. M. (2005) Different HECT domain ubiquitin ligases employ distinct mechanisms of polyubiquitin chain synthesis. *EMBO J,* 24**,** 4324-33.

WANG, X., HERR, R. A., CHUA, W. J., LYBARGER, L., WIERTZ, E. J. & HANSEN, T. H. (2007) Ubiquitination of serine, threonine, or lysine residues on the cytoplasmic tail can induce ERAD of MHC-I by viral E3 ligase mK3. *J Cell Biol,* 177**,** 613-24.

WANG, X., HERR, R. A., RABELINK, M., HOEBEN, R. C., WIERTZ, E. J. & HANSEN, T. H. (2009) Ube2j2 ubiquitinates hydroxylated amino acids on ER-associated degradation substrates. *J Cell Biol,* 187**,** 655-68.

WEBB, J. L., RAVIKUMAR, B., ATKINS, J., SKEPPER, J. N. & RUBINSZTEIN, D. C. (2003) Alpha-Synuclein is degraded by both autophagy and the proteasome. *J Biol Chem,* 278**,** 25009-13.

WEIHOFEN, A., OSTASZEWSKI, B., MINAMI, Y. & SELKOE, D. J. (2008) Pink1 Parkinson mutations, the Cdc37/Hsp90 chaperones and Parkin all influence the maturation or subcellular distribution of Pink1. *Hum Mol Genet,* 17**,** 602-16.

WELCHMAN, R. L., GORDON, C. & MAYER, R. J. (2005) Ubiquitin and ubiquitin-like proteins as multifunctional signals. *Nat Rev Mol Cell Biol,* 6**,** 599-609.

WEST, A. B., LOCKHART, P. J., O'FARELL, C. & FARRER, M. J. (2003) Identification of a novel gene linked to parkin via a bi-directional promoter. *J Mol Biol,* 326**,** 11-9.

WHITBY, F. G., XIA, G., PICKART, C. M. & HILL, C. P. (1998) Crystal structure of the human ubiquitin-like protein NEDD8 and interactions with ubiquitin pathway enzymes. *J Biol Chem,* 273**,** 34983-91.

WIBORG, O., PEDERSEN, M. S., WIND, A., BERGLUND, L. E., MARCKER, K. A. & VUUST, J. (1985) The human ubiquitin multigene family: some genes contain multiple directly repeated ubiquitin coding sequences. *EMBO J,* 4**,** 755-9.

WIESNER, S., OGUNJIMI, A. A., WANG, H. R., ROTIN, D., SICHERI, F., WRANA, J. L. & FORMAN-KAY, J. D. (2007) Autoinhibition of the HECT-type ubiquitin ligase Smurf2 through its C2 domain. *Cell,* 130**,** 651-62.

WILLIAMSON, A., WICKLIFFE, K. E., MELLONE, B. G., SONG, L., KARPEN, G. H. & RAPE, M. (2009) Identification of a physiological E2 module for the human anaphase-promoting complex. *Proc Natl Acad Sci U S A,* 106**,** 18213-8.

WILSON, M. A., COLLINS, J. L., HOD, Y., RINGE, D. & PETSKO, G. A. (2003) The 1.1-A resolution crystal structure of DJ-1, the protein mutated in autosomal recessive early onset Parkinson's disease. *Proc Natl Acad Sci U S A,* 100**,** 9256-61.

WINDHEIM, M., PEGGIE, M. & COHEN, P. (2008) Two different classes of E2 ubiquitin-conjugating enzymes are required for the mono-ubiquitination of proteins and elongation by polyubiquitin chains with a specific topology. *Biochem J,* 409**,** 723-9.

WINN, P. J., RELIGA, T. L., BATTEY, J. N., BANERJEE, A. & WADE, R. C. (2004) Determinants of functionality in the ubiquitin conjugating enzyme family. *Structure,* 12**,** 1563-74.

WOELK, T., OLDRINI, B., MASPERO, E., CONFALONIERI, S., CAVALLARO, E., DI FIORE, P. P. & POLO, S. (2006) Molecular mechanisms of coupled monoubiquitination. *Nat Cell Biol,* 8**,** 1246-54.

WONG, E. S., TAN, J. M., WANG, C., ZHANG, Z., TAY, S. P., ZAIDEN, N., KO, H. S., DAWSON, V. L., DAWSON, T. M. & LIM, K. L. (2007) Relative sensitivity of parkin and other cysteine-containing enzymes to stress-induced solubility alterations. *J Biol Chem,* 282**,** 12310-8.

WU, P. Y., HANLON, M., EDDINS, M., TSUI, C., ROGERS, R. S., JENSEN, J. P., MATUNIS, M. J., WEISSMAN, A. M., WOLBERGER, C. & PICKART, C. M. (2003) A conserved catalytic residue in the ubiquitin-conjugating enzyme family. *EMBO J,* 22**,** 5241-50.

WU, T., MERBL, Y., HUO, Y., GALLOP, J. L., TZUR, A. & KIRSCHNER, M. W. (2010) UBE2S drives elongation of K11-linked ubiquitin chains by the anaphase-promoting complex. *Proc Natl Acad Sci U S A,* 107**,** 1355-60.

XIONG, H., WANG, D., CHEN, L., CHOO, Y. S., MA, H., TANG, C., XIA, K., JIANG, W., RONAI, Z., ZHUANG, X. & ZHANG, Z. (2009) Parkin, PINK1, and DJ-1 form a ubiquitin E3 ligase complex promoting unfolded protein degradation. *J Clin Invest,* 119**,** 650-60.

XU, J., KAO, S. Y., LEE, F. J., SONG, W., JIN, L. W. & YANKNER, B. A. (2002) Dopamine-dependent neurotoxicity of alpha-synuclein: a mechanism for selective neurodegeneration in Parkinson disease. *Nat Med,* 8**,** 600-6.

YAMADA, M., MIZUNO, Y. & MOCHIZUKI, H. (2005) Parkin gene therapy for alpha-synucleinopathy: a rat model of Parkinson's disease. *Hum Gene Ther,* 16**,** 262-70.

YAMAMOTO, A., FRIEDLEIN, A., IMAI, Y., TAKAHASHI, R., KAHLE, P. J. & HAASS, C. (2005) Parkin phosphorylation and modulation of its E3 ubiquitin ligase activity. *J Biol Chem,* 280**,** 3390-9.

YAMOAH, K., OASHI, T., SARIKAS, A., GAZDOIU, S., OSMAN, R. & PAN, Z. Q. (2008) Autoinhibitory regulation of SCF-mediated ubiquitination by human cullin 1's C-terminal tail. *Proc Natl Acad Sci U S A,* 105**,** 12230-5.

YANG, Y., GEHRKE, S., IMAI, Y., HUANG, Z., OUYANG, Y., WANG, J. W., YANG, L., BEAL, M. F., VOGEL, H. & LU, B. (2006) Mitochondrial pathology and muscle and dopaminergic neuron degeneration caused by inactivation of Drosophila Pink1 is rescued by Parkin. *Proc Natl Acad Sci U S A,* 103**,** 10793-8.

YANG, Y., NISHIMURA, I., IMAI, Y., TAKAHASHI, R. & LU, B. (2003) Parkin suppresses dopaminergic neuron-selective neurotoxicity induced by Pael-R in Drosophila. *Neuron,* 37**,** 911-24.

YANG, Y. X., WOOD, N. W. & LATCHMAN, D. S. (2009) Molecular basis of Parkinson's disease. *Neuroreport,* 20**,** 150-6.

YAO, D., GU, Z., NAKAMURA, T., SHI, Z. Q., MA, Y., GASTON, B., PALMER, L. A., ROCKENSTEIN, E. M., ZHANG, Z., MASLIAH, E., UEHARA, T. & LIPTON, S. A. (2004) Nitrosative stress linked to sporadic Parkinson's disease: S-nitrosylation of parkin regulates its E3 ubiquitin ligase activity. *Proc Natl Acad Sci U S A,* 101**,** 10810-4.

YASUDA, T., MIYACHI, S., KITAGAWA, R., WADA, K., NIHIRA, T., REN, Y. R., HIRAI, Y., AGEYAMA, N., TERAO, K., SHIMADA, T., TAKADA, M., MIZUNO, Y. & MOCHIZUKI, H. (2007) Neuronal specificity of alpha-synuclein toxicity and effect of Parkin co-expression in primates. *Neuroscience,* 144**,** 743-53.

YE, Y. & RAPE, M. (2009) Building ubiquitin chains: E2 enzymes at work. *Nat Rev Mol Cell Biol,* 10**,** 755-64.

YIN, Q., LIN, S. C., LAMOTHE, B., LU, M., LO, Y. C., HURA, G., ZHENG, L., RICH, R. L., CAMPOS, A. D., MYSZKA, D. G., LENARDO, M. J., DARNAY, B. G. & WU, H. (2009) E2 interaction and dimerization in the crystal structure of TRAF6. *Nat Struct Mol Biol,* 16**,** 658-66.

YUNUS, A. A. & LIMA, C. D. (2006) Lysine activation and functional analysis of E2-mediated conjugation in the SUMO pathway. *Nat Struct Mol Biol,* 13**,** 491-9.

ZHANG, D., RAASI, S. & FUSHMAN, D. (2008) Affinity makes the difference: nonselective interaction of the UBA domain of Ubiquilin-1 with monomeric ubiquitin and polyubiquitin chains. *J Mol Biol,* 377**,** 162-80.

ZHANG, M., WINDHEIM, M., ROE, S. M., PEGGIE, M., COHEN, P., PRODROMOU, C. & PEARL, L. H. (2005) Chaperoned ubiquitylation--crystal structures of the CHIP U box E3 ubiquitin ligase and a CHIP-Ubc13-Uev1a complex. *Mol Cell,* 20**,** 525-38.

ZHANG, N., WANG, Q., EHLINGER, A., RANDLES, L., LARY, J. W., KANG, Y., HARIRINIA, A., STORASKA, A. J., COLE, J. L., FUSHMAN, D. & WALTERS, K. J. (2009) Structure of the s5a:k48-linked diubiquitin complex and its interactions with rpn13. *Mol Cell,* 35**,** 280-90.

ZHANG, Y., GAO, J., CHUNG, K. K., HUANG, H., DAWSON, V. L. & DAWSON, T. M. (2000) Parkin functions as an E2-dependent ubiquitin- protein ligase and promotes the degradation of the synaptic vesicle-associated protein, CDCrel-1. *Proc Natl Acad Sci U S A,* 97**,** 13354-9.

ZHENG, N., WANG, P., JEFFREY, P. D. & PAVLETICH, N. P. (2000) Structure of a c-Cbl-UbcH7 complex: RING domain function in ubiquitin-protein ligases. *Cell,* 102**,** 533-9.

ZHONG, L., TAN, Y., ZHOU, A., YU, Q. & ZHOU, J. (2005) RING finger ubiquitin-protein isopeptide ligase Nrdp1/FLRF regulates parkin stability and activity. *J Biol Chem,* 280**,** 9425-30.

ZHU, X., MENARD, R. & SULEA, T. (2007) High incidence of ubiquitin-like domains in human ubiquitin-specific proteases. *Proteins,* 69**,** 1-7.

ZIMPRICH, A., BISKUP, S., LEITNER, P., LICHTNER, P., FARRER, M., LINCOLN, S., KACHERGUS, J., HULIHAN, M., UITTI, R. J., CALNE, D. B., STOESSL, A. J., PFEIFFER, R. F., PATENGE, N., CARBAJAL, I. C., VIEREGGE, P., ASMUS, F., MULLER-MYHSOK, B., DICKSON, D. W., MEITINGER, T., STROM, T. M., WSZOLEK, Z. K. & GASSER, T. (2004) Mutations in LRRK2 cause autosomal-dominant parkinsonism with pleomorphic pathology. *Neuron,* 44**,** 601-7.

ZIVIANI, E., TAO, R. N. & WHITWORTH, A. J. (2010) Drosophila parkin requires PINK1 for mitochondrial translocation and ubiquitinates mitofusin. *Proc Natl Acad Sci U S A,* 107**,** 5018-23.